PROTEIN STABILIZING POTENTIAL OF SIMULATED HONEY SUGAR COCKTAIL AND HONEY: A CASE STUDY WITH BOVINE SERUM ALBUMIN, OVALBUMIN AND LYSOZYME

WONG YIN HOW

FACULTY OF SCIENCE
UNIVERSITY OF MALAYA
KUALA LUMPUR

2016

PROTEIN STABILIZING POTENTIAL OF SIMULATED HONEY SUGAR COCKTAIL AND HONEY: A CASE STUDY WITH BOVINE SERUM ALBUMIN, OVALBUMIN AND LYSOZYME

WONG YIN HOW

THESIS SUBMITTED IN FULFILMENT OF THE REQUIREMENTS FOR THE DEGREE OF DOCTOR OF PHILOSOPHY

FACULTY OF SCIENCE
UNIVERSITY OF MALAYA
KUALA LUMPUR

2016

UNIVERSITY OF MALAYA

ORIGINAL LITERARY WORK DECLARATION

Name of Candidate: Wong Yin How

Registration/Matric No: SHC 130027

Name of Degree: Doctor of Philosophy (Ph.D.)

Title of Thesis ("this Work"):

"Protein Stabilizing Potential of Simulated Honey Sugar Cocktail and Honey: A Case Study with Bovine Serum Albumin, Ovalbumin and Lysozyme"

Field of Study: Biochemistry

I do solemnly and sincerely declare that:

(1) I am the sole author/writer of this Work;
(2) This Work is original;
(3) Any use of any work in which copyright exists was done by way of fair dealing and for permitted purposes and any excerpt or extract from, or reference to or reproduction of any copyright work has been disclosed expressly and sufficiently and the title of the Work and its authorship have been acknowledged in this Work;
(4) I do not have any actual knowledge nor do I ought reasonably to know that the making of this work constitutes an infringement of any copyright work;
(5) I hereby assign all and every rights in the copyright to this Work to the University of Malaya ("UM"), who henceforth shall be owner of the copyright in this Work and that any reproduction or use in any form or by any means whatsoever is prohibited without the written consent of UM having been first had and obtained;
(6) I am fully aware that if in the course of making this Work I have infringed any copyright whether intentionally or otherwise, I may be subject to legal action or any other action as may be determined by UM.

Candidate's Signature Date:
(Wong Yin How)

Subscribed and solemnly declared before,

Witness's Signature Date:
Name: Professor Saad Tayyab
Designation: Supervisor

Witness's Signature Date:
Name: Professor Habsah Abdul Kadir
Designation: Supervisor

ABSTRACT

The protein stabilizing potential of honey was elucidated using simulated honey sugar cocktail (SHSC) on three model proteins, namely, bovine serum albumin (BSA), ovalbumin and lysozyme. The chemical (urea and guanidine hydrochloride) and thermal denaturation curves of these proteins were shifted towards higher denaturant concentration or temperature in the presence of different SHSC concentrations (8–30%) in a concentration dependent manner, when monitored by far-UV circular dichroism (CD), fluorescence and UV-difference spectral measurements. A comparison of the spectral properties of the partially-denatured proteins (at the mid-point of transition) in the absence and the presence of SHSC using far-UV and near-UV CD, UV-difference, intrinsic fluorescence, three-dimensional fluorescence and ANS fluorescence measurements showed significant retention of globular conformation in the partially-denatured proteins in the presence of SHSC. Honey quenched the intrinsic fluorescence of BSA in a concentration dependent manner, showing complete quenching in the presence of 5% (w/v) honey. Increasing the protein concentration did not lead to any recovery in the protein fluorescence. Intrinsic fluorescence failed to produce any result in the urea denaturation of BSA in the presence of 5% (w/v) honey. Hence, chemical and thermal stabilizing potential of honey was evaluated on a model protein, BSA using far-UV CD and ANS fluorescence spectroscopy. A comparison of the chemical and thermal transition curves of BSA obtained in the absence and the presence of SHSC or honey showed greater shift of the transition curves towards higher denaturant concentration or temperature in the presence of honey compared to SHSC. Furthermore, greater retention of the globular conformation in the partially-denatured protein was also observed in the presence of honey compared to SHSC. Taken together, all these results suggested significant stabilization of native protein conformation in the presence of

SHSC or honey against chemical and thermal denaturations, being relatively higher in the presence of honey.

ABSTRAK

Potensi penstabilan protein madu telah dikaji dengan menggunakan koktel gula madu simulasi (SHSC) terhadap tiga protein model iaitu albumin serum bovin (BSA), ovalbumin dan lisozim. Lengkung penyahaslian kimia (urea and guanidin hidroklorida) dan terma protein-protein tersebut telah beralih kepada kepekatan penyahasli and suhu yang lebih tinggi secara berkadar langsung dengan kepekatan SHSC dengan penambahan SHSC pada kepekatan 8–30% apabila dikaji dengan menggunakan teknik spektroskopi 'far-UV circular dichroism (CD)', fluoresens dan 'UV-difference'. Perbandingan ciri-ciri spektra 'far-UV and near-UV CD', 'UV-difference', fluoresens intrinsik, fluoresens tiga-dimensi dan fluoresens ANS protein-separa dinyahasli (pada pertengahan transisi protein) menunjukkan pengekalan konformasi globular protein-separa dinyahasli yang signifikan dengan penambahan SHSC. Madu melindapkejutkan fluoresens BSA secara berkadar langsung dengan kepekatan madu dan pelindapkejutan fluoresens penuh BSA berlaku pada kepekatan 5% (w/v) madu. Penambahan kepekatan protein tidak memulihkan fluoresens protein tersebut. Urea denaturasi BSA dengan kehadiran 5% (w/v) madu tidak menunjukkan sebarang keputusan apabila dikaji dengan menggunakan teknik fluoresens. Oleh yang demikian, potensi penstabilan kimia and terma madu dikaji terhadap protein model, BSA dengan menggunakan 'far-UV CD' dan fluoresens ANS. Perbandingan lengkung transisi kimia dan terma BSA tanpa dan dengan penambahan SHSC atau madu menunjukkan peralihan lengkung transisi kepada kepekatan penyahasli dan suhu yang lebih tinggi dengan penambahan madu berbanding dengan SHSC. Tambahan pula, pengekalan konformasi globular protein-separa dinyahasli didapati lebih berkesan dengan penambahan madu berbanding dengan SHSC. Kesemuaan keputusan diatas menunjukkan pencapaian penstabilan protein yang signifikan menentang penyahaslian kimia dan terma dengan penambahan SHSC atau

madu. Penstabilan protein ini didapati lebih berkesan dengan penambahan madu berbanding dengan SHSC.

ACKNOWLEDGEMENTS

It is my pleasure to convey my gratitude to those people who helped me during the completion of this thesis.

First and foremost, I would like to express my deepest and sincere gratitude to my supervisor, **Professor Saad Tayyab** for the invaluable opportunity to undertake this project under him. His excellent guidance, knowledge, never-ceasing help and moral support have been a great value to me. His kind understanding, patience and constructive comments from time to time provided a good basis for completion of this project.

I would like to express my gratitude to my co-supervisor, **Professor Habsah Abdul Kadir** not only for her endless support and encouragement but also providing all necessary facilities during the course of completing this project.

I am grateful to **Associate Dr. Professor Rosli Ramli**, Head, Institute of Biological Sciences, **Professor Zanariah Abdullah**, Dean, Faculty of Science, University of Malaya and **Dr. Zazali Alias**, Coordinator, Biochemistry Programme for providing all necessary facilities.

I am heartily thankful to **Mr. Shevin Rizal Feroz** for being with me through all easy and hard days throughout the project. The journey will not be the same without his advice, moral support, invaluable experiences and encouraging opinions. I would like to thank the members of Laboratory E2.5 especially, **Ms. Adyani Azizah Abdul Halim** and **Mr. Mohammed Suleiman Zaroog** for their constant support and opinions. My thanks and appreciation to **Mr. Izuwan, Ms. Nadia, Ms. Norlida** and all the staffs of Institute of Biological Sciences for their assistance and technical guidance throughout this project. Special thanks are due to **Dr. Hong Sok Lai** and **Dr. Lee Guan Serm** for providing the HIR lab facilities.

Financial support from the University of Malaya in the form of University Malaya Fellowship Scheme and University of Malaya Postgraduate Research Fund (PG072 / 2013B) are gratefully acknowledged.

I wish to express my gratitude to my family for all their understanding, support and encouragement throughout this project.

WONG YIN HOW

June 27, 2015

TABLE OF CONTENTS

LIST OF FIGURES

LIST OF TABLES

LIST OF ABBREVIATIONS / SYMBOLS

Å	Angstrom
Ala	Alanine
ANOVA	One-way analysis of variance
ANS	8-Anilino-1-naphthalene sulfonic acid
Arg	Arginine
Asn	Asparagine
Asp	Aspartic acid
α	Alpha
β	Beta
BSA	Bovine serum albumin
c	Concentration
°C	Degree Celsius
CD	Circular dichroism
cm	Centimeter
C_m	Mid-point concentration
Cys	Cysteine
3-D	Three-dimensional
D	Denatured
deg	Degree
$dmol^{-1}$	per Decimole
ε	Extinction coefficient
F_D	Fraction denatured
g	Gram
GdnHCl	Guanidine hydrochloride

Glu	Glutamic acid
Gln	Glutamine
Gly	Glycine
h	Hour
His	Histidine
I	Intermediate
Ile	Isoleucine
l	Optical path length
Leu	Leucine
Lys	Lysine
Met	Methionine
M	Molar
mM	Milimolar
mol	Mole
mg	Miligram
min	Minute
ml	Mililiter
mm	Milimeter
MRW	Mean residue weight
MRE	Mean residue ellipticity
MRE_{222nm}	Mean residue ellipticity at 222 nm
MW	Molecular weight
nm	Nanometer
N	Native
n	Number
Phe	Phenylalanine

Pro	Proline
s	Second
Ser	Serine
SHSC	Simulated honey sugar cocktail
SD	Standard deviation
Thr	Threonine
T_m	Temperature required to achieve 50% thermal-denatured state
$T_{50\%}$	Temperature at 50% residual activity
Trp	Tryptophan
Tyr	Tyrosine
UV	Ultra violet
V	Volume
Val	Valine
w/v	Weight over volume
λ_{Em}	Emission wavelength
λ_{Ex}	Excitation wavelength
$\Delta\varepsilon$	Molar difference extinction coefficient
μM	Micromolar
Y	Variable parameter at given denaturant concentration
Y_D	Variable parameter for the denatured state
Y_N	Variable parameter for the native state
%	Percentage
Θ_{obs}	Observed ellipticity
~	Approximate
>	Greater than
<	Smaller than

CHAPTER 1

Introduction

1. INTRODUCTION

1.1. Protein stability

Proteins are important macromolecules in living organisms, which play crucial roles in essentially all biological processes. They function as biocatalysts, transport carriers, storage molecules and are involved in immune protection, movement, signal transduction, cell organization and reproduction of living organisms (Berg et al., 2002). Despite their biological importance, proteins have also been widely exploited in various industrial and pharmaceutical applications (Table 1.1) as biocatalysts, therapeutic agents and clinical diagnostic materials (Leader et al., 2008; Gurung et al., 2013). The ability of proteins to accelerate the rate and the specificity of the chemical reactions renders their broad usage as biocatalysts in various industrial processes such as dairy, textile, food and beverage processing as well as paper manufacturing industries (Gurung et al., 2013). Proteins are also widely used in pharmaceutical industries as therapeutic agents and diagnostic tools for some diseases (Leader et al., 2008; Ratnaparkhi et al., 2011). For example, several proteins such as insulin, luteinizing hormone-releasing hormone, vasopressin, adenosine deaminase, bevacizumab *etc.* are used to treat several diseases including hormone deficiency, diabetes insipidus, immunodeficiency and cancer (Leader et al., 2008; Ratnaparkhi et al., 2011). Furthermore, several enzymes have been used as therapeutic agents due to their specific use as oncolytics, anticoagulants, anti-inflammatory agents and as replacements for metabolic deficiency. Besides, proteins have also been used as the diagnostic agents for various diseases such as cancer, myocardial infarction and HIV infection (Leader et al., 2008).

Such a wide range functionality of proteins depends on the three-dimensional structure (native conformation), which is acquired through the folding of the fairly loose and disordered polypeptide chain(s) (Murphy, 1995). Attainment of the correct

Table 1.1. Industrial and pharmaceutical applications of proteins.*

Application		Examples
Industrial biocatalyst	Alcohol / beverage	Amylase, glucanase, protease, β-glucanase, amyloglucosidase, pullulanase and acetolactate decarboxylase
	Fruit drinks	Cellulase and pectinase
	Food processing	Amylase, protease, papain and trypsin
	Dairy	Rennin, lipase and lactase
	Detergent	Protease, amylase, lipase, cellulase and mannanase
	Textile	Amylase, pectinase, cellulase, catalase and protease
	Paper and pulp	Amylase, xylanase, cellulase, hemicellulase, ligninase and esterase
	Rubber	Catalase
	Oil and petroleum	Cellulase, ligninase and mannanase
	Biopolymer / plastic	Laccase, peroxidase, lipase and transglutaminase
	Pharmaceutical	Nitrile hydratase, D-amino acid oxidase, glutaric acid acylase, penicillin acylase, penicillin G acylase and ammonia lyase
	Molecular biology	Restriction enzymes, DNA ligase and polymerase

Table 1.1 Continued

Therapeutic agent	Antibiotic	Lysozyme and penicillin
	Antibiotic resistance	β-Lactamase
	Antiviral	Ribonuclease
	Blood clotting	Antithrombin III, clotting factor VIII, clotting factor IX, protein C concentrate, streptokinase and urokinase
	Cancer	Alemtuzumab, bevacizumab, cetuximab, panitumumab, rituximab
	Inflammation	Trypsin
	Leukemia	Asparaginase, gemtuzumab, glutaminase, ozogamicin and rasburicase
	Skin ulcers	Collagenase
	Gout	Uricase
	Hormone deficiency	Growth hormone, insulin, luteinizing hormone-releasing hormone, pramlintide acetate, mecasermin and somatotropin
	Metabolic enzyme deficiency	Alglucosidase-α, β-glucocerebrosidase, galsulphase, idursulphase and laronidase
	Pulmonary and gastrointestinal tract disorders	Amylase, α-1-proteinase inhibitor, lipase and protease
	Immunodeficiency	Adenosine deaminase and pooled immunoglobulins

Table 1.1 Continued

Therapeutic agent	Autoimmune disease	Anti-Rhesus immunoglobulin G
	Fertility	Human follicle-stimulating hormone and human chorionic gonadotropin and lutropin-α
	Diabetes insipidus	Vasopressin
Diagnostic agent	Infectious disease	Recombinant purified protein derivative
	Appendicitis	Technetium fanolesomab
	Cancer	Arcitumomab, capromab pendetide, nofetumomab, satumomab pendetide, thyroid stimulating hormone and thyrotropin
	Thrombosis	Apcitide
	HIV infection	HIV antigens
	Myocardial infarction	Creatine kinase, imciromab pentetate, myoglobin, troponin I and T

* Adapted from:
Leader et al. (2008)
Ratnaparkhi et al. (2011)
Gurung et al. (2013).

three-dimensional structure of a protein is governed by its linear amino acid sequence (Anfinsen, 1973) and its surrounding biological environment (Ellis & Hartl, 1999; Dobson, 2003). Several non-covalent forces such as hydrogen bonding, *van der waals* forces, electrostatic interactions and hydrophobic interactions as well as disulfide bridges (if present) are involved in the formation and maintenance of the native protein conformation (Anfinsen, 1973; Dill, 1990; Pace et al., 1996). However, the native protein conformation of many proteins is only marginally stable over their denatured counterparts as the free energy of unfolding of most proteins has been determined to be around – 10 kcal / mol (Pace, 1975; Dill, 1990; Taverna & Goldstein, 2002).

In view of the above, proteins progressively loose their functionality and native conformation under *in vitro* conditions such as extreme temperature, pH, pressure and in the presence of various destabilizing agents (salt, alkali, denaturants and surfactants), which are frequently met in different industrial applications. Therefore, stability of proteins used in these applications is a critical issue in industrial and pharmaceutical sectors. Hence, there is a need for further research to achieve greater storage and operational stability of proteins (Iyer & Ananthanarayan, 2008).

1.2. Protein stabilization approaches

For the past few decades, extensive research has been directed towards the enhancement of protein stability (Matthews et al., 1987; Matsumura et al., 1989; Fágáin, 1995; Bryan, 2000; Khajeh et al., 2001; Fágáin, 2003; Iyer & Ananthanarayan, 2008; Singh et al., 2011; Singh et al., 2013). Several strategies have been adopted to meet the above objective, which include protein engineering, chemical modifications and use of solvent additives.

1.2.1. Protein engineering

Protein engineering is a genetic approach to modify protein's amino acid sequence and thus its structure through substitution, deletion or insertion of amino acid residues (Singh et al., 2013). Different procedures such as site-directed mutagenesis, disulphide bond engineering and modification of ion binding sites have been employed to modify the protein structure in order to achieve greater protein stability (Fágáin, 1995). A few examples showing the effect of different protein engineering approaches on protein stability are given in Table 1.2.

Site-directed mutagenesis involves production of mutant proteins by altering the amino acid sequence in such a way so that the mutant proteins should have greater stability. For example, introduction of Pro residues or removal of Gly residues from the original amino acid sequence of bacteriophage T4 lysozyme have been shown to successfully increase its thermal stability (Matthews et al., 1987). Substitution of Gly residue at position 28 with Ser residue has also been found to increase thermal stability of *Bacillus pumilus* lipase (Bustos-Jaimes et al., 2010). Site-directed mutagenesis of maltogenic amylase involving substitution of Gly with Ala or Lys with Arg has also resulted in greater thermal stability of the enzyme (Ben Mabrouk et al., 2011). On the other hand, substitution of Lys-27, Arg-59 or His-102 with Ala though increased the thermal stability of barnase but produced a large decrease in its enzyme activity (Meiering et al., 1992).

Introduction of disulphide bonds in the protein has also been used as an approach to stabilize the protein molecule (Matsumura et al., 1989; Fágáin, 1995; Le et al., 2012). In this approach, one or several Cys residues are usually added to the protein's original amino acid sequence either by insertion or substitution, which may lead to the formation of disulphide bonds in the protein, thus affecting its stability. However, addition of the

Table 1.2. Effect of different protein engineering approaches on protein stability.

Stabilizing approach	Protein	Amino acid change	Effect on stability	Reference
Site-directed mutagenesis	Apomyoglobin	Cys-110 → Leu	C_m ↑ (0.9 pH unit)	Hughson and Baldwin (1989)
	β-Agarase AgaA	Ser-63 → Lys	Activity at 45°C ↑ (125%)	Lee et al. (2011)
	β-Glucosidase	Pro-172 → Leu Phe-250 → Ala	T_m ↑ (6.7°C)	Lee et al. (2012)
	Cholesterol oxidase	Gln-153 → Glu Phe-128 → Leu	Activity at 50°C ↑ (47%)	Sun et al. (2011)
	Endo-1,4-β-xylanase II	Asn-97 → Arg Phe-93 → Trp His-144 → Lys	$T_{50\%}$ ↑ (4–5°C)	Fenel et al. (2006)
	Endoglucanase	Tyr-95 → Phe	k_{cat} ↑ (4.4 fold)	Srikrishnan et al. (2012)
	Formate dehydrogenase	Cys-262 → Val	T_m ↓ (8°C)	Slusarczyk et al. (2000)
	Isopropylmalate dehydrogenase	Ala-172 → Asp	T_m ↓ (3°C)	Akanuma et al. (1997)
	Lipase	Gly-28 → Ser	Half-life ↑ (25 fold)	Bustos-Jaimes et al. (2010)
		Ala-132 → Asp	Half-life ↑ (173 fold)	Bustos-Jaimes et al. (2010)

Table 1.2 Continued

Site-directed mutagenesis	Lipase	Asn-166 → Tyr Ala-132 → Asp	C_m ↑ (1 M urea)	Acharya et al. (2004)
		Asn-166 → Tyr Ala-132 → Asp Leu-114 → Pro	Half-life ↑ (270 fold)	Acharya et al. (2004)
	Superoxide dismutase	Cys-95 → Ala	Thermostability ↑ (2 fold)	Kumar et al. (2012)
	Xylanase	Thr-25 → Arg Thr-65 → Arg Ser-67 → Arg Ser-184 → Arg	Half-life ↑ (17 fold)	Sriprang et al. (2006)
	Xylose isomerase	Gln-58 → Pro	Half-life ↑ (43%)	Sriprapundh et al. (2000)
	T4 Lysozyme	Arg-96 → His	T_m ↓ (7°C)	Wetzel et al. (1988)
		Gly-77 → Ala	T_m ↑ (0.9°C)	Matthews et al. (1987)
		Ala-82 → Pro	T_m ↑ (2.1°C)	Matthews et al. (1987)
		Asn-144 → Glu	T_m ↑ (1.5°C)	Sun et al. (1991)
		Ser-38 → Asp	T_m ↑ (1.6°C)	Nicholson et al. (1988)
		Ser-117 → Val	T_m ↑ (5.1°C)	Shoichet et al. (1995)

Table 1.2. Continued

Disulphide bond engineering	Acetylcholinesterase	Ile-327 → Cys Asp-375 → Cys	Activity at 50°C ↑ (170 fold) Activity in 4 M urea ↑ (12 fold)	Siadat et al. (2006)
	Barnase	Ala-43 → Cys Ser-80 → Cys	C_m ↑ (1.2 M urea)	Clarke and Fersht (1993)
		Ser-85 → Cys His-102 → Cys	C_m ↑ (1 M GdnHCl)	Clarke and Fersht (1993)
	Endo-1,4-β-xylanase II	Thr-2 → Cys Thr-28 → Cys	$T_{50\%}$ ↑ (~15°C)	Fenel et al. (2004)
	Lipase B	Ala-162 → Cys Lys-308 → Cys	$T_{50\%}$ ↑ (8.5°C)	Le et al. (2012)
	Plastocyanin	Ile-21 → Cys Glu-25 → Cys	T_m ↓ (4.7°C)	Guzzi et al. (2004)
	Ribonuclease	Asn-44 → Cys	T_m ↑ (11.8°C)	Kanaya et al. (1991)
	Subtilisin	Asp-41 → Cys Gly-80 → Cys	Half-life ↓ (5 fold)	Mitchinson and Wells (1989)
	T4 lysozyme	Ile-3 → Cys	T_m ↑ (3°C)	Wetzel et al. (1988)
		Thr-3 → Cys	T_m ↑ (11°C)	Jacobson et al. (1992)
		Ile-9 → Cys Leu-164 → Cys	T_m ↑ (6.5°C)	Matsumura et al. (1989)

Cys residues should be targeted at an appropriate distance in the three-dimensional structure of a protein to allow proper disulphide bond pairing (Fágáin, 1995). Using this strategy, more stable enzyme such as lysozyme, subtitisin and lipase B have been produced (Pantoliano et al., 1988; Matsumura et al., 1989; Bryan, 2000; Le et al., 2012). The disulphide bond engineering may also lead to protein destabilization, (Dombkowski et al., 2014) as the melting temperature of a poplar plastocyanin has been shown to decrease by about 4°C compared to the wild type protein (Guzzi et al., 2004).

Modification of the ion binding sites in proteins has been employed to engineer the low affinity ion binding sites into high affinity ion binding sites through genetic modifications of the desired amino acid residues (Bryan, 2000; Iyer & Ananthanarayan, 2008). For instance, increasing the affinity of one of the calcium binding sites in subtilisin has been found to increase its thermal stability (Bryan, 2000). Modification of the calcium binding site in *Bacillus licheniformis* α-amylase through substitution of Ala-181 with Thr has been shown to stabilize the enzyme against thermal denaturation (Bisgaard-Frantzen et al., 1999; Nielsen & Borchert, 2000).

In general, protein engineering is purely based on a hit and trial method, producing mutant proteins of both higher and lower stability (Marshall et al., 2003). Furthermore, it may also produce adverse effects with respect to the protein function / activity as these mutations are random in nature (Brannigan & Wilkinson, 2002). For example, engineered mutants may have greater stability than the wild type but without any activity or poor activity. Lack of a theory for structure design and a general approach for sequence design are some of the obstacles in limiting the applications of protein engineering in protein stabilization (Leisola & Turunen, 2007).

1.2.2. Chemical modification

Chemical modification of proteins has remained a useful approach for protein stabilization, despite being overshadowed in recent years by protein engineering (Fágáin, 2003). Protein stabilization through chemical modification can be achieved using several methods, which include modification of the surface groups, intra- or intermolecular cross-linking and covalent coupling with polymers such as polyethylene glycol (PEG) or polysaccharides (Lundblad & Noyes, 1984; Imoto & Yamada, 1989; Means & Feeney, 1990). Table 1.3 shows a few examples of chemical modification of proteins and its effect on protein stability. Generally, chemical modification of a protein is restricted to the side chains of the amino acid residues and involves oxidation, reduction, nucleophilic and electrophilic substitutions, racemization, β-elimination and other reactions with chemical reagents (Feeney et al., 1982). This is achievable as many amino acid residues of a protein possess an active functional group, accessible for chemical modification. According to Means and Feeney (1990), at least nine of the twenty different amino acids, namely, Cys, Lys, Asp, Glu, Arg, His, Trp, Tyr and Met contain a side chain that can be chemically modified by specific reagents under mild conditions and the modified protein may show greater stability. For example, modification of the Lys side chains of α-amylase from mesophilic *B. amyloliquefaciens* and thermophilic *B. licheniformis* with citraconic anhydride has yielded the enzymes with higher activity than the wild type at 70°C and 80°C (Khajeh et al., 2001). Modification of the surface Lys residues of α-chymotrypsin with cyclic anhydrides of aromatic carboxylic acids has also shown increased stability of the enzyme. Similarly, stability of trypsin can be increased by converting the surface Tyr residues to aminotyrosines (Mozhaev et al., 1988).

Formation of the cross-link within the protein molecule or between the protein molecules with an artificial cross-linker has been demonstrated as an effective approach to increasing protein stability (Wong & Wong, 1992). For example, treatment of

Table 1.3. Effect of different chemical modification approaches on protein stability.

Stabilizing approach	Protein	Modification	Effect on stability	Reference
Cross-linking	Alkaline phosphatase	Poly(phosphorothioates) cross-link	Activity at 45°C ↑ (35%)	Bieniarz et al. (1998)
	Creatine kinase	Dimethylsuberimidate	Shelf-life at 4°C ↑	Sheehan et al. (1990)
	Glucose oxidase	Poly(phosphorothioates) cross-link	Stability at 37°C ↑ (8 fold)	Bieniarz et al. (1998)
	Horseradish peroxidase	Suberic acid bis (N-hydroxy-succinimide ester)	Half-life ↑ (6–23 fold)	Ryan et al. (1994)
		Ethylene glycol-bis(succinic acid N-hydroxysuccinimide ester)	Half-life ↑ (6–23 fold)	Ryan et al. (1994)
	Lysozyme	Lys-2 – His-15 cross-link	T_m ↑ (14°C)	Ueda et al. (2000)
	Ribonuclease A	Malonaldehyde	Enzyme inactivation	Chio and Tappel (1969)
Attachment to polymer	Invertase	Chitosan	T_m ↑ (10°C)	Gómez and Villalonga (2000)
		Pectin	T_m ↑ (7°C)	Gómez and Villalonga (2000)

Table 1.3 Continued

Attachment to polymer	Lysozyme		Glucose stearic acid monoester	T_m ↑ (2°C)	Takahashi et al. (2000)
	Ribonuclease A		Polyunsaturated fatty acid	Enzyme inactivation	Chio and Tappel (1969)
	Soy protein		Glutaraldehyde	Foam stability ↑ (3 fold)	Park et al. (2000)
	Trypsin		PEG5000	Half-life ↑ (3.8 fold)	Treetharnmathurot et al. (2008)
Surface group modification	α-Amylase		Lys - Citraconic anhydride	Activity at 70°C ↑	Khajeh et al. (2001)
	α-Chymotrypsin		Lys - Aromatic carboxylic acids	Thermal stability ↑ (3 fold)	Mozhaev et al. (1988)
	Lysozyme		Trp-62 → N-formylkynurenine	T_m ↓ (0.3°C)	Okajima et al. (1990)
			Trp-62 → Kynurenine	T_m ↓ (3.1°C)	Okajima et al. (1990)
			Succinylation	T_m ↓ (16°C)	van der Veen et al. (2005)
			Succinylation	C_m ↓ (1.6 M GdnHCl)	Ong et al. (2009)
	Ribonuclease T1		Trp-59 → N-formylkynurenine	T_m ↓ (23.4°C)	Okajima et al. (1990)
			Trp-59 → Kynurenine	T_m ↓ 14.8°C	Okajima et al. (1990)
	Trypsin		Tyr → Aminotyrosines	Thermal stability ↑ (100%)	Mozhaev et al. (1988)

horseradish peroxidase with suberic acid bis(N-hydroxysuccinimide ester) and ethylene glycol-bis(succinic acid N-hydroxysuccinimide ester) has induced greater thermal stability of the enzyme (Ryan et al., 1994). Chemical cross-linking of beef heart creatinine kinase with dimethylsuberimidate produced a dimeric enzyme with higher thermal stability despite showing some loss in its activity. However, the dimeric enzyme was found resistant to activity loss in the presence of chemical denaturants such as guanidine hydrochloride (GdnHCl) and urea (Sheehan et al., 1990).

Increase in protein stability can also be accomplished by attaching a soluble polymer to the target protein. Many enzymes have been stabilized using this method. Thermal stability of trypsin has been increased with the attachment of PEG to the enzyme (Mozhaev et al., 1988; Treetharnmathurot et al., 2008). Furthermore, PEG-treated trypsin has been found chemically resistant against denaturation induced by sodium dodecyl sulfate (Gaertner & Puigserver, 1992). Attachment of naturally occurring carbohydrates such as chitosan and pectin to yeast invertase yielded a thermostable enzyme, showing an increase in the melting temperature by 10°C and 7°C for chitosan and pectin, respectively. Furthermore, half-life of the protein at 65°C has been extended from 5 minutes to 2 days for pectin-modified invertase compared to 5 hours for chitosan-modified invertase (Gómez et al., 2000; Gómez & Villalonga, 2000).

Although chemical modification of proteins results in increased stability in many cases, unexpected side effects such as activity loss or altered pH optimum may also arise. Since a few side chains of the amino acids are essential for the function as well as to maintain the three-dimensional structure of a protein, modification of these side chains may lead to protein inactivation (Feeney et al., 1982; Means & Feeney, 1990). For example, cross-linking of two *Aspergillus niger* glucoamylase molecules together yielded

an oligomerized glucoamylase with lower thermal stability than the native enzyme and loss of its enzymatic activity (Sasvari & Asboth, 1999).

1.2.3. Solvent additives

Various organisms adapt to life-threatening environmental conditions including extremes of temperature and pH, cellular dehydration, desiccation and high extracellular salt by accumulating small organic molecules known as osmolytes (Yancey et al., 1982; Yancey, 2003; 2004). The idea of osmolyte-induced cellular protein stabilization has been exploited in various applications to maintain protein stability (Singh et al., 2011). Osmolytes have been grouped into three major classes on the basis their chemical structure. These groups are polyols, free amino acids and their derivatives as well as methylammonium salts. A list of a number of osmolytes categorized under these classes has been given in Table 1.4.

Based on their effects on the protein's functional activity, osmolytes have been classified as counteracting and compatible osmolytes (Yancey, 2004). Counteracting osmolytes alter the protein functions and belong to the methylammonium class of osmolytes (Taravati et al., 2007; Singh et al., 2011). On the other hand, compatible osmolytes do not affect protein's function and consist of nitrogenous compounds (*e.g.* proline, glutamate, ectoine, glycine *etc.*), polyols (*e.g.* glycerol) and carbohydrates (sucrose, fructose, trehalose *etc.*) (Yancey, 2004). Compatibility of these osmolytes with protein functions may be embarked due to the absence of any interaction between osmolytes and proteins, substrate or co-factors. Hence, macromolecular-solvent interactions would remain unperturbed in the presence of these osmolytes (Singh et al., 2011).

Osmolytes such as amino acids and sugars has been proven compatible with protein structure as their presence in the protein solution does not alter the native protein

Table 1.4. Classification of naturally occurring osmolytes used by organisms under various stress conditions.*

Class of osmolyte	Example of osmolyte
Polyols and sugars	Glycerol, sorbitol, manitol, pinitol, inositol, glucose, fructose, sucrose, raffinose, stachyose, trehalose, maltose and mammosylglycerate
Amino acids and derivatives	Proline, phenylalanine, valine, leucine, isoleucine, serine, glutamine, arginine, lysine, glycine, aspartate, β-alanine, ectonine, taurine, hypotaurine and thiotaurine
Methylammonium salts	Glycine betaine, L-carnitine, choline, creatine, trimethylamine N-oxide, sarcosine, N-methyltaurine and glycerophosphorylcholine

* Adapted from Singh et al. (2011)

conformation. The far-UV and the near-UV circular dichroism as well as near-UV absorption spectra of many proteins have been found identical within experimental error both in the absence and the presence of these osmolytes, suggesting that the secondary and tertiary structures of these proteins remain unchanged even in the presence of osmolytes (Lee & Timasheff, 1981; Kim et al., 2003; Haque et al., 2005; Poddar et al., 2008).

In general, osmolytes (solvent additives) do not interact directly with the protein rather they alter the solvent properties (viscosity and surface tension) and thus the protein-solvent interactions (Schein, 1990; Timasheff, 1993). The protein stabilizing effect of these osmolytes has been well established, as reflected from the increase in the mid-point of denaturation induced by heat or chemical agents, in the presence of osmolytes (Lee & Timasheff, 1981; Allison et al., 1996; Miroliaei & Nemat-Gorgani, 2001; Kaushik & Bhat, 2003; Chebotareva et al., 2004; Saadati & Bordbar, 2008). Table 1.5 shows a few examples of proteins, which have been stabilized by different osmolytes. More specifically, sugars have been shown to increase protein stability especially, thermal stability (Baier & McClements, 2001; Yancey, 2005; Gheibi et al., 2006; Miroliaei et al., 2007; Bellavia et al., 2009) under a variety of experimental conditions such as dehydration, variable pH, freezing, high salinity or in the presence of chemical denaturants (Yancey, 2005; Singh et al., 2011). For example, addition of 0.5 M of trehalose to a lipolytic enzyme, cutinase has increased the mid-point of the thermal denaturation by 4°C and 2.6°C at pH 9.2 and 10.5, respectively (Baptista et al., 2000). The T_m of lysozyme has also been found to increase by 18°C upon addition of 2.0 M trehalose (Kaushik & Bhat, 2003).

Use of different solvent additives such as sugars can enhance the protein stability to the extent, achievable with chemical or genetic modifications. For instance,

Table 1.5. Effect of osmolytes on protein stability.

Protein	Osmolyte	Effect on stability	Reference
Alcohol dehydrogenase	0.5 M Trehalose	Activity at 50°C ↑ (20%)	Ramos et al. (1997)
α-Chymotrypsin	2 M Trehalose	T_m in 4 M urea ↑ (22°C)	Kumar et al. (2010)
β-Lactoglobulin	10% (w/v) Trehalose	GdnHCl stability ↑ (11%)	Saadati and Bordbar (2008)
	10% (w/v) Sucrose	GdnHCl stability ↑ (7%)	
	10% (w/v) Sorbitol	GdnHCl stability ↑ (4%)	
	10% (w/v) Mannitol	GdnHCl stability ↑ (2%)	
BSA	2 M Arginine	Aggregation temperature delayed (16°C)	Arakawa et al. (2007)
	PEG8000	T_m ↑ (1.2°C)	Farruggia et al. (1999)
Creatine kinase	30% (w/v) Glycerol	T_m ↑ (3.3°C)	Meng et al. (2004)

Table 1.5. Continued

Cytochrome c	1 M Glycine	T_m ↑ (3.3°C)	Taneja and Ahmad (1994)
	0.7 M Alanine	T_m ↑ (6.5°C)	
	1 M Serine	T_m ↑ (3.5°C)	
	0.3 M Valine	T_m ↑ (1.8°C)	
	1 M Proline	T_m ↑ (4.3°C)	
	1.5 M Trehalose	T_m ↑ (8.5°C)	Kaushik and Bhat (2003)
Ferricytochrome c	0.6 M Trehalose	Mid-point ↑ (0.9 M urea)	Zhang et al. (2013)
Hexokinase A	1.5 M Glycerol	T_m ↑ (3.9°C)	Tiwari and Bhat (2006)
	1.5 M Erythritol	T_m ↑ (7.2°C)	
	1.5 M Xylitol	T_m ↑ (9.7°C)	
	1.5 M Sorbitol	T_m ↑ (13.4°C)	
Hexokinase B	1.5 M Glucose	T_m ↑ (15.5°C)	Catanzano et al. (1997)

Table 1.5. Continued

Lactate dehydrogenase	0.5 M Trehalose	Activity at 50°C ↑ (20%)	Ramos et al. (1997)
Lysozyme	2 M Trehalose	T_m ↑ (18°C)	Kaushik and Bhat (2003)
	40% (w/v) Sorbitol	T_m ↑ (7.5°C)	Haque et al. (2005)
	40% (w/v) Glycerol	T_m ↑ (3°C)	
	1 M Xylitol	T_m ↑ (3°C)	
	1 M Adonitol	T_m ↑ (2°C)	
	1 M Mannitol	T_m ↑ (2.5°C)	
Papain	30% (w/v) Sucrose	T_m ↑ (4°C)	Sathish et al. (2007)
	30% (w/v) Xylose	T_m ↑ (5°C)	
Ribonuclease A	5 M Betaine	T_m ↑ (8.8°C)	Knapp et al. (1999)
	3 M β-Hydroxyectoine	T_m ↑ (12°C)	
	2 M Trehalose	T_m ↑ (13°C)	Kaushik and Bhat (2003)

Table 1.5. Continued

Ribonuclease A	40% (w/v) Sorbitol	T_m ↑ (9.1°C)	Haque et al. (2005)
	1 M Adonitol	T_m ↑ (1.3°C)	
	40% (w/v) Glycerol	T_m ↑ (2.2°C)	
	1 M Xylitol	T_m ↑ (2°C)	Poddar et al. (2008)
	1 M Mannitol	T_m ↑ (1.1°C)	
	2 M Glucose	T_m ↑ (8.6°C)	
	1 M Galactose	T_m ↑ (3.8°C)	
	1.5 M Sucrose	T_m ↑ (9.4°C)	
	0.4 M Raffinose	T_m ↑ (2.9°C)	
	0.75 M Stachyose	T_m ↑ (6.8°C)	
Trypsin inhibitor	1.5 M Trehalose	T_m ↑ (15.5°C)	Kaushik and Bhat (2003)

trehalose-induced lysozyme stabilization showed an increase in its T_m by 18°C (Kaushik & Bhat, 2003), which was comparable to that obtained with disulphide bond engineering (11°C) (Jacobson et al., 1992) or chemical cross-linking (14°C) (Ueda et al., 2000). Such protein stabilizing effect offered by osmolytes is advantageous over to protein engineering and chemical modification approaches in being generalized rather than being specific for a single protein (Fágáin, 1995). In other words, a stabilizing formulation of osmolytes can be designed for a large number of proteins (Fágáin, 1995). On the other hand, protein engineering and chemical modification approaches are based on a hit and trial method and require a detailed theoretical knowledge on the structure and function of the target protein (Leisola & Turunen, 2007). This is important as in some cases, these strategies have produced destabilizing effect rather than stabilizing the proteins. For example, a site-directed mutant of lysozyme has been found thermolabile with a decrease in its T_m by 7°C (Wetzel et al., 1988) and succinylation of lysozyme was found to lower its T_m by about 16°C (van der Veen et al., 2005). In view of the above, use of solvent additives seems to be more promising over to other strategies for protein stabilization.

The protein stabilizing effect of osmolyte mixture has been shown to be additive and synergistic, where greater protein stabilization is achieved with a mixture of osmolytes compared to that observed in the presence of single osmolyte (Poddar et al., 2008; Poddar et al., 2010; Singh et al., 2011). Nature has created such a system of osmolyte mixture where different osmolytes seem to cooperate each other to protect cellular functions against adverse environmental conditions. Therefore, use of naturally occurring osmolyte mixture seems to be a better choice towards increasing protein stability against different denaturing conditions.

1.3. Honey

U.S. Federal Food and Drug Act 1906 has defined honey as "The nectar and saccharine exudation of plants, gathered, modified and stored in the comb by honey bees (*Apis mellifera* and *Apis dorsata*); is levorotatory; contains not more than 25% water, not more than 0.25% ash and not more than 8% sucrose". Honey is an important food and natural sweetener for *Homo sapiens* from early civilization (Crane, 1983). Honey is a mixture of compounds with high-carbohydrate content and rich diversity of minor constituents such as proteins, amino acids, minerals, vitamins and polyphenolic compounds, which offer nutritional benefits to human. It is used as the medicine or special tonic rather than as an everyday food in many countries. The anti-microbial, anti-bacterial and antioxidant properties of honey have allowed its use in the treatment of some gastrointestinal, respiratory and ophthalmic disorders. Furthermore, honey is also used as a topical agent in wound healing treatment due to its wound healing properties (Bogdanov et al., 2008).

Major component of honey is carbohydrate, which constitutes about 95−97% of honey dry weight (White & Kushnir, 1967). The sugar composition of honey shows fructose (~51.6%) and glucose (~46.6%) as the major sugar components (Table 1.6), which are the hydrolyzed products of sucrose (Rybak-Chmielewska & Szczęsna, 1995). Various disaccharides such as sucrose, maltose, turanose and trehalose are also present in honey in small amounts. Whereas trisaccharides such as erlose, melezitose and panose have been characterized in honey from different origin (Doner, 1977), tetra- and pentasaccharides have also been detected in trace amount in honey (Bogdanov et al., 2008).

In addition of sugars, honey also contains small amount of proteins (~0.5%), which include enzymes and free amino acids (Bogdanov et al., 2008). The most

Table 1.6. Sugar composition in honey and simulated honey sugar cocktail (SHSC).

Sugar	Percentage content	
	Honey [a] (w/v)	60% (w/v) SHSC [b] (w/v)
Fructose	51.60	30.96
Glucose	46.59	27.95
Sucrose	0.27	0.16
Maltose and trehalose (1:1)	1.26	0.38
Melibiose and other sugars	0.28	–

[a] Adapted from Rybak-Chmielewska and Szczęsna (1995).
[b] Weight of sugar in grams per 100 ml of 60 mM sodium phosphate buffer, pH 7.4 / 7.0.

significant enzyme present in honey is α-glucosidase (invertase or sucrase), which is responsible for the conversion of sucrose into fructose and glucose. This enzyme also catalyzes the formation of several higher sugars such as maltose, turanose, trehalose and erlose via transglucosylation reactions (Doner, 2003). Another enzyme, glucose oxidase has also been characterized in various honey samples, which contributes to the anti-bacterial property of honey via production of hydrogen peroxide and gluconic acid (Doner, 2003). Several other enzymes such as diastase (amylase), acid phosphatase and catalase have also been characterized in honey (White, 1978). About 20 different non-enzymatic proteins (globulin, albumin *etc*.) have been found in honey from different origins. Honey is also a rich source of all physiological amino acids in which proline accounts for about half of the total amino acid content (Doner, 2003).

Several minerals also exist in honey, though in small quantities (0.1−0.3%) (White, 1975; Bogdanov et al., 2007). The most abundant mineral element in honey is potassium, contributing about one third to the total mineral content. Other major mineral elements of honey are sodium, calcium and magnesium, mixed with a variety of different trace elements such as iron, manganese, copper, chlorine, phosphorus, sulphur and silicon (Doner, 2003). Different types of vitamins (riboflavin, pantothenic acid, niacin, thiamine, pyridoxine, phyllochinon and ascorbic acid) are also observed at a measureable amount, although the vitamin content is relatively low, being 5 mg / 100 gm of honey (White, 1978).

Polyphenolic compounds such as flavonoids (*e.g.* quercetin, luteolin, kaempferol, apigenin, chrysin, galangin), phenolic acids and their derivatives constitute another important class of compounds (Tomás-Barberán et al., 2001), being present as 500 mg / kg of honey (Al-Mamary et al., 2002; Gheldof & Engeseth, 2002). Anti-oxidant property of honey can be attributed to the presence of these flavonoids.

Water contributes less than 18.6% to honey total weight and any increase in the percentage content of water indicates the fermentation process (Doner, 2003). Honey also contains several acids such as formic, acetic, butyric, lactic and gluconic acids, whose flavors are masked by the presence of high sugar content. These acids constitute ~0.5% of honey weight and render a low pH (3.99) to honey, which can be accounted for its excellent stability (Doner, 2003).

Since honey contains high sugar content and other osmolyte (amino acids), it can be used as a solvent additive for protein stabilization. Hence, both simulated honey sugar cocktail and honey were selected as the subject for protein stabilization studies on different model proteins against chemical and thermal denaturations.

1.4. Model proteins

Bovine serum albumin, ovalbumin and lysozyme have been extensively used as the model proteins in various protein structure-function studies due to their easy availability in pure form, lower cost, single polypeptide nature and well known three-dimensional structures.

1.4.1. Bovine serum albumin

The word ‘albumin’ derives from the Latin word *Albus* (white), which refers to the colour of the part surrounding the egg yolk when cooked. The ending ‘–in’ refers to the specific protein from blood plasma (Peters, 1996). The origin of the word ‘albumin’ dates back to the recognition of the albumen of an egg, which appears white after coagulation and is mostly protein in nature. Being the major component of the blood with a concentration of 5 g / 100 ml, serum albumin is considered as the most abundant protein in mammalian blood circulation (Carter & Ho, 1994).

The synthesis of mammalian albumin takes place in the liver (Peters & Anfinsen, 1950) at a rate of 0.7 mg / g liver tissue per hour (Peters, 1985). Its synthesis is highly dependent on the dietary supply of amino acids (Kaysen et al., 1989). The average half-life of albumin is about 19 days after which it is degraded and replaced by the hepatic synthesis (Waldmann, 1977). The plasma albumin concentration is being maintained through transcriptional regulation of the albumin gene by several anabolic hormones, insulin and somatotropin (Hutson et al., 1987).

1.4.1.1. Physicochemical properties

Some physicochemical properties of bovine serum albumin (BSA) are summarized in Table 1.7. The molecular weight obtained from hydrodynamic data is around 66,700 (Squire et al., 1968) for defatted monomeric BSA, which is found to be slightly higher than the molecular weight (66,267), calculated from its amino acid composition (Peters, 1985). Hydrodynamically, BSA shows a sedimentation coefficient ($S^{o}_{20,\ w}$) of 4.5×10^{-13} s (Squire et al., 1968), diffusion coefficient ($D^{o}_{20,\ w}$) of 5.9×10^{-7} cm^2 / s (Wagner & Scheraga, 1956) and a partial specific volume of 0.733 cm^3 / g (Hunter, 1966). The intrinsic viscosity of BSA has been determined as 4.1 cc / g (McMillan, 1974). The BSA molecule is considered as a prolate ellipsoid with dimensions of 41.6×140.9 Å for the major and minor exes, which gives a value of the axial ratio as 3.4:1 (Wright & Thompson, 1975). Defatted BSA has an isoelectric point of 4.7 (Longsworth & Jacobsen, 1949), suggesting acidic nature of the protein. The protein has been classified as a helical protein due to the predominance of the α-helix (55%) compared to 16% β-pleated sheet (Reed et al., 1975; Foster, 1977).

1.4.1.2. Amino acid composition

Albumin is a nonglycoprotein with a carbohydrate content lesser than 0.05% (w/w) (Cohn et al., 1947). Table 1.8 shows the amino acid composition of BSA. BSA is

Table 1.7. Physicochemical properties of BSA.

Property	Value	Reference
Molecular weight		
– Amino acid composition	66,267	Peters (1985)
– Hydrodynamic data	66,700	Squire et al. (1968)
Sedimentation coefficient, $S^{o}_{20,w}$ (s)	4.5×10^{-13}	Squire et al. (1968)
Diffusion coefficient, $D^{o}_{20,w}$ (cm^2 / s)	5.9×10^{-7}	Wagner and Scheraga (1956)
Partial specific volume (cm^3 / g)	0.733	Hunter (1966)
Intrinsic viscosity, [η] (cc / g)	4.1	McMillan (1974)
Overall dimension (Å)	41.6 × 140.9	Wright and Thompson (1975)
Axial ratio	3.4:1	Wright and Thompson (1975)
Isoelectric point	4.7	Longsworth and Jacobsen (1949)
Isoionic point	5.15	Foster (1960)
$E^{1\%}_{1\,cm}$	6.67	Janatova et al. (1968)
Secondary structures		
– α- helix (%)	55	Foster (1977)
– β-pleated sheet (%)	16	Reed et al. (1975)

Table 1.8. Amino acid composition of BSA.*

Amino acid	Abbreviation	Number of residues
Alanine	Ala	46
Arginine	Arg	23
Asparagine	Asn	13
Aspartic acid	Asp	41
Cysteine	Cys	35
Glutamic acid	Glu	59
Glutamine	Gln	20
Glycine	Gly	16
Histidine	His	17
Isoleucine	Ile	14
Leucine	Leu	61
Lysine	Lys	59
Methionine	Met	4
Phenylalanine	Phe	27
Proline	Pro	28
Serine	Ser	28
Threonine	Thr	34
Tryptophan	Trp	2
Tyrosine	Tyr	19
Valine	Val	36
Total		582

* Adapted from Peters (1985)

characterized by the low content of Trp (2) and Met (4) residues. On the other hand, it has high content of Cys (35) and other charged residues such as Asp (41), Glu (59), Arg (23) and Lys (59) residues. The odd number of Cys residues indicates the presence of free thiol group. The overall charge of BSA has been determined as –18 based on the calculation from the amino acid composition.

1.4.1.3. Primary structure

The complete amino acid sequence of BSA is shown on Figure 1.1. BSA contains a total of 582 residues in a single polypeptide chain. Thirty five Cys residues form 17 disulphide bonds while leaving one Cys residue free at the position 34. The arrangement of disulphide bonds leads to a unique organization of the albumin molecule into 9 loops. These loops are repeated in a triplet fashion of large-small-large loops and are further grouped into 3 homologous domains (I, II and III) of three loops each (Figure 1.1). All but the first of the nine loops are double loops, based upon a repeating Cys–Cys sequence, which occurs eight times in the chain (Peters, 1985). The shorter loops are formed by mostly negatively charged residues and lack the presence of aromatic amino acids. Domains I, II, and III are comprised of residues 1–183, 184–376 and 377–582, respectively (Brown, 1977; Saber et al., 1977).

The Trp residues in BSA are located at positions 134 in the loop 3 of domain I and 212 in the loop 4 of domain II. The different amino acid residues in BSA molecule are not evenly distributed throughout the albumin structure leading to the accumulation of certain amino acid residues at defined positions. For example, Gly residues are more confined in the amino half of the albumin, whereas Thr residues are more populated in the carboxyl half of the albumin molecule. The Asn and Gln residues are more frequently found at both ends rather than in the middle of the chain. The Tyr residues are confined

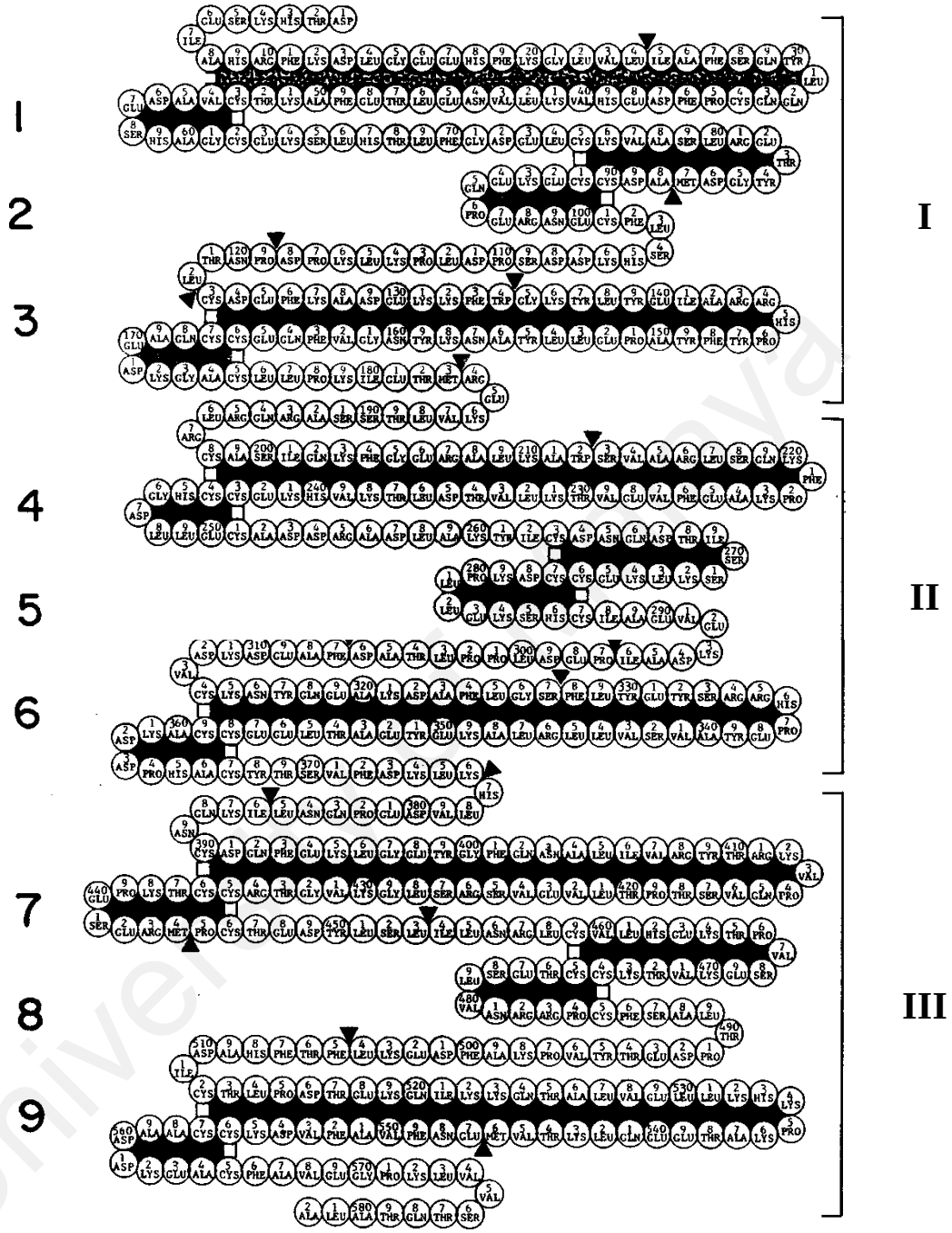

Figure 1.1. Amino acid sequence and disulphide bond pattern of BSA. The nine loops are labelled on the left while the three domains are labelled on the right. (Adapted from Peters, 1985)

in the loops 3 and 6 of BSA (Peters, 1985). In view of the above, the charge distribution of BSA molecule is not even along the length of the molecule, due to which domains I, II and III possess different net charge. At pH 7.0, the net charge on domains I, II and III is –10, –8 and 0, respectively, thus making the amino terminal of BSA highly negatively charged whereas the carboxyl terminal being rather neutral (Peters, 1985).

1.4.1.4. Three-dimensional structure

The three-dimensional structure of serum albumin has been determined by x-ray crystallography (Carter & Ho, 1994). The three homologous domains (I, II and III) form a heart-shaped structure. Each of the domains in BSA is subdivided into subdomains A and B (Figure 1.2), which share the same structural motifs (Huang et al., 2004). These subdomains are predominantly helical structures (Figure 1.2) and are cross-linked by several disulphide bonds (Carter & Ho, 1994). About 76% of the total amino acid residues of serum albumin are involved in the formation of 28 α-helical segments (Carter & Ho, 1994). There are 10 principal helical structures (h1–h10) present in each domain. The subdomain A is comprised of h1–h6 helices while h7–h10 helices form subdomain B. The hydrophobic helix packing interactions among h2, h3 and h8 are responsible to assemble subdomains A and B together. Domains I and II are connected by a helical extension formed between h10 of domain I and h1 of domain II while the helical extension between h10 of domain II and h1 of domain III links domains II and III. Due to the extension of these helices, the total number of helical segments is therefore reduced to 28 (Peters, 1985).

1.4.1.5. Denaturation

Denaturation behavior of serum albumin has been extensively studied under different experimental conditions. Although serum albumin possesses a multidomain structure, its denaturation behavior has been found reversible as it is able to recover from

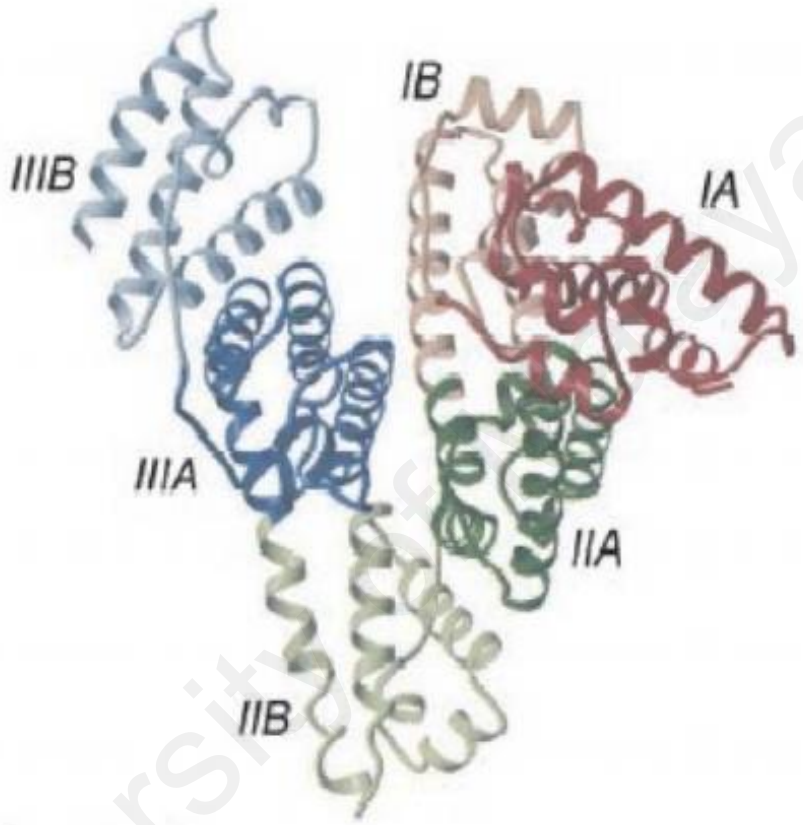

Figure 1.2. Diagram showing domain and subdomain structure of BSA based on crystallographic data. The heart-shaped BSA molecule consists of three homologous helical domains (I, II and III), which are comprised of two subdomains (A and B). (Adapted from Huang et al., 2004)

structural changes induced by many variables except heat denaturation in strong alkali (Peters, 1996). Albumin molecule shows temporary loss of its α-helical structure in the presence of 8 M urea or 6 M GdnHCl at 44°C (Tanford, 1968). However, prolonged or repeated heating of albumin may promote dimerization, unfolding and aggregation thus leading to irreversible denaturation (Peters, 1985). Alterations in the disulphide-bonded loops and domains have been suggested to contribute to the irreversible denaturation of serum albumin (Aoki et al., 1973; Brandt & Andersson, 1976).

i. Chemical denaturation: The most commonly used chemical denaturants are urea and GdnHCl. These denaturants weaken the hydrophobic as well as polar interactions when present at a high concentration (Dill & Shortle, 1991). Urea / GdnHCl denaturation of albumin has been extensively studied by various groups using different techniques (Khan et al., 1987; Ahmad & Qasim, 1995; Farruggia & Pico, 1999; Muzammil et al., 2000a; Tayyab et al., 2000; Santra et al., 2004; Leggio et al., 2009; Galantini et al., 2010). Whereas little changes in the albumin molecule have occurred below 2 M urea (Qasim & Salahuddin, 1978; Khan et al., 1987; Muzammil et al., 2000a; Leggio et al., 2009) or 1.3 M GdnHCl (Farruggia & Pico, 1999; Muzammil et al., 2000a; Ahmad et al., 2005), stepwise alteration in the structure has been reported up to about 8 M urea or 5.5 M GdnHCl (Qasim & Salahuddin, 1978; Khan et al., 1987; Farruggia & Pico, 1999; Muzammil et al., 2000a; Ahmad et al., 2005; Leggio et al., 2009).

Many groups have demonstrated urea denaturation of serum albumin as a two-step, three-state transition with the existence of a stable intermediate around 4.0–5.2 M urea (Khan et al., 1987; Ahmad & Qasim, 1995; Muzammil et al., 2000a; Leggio et al., 2009; Galantini et al., 2010). Involvement of domain III has been suggested in the formation of the intermediate, as urea denaturation of a large serum albumin fragment (comprised of domains II and III) has been shown to proceed with the changes in the more loosely folded

domain III, indicating unfolding and separation of its subdomains around 4 M urea (Khan et al., 1987). Furthermore, studies on urea denaturation of serum albumin with domain specific ligands have also suggested the unfolding of domain III during first transition of urea denaturation while the second transition corresponds to the changes in domains I and II (Tayyab et al., 2000; Ahmad et al., 2005). On the other hand, GdnHCl denaturation of serum albumin has been shown to occur as a single-step, two-state transition without the existence of intermediate (Farruggia & Pico, 1999; Ahmad et al., 2005). A comparative study using domain specific ligands has also suggested that GdnHCl-induced denaturation of serum albumin starts with the unfolding of domain III followed by domains I and II (Ahmad et al., 2005).

ii. Thermal denaturation: Many groups have studied thermal denaturation of serum albumin (Pico, 1997; Farruggia et al., 1999; Farruggia & Pico, 1999; Muzammil et al., 2000b; Moriyama et al., 2003; Kragh-Hansen et al., 2005; Moriyama et al., 2008). Pico (1997) has demonstrated the thermal denaturation of serum albumin as a reversible process up to 75°C, beyond which irreversible changes may occur. Whereas minor structural alterations occur within 30–50°C (Farruggia et al., 1999; Kragh-Hansen et al., 2005; Moriyama et al., 2008), pronounced structural changes in the serum albumin have been reported between 50°C and 80°C, followed by smaller changes in the structure up to 100°C (Muzammil et al., 2000b; Moriyama et al., 2008). Thermal denaturation of serum albumin even at high temperature (130°C) has not resulted in complete loss in its secondary structure as about 16% α-helical structure has been shown even at 130°C (Moriyama et al., 2008).

1.4.2. Ovalbumin

Ovalbumin (also known as chicken egg white albumin) is a major protein of avian egg white, constituting about 54% of its total protein content (Burley & Vadehra, 1989). Due to its primary and tertiary structural similarities, ovalbumin has been grouped into serine protease family inhibitors (Hassan et al., 2011). Ovalbumin is a monomeric phosphoglycoprotein with about 3.5% carbohydrate moiety (Vadehra et al., 1973; Alleoni, 2006), which has been characterized as mannose and glucosamine in a ratio of 5:3 (Cunningham et al., 1963). The carbohydrate side chain is covalently attached to the amide nitrogen of Asn-292 by glycosyltransferases (Lee & Montgomery, 1962; Nisbet et al., 1981). Although the carbohydrate chain of ovalbumin is heterogeneous in nature, the molecular weight of different ovalbumin glycopeptides lies between 1560 and 1580 (Lee et al., 1964; Montgomery et al., 1965). In addition, the carbohydrate chain shares a common core structure with at least one mannose linked to two N-acetylglucosamine by a β–(1-4) linkage (Tai et al., 1975; Conchie & Strachan, 1978). Ovalbumin contains two phosphorylation sites at Ser-68 and Ser-344 residues (Nisbet et al., 1981). Different degrees of phosphorylation characterize the three isoforms of ovalbumin as A_1, A_2 and A_3 with zero, one and two phosphate group(s), respectively. These isoforms are present in the egg white in an approximate ratio of 81–84 : 14–16 : 2–4 (Longsworth et al., 1940; Cann, 1949; Perlmann, 1952).

1.4.2.1. Physicochemical properties

The physicochemical properties of ovalbumin are listed in Table 1.9. Using the physical techniques such as sedimentation equilibrium and light scattering, the molecular weight of ovalbumin has been determined as 45,000 (Warner, 1954). The molecular weight of ovalbumin calculated from its amino acid composition (44,300) is slightly lower than the value obtained using physical techniques (Tai et al., 1977). Ovalbumin is a globular protein with the sedimentation coefficient ($S^o_{20,w}$) of 3.50×10^{-13} s

Table 1.9. Physicochemical properties of ovalbumin.

Property	Value	Reference
Molecular weight		
– Amino acid composition	44,300	Tai et al. (1977)
– Sedimentation equilibrium	45,000	Warner (1954)
Sedimentation coefficient, $S^{o}_{20,w}$ (s)	3.50×10^{-13}	Fothergill and Fothergill (1970)
Diffusion coefficient, $D^{o}_{20,w}$ (cm^2 / s)	7.76×10^{-7}	Tanford (1961)
Intrinsic viscosity, [η] (cc / g)	3.9	Qasim and Salahuddin (1979)
Partial specific volume (cm^3 / g)	0.748	Dayhoff et al. (1952)
Stokes radius (nm)	2.7	Qasim and Salahuddin (1978)
Overall dimension (nm)	$6.3 \times 8.5 \times 7.2$	Stein et al. (1990)
Axial ratio	1.5:1	Harding (1981)
Isoelectric point	4.9	Kidwai et al. (1976)
Isoionic point	4.88	Sørensen et al. (1927)
$E^{1\%}_{1\,cm}$	7.12	Glazer et al. (1963)
Secondary structures		
– α- helix (%)	25–30	Timasheff and Gorbunoff (1967)
– β-sheet (%)	32	Stein et al. (1991)

(Fothergill & Fothergill, 1970) and a partial specific volume of 0.748 cm^3 / g (Dayhoff et al., 1952). The intrinsic viscosity, diffusion coefficient and stokes radius of ovalbumin have been determined as 3.9 cc / g (Qasim & Salahuddin, 1979), 7.76×10^{-7} cm^2 /s (Tanford, 1961) and 2.7 nm (Qasim & Salahuddin, 1978), respectively. Based on the crystallographic studies, ovalbumin has an ellipsoidal shape with dimensions of 6.3 × 8.5 × 7.2 nm (Stein et al., 1990) and the axial ratio of 1.5:1 (Harding, 1981). Ovalbumin possesses an isoionic and isoelectric points of 4.88 and 4.9, respectively (Sørensen et al., 1927; Kidwai et al., 1976). About 25–30% α-helix and 32% β-sheet structure are present in ovalbumin (Timasheff & Gorbunoff, 1967; Stein et al., 1991).

1.4.2.2. Amino acid composition

The single polypeptide chain of ovalbumin is comprised of 385 amino acid residues. The amino acid composition of ovalbumin is given in Table 1.10. Nearly half of the amino acid residues of ovalbumin are hydrophobic in nature, whereas the charged amino acid residues constitute about one third of the total amino acid residues (Table 1.10). Most of the charged amino acid residues in ovalbumin are acidic thus allowing ovalbumin an isoelectric point of 4.9. There are 6 Cys and 16 Met residues in ovalbumin. Ovalbumin also contains a high number of aromatic amino acid residues (33), comprising of 20 Phe, 10 Tyr and 3 Trp residues.

1.4.2.3. Primary structure

The primary structure of ovalbumin is shown in Figure 1.3. The C-terminal of ovalbumin has been characterized as Pro residue (Fothergill & Fothergill, 1970) while the Gly residue at the N-terminal end is acetylated (Narita, 1961). The hydrophobic sequence between position numbers 21 and 47 has been shown to act as an internal signal for membrane translocation (Robinson et al., 1986). Out of the 6 Cys residues (Cys-11, Cys-30, Cys- 73, Cys-120, Cys-367 and Cys-382) found in ovalbumin, only Cys-73 and

T**able 1.10.** Amino acid composition of ovalbumin.*

Amino acid	Number of residues
Alanine	35
Arginine	15
Aspartic acid	14
Asparagine	17
Cysteine	6
Glutamic acid	33
Glutamine	15
Glycine	19
Histidine	7
Isoleucine	25
Leucine	32
Lysine	20
Methionine	16
Phenylalanine	20
Proline	14
Serine	38
Threonine	15
Tryptophan	3
Tyrosine	10
Valine	31
Total	385

* Adapted from Nisbet et al. (1981)

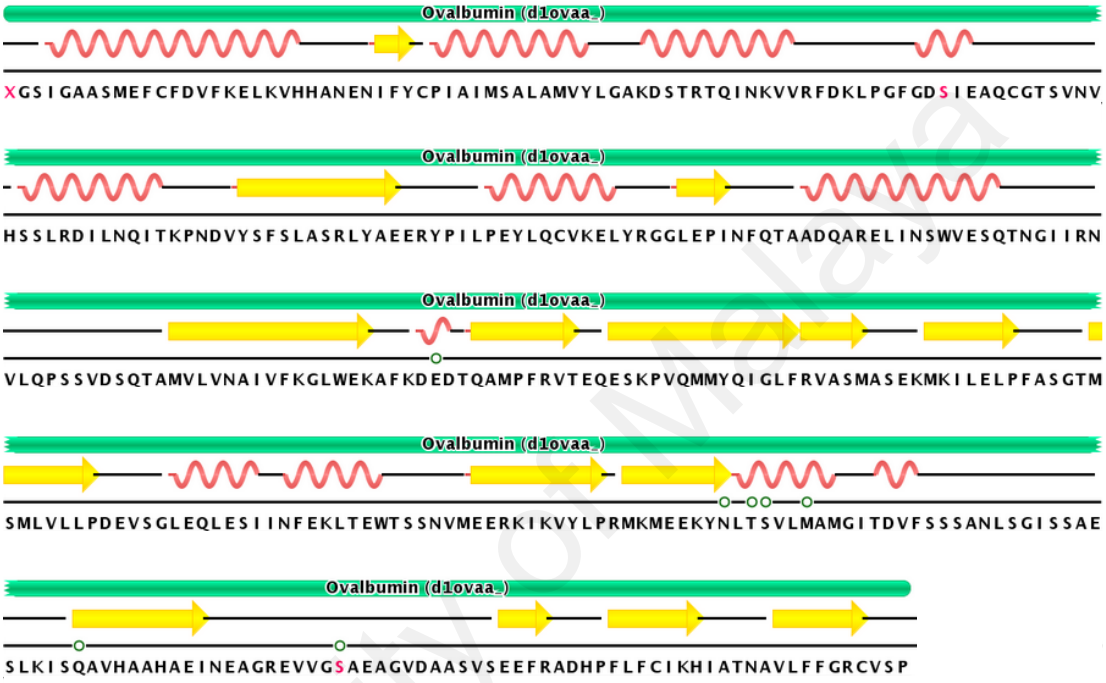

Figure 1.3. Primary structure of ovalbumin. The complete amino acid sequence is adapted from Protein Data Bank (entry code 1OVA). The positions of α-helices and β-sheets, as determined from ovalbumin crystal structure (Stein et al., 1991) are indicated by pink spirals and yellow arrows, respectively.

(Taken from http://www.rcsb.org/pdb/explore/remediatedSequence.do?structureId=1OVA)

Cys-120 are involved in disulphide bond formation, leaving 4 free thiol groups in ovalbumin (Fothergill & Fothergill, 1968).

1.4.2.4. Three-dimensional structure

The secondary structures of ovalbumin have been determined from its crystal structure (Stein et al., 1991) and locations of α-helices and β-sheets are shown in Figure 1.3. The three-dimensional structure of ovalbumin (Figure 1.4) shows the presence of five β-sheets running parallel to the long axis of the ovalbumin molecule (Stein et al., 1991). The sole disulphide bond in ovalbumin interconnects two part of the chain (Hassan et al., 2011) and is located in solvent accessible environment. The rest of the Cys residues are buried in the protein interior (Tani et al., 1997). All three Trp residues of ovalbumin (Trp-148, Trp-184 and Trp-267) are located in the protein interior and are positioned in different α-helices (Trp-148 and Trp-267) and β-sheet (Trp-184) (Wright et al., 1990).

1.4.2.5. Denaturation

The denaturation studies on ovalbumin under different denaturing conditions have been made by monitoring the changes in the optical rotation, viscosity, circular dichroism, fluorescence, UV-absorption and sedimentation velocity (Simpson & Kauzmann, 1953; Steven & Tristram, 1959; McKenzie et al., 1963; Gagen & Holme, 1964; Holt & Creeth, 1972; Ahmad & Salahuddin, 1976; Batra et al., 1989; Zemser et al., 1994).

i. Chemical denaturation: Denaturation of ovalbumin in the presence of urea and GdnHCl has been shown to be a reversible process (Holt & Creeth, 1972; Ahmad & Salahuddin, 1976; Zemser et al., 1994). In urea denaturation of ovalbumin, major structural changes have been observed above 3 M urea and is reported to be fully denatured around 8 M urea (Hayakawa et al., 1992; McKenzie & Frier, 2003; Covaciu et al., 2004). McKenzie and Frier (2003) have shown no significant variation in terms of the transition characteristics in the urea denaturation of commercial ovalbumin (mixture of A1, A2 and A3 isoforms)

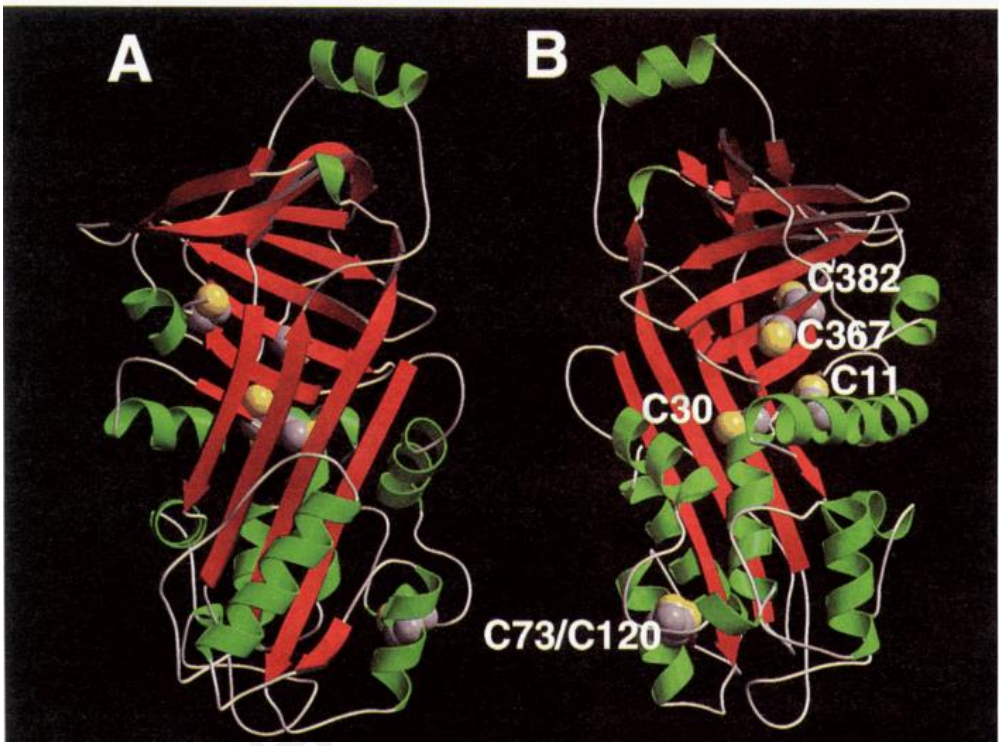

Figure 1.4. Three-dimensional structure of ovalbumin (A: front view and B: back view). The α-helices are shown as green helical ribbons while the β-sheets are indicated by red arrows. Sulphur atoms and both α- and β-carbon atoms in Cys residues are shown as yellow and grey spheres, respectively. (Adapted from Tani et al., 1997)

and independent isoforms. On the other hand, GdnHCl denaturation of ovalbumin displayed a shorter transition compared to urea denaturation due to the stronger denaturing effect of GdnHCl, with the start- and the end-points occurring at 1 M and 5 M GdnHCl, respectively (Holt & Creeth, 1972; Ahmad & Salahuddin, 1976; Hayakawa et al., 1992). GdnHCl-induced structural disorganization of ovalbumin involved a helix-to-coil transition (Zemser et al., 1994), where the decrease in the α-helical content was accompanied by the increase in the random coil (Batra et al., 1989).

ii. Thermal denaturation: Unlike the reversible urea and GdnHCl denaturations of ovalbumin, thermal denaturation of ovalbumin has been found as an irreversible reaction due to the formation of aggregates (Kato & Takagi, 1988; Koseki et al., 1989; Tani et al., 1997; Dong et al., 2000; Tani et al., 2004; Pearce et al., 2007). The major structural changes in ovalbumin against thermal denaturation occur between 60°C and 80°C (Dong et al., 2000; Pearce et al., 2007). The minor structural derangement takes place below 60°C as reflected from the smaller change in the fluorescence and circular dichroism spectral signals (Pearce et al., 2007). The major structural change of ovalbumin involved an increase in the β-sheet structure concomitant to the decrease in its α-helical content (Pearce et al., 2007). The formation of aggregates of ovalbumin upon thermal denaturation seems to involve an intermolecular β-sheet developed between two protein molecules during the heat treatment (Kato & Takagi, 1988; Dong et al., 2000; Pearce et al., 2007).

1.4.3. Lysozyme

Lysozyme (EC 3.2.1.17) was first discovered in 1922 by Sir Alexander Fleming in nasal mucus for its bacteriolytic activity on *Micrococcus lysodeikticus* suspension. The protein was named as lysozyme, where 'lyso' means capability to lyse bacteria and 'zyme' refers to enzyme. Lysozyme inhibits activity of bacterial colonies, particularly

Gram-positive bacteria due to its ability to hydrolyze the thick peptidoglycan layer of the bacterial cell wall. Apart from nasal mucus, the enzyme can be found in tears, saliva, blood serum, milk and placenta of human, bacteriophage lamda and avian egg white (Jollès, 1960; 1969; Mouton & Jolles, 1969; Raftery & Dahlquist, 1969; Imoto et al., 1972). Lysozyme can be categorized into three different types based on its origin. The c-type (chicken or conventional type), the g-type (goose-type) and the i-type (invertebrate type) lysozymes have been identified in animal kingdom while the v-type lysozyme has been found in bacteriophage lambda (Evrard et al., 1998; Callewaert & Michiels, 2010). Out of all these different types of lysozyme, the c-type lysozyme from hen egg white has been extensively studied due to its easy availability in purified form.

1.4.3.1. Physicochemical properties

Table 1.11 summarizes some physicochemical properties of lysozyme. The molecular weight of lysozyme has been calculated from its amino acid composition as 14,300 (Canfield, 1963a), which is slightly lower than the molecular weight (14,400), determined from sedimentation equilibrium (Sophianopoulos et al., 1962). The hydrodynamic data of lysozyme shows the values of sedimentation coefficient ($S^{o}_{20,w}$), diffusion coefficient ($D^{o}_{20,w}$) and partial specific volume as 1.9×10^{-13} s, 11.2×10^{-7} cm^2 / s and 0.703 cm^3 / g, respectively (Alderton et al., 1945; Sophianopoulos et al., 1962). Lysozyme has an intrinsic viscosity of 3.0 cc / g. It has an ellipsoidal shape with the dimensions of 4.5 × 3.0 × 3.0 nm (Blake et al., 1965) and an axial ratio of 1.5:1 (Monkos, 1997). The Stokes radius of lysozyme has been determined as 2.0 nm (Uversky, 1993). Higher values of the isoionic point (11.1) and the isoelectric point (11.35) of lysozyme (Wetter & Deutsch, 1951; Beychok & Warner, 1959) clearly suggest its basic nature and it possesses a net charge of + 8 at physiological pH (van der Veen et al., 2004). Lysozyme contains higher content of α-helix (29%) than β-sheets structure (11%) (Greenfield & Fasman, 1969). The enzyme shows its activity over a pH range, 6.0–7.0

T**able 1.11.** Physicochemical properties of lysozyme.

Property	Value	Reference
Molecular weight		
– Amino acid composition	14,300	Canfield (1963a)
– Sedimentation equilibrium	14,400	Sophianopoulos et al. (1962)
Sedimentation coefficient, $S^{o}_{20,w}$ (s)	1.9×10^{-13}	Alderton et al. (1945)
Diffusion coefficient, $D^{o}_{20,w}$ (cm^2 / s)	11.2×10^{-7}	Alderton et al. (1945)
Intrinsic viscosity, [η] (cc / g)	3.0	Sophianopoulos et al. (1962)
Partial specific volume (cm^3 / g)	0.703	Sophianopoulos et al. (1962)
Overall dimension (nm)	$4.5 \times 3.0 \times 3.0$	Blake et al. (1965)
Axial ratio	1.5:1	Monkos (1997)
Stokes radius (nm)	2.0	Uversky (1993)
Isoelectric point	11.35	Wetter and Deutsch (1951)
Isoionic point	11.1	Beychok and Warner (1959)
E^{mM}_{1cm} at 280 nm	36	Davies et al. (1969)
Optimal pH	6.2	Davies et al. (1969)
Secondary structures		
– α- helix (%)	29	Greenfield and Fasman (1969)
– β-sheet (%)	11	
– Random coil (%)	60	

with the pH optimum occurring at pH 6.2 (Davies et al., 1969).

1.4.3.2. Amino acid composition

Lysozyme is a single polypeptide chain of 129 amino acid residues (Canfield, 1963b; 1963a; Jollès et al., 1963; Canfield & Liu, 1965). The amino acid composition of lysozyme is given in Table 1.12. Lysozyme is a small and simple non-glycosylated protein without any non-protein moiety. It contains a total of 12 aromatic amino acid residues, dominated by Trp (6) residues, followed by Tyr and Phe residues (3 each) (Canfield, 1963b). The Cys residues (8) of lysozyme are involved in the formation of 4 disulphide bonds. Lysozyme has a high content of polar and charged residues such as Asn, Ser, Arg and Asp with fewer His, Glu, Met and Pro residues (Table 1.12).

1.4.3.3. Primary structure

Figure 1.5 shows the primary structure of lysozyme as determined by Canfield and Liu (1965). The N-terminal and C-terminal residues of lysozyme have been characterized as Lys and Leu, respectively (Thompson, 1955). The locations of the four disulphide bonds between 8 Cys residues in lysozyme are at positions 6–127, 30–115, 64–80 and 76–94 (Canfield & Liu, 1965). These disulphide bonds are believed to be the major stabilizing force of lysozyme (Imoto et al., 1972).

1.4.3.4. Three-dimensional structure

The three-dimensional structure of lysozyme was the first enzyme structure, determined by X-ray crystallography (Phillips, 1967). The locations of the catalytic residues (Glu-35 and Asp-52) as well as different secondary structures of lysozyme are shown in Figure 1.6. Most of the polar amino acid residues (Lys, Arg, His, Asp and Glu) of lysozyme are located on the protein surface while non-polar amino acid residues are buried in the protein interior (Blake et al., 1965; Lesnierowski & Kijowski, 2007).

Table 1.12. Amino acid composition of lysozyme.*

Amino acid	Number of residues
Alanine	12
Arginine	11
Asparagine	14
Aspartic acid	7
Cysteine	8
Glutamic acid	2
Glutamine	3
Glycine	12
Histidine	1
Isoleucine	6
Leucine	8
Lysine	6
Methionine	2
Phenylalanine	3
Proline	2
Serine	10
Threonine	7
Tryptophan	6
Tyrosine	3
Valine	6
Total	129

* Adapted from Canfield (1963a)

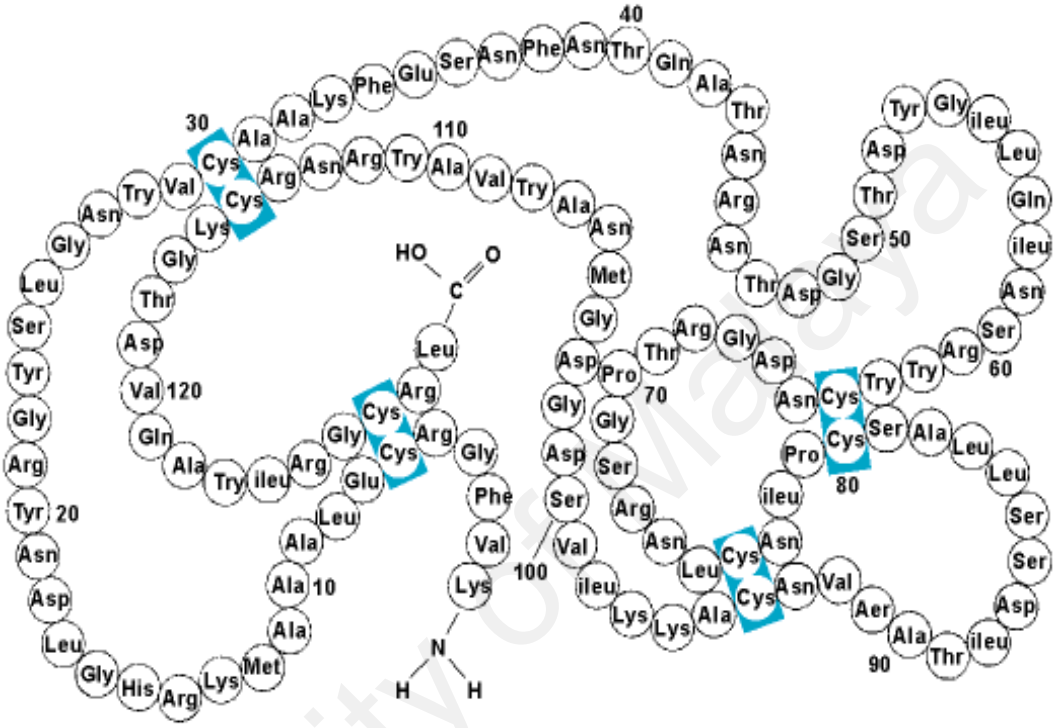

Figure 1.5. Amino acid sequence and disulphide bond linkages of lysozyme. (Adapted from Canfield & Liu, 1965)

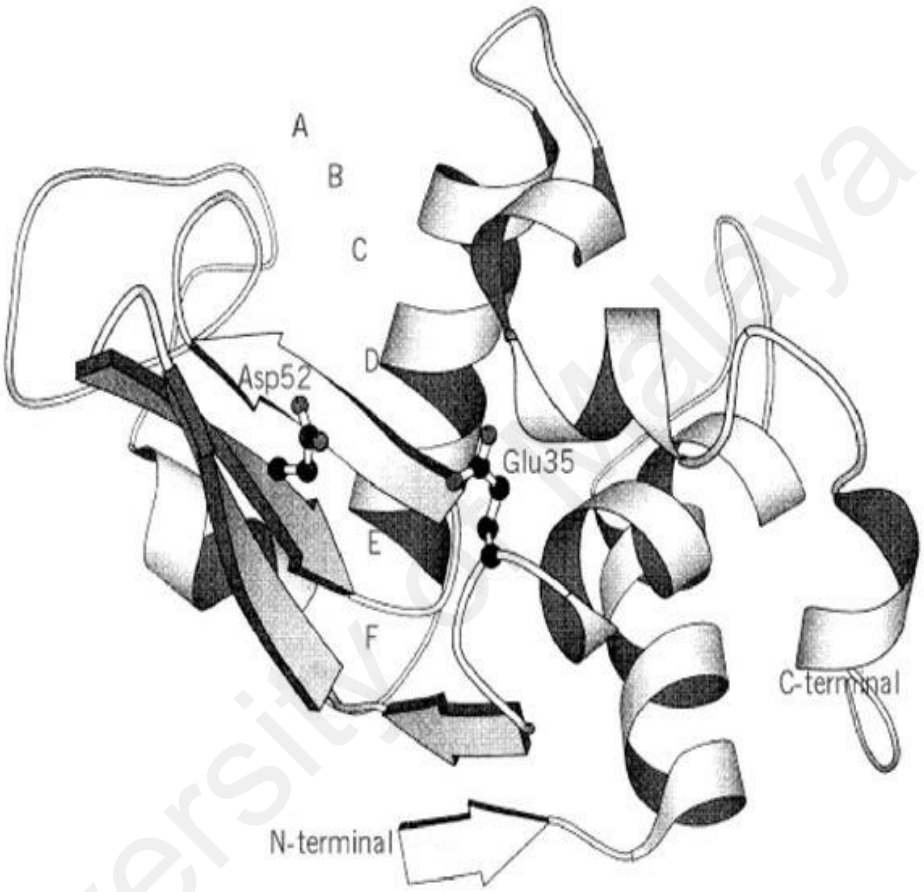

Figure 1.6. Three dimensional structure of lysozyme. Catalytic residues Glu-35 and Asp-52 as well as the binding site of substrate are shown. (Adapted from Imoto et al., 1972)

Interestingly, some hydrophobic amino acid such as Trp-62, Trp-63, Ile-98, Val-109 and Trp-123 are found on protein surface (Phillips, 1967). Lysozyme contains a total of four α-helices, which are comprised of residues 5–15, 24–34, 80–85 and 88–96 (Blake et al., 1965). Blake et al. (1965) also characterized the presence of two strands of antiparallel β-pleated sheet, involving residues 41–46 and 49–54.

Lysozyme possesses a prolate ellipsoid structure, which is separated into two domains, α and β, by a deep active site cleft running at the entire length of the structure (Blake et al., 1965; 1967; Imoto et al., 1972; Jollès & Jollès, 1984). These domains are separated by a helix-loop-helix motif formed along residues, 87–114 (Lesnierowski & Kijowski, 2007). The α-domain, made up of residues 1−39 and 85−129, consists of four α-helices along with a 3_{10}-helix and a short β-turn. On the other hand, the smaller β-domain (residues 36–84) is comprised of triple- and a double-stranded anti-parallel β-sheet involving residues 41−54, a 3_{10}-helix and an irregular loop (Blake et al., 1965; 1967; Imoto et al., 1972; Jollès & Jollès, 1984) . Two disulphide bonds of lysozyme (Cys-6–Cys-127 and Cys-30–Cys-115) are located in domain α while domain β contains one disulphide bond (Cys-64–Cys-80). The remaining disulphide bond links both domains α and β (Imoto et al., 1972; van den Berg et al., 1999b; 1999a; Lesnierowski & Kijowski, 2007).

1.4.3.5. Denaturation

Lysozyme can be easily denatured in the presence of different denaturants such as urea, GdnHCl, heat, acid *etc*. (Aune & Tanford, 1969; Greene & Pace, 1974; Ahmad & Bigelow, 1982; Ahmad et al., 1983; Ahmad et al., 1992; Laurents & Baldwin, 1997; Chang & Li, 2002; Bonincontro et al., 2004; Wu et al., 2008). Various techniques such as UV-difference spectroscopy, intrinsic fluorescence, circular dichroism, viscosity,

differential scanning calorimetry and optical rotation have been used to study the lysozyme denaturation under different experimental conditions.

i. Chemical denaturation: The unfolding pathway of lysozyme has been well studied and is shown to follow a reversible single step, two state transition with GdnHCl even under acidic (pH 1−4) conditions (Aune & Tanford, 1969; Ahmad & Bigelow, 1982; Ahmad et al., 1983; Ahmad et al., 1992; Wu et al., 2008). GdnHCl denaturation of lysozyme has been characterized by the start-, the mid- and the end-points at around 3.5 M, 4.1 M and 5.0 M GdnHCl, respectively at neutral pH, 25°C (Hamaguchi & Kurono, 1963; Ahmad & Bigelow, 1982; Wu et al., 2008). However, urea denaturation of lysozyme has shown some structural changes around 7–8 M urea and the enzyme has not been found fully denatured even at 9 M urea (Léonis, 1956; Hamaguchi & Kurono, 1963; Chang & Li, 2002). Lysozyme seems to be relatively resistant towards urea denaturation (Steiner, 1964; Greene & Pace, 1974).

ii. Thermal denaturation: Thermal denaturation of lysozyme has been found to be a single-step, two-state transition (Arai & Hirai, 1999; Yamamoto et al., 2006; Venkataramani et al., 2013). Overall, the structure of lysozyme remains unchanged below 60°C and shows marked changes in the temperature range, 60–90°C (Sugahara et al., 2002; Yamamoto et al., 2006). The mid-point of the transition has been characterized at around 72°C (Yamamoto et al., 2006; Venkataramani et al., 2013). The major structural alterations of lysozyme in the temperature range, 60–90°C involve loss in both the α-helical and the β-sheets structures (Venkataramani et al., 2013).

Several approaches such as protein engineering, chemical modification and use of solvent additives have been adopted to enhance protein stability. However, employment of solvent additives seems to be a better choice for protein stabilization, as protein engineering and chemical modification approaches are purely based on a hit and trial method, which may produce both protein stabilizing and destabilizing effects. Although use of different osmolytes as solvent additives has been shown to induce greater protein stability, only a few reports are available on the use of osmolyte mixtures in protein stabilization. Furthermore, these reports are mainly focused on the mixture of two to three osmolytes at a fixed ratio. The protein stabilizing potential of a complex mixture of osmolytes is yet to be explored. Since honey represents a naturally occurring mixture of different sugars (osmolytes), it would be of interest to study the protein stabilizing potential of honey. However, presence of several other components such as proteins, polyphenolic compounds and flavonoids in honey may interfere in protein stabilization studies using fluorescence spectroscopy, which is a popular technique due to its sensitivity and requirement of low protein concentration. Hence, simulated honey sugar cocktail (SHSC) would be a better substitute for honey to study the protein stabilizing potential of honey sugars on different model proteins using fluorescence spectroscopic probe. Furthermore, presence of other components in honey such as amino acids, minerals, vitamins and flavonoids might have added to the protein stabilizing potential of honey sugars. Hence, it would be of interest to compare the protein stabilizing potential of SHSC and honey using far-UV circular dichroism spectroscopy.

Problem statement

In view of the above, several research questions arise in mind:

1. Can SHSC be used as solvent additive for protein stabilization?
2. Does the formulated SHSC possess similar protein stabilizing potential as acquired by honey?

3. Does honey interfere with the fluorimetric investigation of honey-induced protein stabilization?

Objectives of the study

In order to address the above questions, the work presented in this thesis was undertaken to meet the following objectives:

- To study the chemical (urea and GdnHCl) stabilizing potential of SHSC on model proteins *i.e.* BSA, ovalbumin and lysozyme.
- To investigate the thermal stabilizing potential of SHSC on BSA, ovalbumin and lysozyme.
- To study the interference of honey in the fluorimetric investigation of honey-induced protein stabilization.
- To evaluate the chemical and thermal stabilizing potentials of honey on a model protein, BSA, using circular dichroism spectroscopy.
- To compare the chemical and thermal stabilizing potentials of SHSC and honey on a model protein, BSA.

CHAPTER 2

Materials & Methods

2. MATERIALS AND METHODS

2.1. Materials

2.1.1. Proteins

Bovine serum albumin (BSA), essentially fatty acid free (type A-6003; Lot 080M7405V), albumin from chicken egg white (ovalbumin) (type A-2512; Lot SLBB9019V) and lysozyme from chicken egg white (type L-6876; Lot 061M129V) were procured from Sigma-Aldrich Co., USA. The protein preparations were used as such throughout these studies.

2.1.2. Reagents used in denaturation studies

Urea ultrapure (type U-0631; Lot BCBJ2674V), guanidine hydrochloride (GdnHCl) (type G-4505; Lot 081M5405V) and 1-anilinonaphthalene-8-sulfonic acid (ANS) (type A-3125; Lot 104K2510) were obtained from Sigma-Aldrich Co., USA.

2.1.3. Reagents used in the preparation of simulated honey sugar cocktail and honey solutions

D (+) glucose (type G-8270; Lot 080M0175V), D (–) fructose (type F-0127; Lot 110M0185V) and D (+) trehalose dihydrate (type T-5251; Lot 113K3775 / type T-9449; Lot 011M7000V) were purchased from Sigma-Aldrich Co., USA. Analytical pure samples of sucrose and maltose were supplied by Systerm, Malaysia and R & M Chemicals, UK, respectively. Unblended raw clover honey from New Zealand (Batch 120708) was supplied by Cammells Honey Ltd., New Zealand.

2.1.4. Other reagents

Analytical grade samples of sodium hydroxide, sodium dihydrogen phosphate, disodium hydrogen phosphate and phosphoric acid were purchased from Systerm,

Malaysia. Standard buffers (pH 7.0 and pH 10.0) were obtained from Sigma-Aldrich Co., USA.

2.1.5. Miscellaneous

Millipore filters (pore size = 0.22 μm and 0.45 μm) were obtained from Merck Millipore, Germany. Parafilm 'M' was the product of Bemis Company Inc., USA.

All-glass double-distilled water or ultrapure water (type 1) obtained from Mili-Q system, Merck Millipore, Germany was used throughout these studies.

All the experiments were performed at room temperature (~25°C) unless otherwise stated.

2.2. Methods

2.2.1. pH measurements

pH measurements were performed on a Metler-Toledo pH meter, model Delta 320 using a BNC's combined electrode, type HA405-K2/120. The pH meter was routinely calibrated with standard buffers of pH 7.0 and pH 10.0 for pH measurements in the neutral and alkaline ranges, respectively. The least count of the pH meter was 0.01 pH unit.

2.2.2. Analytical procedures

The stock solutions of different proteins (BSA, ovalbumin and lysozyme) and denaturants (urea and GdnHCl) as well as ANS were prepared in 60 mM sodium phosphate buffer, pH 7.4 / 7.0 and were filtered through 0.45 μm Millipore filters before use.

2.2.2.1. Protein concentration

The protein concentrations of the stock BSA, ovalbumin and lysozyme solutions were determined spectrophotometrically on a Shimadzu double-beam spectrophotometer,

model UV-2450, using extinction coefficient values of $E_{1\,cm}^{1\%}$ = 6.67 at 279 nm for BSA (Janatova et al., 1968); $E_{1\,cm}^{1\%}$ = 7.12 at 280 nm for ovalbumin (Glazer et al., 1963) and E_{1cm}^{mM} = 36 at 280 nm for lysozyme (Davies et al., 1969). Scattering corrections, if required were made by extrapolation of the absorbance values in the wavelength range, 340–360 nm to the desired wavelength.

2.2.2.2. ANS concentration

The concentration of the stock ANS solution was determined spectrophotometrically using a molar extinction coefficient, E_M of 5000 $M^{-1}cm^{-1}$ at 350 nm (Mulqueen & Kronman, 1982).

2.2.2.3. Denaturant concentration

The concentrations of the stock urea and GdnHCl solutions were determined based on recorded weights, as described by Pace and Scholtz (1997). Weight fraction area (*W*) of the denaturant solution was calculated using the following equation:

$$W = \frac{\text{Weight of solid urea / GdnHCl (g)}}{\text{Weight of urea / GdnHCl solution (g)}} \quad (1)$$

The value of *W*, thus obtained, was used to calculate the ratio of the density of the denaturant solution (*d*) to the density of water (d_o) using equation (2) for urea and equation (3) for GdnHCl:

$$d/d_o = 1 + 0.2658W + 0.0330W^2 \quad (2)$$

$$d/d_o = 1 + 0.2710W + 0.0330W^2 \quad (3)$$

The d/d_o ratio was used to determine the volume (V) of the stock urea / GdnHCl solution using the following equation:

$$V\ (ml) = \frac{\text{Weight of urea / GdnHCl solution (g)}}{d/d_o} \quad (4)$$

Finally, the concentration of the stock urea / GdnHCl solution was obtained using equation (5):

$$\text{Concentration of stock urea / GdnHCl solution (M)} = \frac{\text{Weight of solid urea / GdnHCl (g)}}{MW \times (V \div 1000)} \quad (5)$$

where MW is the molecular weight of urea (60.056 g / mol) or GdnHCl (95.533 g / mol).

2.2.2.4. Curve fitting

The lines of all curves were made as a guide for the eyes using the non-linear curve fitting mode of OriginPro 9.0 software (Originlab Co., USA).

2.2.2.5. Statistical analysis

All the experiments were repeated atleast three times and the results are expressed as the mean value ± standard deviation (SD) of three independent experiments. One-way analysis of variance (ANOVA) was used to compare the means, if required and the difference was considered significant at $p < 0.05$. All statistical analysis was made using either OriginPro 9.0 software (Originlab Co., USA) or Microsoft Excel.

2.2.3. Preparation of the stock simulated honey sugar cocktail and honey solutions

The stock solution [60% (w/v)] of simulated honey sugar cocktail (SHSC) was prepared by dissolving 309.6 g fructose, 279.5 g glucose, 1.62 g sucrose and 3.78 g each of maltose and trehalose in 60 mM sodium phosphate buffer, pH 7.4 / 7.0 in a total volume of 1000 ml. The sugars' concentrations required in the preparation of the stock SHSC solution corresponded to the sugar composition of the honey as shown in Table 1.6 (Rybak-Chmielewska & Szczęsna, 1995).

The stock honey solution [60% (w/v)] was prepared by mixing 600 g of honey with 60 mM sodium phosphate buffer, pH 7.4 in a total volume of 1000 ml.

The pH of the stock SHSC or honey solutions was adjusted to pH 7.4 / 7.0 with sodium hydroxide. These solutions were diluted with the same buffer to get the desired SHSC or honey concentrations.

2.2.4. Spectral measurements

2.2.4.1. Circular dichroism spectroscopy

Circular dichroism (CD) spectral measurements in the far-UV (200–250 nm) and the near-UV (250–300 nm) regions were made on a Jasco spectropolarimeter, model J-815, equipped with a peltier type temperature controller (PTC-423S/15) under constant nitrogen flow. All CD spectral measurements were performed at 25°C (unless otherwise stated) at a scan speed of 100 nm.min^{-1} and a response time of 1 s after calibrating the instrument with (+)-10-camphorsulfonic acid. Each spectrum was the average of four scans and it was corrected using suitable blanks. The far-UV CD and the near-UV CD spectra were recorded with a protein concentration of 2 μM and 20 μM for BSA; 5 μM and 40 μM for ovalbumin; 10 μM and 25 μM for lysozyme in a 1 mm and 10 mm path length cells, respectively. The CD results are expressed as mean residue ellipticity (MRE) in deg.cm^2.dmol^{-1}, which is defined as:

$$\text{MRE} = \frac{\theta_{obs} \times MRW}{10 \times l \times c} \quad (6)$$

where θ_{obs} is the measured ellipticity in millidegrees, *MRW* is the mean residue weight [molecular weight of the protein (66,700 for BSA; 45,000 for ovalbumin; 14,300 for lysozyme) divided by the total number of amino acid residues (582 for BSA; 385 for

ovalbumin; 129 for lysozyme)], *l* is the path length of the cell in cm and *c* is the protein concentration in mg / ml (Kelly et al., 2005).

The MRE values were transformed into relative MRE, if required, by taking the MRE value of the protein in the absence of the denaturant as 100.

The α-helical content was calculated from the MRE value at 222 nm (MRE_{222nm}) using the following equation (Chen et al., 1972):

$$\% \text{ α-Helix} = \frac{MRE_{222nm} - 2340}{30300} \times 100 \quad (7)$$

2.2.4.2. Fluorescence spectroscopy

Fluorescence measurements were performed either on a Hitachi fluorescence spectrophotometer, model F-2500 or on a Jasco spectrofluorometer, model FP-6500, equipped with a temperature-controlled cell holder, attached to a Protech 632D circulating water bath, using quartz cuvette of 10 mm path length at 25°C (unless otherwise stated). Both excitation and emission slits were set at 10 nm each. Each sample was used once in fluorescence spectral measurements. All fluorescence spectra were corrected by subtracting the fluorescence intensity of the appropriate blank solutions at each wavelength, if required.

Intrinsic fluorescence spectra of BSA samples were recorded in the wavelength range, 300–400 / 450 nm upon excitation at 280 nm, using a protein concentration of 2 μM / 5 μM. Fluorescence intensity values were transformed into relative fluorescence intensity, if required, by taking the fluorescence intensity of BSA in buffer as 100.

Tryptophan fluorescence spectra of ovalbumin and lysozyme samples were made in the wavelength range, 310–390 nm upon excitation at 295 nm, using a protein concentration of 2.5 μM and 1 μM, respectively.

Honey samples were excited at 280 nm to obtain the fluorescence spectra in the wavelength range of 300–450 nm.

ANS fluorescence measurements were made by recording either the emission spectra in the wavelength range, 400–600 nm or the fluorescence intensity at 470 nm upon excitation at 380 nm, using a protein concentration of 0.2 μM / 1.5 μM for BSA; 0.2 μM for ovalbumin and 1 μM for lysozyme. The ANS/protein molar ratio was fixed at 50:1 or 100:1 in all ANS binding experiments (Cardamone & Puri, 1992).

Three-dimensional (3-D) fluorescence spectra of different protein samples (2 μM for BSA and 2.5 μM for ovalbumin) were recorded between 220 nm and 500 nm after setting the excitation wavelength range at 220–350 nm with an increment of 10 nm.

2.2.4.3. UV-difference spectroscopy

UV-absorption measurements were made on a Shimadzu double-beam spectrophotometer, model UV-2450 at 25°C, using quartz cuvettes of 10 mm path length. Absorption spectra of various protein samples (20 μM for BSA; 40 μM for ovalbumin) in the absence and the presence of different urea concentrations were recorded in the wavelength range, 250–300 / 310 nm against their respective blanks. The difference spectrum was obtained by subtracting the absorbance values of the native protein from the absorbance values of the protein in different urea concentrations, at each wavelength. Values of absorbance difference were transformed into molar difference extinction coefficient (Є) and were plotted against wavelength.

2.2.5. Fluorimetric interference studies

All the solutions used in honey-induced fluorimetric interference studies were prepared in 60 mM sodium phosphate buffer, pH 7.4. To a constant volume (125 μl and 313 μl) of the stock protein solution (80 μM) taken in different tubes, increasing volumes

of the stock honey solution [60% (w/v)] were added to obtain the desired honey concentration and the final volume in each tube was made to 5 ml with the above buffer. The blank solutions were prepared in the same way except that the buffer was used instead of the protein solution. The contents were mixed thoroughly and the tubes were incubated for 1 h at 25°C before fluorescence spectral measurements.

2.2.6. Denaturation studies

Denaturation studies involving BSA and ovalbumin were made in 60 mM sodium phosphate buffer, pH 7.4, whereas, 60 mM sodium phosphate buffer, pH 7.0 was used in denaturation studies on lysozyme.

2.2.6.1. Urea / GdnHCl denaturation

For denaturation experiments, different volumes of the buffer were mixed with a constant volume of the stock protein solution taken in different tubes. This was followed by the addition of different volumes of the stock urea (11 M) / GdnHCl (8 M) solution to obtain the desired concentration of urea / GdnHCl. The solution mixture (5 ml) was incubated for 12 h at 25°C for equilibrium attainment (Simko & Kauzmann, 1962; Mustafa et al., 2011) before spectral measurements.

Experiments involving SHSC or honey were carried out in the same way except that all solutions contained the desired concentration of SHSC or honey.

2.2.6.2. Thermal denaturation

Thermal denaturation studies of BSA, ovalbumin and lysozyme were carried out in the temperature range, 20−100°C, using far-UV CD spectroscopy. The spectra of the freshly prepared protein samples (5 ml) were recorded in the same way as described in the section 2.2.4.1 after equilibrating the samples at each temperature for 6 min in the given temperature range (Moosavi-Movahedi et al., 1996). The protein samples contained

the desired concentration of SHSC or honey for thermal denaturation studies of these proteins in the presence of SHSC or honey.

2.2.6.3. Data analysis

The denaturation data, obtained by different techniques were transformed into the fraction denatured, $F_{D,}$ using the following equation:

$$F_D = \frac{Y - Y_N}{Y_D - Y_N} \quad (8)$$

where Y is the observed variable parameter at a given denaturant concentration or temperature; Y_N and Y_D represent the values of the variable characteristic of the native and the denatured states, respectively (Pace, 1986), which were obtained by linear extrapolation of the pre- and the post-transition regions.

The mid-point of the denaturation curve was determined from the X-axis value (denaturant concentration), corresponding to the Y-axis value (F_D) of 0.5.

For thermal denaturation studies, the mid-point of the denaturation curve (T_m) *i.e.* the temperature required to achieve 50% thermal-denatured state, was determined directly from the transition curves.

Flow chart of the research work flow.

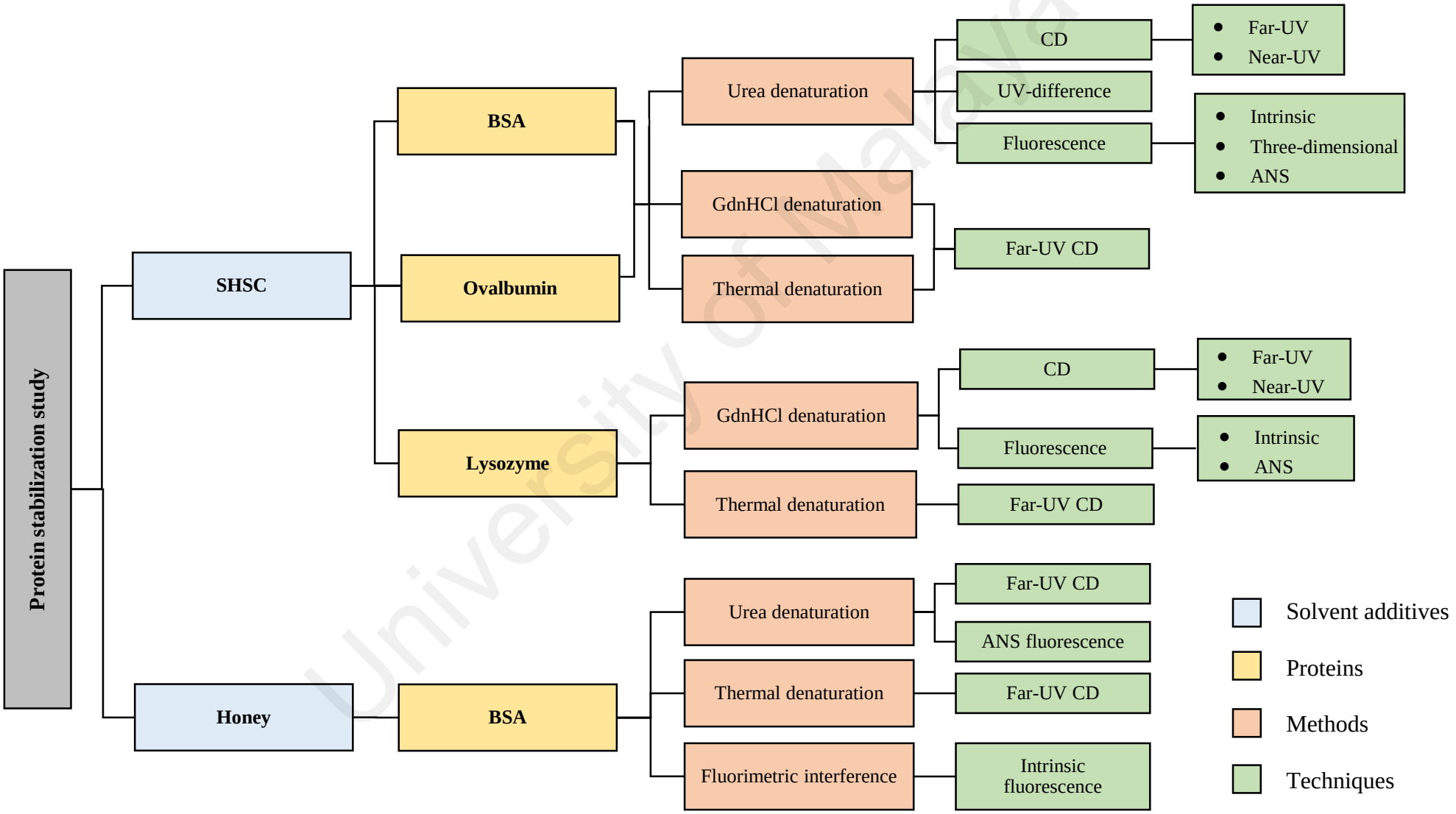

CHAPTER 3

Results & Discussion

3. RESULTS AND DISCUSSION

3.1. SHSC-induced stabilization of BSA

Urea, GdnHCl and thermal denaturation studies of BSA were made in the absence and the presence of SHSC to evaluate the protein stabilizing effect of SHSC.

3.1.1. Urea denaturation of BSA in the absence and the presence of SHSC

Protein stabilizing potential of SHSC on BSA against urea denaturation was studied by far-UV CD, intrinsic fluorescence and UV-difference spectral measurements in the absence and the presence of different SHSC concentrations.

3.1.1.1. Far-UV CD spectra

Far-UV CD spectroscopy is generally employed to probe secondary structural changes in proteins under various experimental conditions (Pelton & McLean, 2000; Botelho et al., 2003; Kelly et al., 2005; Carrotta et al., 2009). Figure 3.1 shows the far-UV CD spectra of BSA, obtained in the absence and the presence of increasing urea (2.5–9.3 M) concentrations. The far-UV CD spectra, obtained at lower (< 2.5 M) and higher (> 9.3 M) urea concentrations are omitted for clarity due to overlapping nature of the spectra in these concentration ranges. The far-UV CD spectrum of the native BSA was characterized by the presence of two minima at 208 nm and 222 nm, characteristics of the α-helical structures in proteins (Pelton & McLean, 2000; Kelly et al., 2005). Presence of increasing urea concentrations within this range produced a gradual decrease in the MRE values throughout the wavelength range, 200–250 nm, indicating loss in the protein's secondary structures. It should be noted that the far-UV CD spectra of BSA in the presence of urea could not be recorded below 210–216 nm due to high signal to noise ratio (saturation of detector / amplifier due to high absorption of denaturant).

Transformation of the MRE_{222nm} values, obtained at different urea concentrations into F_D was made following the procedure described in the section 2.2.6.3 and the F_D

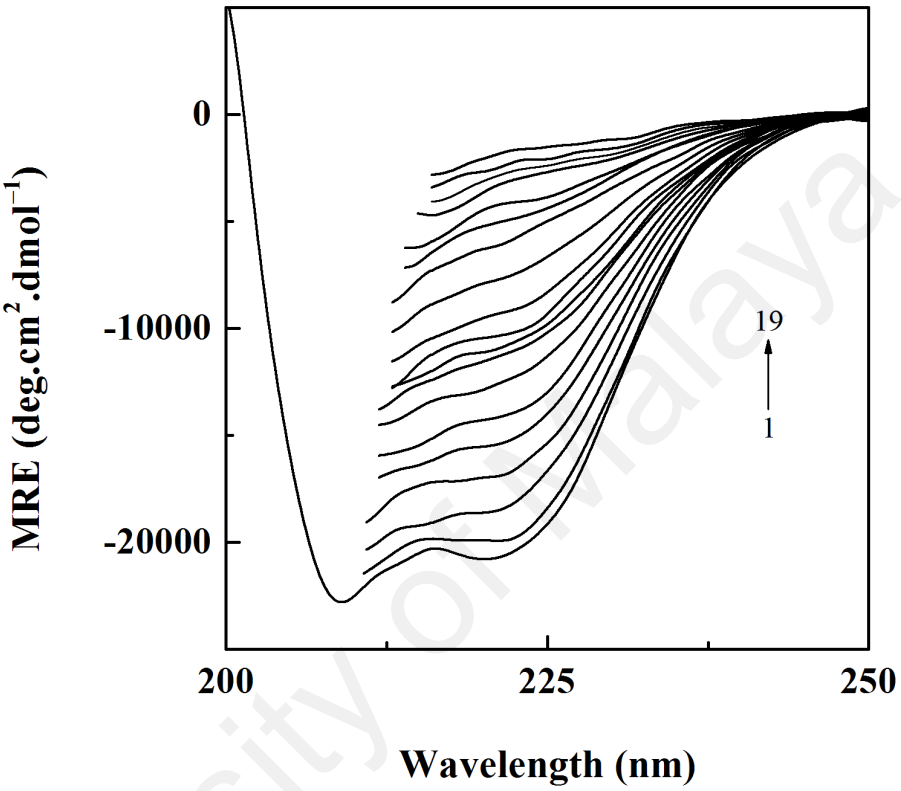

Figure 3.1. Far-UV CD spectra of BSA (2 μM), obtained in 60 mM sodium phosphate buffer, pH 7.4 in the absence and the presence of increasing urea concentrations (0–9.3 M urea). The urea concentrations (from bottom to top) were: 0, 2.5, 3.0, 3.25, 3.5, 4.0, 4.5, 4.6, 4.8, 5.0, 5.25, 5.5, 6.0, 6.5, 7.0, 8.0, 8.5, 9.0 and 9.3 M.

values were plotted against urea concentration (Figure 3.2). MRE_{222nm} values of BSA, obtained at different urea concentrations but in the presence of SHSC were also treated in the same way. Figure 3.2 shows normalized urea denaturation curves of BSA in the absence and the presence of increasing SHSC concentrations, as monitored by MRE_{222nm} measurements. As can be seen from the figure, urea denaturation of BSA was characterized by a two-step, three-state transition, from the native (N) state to the denatured state (D) via a stable intermediate (I) state, which accumulated around 4.6–5.0 M urea. The first transition ($N \rightleftharpoons I$) started at 2.0 M urea and completed at 4.6 M urea, whereas the second transition, showing the transformation from the intermediate (I) state to the denatured (D) state ($I \rightleftharpoons D$) started at 5.0 M urea and ended at 9.3 M urea. These results were in agreement with previous reports on urea denaturation of serum albumin (Muzammil et al., 2000a; Leggio et al., 2009). Involvement of domain III in the formation of the intermediate state during urea denaturation has been suggested in earlier reports (Muzammil et al., 2000a; Tayyab et al., 2000).

Presence of increasing concentrations [8–20% (w/v)] of SHSC in the incubation mixture significantly affected the transition both in terms of the nature and the origin. Values of the start-, the mid- and the end-points of the urea transition curves of BSA in the absence and the presence of different SHSC concentrations, as monitored by MRE_{222nm} measurements are given in Table 3.1. The transition became a single-step transition without any detection of the intermediate state in the presence of 8–20% (w/v) SHSC (Figure 3.2). Furthermore, the transition was also shifted towards higher urea concentrations, being positively correlated with SHSC concentrations. In other words, the shift in the transition curve towards higher urea concentrations was more pronounced in the presence of 20% (w/v) SHSC compared to that obtained in the presence of 8% (w/v) SHSC. More evidently, the start- and the mid-points of the transition curve were increased

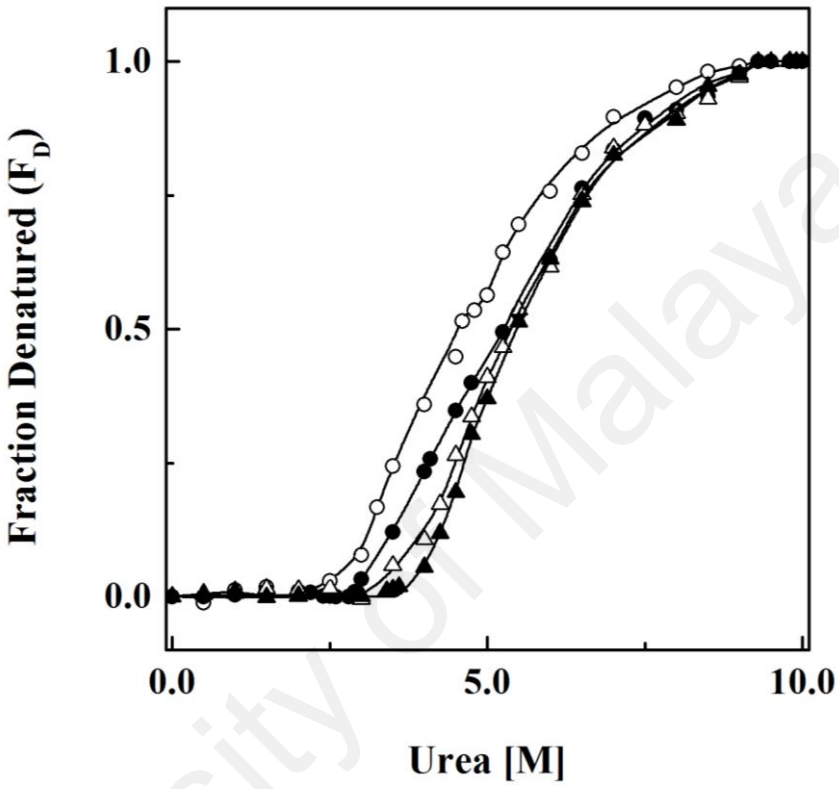

Figure 3.2. Normalized urea denaturation curves of BSA (2 μM) in 60 mM sodium phosphate buffer, pH 7.4, as studied by MRE_{222nm} measurements in the absence (○) and the presence of 8% (●), 10% (△) or 20% (▲) (w/v) SHSC.

Table 3.1. Characteristics of urea denaturation of BSA in the absence and the presence of different SHSC concentrations, as monitored by MRE_{222nm} measurements.

Protein sample	Urea-induced transition			Transition pattern
	Start-point [M]	Mid-point [M]	End-point [M]	
BSA				
– First transition	2.0 ± 0.11	3.6 ± 0.10	4.6 ± 0.06	Two-step, three-state
– Second transition	5.0 ± 0.06	6.1 ± 0.10	9.3 ± 0.12	
BSA + 8% (w/v) SHSC	2.8 ± 0.06	5.3 ± 0.03	9.3 ± 0.12	Single-step, two-state
BSA + 10% (w/v) SHSC	3.0 ± 0.06	5.4 ± 0.03	9.3 ± 0.00	
BSA + 20% (w/v) SHSC	3.6 ± 0.06	5.5 ± 0.06	9.3 ± 0.12	

Each value is expressed as the mean ± SD of three independent experiments.

from 2.8 M and 5.3 M urea (in the presence of 8%, w/v SHSC) to 3.6 M and 5.5 M urea (in the presence of 20%, w/v SHSC), respectively (Figure 3.2; Table 3.1).

3.1.1.2. Intrinsic fluorescence spectra

Fluorescence spectroscopy is widely used in proteins' structural studies (Royer, 1995), where the changes in the proteins' tertiary structures are reflected by the alteration in the fluorescence characteristics *i.e.* fluorescence intensity and emission maxima of proteins (Lakowics, 1999; Royer, 2006). Therefore, urea denaturation of BSA in the absence and the presence of different SHSC concentrations was also studied using intrinsic fluorescence measurements. The intrinsic fluorescence spectra of BSA in the absence and the presence of increasing urea (2.1–8.0 M) concentrations upon excitation at 280 nm are shown in Figure 3.3. The fluorescence spectra of BSA at lower (< 2.1 M) and higher (> 8.0 M) urea concentrations overlapped each other due to smaller changes in the spectral signal and therefore, have been omitted for clarity. Appearance of an emission maxima at 341 nm characterized the intrinsic fluorescence spectrum of the native BSA due to the presence of Trp residues (Royer, 2006; Kumaran & Ramamurthy, 2011), which was in agreement with previous reports (Khan et al., 1987; Kumaran & Ramamurthy, 2011). BSA contains two Trp residues, which are located at positions 134 and 212 in the primary sequence (Peters, 1996). The fluorescence intensity of BSA at 341 nm showed a progressive decrease with increasing urea concentrations, suggesting microenvironmental perturbation around Tyr and Trp residues from non-polar to polar (Royer, 2006), owing to tertiary structural changes in the protein (Figure 3.3). Furthermore, emission maxima was shifted from 341 nm to 335 nm in the presence of 5.0 M urea but showed a red shift of 11 nm from 335 nm at 8.0 M urea. The initial blue shift in the emission maxima can be ascribed to the internalization of the Trp residues in the protein interior due to rearrangement of domains I and II, whereas the red shift beyond 5.0 M urea indicated an increase in the microenvironmental polarity of Trp residues,

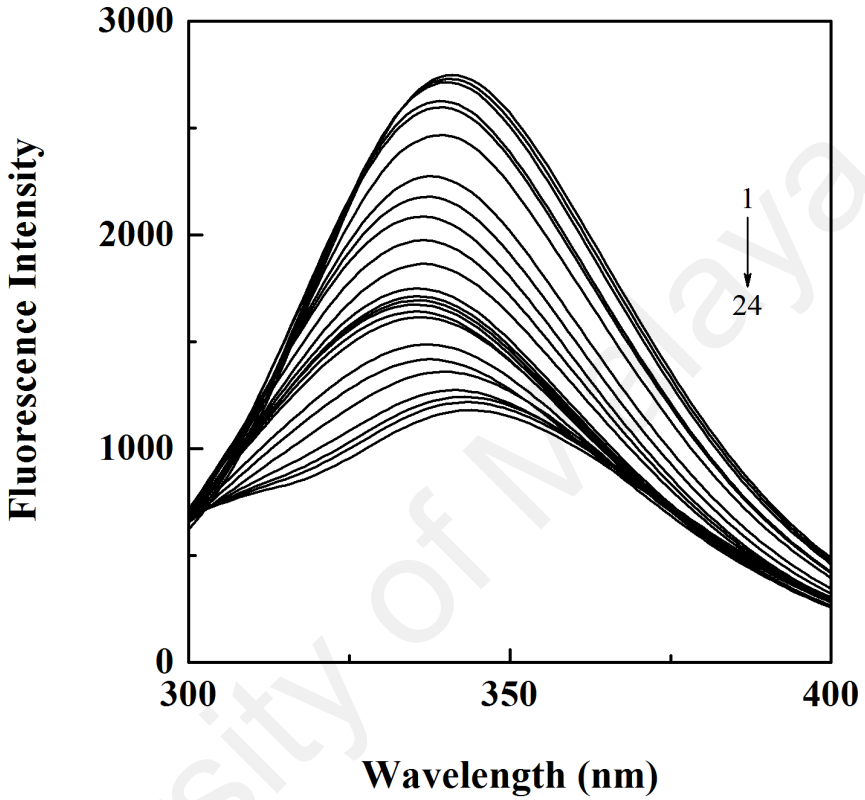

Figure 3.3. Fluorescence spectra of BSA (2 μM), obtained in 60 mM sodium phosphate buffer, pH 7.4 in the absence and the presence of increasing urea concentrations (0–8.0 M urea) upon excitation at 280 nm. The urea concentrations (from top to bottom) were: 0, 2.1, 2.2, 2.4, 2.5, 2.75, 3.0, 3.25, 3.5, 3.75, 4.0, 4.3, 4.4, 4.5, 4.6, 4.8, 5.0, 5.2, 5.5, 6.0, 6.5, 7.0, 7.5 and 8.0 M.

resulted from the unfolding of domains I and II of BSA (Leggio et al., 2009).

Normalization of the fluorescence intensity values at 341 nm, obtained at different urea concentrations into F_D, following the procedure described above produced the urea denaturation curve. As shown in Figure 3.4, urea denaturation curves of BSA in the absence and the presence of different SHSC concentrations were found similar to those obtained using MRE_{222nm} measurements (Figures 3.2). The two-step, three-state transition of BSA was transformed into a single-step, two-state transition and the denaturation curve was shifted towards higher urea concentrations in the presence of 8–20% (w/v) SHSC in a concentration dependent manner (Figure 3.4). However, values of the start-, the mid- and the end-points of the transition, as studied by intrinsic fluorescence measurements (Table 3.2) were found different from those obtained with MRE_{222nm} measurements (Table 3.1). Such differences in the transition characteristics were not unusual and have been shown earlier (Hung & Chang, 2001; Kishore et al., 2012).

3.1.1.3. UV-difference spectra

SHSC-induced stabilization of BSA against urea denaturation was further studied by UV-difference spectral measurements. Figure 3.5 shows the UV-difference spectra of BSA in the presence of increasing urea (0.5–8.5 M) concentrations. These spectra were characterized by the presence of a negative peak at 288 nm along with a shoulder at 280 nm, which were indicative of microenvironmental perturbation around Tyr residues (Sogami & Ogura, 1973). Additionally, several positive fine structures, 'wiggles' were also observed in the wavelength range, 250–275 nm, reflecting microenvironmental fluctuation around Phe residues (Horowitz & Butler, 1993). These UV-difference spectral features clearly indicated urea-induced disruption of the tertiary structure of BSA. Similar to those observed with far-UV CD and intrinsic fluorescence measurements, UV-difference spectra at lower (< 3.0 M) and higher (> 8.5 M) urea concentrations showed overlapping patterns and hence, are omitted for clarity. A quantitative analysis

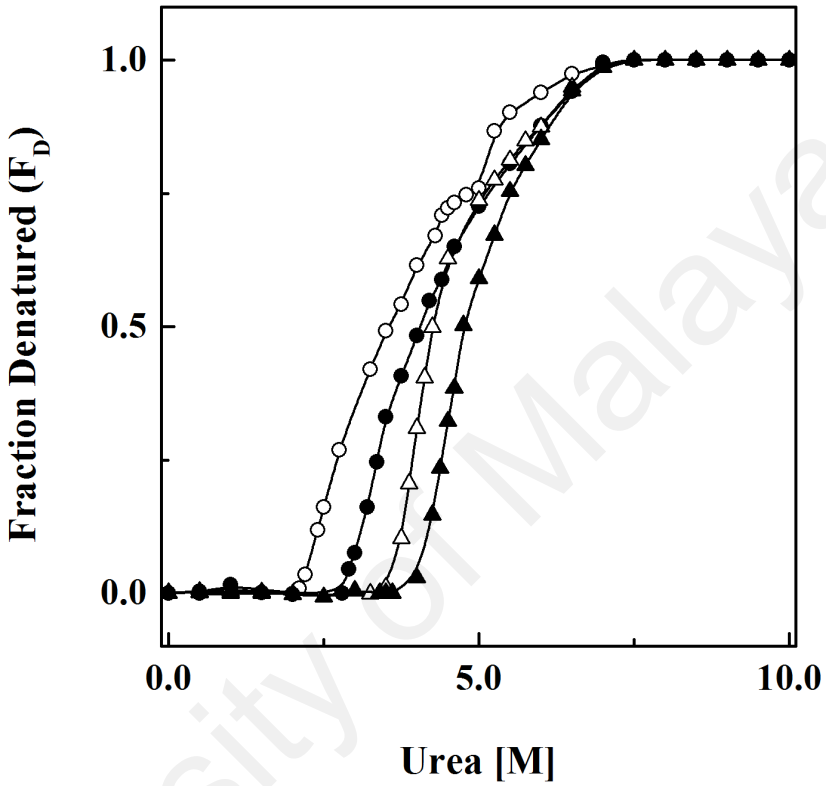

Figure 3.4. Normalized urea denaturation curves of BSA (2 μM) in 60 mM sodium phosphate buffer, pH 7.4, as studied by intrinsic fluorescence measurements at 341 nm upon excitation at 280 nm in the absence (○) and the presence of 8% (●), 10% (△) or 20% (▲) (w/v) SHSC.

Table 3.2. Characteristics of urea denaturation of BSA in the absence and the presence of different SHSC concentrations, as monitored by intrinsic fluorescence measurements at 341 nm upon excitation at 280 nm.

Protein sample	Urea-induced transition			Transition pattern
	Start-point [M]	Mid-point [M]	End-point [M]	
BSA				
– First transition	2.0 ± 0.06	3.1 ± 0.06	4.5 ± 0.10	Two-step, three-state
– Second transition	5.0 ± 0.06	5.1 ± 0.03	8.0 ± 0.25	
BSA + 8% (w/v) SHSC	2.8 ± 0.12	3.7 ± 0.03	8.0 ± 0.00	Single-step, two-state
BSA + 10% (w/v) SHSC	3.25 ± 0.09	4.3 ± 0.03	8.0 ± 0.15	
BSA + 20% (w/v) SHSC	3.6 ± 0.06	4.7 ± 0.06	8.0 ± 0.29	

Each value is expressed as the mean ± SD of three independent experiments.

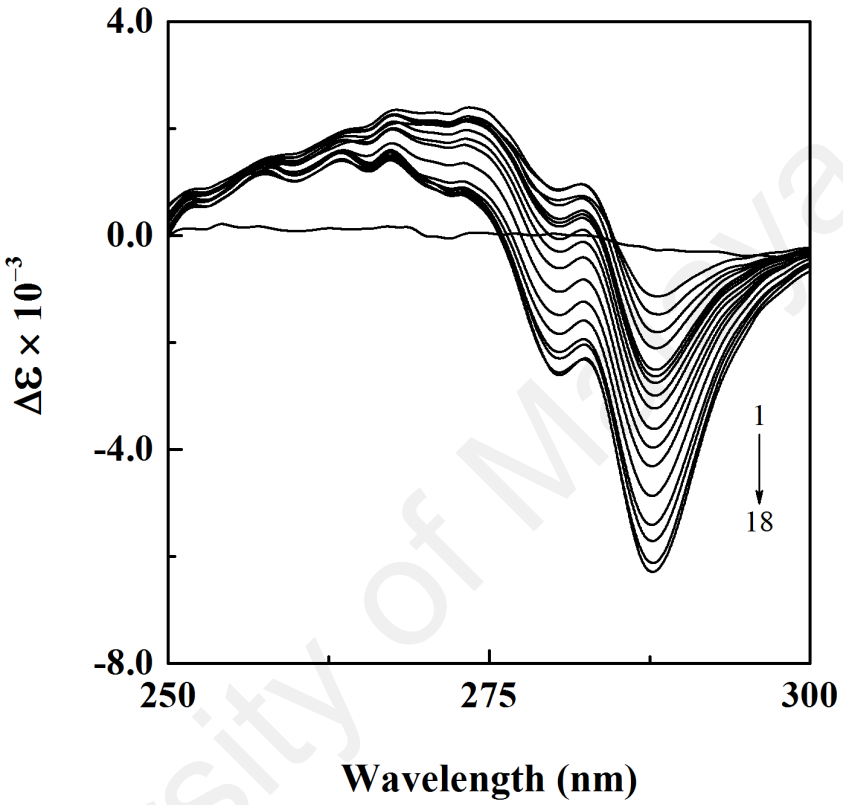

Figure 3.5. UV-difference spectra of BSA (20 μM), obtained in 60 mM sodium phosphate buffer, pH 7.4 in the presence of increasing urea concentrations (0.5–8.5 M urea). The urea concentrations (from top to bottom) were: 0.5, 3.0, 3.25, 3.5, 4.0, 4.2, 4.4, 4.6, 4.8, 5.0, 5.25, 5.5, 6.0, 6.5, 7.0, 7.5, 8.0 and 8.5 M urea.

of the UV-difference spectra revealed a progressive decrease in the molar difference extinction coefficient values at 288 nm with increasing urea concentrations, suggesting loss in the tertiary structure of BSA.

Transformation of the molar difference extinction coefficient values at 288 nm into F_D, using the same procedure as described in the section 2.2.6.3 yielded the denaturation curve, shown in Figure 3.6. UV-difference spectral data obtained in the presence of different SHSC concentrations were treated in the same way and the results are included in Figure 3.6. These transition curves were qualitatively similar to those obtained with MRE_{222nm} and intrinsic fluorescence measurements as shown in Figures 3.2 and 3.4, respectively. However, quantitative differences were noticed in the values of the start-, the mid- and the end-points of the transition (Tables 3.1; 3.2; 3.3). The start- and the end-points of the transition were observed at 2.5 M and 8.5 M urea, respectively, with the accumulation of the intermediate around 4.2–4.6 M urea. An earlier report on urea denaturation of BSA has also shown similar characteristics of the denaturation curve, when studied by UV-difference spectroscopy (Ahmad & Qasim, 1995). The denaturation curves obtained in the presence of different SHSC concentrations were characterized by the absence of the intermediate state and the late transition, when compared to the one obtained in the absence of SHSC (Figure 3.6; Table 3.3). These characteristics were similar to those obtained with MRE_{222nm} and intrinsic fluorescence measurements with slight variation in the values of start-, the mid- and the end-points of the transition. Since urea concentration range for the denaturation transition was found different with different probes, variation in the mid-point values is expected. In several earlier reports, such type of variation has been shown (Khan et al., 1987; Ahmad & Qasim, 1995; Muzammil et al., 2000a; Hung & Chang, 2001; Tayyab et al., 2002).

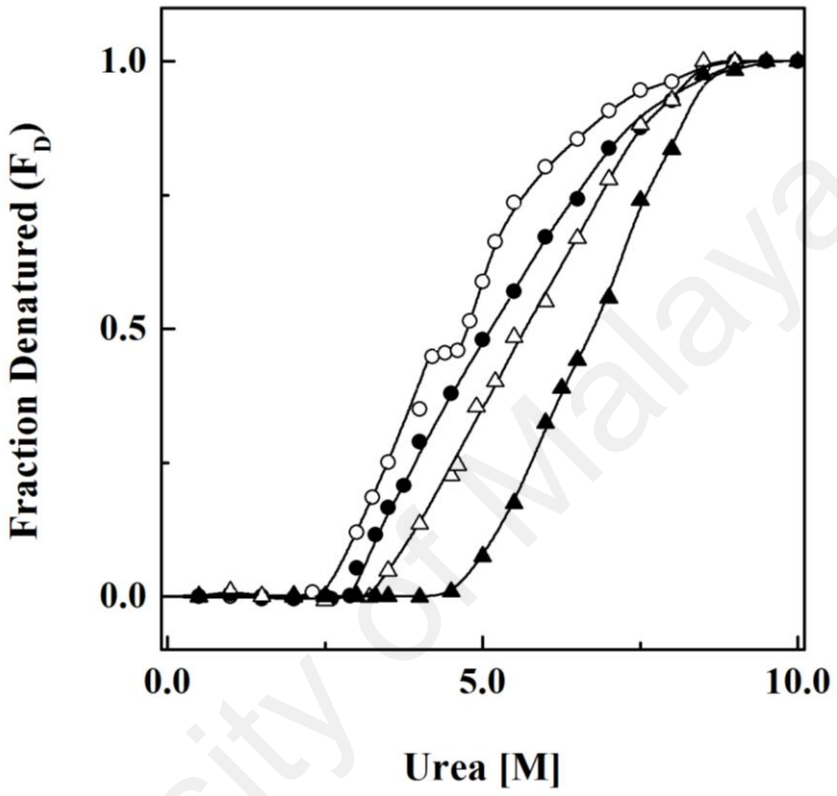

Figure 3.6. Normalized urea denaturation curves of BSA (20 μM) in 60 mM sodium phosphate buffer, pH 7.4, as studied by molar difference extinction coefficient measurements at 288 nm in the absence (○) and the presence of 8% (●), 10% (△) or 20% (▲) (w/v) SHSC.

Table 3.3. Characteristics of urea denaturation of BSA in the absence and the presence of different SHSC concentrations, as monitored by molar difference extinction coefficient measurements at 288 nm.

Protein sample	Urea-induced transition			Transition pattern
	Start-point [M]	Mid-point [M]	End-point [M]	
BSA				
– First transition	2.5 ± 0.06	3.4 ± 0.06	4.2 ± 0.10	Two-step, three-state
– Second transition	4.6 ± 0.11	5.4 ± 0.05	8.5 ± 0.14	
BSA + 8% (w/v) SHSC	2.9 ± 0.10	5.0 ± 0.06	8.5 ± 0.29	Single-step, two-state
BSA + 10% (w/v) SHSC	3.2 ± 0.06	5.5 ± 0.10	8.5 ± 0.14	
BSA + 20% (w/v) SHSC	4.0 ± 0.14	6.6 ± 0.10	8.5 ± 0.00	

Each value is expressed as the mean ± SD of three independent experiments.

Both shift in the transition curve towards higher urea concentrations and abolishment of the intermediate state observed in the presence of different SHSC concentrations using different probes indicated stabilization of the protein by SHSC. In view of the involvement of domain III in the intermediate formation (Khan et al., 1987; Muzammil et al., 2000a), SHSC seems to stabilize this domain, leading to the abolishment of the intermediate state in the urea denaturation. Previous reports on urea denaturation of BSA in the presence of fatty acids and salts have also shown a single-step transition with the abolishment of the intermediate state (Ahmad & Qasim, 1995; Muzammil et al., 2000a).

3.1.2. Characterization of the partially-denatured BSA in the absence and the presence of SHSC

In order to further investigate the stabilizing effect of SHSC on BSA, 4.6 M urea-denatured BSA (representing the intermediate state) was equilibrated with 20% (w/v) SHSC and its properties were studied using far-UV and near-UV CD spectra, UV-difference spectra, intrinsic florescence and three-dimensional fluorescence spectra as well as ANS binding.

3.1.2.1. Far-UV CD spectra

Figure 3.7 shows the effect of 20% (w/v) SHSC on the far-UV CD spectrum of the partially-denatured BSA, obtained in the presence of 4.6 M urea at pH 7.4. The far-UV CD spectrum of the native BSA at pH 7.4 is also included for comparison. The far-UV CD spectra of the partially-denatured BSA at 4.6 M urea in the absence and the presence of 20% (w/v) SHSC retained the characteristic feature of the α-helical structure, showing a minima at 222 nm. However, the MRE_{222nm} value was found higher (28%) in the presence of 20% (w/v) SHSC compared to that obtained in its absence, but was still lower (25%) than the MRE_{222nm} value of the native BSA (Figure 3.7; Table 3.4).

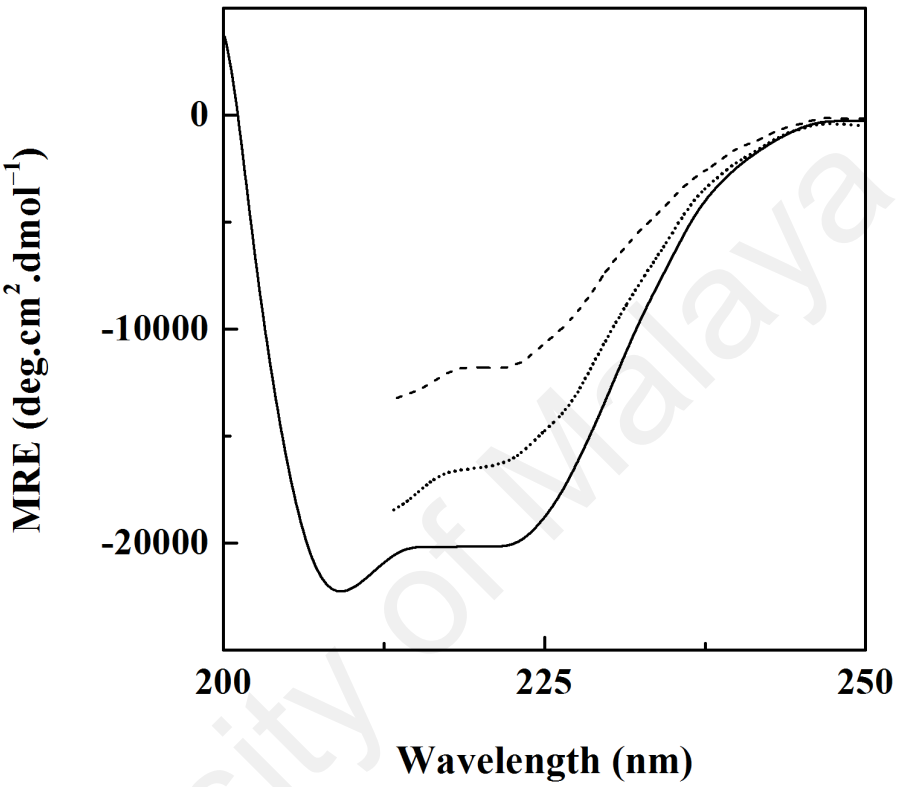

Figure 3.7. Far-UV CD spectra of BSA (——) and 4.6 M urea-denatured BSA in the absence (- - -) and the presence (·····) of 20% (w/v) SHSC at pH 7.4. The protein concentration was 2 μM.

Table 3.4. Spectral characteristics of BSA under various experimental conditions, as monitored by different probes.

Spectral characteristics	Native BSA	4.6 M urea-denatured BSA	4.6 M urea-denatured BSA + 20% (w/v) SHSC
Far-UV CD spectra			
– MRE at 222 nm (deg.cm^2.dmol^{-1})	–20,127.1 ± 138	–11,769.4 ± 77	–15,116.6 ± 36
– α-Helical content[a]	~58 ± 0.45%	~31 ± 0.25%	~42 ± 0.12%
Near-UV CD spectra			
– MRE at 262 nm (deg.cm^2.dmol^{-1})	–135.1 ± 23	–72.2 ± 6	–105.1 ± 6
– MRE at 268 nm (deg.cm^2.dmol^{-1})	–126.0 ± 20	–64.8 ± 5	–101.0 ± 7
UV-difference spectra			
– Molar difference extinction coefficient at 288 nm	–	– 2.8 ± 0.06 × 10^3	– 0.9 ± 0.04 × 10^3
ANS fluorescence spectra			
– Fluorescence intensity at 469 nm	273.3 ± 12	33.6 ± 3	112.8 ± 10
Intrinsic fluorescence spectra			
– Fluorescence intensity at 341 nm	2,756.3 ± 54	1,638.3 ± 116	2,284.6 ± 145
– Emission maximum (nm)	341 ± 0.00	336 ± 0.58	338 ± 1.00

Each value is expressed as the mean ± SD of three independent experiments.
[a] Calculated by the method of Chen et al. (1972).

It should be noted that the far-UV CD spectra of the partially-denatured BSA at 4.6 M urea both in the absence and the presence of 20% (w/v) SHSC could not be obtained below 213 nm due to high signal to noise ratio.

A more quantitative analysis of the far-UV CD spectra was made by calculating the percentage the α-helical content using the method of Chen et al. (1972) and the values of the α-helical content are given in Table 3.4. As can be seen from the table, the α-helical content decreased from ~58% (for native BSA) to ~31% in the presence of 4.6 M urea, showing a decrease of 27%. Similar decrease in the α-helical content in the urea-induced intermediate of serum albumin has also been reported earlier (Muzammil et al., 2000a). Interestingly, addition of 20% (w/v) SHSC in the incubation mixture stabilized the native protein conformation by inducing 11% increase in the α-helical content at the same urea concentration (Table 3.4). Although this stabilizing effect was significant but was not enough to retain the native protein structure within this urea concentration range. In view of the involvement of domain III in the intermediate formation during urea denaturation (Ahmad & Qasim, 1995; Tayyab et al., 2000), it seems that 20% (w/v) SHSC stabilized this domain to a significant extent during urea denaturation. The far-UV CD spectrum of BSA was also determined in the presence of 20% (w/v) SHSC and the overlapping CD spectra (figure not shown) suggested that the structural integrity of BSA was retained in the presence of SHSC.

3.1.2.2. Near-UV CD spectra

The stabilizing effect of 20% (w/v) SHSC on the tertiary structure of the partially-denatured BSA can be seen from Figure 3.8, showing the near-UV CD spectra of 4.6 M urea-denatured BSA in the absence and the presence of 20% (w/v) SHSC along with the near-UV CD spectrum of the native BSA. Presence of two troughs at 262 nm and 268 nm along with two shoulders at 275 nm and 292 nm characterized the

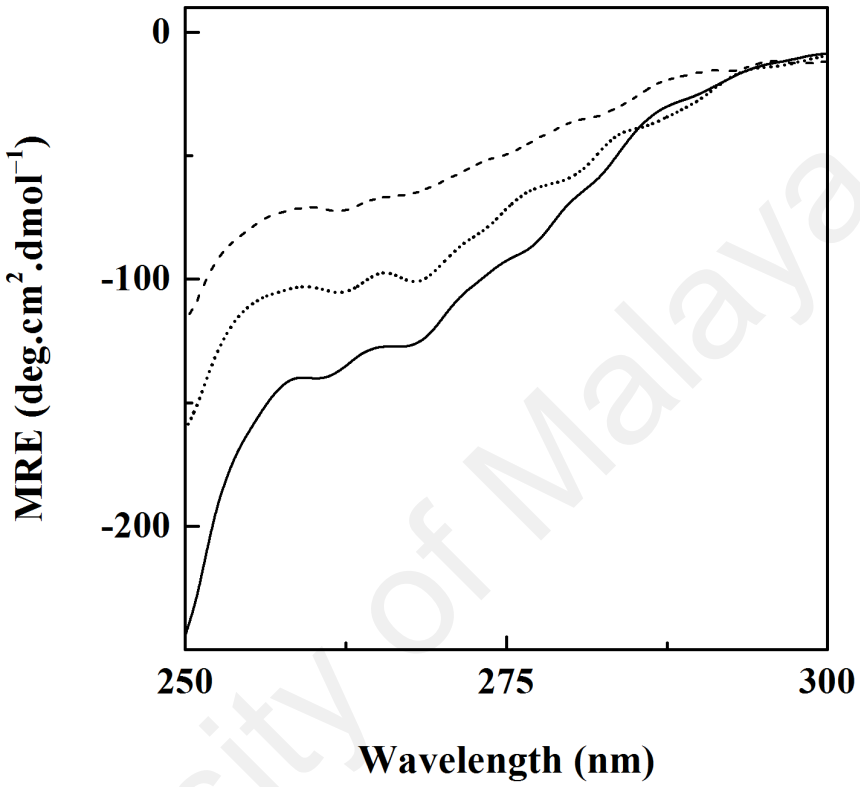

Figure 3.8. Near-UV CD spectra of BSA (——) and 4.6 M urea-denatured BSA in the absence (- - -) and the presence (·····) of 20% (w/v) SHSC at pH 7.4. The protein concentration was 20 μM.

near-UV CD spectrum of the native BSA. Previous studies have also shown the presence of these spectral features in the near-UV CD spectrum of BSA (Pelton & McLean, 2000; Carrotta et al., 2009). The origin of these spectral features has been ascribed to the presence of disulphide bonds and aromatic chromophores (Lee & Hirose, 1992). Decrease in the MRE values at 262 nm and 268 nm, observed in the near-UV CD spectrum of the partially-denatured BSA indicated significant loss in the tertiary structure of the protein (Table 3.4). Significant stabilization of the native protein structure by 20% (w/v) SHSC was evident from the near-UV CD spectrum of the partially-denatured BSA, obtained in the presence of 20% (w/v) SHSC (Figure 3.8). The MRE values at 262 nm and 268 nm were found to be significantly higher (46% and 56%, respectively) than those obtained for 4.6 M urea-denatured BSA (Table 3.4). These results were similar to those obtained with far-UV CD spectra, suggesting stabilizing potential of 20% (w/v) SHSC against urea denaturation of BSA.

3.1.2.3. UV-difference spectra

Figure 3.9 shows UV-difference spectra of the partially-denatured BSA at 4.6 M urea in the absence and the presence of 20% (w/v) SHSC. The UV-difference spectrum of the partially-denatured BSA against native BSA was characterized by the presence of a pronounced trough at 288 nm along with a shoulder at 280 nm. Similar spectral features in the UV-difference spectrum of the urea-denatured BSA have been reported earlier (Ahmad & Qasim, 1995). These spectral features of the UV-difference spectrum were indicative of the microenvironmental perturbation around Tyr residues (Sogami & Ogura, 1973). A slight bulging near 292–295 nm in the UV-difference spectra of 4.6 M urea-denatured BSA both in the absence and the presence of 20 % (w/v) SHSC was suggestive of the microenvironmental fluctuations around Trp residues (Trp-134 and Trp-212) of BSA at 4.6 M urea (Peters, 1996). Presence of 20% (w/v) SHSC offered significant stabilization to BSA against urea denaturation as reflected from the marked

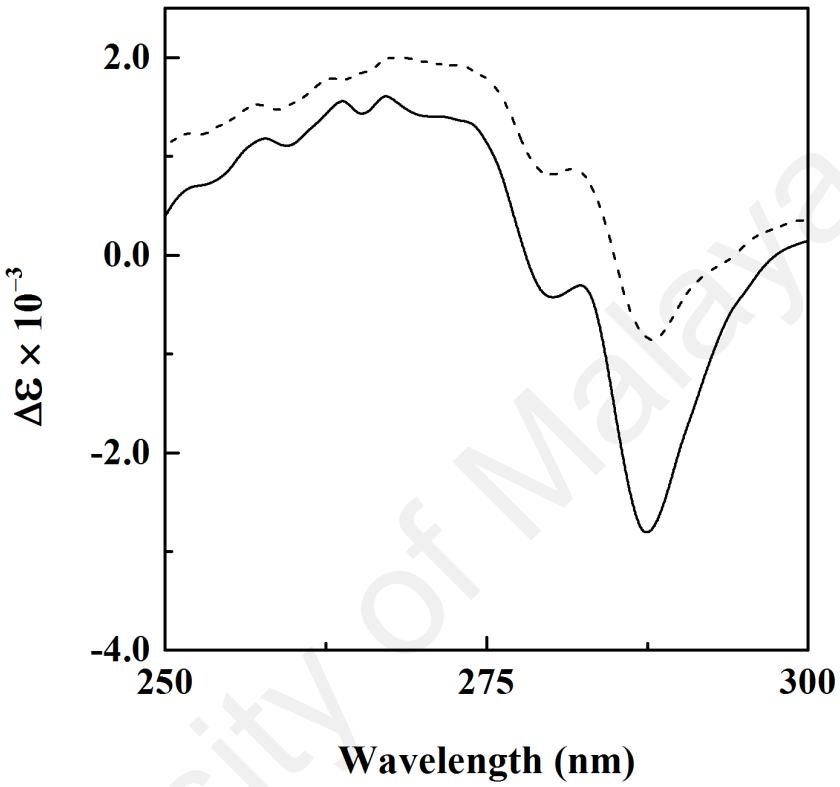

Figure 3.9. UV-difference spectra of 4.6 M urea-denatured BSA in the absence (——) and the presence (- - -) of 20% (w/v) SHSC at pH 7.4. The protein concentration was 20 μM.

decrease in the magnitude of the UV-difference spectrum of the partially-denatured BSA in the presence of 20% (w/v) SHSC. The significant decrease in the molar difference extinction coefficient at 288 nm (Figure 3.9; Table 3.4) suggested stabilization of domains I and II of BSA in the presence 20% (w/v) SHSC, as most of the Tyr residues are located in domains IB and IIB of BSA (Peters, 1996).

3.1.2.4. ANS fluorescence spectra

ANS binding was used to investigate the exposure of hydrophobic regions in BSA under different experimental conditions. Figure 3.10 shows ANS fluorescence spectra of the native BSA and 4.6 M urea-denatured BSA, obtained in the absence and the presence of 20% (w/v) SHSC. ANS in free form shows little fluorescence and produces a marked increase in the fluorescence upon binding to hydrophobic regions in proteins (Stryer, 1965). Native BSA produced a significant ANS fluorescence spectrum in the wavelength range, 400–600 nm, which was suggestive of the presence of significant surface hydrophobicity in the native protein. These results were in accordance to a previous report showing about 10 ANS binding sites available in the native BSA (Cardamone & Puri, 1992). There was a remarkable decrease (88%) in ANS fluorescence in the presence of 4.6 M urea, as shown by ANS fluorescence spectrum of the partially-denatured BSA (Figure 3.10; Table 3.4). Although more hydrophobic residues would have been exposed in 4.6 M urea-denatured BSA, nevertheless, binding of ANS to BSA required the organized hydrophobic clusters instead of individual hydrophobic residues (Horowitz & Butler, 1993), which would have been disorganized in the presence of 4.6 M urea. Additionally, presence of urea would have disrupted the hydrophobic interactions involved in the binding of ANS to these exposed hydrophobic regions (Horowitz & Butler, 1993). In view of the above, decrease in the ANS fluorescence of BSA in the presence of 4.6 M urea was not astonishing. Similar observations on the decrease in ANS fluorescence of other proteins in the presence of urea have been reported earlier

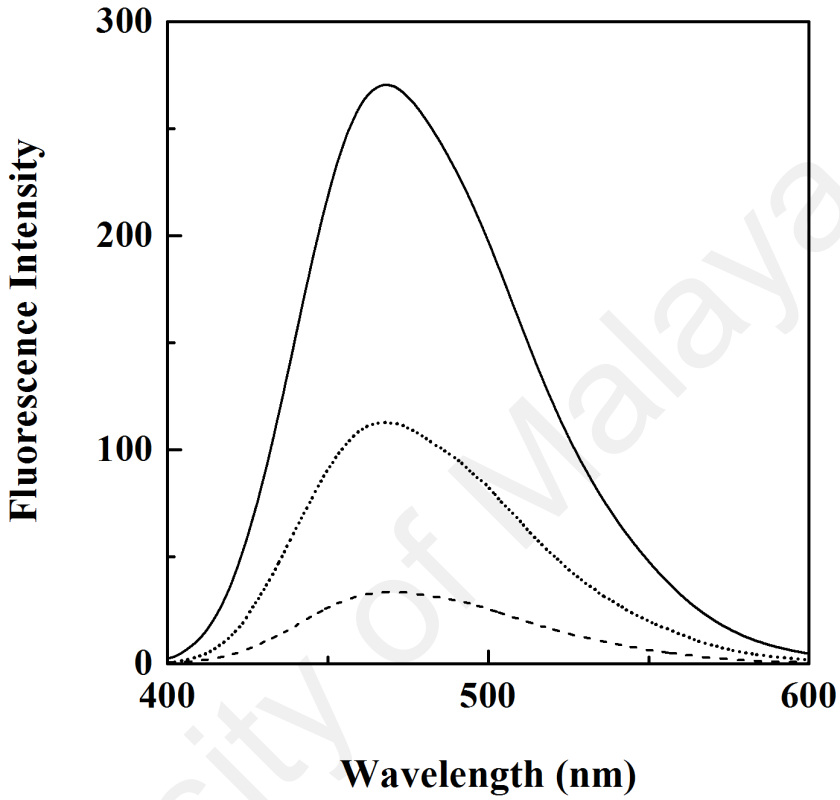

Figure 3.10. ANS fluorescence spectra of BSA (——) and 4.6 M urea-denatured BSA in the absence (- - -) and the presence (·····) of 20% (w/v) SHSC at pH 7.4 upon excitation at 380 nm. The protein concentration was 0.2 μM while the ANS concentration was set as 20 μM.

(Horowitz & Butler, 1993; Botelho et al., 2003). Stabilizing effect of 20% (w/v) SHSC on BSA against urea denaturation can be clearly seen from the ANS fluorescence spectrum of 4.6 M urea-denatured BSA in the presence of 20% SHSC. A significant recovery in the ANS fluorescence exhibited by the partially-denatured BSA in the presence of 20% (w/v) SHSC [3.35 fold higher than that observed in the absence of 20% (w/v) SHSC] indicated significant retention of native-like structure with more hydrophobic clusters in this preparation (Figure 3.10; Table 3.4). These results suggested that the conformation of 4.6 M urea-denatured BSA in the presence of 20% (w/v) SHSC was more conserved.

3.1.2.5. Intrinsic fluorescence spectra

Intrinsic fluorescence spectra of the native BSA and 4.6 M urea-denatured BSA in the absence and the presence of 20% (w/v) SHSC are shown in Figure 3.11. As can be seen from the figure, about 40% reduction in the fluorescence intensity at 341 nm along with 5 nm blue shift were noticed in 4.6 M urea-denatured BSA (Table 3.4), suggesting significant disruption of the protein's tertiary structure. Unfolding of domain III along with rearrangement of domains I and II of BSA may account for the observed changes in the fluorescence characteristics of 4.6 M urea-denatured BSA (Leggio et al., 2009). Interestingly, the fluorescence characteristics of 4.6 M urea-denatured BSA were normalized to a significant extent in the presence of 20% (w/v) SHSC, showing lesser reduction (17%) in the fluorescence intensity at 341 nm and smaller blue shift (3 nm) in the emission maxima (Table 3.4). These fluorescence characteristics of 4.6 M urea-denatured BSA were indicative of protein's tertiary structure stabilization by 20% (w/v) SHSC.

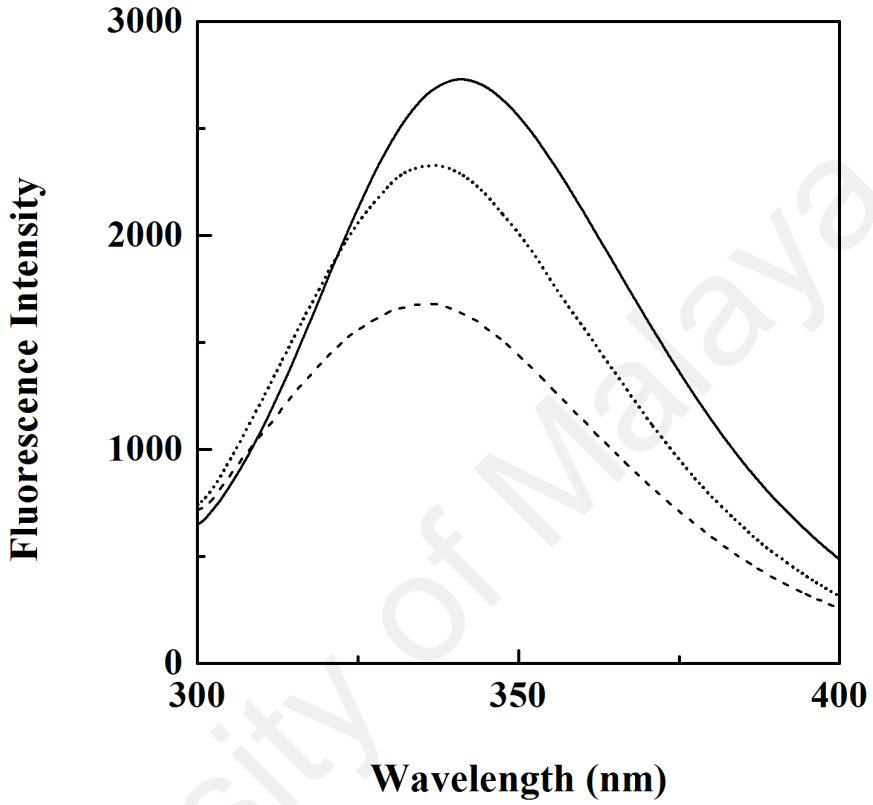

Figure 3.11. Intrinsic fluorescence spectra of BSA (——) and 4.6 M urea-denatured BSA in the absence (- - -) and the presence (·····) of 20% (w/v) SHSC at pH 7.4 upon excitation at 280 nm. The protein concentration was 2 μM. The spectrum of 4.6 M urea-denatured BSA in the presence of 20% (w/v) SHSC was normalized with the help of the spectrum of native BSA, obtained in the presence of 20% (w/v) SHSC.

3.1.2.6. Three-dimensional fluorescence spectra

Three-dimensional fluorescence has been used as probe to study conformational changes in protein (Li et al., 2011; Deng & Liu, 2012; Shahani et al., 2014). The 3-D fluorescence spectra and corresponding contour maps of the native BSA and the partially-denatured BSA at 4.6 M urea in the absence and the presence of 20% (w/v) SHSC are shown in Figures 3.12 and 3.13, respectively. The spectral characteristics of the 3-D fluorescence spectra are listed in Table 3.5. As shown in Figures 3.12 and 3.13, peaks 'a' and 'b' represented the Rayleigh scattering peak ($\lambda_{em} = \lambda_{ex}$) and the second-order scattering peak ($\lambda_{em} = 2\ \lambda_{ex}$), respectively. Two additional peaks, namely, 'peak 1' (λ_{ex} = 280 nm) and 'peak 2' (λ_{ex} = 230 nm), representing protein fluorescence peaks were also observed. Both these peaks mainly revealed the spectral behavior of Tyr and Trp residues in the three-dimensional structure of the protein. The emission maxima and the fluorescence intensity of the peaks characterize the polarity of the fluorophores' microenvironment (Deng & Liu, 2012). Presence of 4.6 M urea significantly reduced the fluorescence intensity of peaks '1' and '2' compared to that obtained with the native BSA in a ratio of 0.67:1.00 and 0.42:1.00, respectively (Figure 3.12; Table 3.5). In addition, 5 nm and 9 nm blue shift in the emission maxima of peaks '1' and '2', respectively, were also noticed (Table 3.5). Decrease in the fluorescence intensity of both peaks in the presence of 4.6 M urea may result from the unfolding of domain III leading to a loss in the tertiary structure of BSA, whereas rearrangement of domains I and II may account for the observed blue shift (Leggio et al., 2009). Interestingly, there was a significant recovery in the fluorescence intensity of both peaks of 4.6 M urea-denatured BSA in the presence of 20% (w/v) SHSC, as the ratio of the fluorescence intensity of peaks 1 and peak 2 of 4.6 M urea-denatured BSA to that of native BSA was increased to 0.88:1.00 and 0.53:1.00, respectively, in the presence of 20% (w/v) SHSC. Furthermore, increase in the blue shift of peak 1 (9 nm) observed with 4.6 M urea-denatured BSA in the presence

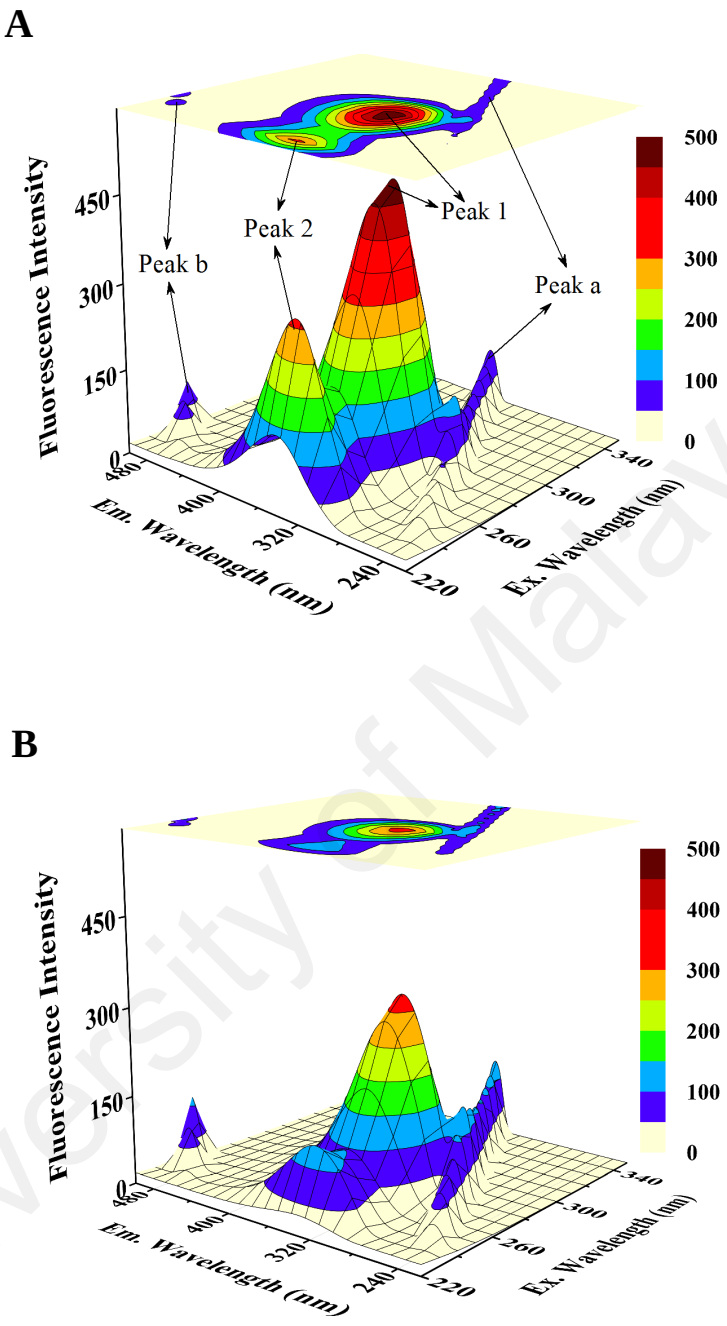

Figure 3.12. Three-dimensional fluorescence spectra and corresponding contour maps of BSA (A) and 4.6 M urea-denatured BSA (B). The protein concentration was 2 μM.

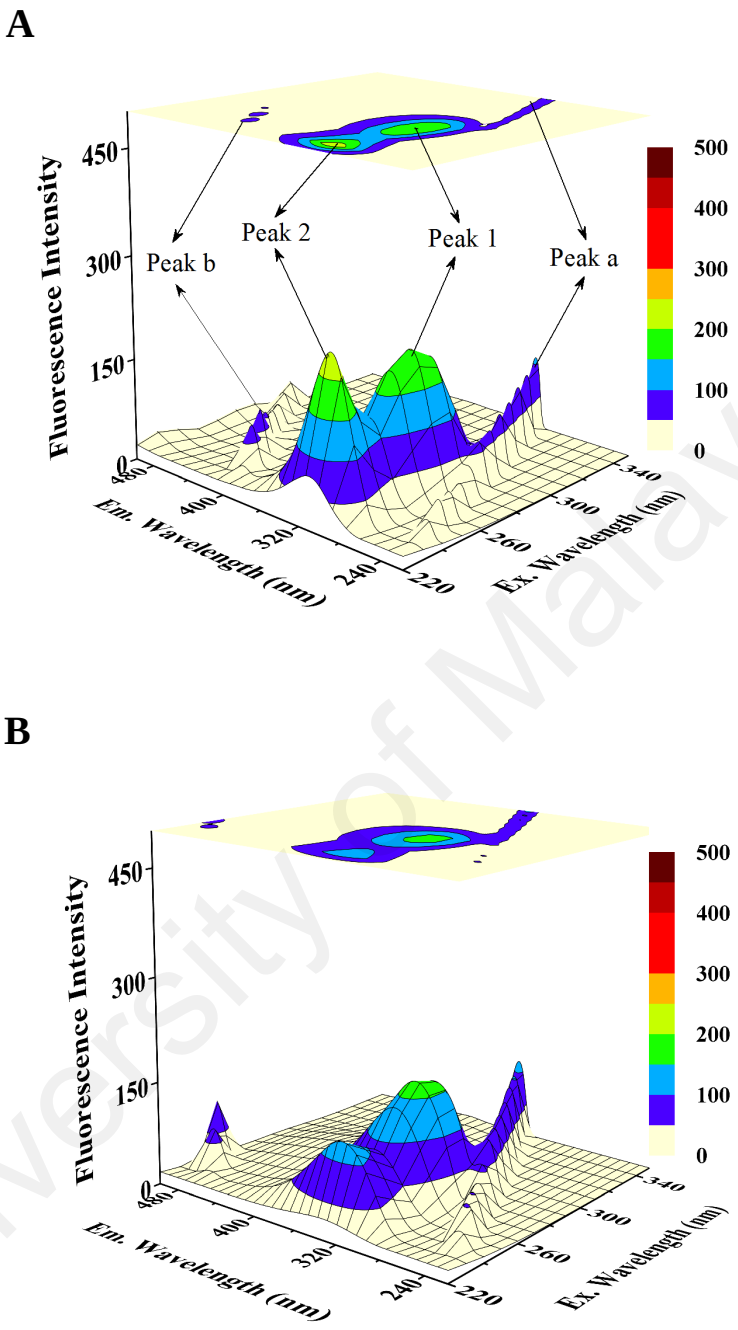

Figure 3.13. Three-dimensional fluorescence spectra and corresponding contour maps of BSA (A) and 4.6 M urea-denatured BSA (B) both in the presence of 20% (w/v) SHSC. The protein concentration was 2 μM.

Table 3.5. Three-dimensional fluorescence spectral characteristics of BSA under various experimental conditions.

Protein sample	Peak	Peak position [$\lambda_{ex}/\lambda_{em}$ (nm/nm)]	Intensity
Native BSA	a	230/230 → 350/350	17.7 → 91.8
	b	250/500	85.9
	1	280/341	485.2
	2	230/341	313.7
4.6 M urea-denatured BSA	a	230/230 → 350/350	16.8 → 129.8
	b	250/500	114.5
	1	280/336	324.1
	2	230/332	132.2
Native BSA + 20% (w/v) SHSC	a	230/230 → 350/350	17.1 → 108.2
	b	250/500	80.3
	1	280/339	182.1
	2	230/342	233.8
4.6 M urea-denatured BSA + 20% (w/v) SHSC	a	230/230 → 350/350	15.4 → 114.9
	b	250/500	92.5
	1	280/330	160.0
	2	230/332	124.8

of 20% (w/v) SHSC may be ascribed to a greater internalization of Trp residues, as compared to the shift noticed in the absence of 20% (w/v) SHSC. The stabilizing effect of 20% (w/v) SHSC on the tertiary structure of protein, as shown by 3-D fluorescence spectral results was in agreement with the near-UV CD spectral results, shown in Figure 3.8.

3.1.3. GdnHCl denaturation of BSA in the absence and the presence of SHSC

Protein stabilizing potential of SHSC was further evaluated using GdnHCl denaturation studies of BSA in the absence and the presence of 20% (w/v) SHSC. Figure 3.14 shows the far-UV CD spectra of BSA, obtained in the absence and the presence of increasing GdnHCl (0–5.5 M) concentrations. The far-UV CD spectra, obtained at lower (< 1.4 M) and higher (> 5.5 M) GdnHCl concentrations showed minimal difference in the spectral signal and therefore, are omitted for clarity. The far-UV CD spectra of BSA in the presence of GdnHCl could not be recorded below 212–219 nm due to high signal to noise ratio. Similar to the effect observed in the presence of urea, MRE values of BSA showed a gradual reduction with increasing GdnHCl concentrations, which was suggestive of protein denaturation.

The MRE_{222nm} values, obtained from these spectra were normalized and plotted against GdnHCl concentrations. Figure 3.15 shows GdnHCl denaturation curves of BSA in the absence and the presence of 20% (w/v) SHSC, as studied by MRE_{222nm} measurements. The GdnHCl denaturation of BSA was characterized by a single-step, two-state transition, which started at 1.3 M and completed at 5.5 M GdnHCl concentrations. A previous study on denaturation of serum albumin by GdnHCl has shown similar results (Muzammil et al., 2000a). The denaturation curve of BSA was shifted towards a higher GdnHCl concentration in the presence of 20% (w/v) SHSC, showing the start- and the mid-points of the transition at 1.6 M and 2.3 M GdnHCl against

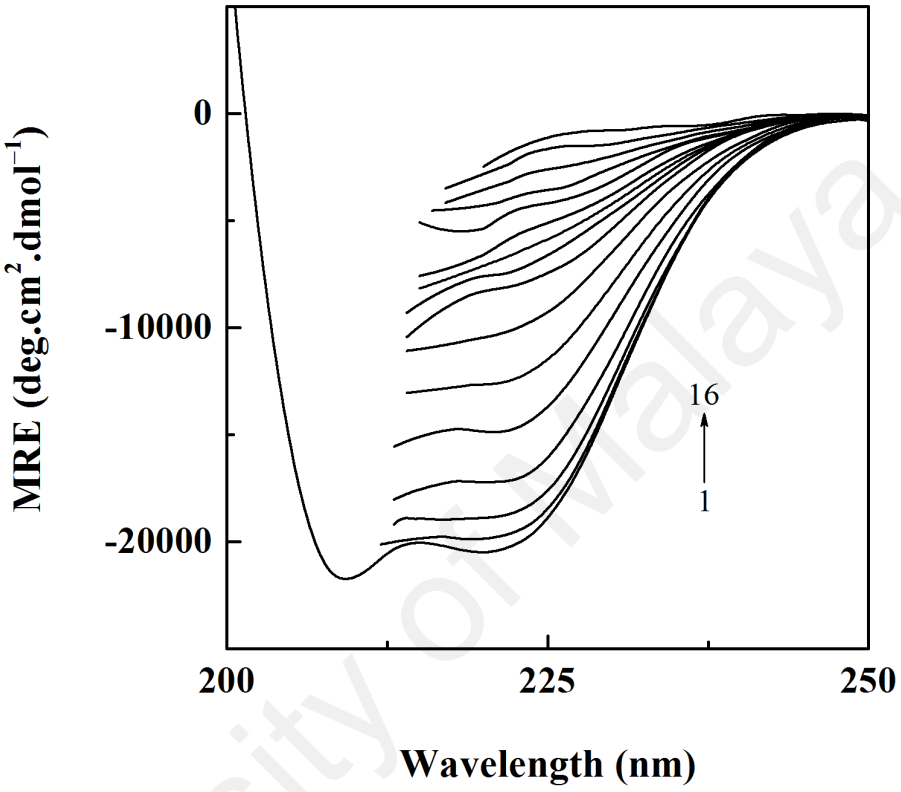

Figure 3.14. Far-UV CD spectra of BSA (2 μM), obtained in 60 mM sodium phosphate buffer, pH 7.4 in the absence and the presence of increasing GdnHCl concentrations (0–5.5 M GdnHCl). The GdnHCl concentrations (from bottom to top) were: 0, 1.4, 1.5, 1.6, 1.75, 1.8, 1.95, 2.25, 2.5, 2.75, 3.0, 3.5, 4.0, 4.5, 5.0 and 5.5 M.

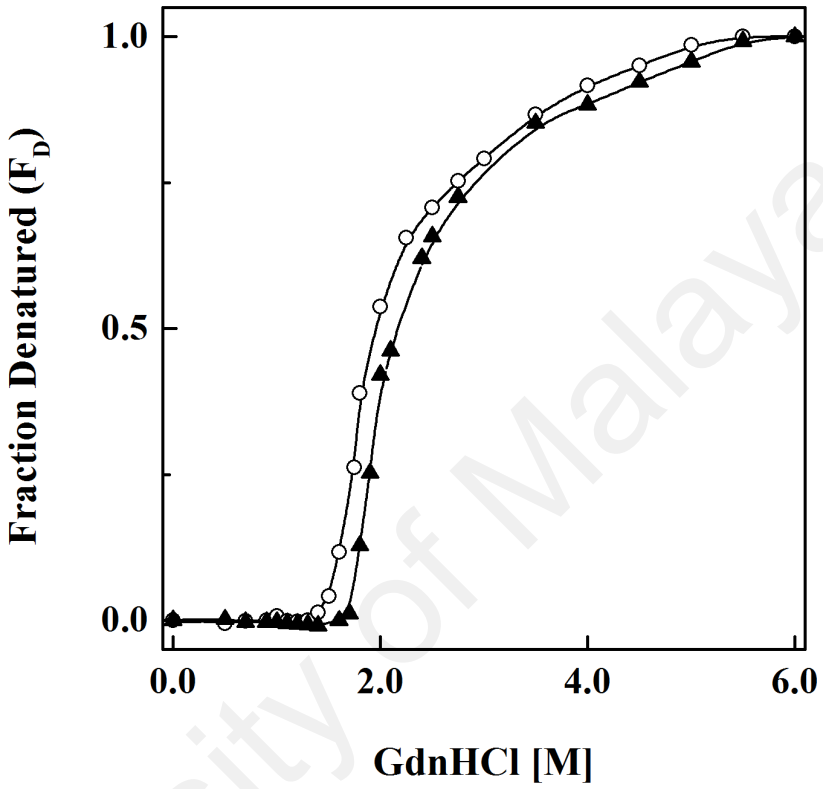

Figure 3.15. Normalized GdnHCl denaturation curves of BSA (2 μM) in 60 mM sodium phosphate buffer, pH 7.4, as studied by MRE_{222nm} measurements in the absence (○) and the presence of 20% (▲) (w/v) SHSC.

1.3 M and 1.9 M GdnHCl, respectively, observed in its absence (Table 3.6). The shift of the whole transition curve was indicative of protein stabilization by 20% (w/v) SHSC. A lesser shift in the GdnHCl denaturation curve compared to that observed with urea denaturation curve in the presence of 20% (w/v) SHSC can be attributed to the stronger protein denaturing action of GdnHCl (Greene & Pace, 1974). As supportive evidence, the far-UV CD spectra of the native BSA and the partially-denatured BSA at 1.9 M GdnHCl in the absence and the presence of 20% (w/v) SHSC are shown in Figure 3.16. The far-UV CD spectrum of 1.9 M GdnHCl-denatured BSA in the presence of 20% (w/v) SHSC showed a significant shift towards the native spectrum of BSA within the whole wavelength range studied, which indicated significant retention of the secondary structural characteristics, particularly, α-helical content. Values of the MRE_{222nm} and respective α-helical content of the native BSA and 1.9 M GdnHCl-denatured BSA in the absence and the presence of 20% (w/v) SHSC are given in Table 3.6. As can be seen from the table, the α-helical content of 1.9 M GdnHCl-denatured BSA increased from ~25% to ~40% in the presence of 20% (w/v) SHSC, suggestive of SHSC-induced protein stabilization.

3.1.4. Thermal denaturation of BSA in the absence and the presence of SHSC

Thermal denaturation profiles of BSA, as monitored by MRE_{222nm} in the absence and the presence of 20% (w/v) SHSC are shown in Figure 3.17. As can be seen from the figure, the MRE_{222nm} value of BSA decreased with increasing temperature, indicative of structural disruption of BSA. However, the decrease was found slower within the temperature range, 25–45°C, became more pronounced during 45–80°C and slowed down above 85°C. Increase in enthalpy change within 45–80°C was primarily responsible for the observed structural disorganization (Makhatadze et al., 1993). Similar helical structural changes within this temperature range have been shown earlier (Moriyama et al., 2003; 2008). Thermal denaturation of BSA in the presence of 20% (w/v) SHSC

Table 3.6. Characteristics of GdnHCl denaturation of BSA in the absence and the presence of 20% (w/v) SHSC, as monitored by MRE_{222nm} measurements.

Characteristics	BSA	BSA + 20% (w/v) SHSC
GdnHCl-induced transition		
– Start-point [M]	1.3 ± 0.06	1.6 ± 0.06
– Mid-point [M]	1.9 ± 0.06	2.3 ± 0.08
Far-UV CD spectra		
– MRE at 222 nm ($deg.cm^2.dmol^{-1}$) [α-Helical content[a]]		
• Native	–20,353.7 ± 135 [~59 ± 0.44%]	–20,227.1 ± 78 [~59 ± 0.26%]
• 1.9 M GdnHCl-denatured	–9,800.1 ± 76 [~25 ± 0.25%]	–14,423.3 ± 212 [~40 ± 0.70%]

Each value is expressed as the mean ± SD of three independent experiments.
[a] Calculated by the method of Chen et al. (1972).

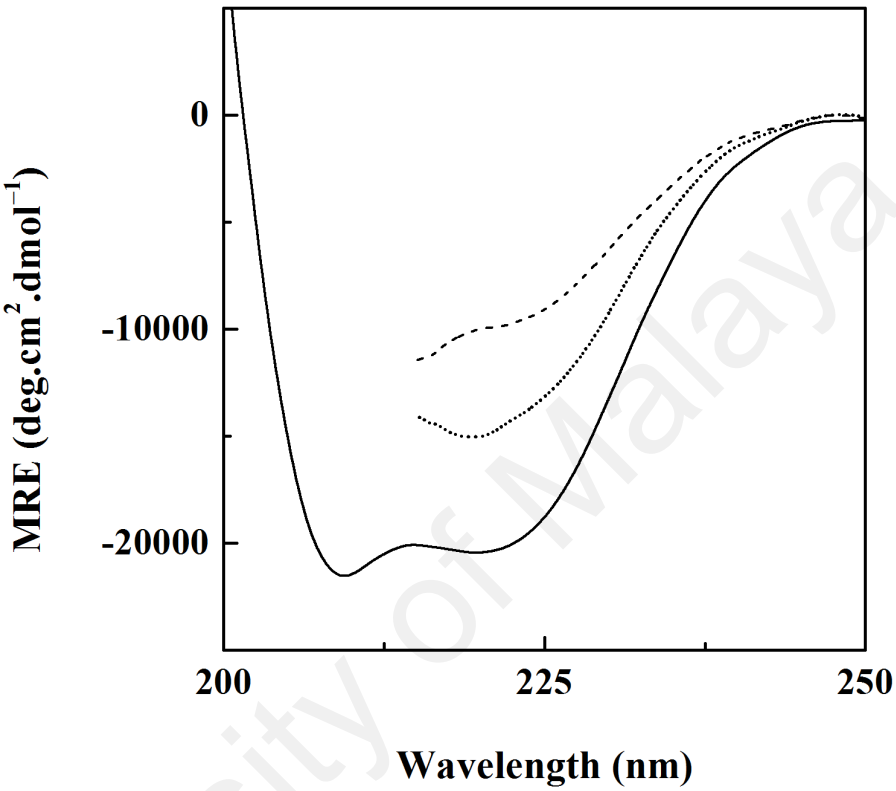

Figure 3.16. Far-UV CD spectra of BSA (——) and 1.9 M GdnHCl-denatured BSA in the absence (- - -) and the presence (·····) of 20% (w/v) SHSC at pH 7.4. The protein concentration was 2 μM.

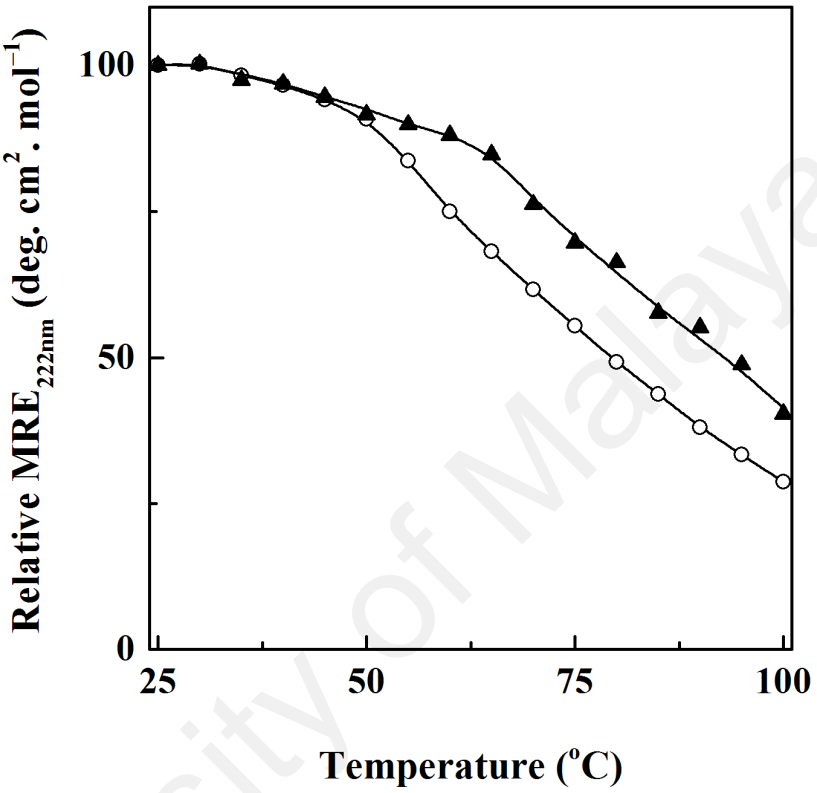

Figure 3.17. Thermal denaturation curves of BSA (2 μM) in 60 mM sodium phosphate buffer, pH 7.4, as studied by MRE_{222nm} measurements in the absence (○) and the presence of 20% (▲) (w/v) SHSC.

followed the similar pattern up to 45°C, as that observed in the absence of 20% (w/v) SHSC. In contrast, it showed extension in the slow phase up to 60°C beyond which a sharp decrease in the MRE_{222nm} value was noticed up to 100°C in the presence of 20% (w/v) SHSC (Figure 3.17; Table 3.7). In other words, thermal denaturation curve of BSA in the presence of 20% (w/v) SHSC was shifted towards higher temperature range, indicating thermal stabilization of BSA induced by SHSC. At any given temperature within the temperature range, 60–100°C, values of the MRE_{222nm}, representing the α-helical content in BSA, were found higher in the presence of 20% (w/v) SHSC compared to those obtained in its absence.

Figure 3.18 shows the far-UV CD spectra of BSA at 25°C as well as 65°C in the absence and the presence of 20% (w/v) SHSC. As evident from the figure, the far-UV CD spectrum of BSA at 65°C showed lesser secondary structural features (~35% α-helix) than those obtained at 25°C (~60% α-helix), indicative of thermal denaturation (Table 3.7). However, the far-UV CD spectrum of BSA obtained at 65°C but in the presence of 20% (w/v) SHSC showed significant retention in the secondary structures (~46% α-helix), which was suggestive of protein stabilization by 20% (w/v) SHSC (Table 3.7). The spectra of BSA at 65°C, obtained in the presence of 20% (w/v) SHSC could not be recorded below 208 nm due to high signal to noise ratio.

No sign of Maillard reaction in the SHSC-BSA mixture was seen up to 85°C. However, little Maillard reaction occurred at temperatures above 85°C. This would not affect the overall conclusion that 20% (w/v) SHSC provided significant thermal stabilization to BSA as indicated in Figures 3.17 and 3.18 within the temperature range, 50−85°C. Moreover, in a previous study on the thermal denaturation of ribonuclease A in the presence of reducing sugars, Poddar et al. (2008) have not observed the occurrence of Maillard reaction up to 85°C.

Table 3.7. Characteristics of thermal denaturation of BSA in the absence and the presence of 20% (w/v) SHSC, as monitored by MRE_{222nm} measurements

Characteristics	BSA	BSA + 20% (w/v) SHSC
Thermal-induced transition (Second phase)		
– Start-point (°C)	45 ± 1.0	60 ± 1.8
Far-UV CD spectra		
– MRE at 222 nm ($deg.cm^2.dmol^{-1}$) [α-Helical content[a]]		
• 25°C	–20,370.6 ± 135 [~60 ± 0.45%]	–20,244.0 ± 68 [~59 ± 0.23%]
• 65°C	–12,972.0 ± 116 [~35 ± 0.38%]	–16,317.0 ± 128 [~46 ± 0.42%]

Each value is expressed as the mean ± SD of three independent experiments.
[a] Calculated by the method of Chen et al. (1972).

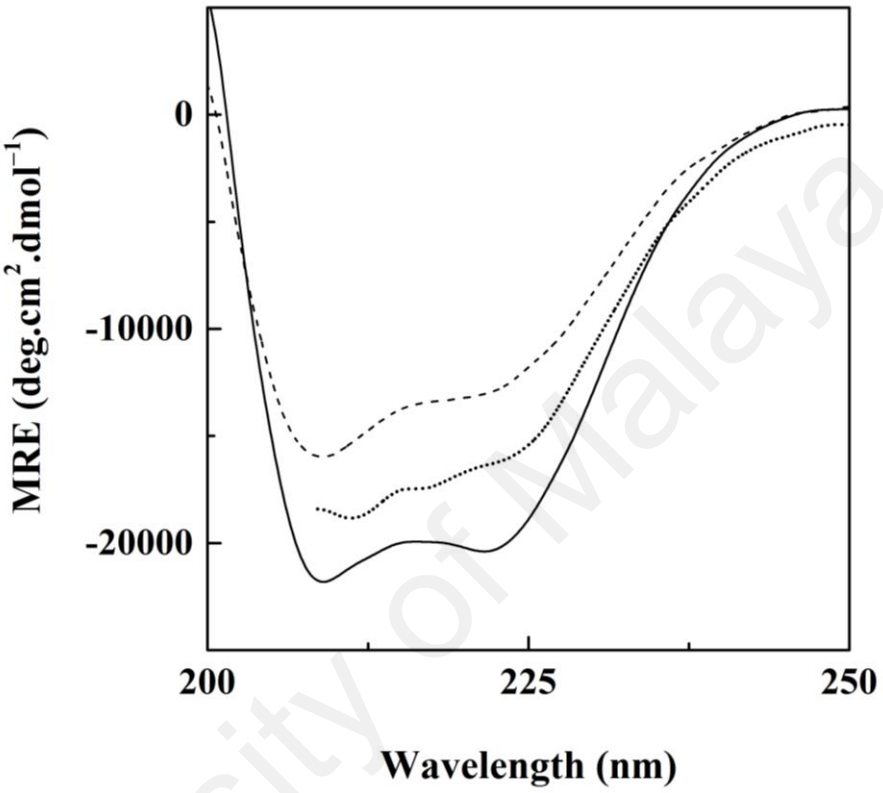

Figure 3.18. Far-UV CD spectra of BSA at 25°C (——) and 65°C in the absence (- - -) and the presence (·····) of 20% (w/v) SHSC at pH 7.4. The protein concentration was 2 μM.

3.2. SHSC-induced stabilization of ovalbumin

The stabilizing effect of SHSC was studied on another model protein, ovalbumin against chemical (urea and GdnHCl) and thermal denaturations.

3.2.1. Urea denaturation of ovalbumin in the absence and the presence of SHSC

Far-UV CD and Trp fluorescence spectroscopy were used to study urea denaturation of ovalbumin in the absence and the presence of different SHSC concentrations.

3.2.1.1. Far-UV CD spectra

The far-UV CD spectra of ovalbumin, obtained in the absence and the presence of increasing urea (3.3–8.5 M) concentrations are shown in Figure 3.19. The far-UV CD spectra of ovalbumin at lower (< 3.3 M) and higher (> 8.5 M) urea concentrations showed smaller changes in the spectral signal and are therefore omitted for clarity. Furthermore, the far-UV CD spectra of ovalbumin in the presence of urea could not be recorded below 210–215 nm due to high signal to noise ratio. Presence of two minima at 208 nm and 222 nm characterized the far-UV CD spectrum of ovalbumin due to the presence of the α-helical structure (Batra & Uetrecht, 1990). However, ovalbumin showed a lesser magnitude of the MRE values compared to those observed with BSA (Figure 3.1). The MRE values of ovalbumin gradually decreased in the presence of increasing urea concentrations, suggesting protein denaturation with the loss in the secondary structure. The decrease in the MRE value at 222 nm was used to probe urea denaturation of ovalbumin. Denaturation data, obtained in the absence and the presence of SHSC were normalized in the same way as described in the section 2.2.6.3 and were plotted against urea concentration (Figure 3.20).

Unlike the two-step, three-state urea transition of BSA, urea denaturation of ovalbumin displayed a single-step, two-state transition, which started at 3.2 M urea and

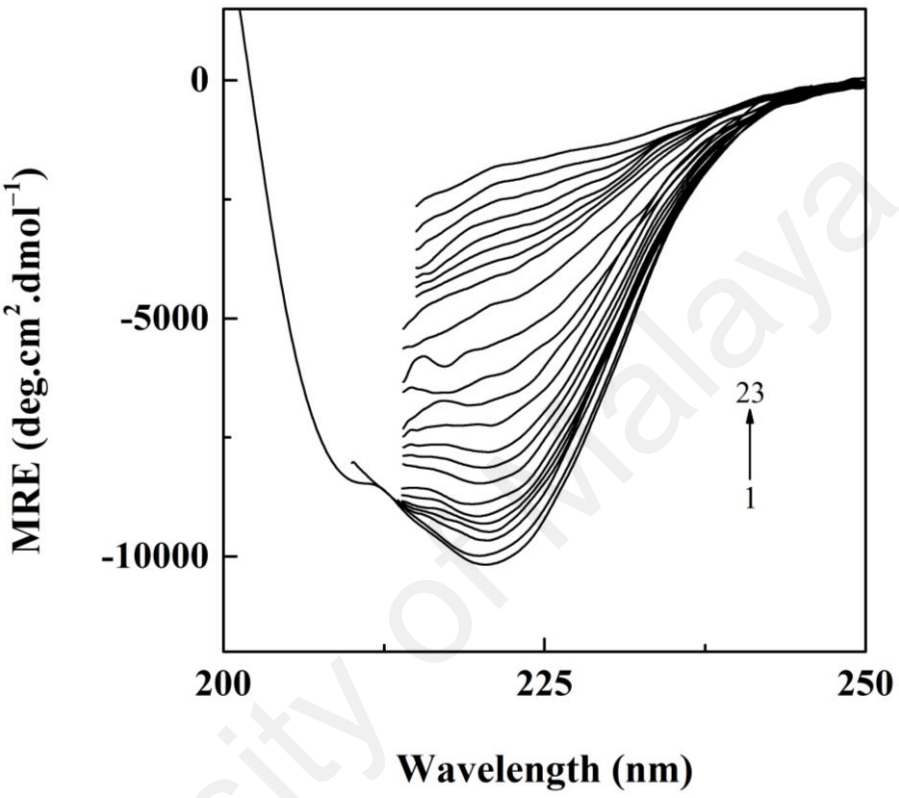

Figure 3.19. Far-UV CD spectra of ovalbumin (5 μM), obtained in 60 mM sodium phosphate buffer, pH 7.4 in the absence and the presence of increasing urea concentrations (0–8.5 M urea). The urea concentrations (from bottom to top) were: 0, 3.3, 3.5, 3.8, 4.0, 4.2, 4.4, 4.6, 5.0, 5.2, 5.4, 5.6, 5.8, 6.0, 6.2, 6.4, 6.6, 6.8, 7.0, 7.25, 7.5, 8.0 and 8.5 M.

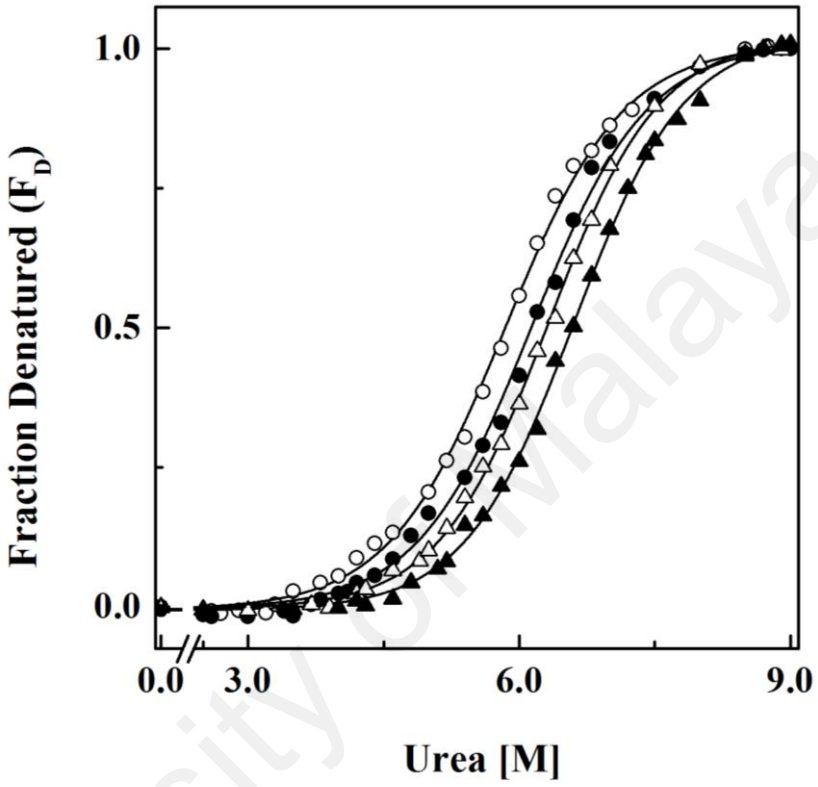

Figure 3.20. Normalized urea denaturation curves of ovalbumin (5 μM) in 60 mM sodium phosphate buffer, pH 7.4, as studied by MRE_{222nm} measurements in the absence (○) and the presence of 8% (●), 10% (△) or 20% (▲) (w/v) SHSC.

ended at 8.5 M urea with the occurrence of the mid-point at 5.9 M urea (Figure 3.20; Table 3.8). The nature of the denaturation curve of ovalbumin was in close agreement with the denaturation curve shown in a previous report, using UV-difference absorption spectroscopy (Glazer et al., 1963). Interestingly, the denaturation curve of ovalbumin was shifted towards higher urea concentrations in the presence of different SHSC concentrations, suggesting protein's secondary structure stabilization. This shift was characterized by the increase in the start- and the mid-points of the transition curve, being more significant at higher SHSC concentrations. Evidently, the start- and the mid-points of the transition curve were shifted from 3.2 M and 5.9 M urea (for ovalbumin) to 4.3 M and 6.6 M urea, respectively, in the presence of 20% (w/v) SHSC (Figure 3.20; Table 3.8).

3.2.1.2. Tryptophan fluorescence spectra

SHSC-induced stabilization of ovalbumin against urea denaturation was also supported by Trp fluorescence results. Figure 3.21 shows the Trp fluorescence spectra of ovalbumin, obtained in the absence and the presence of increasing urea (3.4–8.5 M) concentrations upon excitation at 295 nm. The fluorescence spectra below 3.4 M and above 8.5 M urea are not included in the Figure 3.21 due to their coinciding nature. The Trp fluorescence spectrum of ovalbumin was featured by the presence of an emission maxima at 336 nm, spectral characteristic of Trp residues in proteins (Royer, 2006). This agreed well with previous reports, showing occurrence of the emission maxima at the same wavelength (Tani et al., 1997; Naeem et al., 2011). Presence of increasing urea concentrations in the incubation mixture produced a progressive decrease in the fluorescence intensity of ovalbumin at 336 nm and red shift in the emission maxima (Figure 3.21). About 59% decrease in the fluorescence intensity at 336 nm along with 15 nm red shift in the emission maxima were observed in the presence of 8.5 M urea. Both these changes in the fluorescence characteristics of ovalbumin were indicative of

Table 3.8. Characteristics of urea denaturation of ovalbumin in the absence and the presence of different SHSC concentrations, as monitored by MRE_{222nm} measurements.

Protein sample	Urea-induced transition		
	Start-point [M]	Mid-point [M]	End-point [M]
Ovalbumin	3.2 ± 0.10	5.9 ± 0.06	8.5 ± 0.00
Ovalbumin + 8% (w/v) SHSC	3.5 ± 0.06	6.1 ± 0.03	8.5 ± 0.10
Ovalbumin + 10% (w/v) SHSC	3.9 ± 0.03	6.3 ± 0.06	8.5 ± 0.12
Ovalbumin + 20% (w/v) SHSC	4.3 ± 0.06	6.6 ± 0.06	8.5 ± 0.06

Each value is expressed as the mean ± SD.

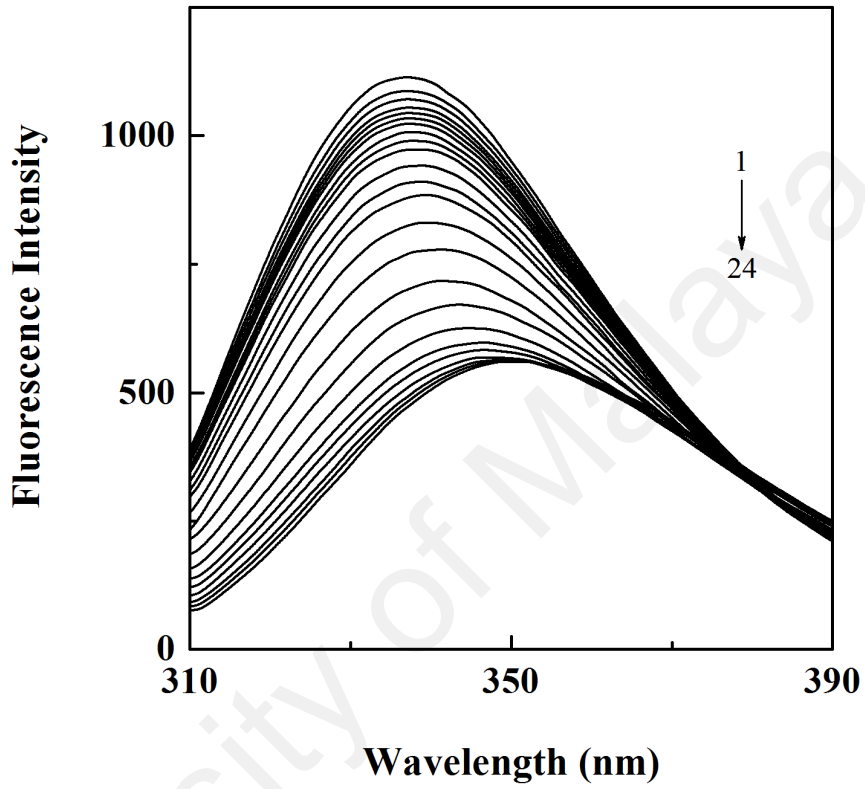

Figure 3.21. Fluorescence spectra of ovalbumin (2.5 μM), obtained in 60 mM sodium phosphate buffer, pH 7.4 in the absence and the presence of increasing urea concentrations (0–8.5 M urea) upon excitation at 295 nm. The urea concentrations (from top to bottom) were: 0, 3.4, 3.6, 3.7, 3.9, 4.0, 4.2, 4.4, 4.6, 4.8, 5.0, 5.2, 5.4, 5.6, 5.8, 6.0, 6.2, 6.4, 6.6, 6.8, 7.0, 7.5, 8.0 and 8.5 M.

significant alteration in the microenvironment around Trp residues from non-polar to polar (Tani et al., 1997), owing to protein denaturation with loss in the tertiary structure.

Urea denaturation results of ovalbumin, as followed by Trp fluorescence measurements at 336 nm (Figure 3.21) yielded the denaturation curve shown in Figure 3.22 upon treatment in the same way as described for Figure 3.20. The denaturation curve of ovalbumin was found to be qualitatively similar to that obtained with MRE_{222nm} measurements in terms of the transition pattern (Figures 3.20; 3.22). However, quantitative differences were noticed in the mid- and the end-points of the denaturation curve, as the values were found to be 5.6 M and 8.0 M urea against 5.9 M and 8.5 M urea, respectively, obtained with MRE_{222nm} measurements (Tables 3.8; 3.9). Nonetheless, these results were in accordance with previous report on urea denaturation of ovalbumin, as monitored by fluorescence measurements (Covaciu et al., 2004). Addition of SHSC to ovalbumin produced a shift in the denaturation curve towards higher urea concentrations (Figure 3.22), suggesting SHSC-induced protein's tertiary structure stabilization against urea denaturation. In particular, the start- and the mid-points of the transition curve were increased from 3.2 M and 5.6 M urea to 4.6 M and 6.7 M urea, respectively, in the presence of 20% (w/v) SHSC (Table 3.9). Small differences in the transition characteristics obtained from MRE_{222nm} and Trp fluorescence measurements can be attributed to the use of different probes and have been observed earlier (Kishore et al., 2012; Zaroog & Tayyab, 2012).

3.2.2. Characterization of the partially-denatured ovalbumin in the absence and the presence of SHSC

The protein stabilizing effect of SHSC on ovalbumin was further evaluated by equilibrating 5.9 M urea-denatured ovalbumin, representing the partially-denatured state at the mid-point of the transition, with 20% (w/v) SHSC. Characterization of all three

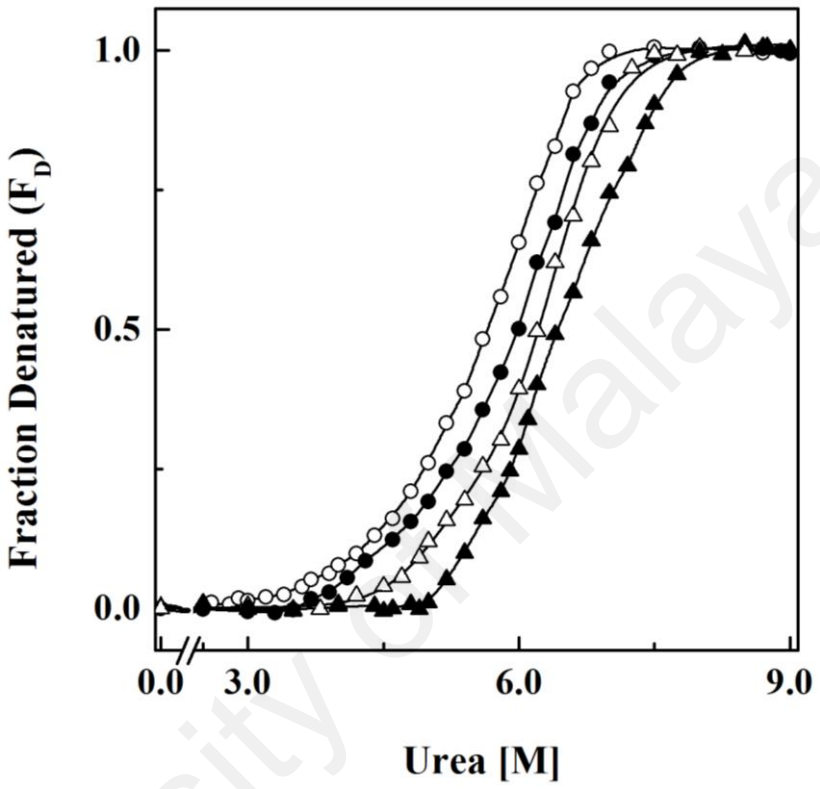

Figure 3.22. Normalized urea denaturation curves of ovalbumin (2.5 μM) in 60 mM sodium phosphate buffer, pH 7.4, as studied by Trp fluorescence measurements at 336 nm upon excitation at 295 nm in the absence (○) and the presence of 8% (●), 10% (△) or 20% (▲) (w/v) SHSC.

Table 3.9. Characteristics of urea denaturation of ovalbumin in the absence and the presence of different SHSC concentrations, as monitored by tryptophan fluorescence measurements at 336 nm upon excitation at 295 nm.

Protein sample	Urea-induced transition		
	Start-point [M]	Mid-point [M]	End-point [M]
Ovalbumin	3.2 ± 0.10	5.6 ± 0.06	8.0 ± 0.00
Ovalbumin + 8% (w/v) SHSC	3.5 ± 0.03	5.9 ± 0.03	8.0 ± 0.10
Ovalbumin + 10% (w/v) SHSC	4.0 ± 0.12	6.2 ± 0.06	8.0 ± 0.14
Ovalbumin + 20% (w/v) SHSC	4.6 ± 0.06	6.7 ± 0.06	8.0 ± 0.00

Each value is expressed as the mean ± SD of three independent experiments.

states of the protein [native, 5.9 M urea-denatured ovalbumin in the absence and the presence of 20% (w/v) SHSC] was made by far-UV CD, near-UV CD, UV-difference ANS fluorescence, Trp fluorescence and 3-D fluorescence spectra.

3.2.2.1. Far-UV CD spectra

Figure 3.23 shows the effect of 20% (w/v) SHSC on the secondary structure stabilization of 5.9 M urea-denatured ovalbumin. The far-UV CD spectrum of the native ovalbumin is also included in the figure. Although the spectral signal at 222 nm was retained in the far-UV CD spectrum of 5.9 M urea-denatured ovalbumin (Figure 3.23), MRE_{222nm} value was significantly reduced (44%), indicating loss in the protein's secondary structures (Figure 3.23 and Table 3.10). The spectral signal at 208 nm could not be detected due to high signal to noise ratio below 214 nm. A lesser decrease (11%) in the MRE_{222nm} value of 5.9 M urea-denatured ovalbumin, observed in the presence of 20% (w/v) SHSC, suggested significant retention of the secondary structure in 5.9 M urea-denatured ovalbumin in the presence of 20% (w/v) SHSC. In addition to the minima at 222 nm, another minima at 218 nm was also visible in the far-UV CD spectra of 5.9 M urea-denatured ovalbumin in the absence and the presence of 20% (w/v) SHSC. The induced signal at 218 nm in 5.9 M urea-denatured ovalbumin reflected the formation of β-structure (Pearce et al., 2007), concomitant to the loss in the α-helical structure.

The calculated α-helical content of the native ovalbumin was found to be ~27%, which was in agreement with the previously reported value (Timasheff & Gorbunoff, 1967). However, the α-helical content in 5.9 M urea-denatured ovalbumin was reduced to ~12% (Table 3.10). On the other hand, presence of 20% (w/v) SHSC showed a significant retention in the α-helical content (~23%) in 5.9 M urea-denatured ovalbumin. Such stabilizing effect was significant, as the value of the α-helical content was slightly lower than that of the native ovalbumin.

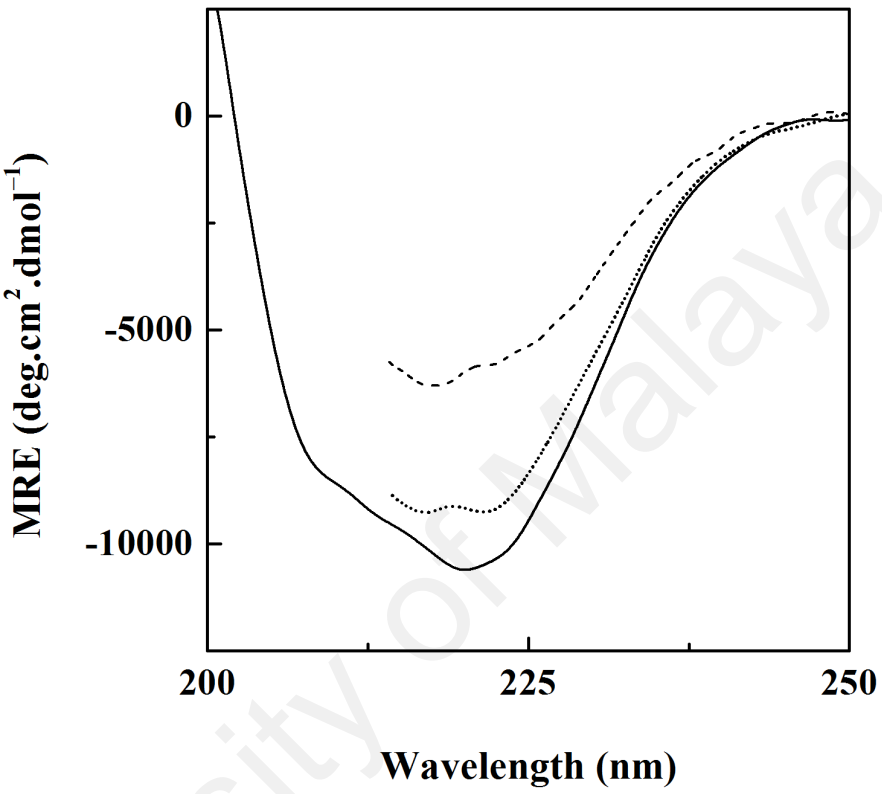

Figure 3.23. Far-UV CD spectra of ovalbumin (——) and 5.9 M urea-denatured ovalbumin in the absence (- - -) and the presence (·····) of 20% (w/v) SHSC at pH 7.4. The protein concentration was 5 μM.

Table 3.10. Spectral characteristics of ovalbumin under various experimental conditions, as monitored by different probes.

Spectral characteristics	Native ovalbumin	5.9 M urea-denatured ovalbumin	5.9 M urea-denatured ovalbumin + 20% (w/v) SHSC
Far-UV CD spectra			
– MRE at 222 nm (deg.cm^2.dmol^{-1})	–10,426.6 ± 208	–5,810.6 ± 92	–9,233.8 ± 146
– α-Helical content[a]	~27 ± 0.68%	~12 ± 0.30%	~23 ± 0.48%
Near-UV CD spectra			
– MRE at 260 nm (deg.cm^2.dmol^{-1})	76.2 ± 3.81	–24.2 ± 0.31	56.6 ± 1.44
– MRE at 268 nm (deg.cm^2.dmol^{-1})	78.1 ± 4.41	–51.2 ± 0.72	20.9 ± 0.51
– MRE at 276 nm (deg.cm^2.dmol^{-1})	114.3 ± 5.37	–29.9 ± 0.33	31.6 ± 0.84
UV-difference spectra			
– Molar difference extinction coefficient at 287 nm	–	– 2.8 ± 0.03 × 10^3	– 0.8 ± 0.01 × 10^3
– Molar difference extinction coefficient at 293 nm	–	– 2.4 ± 0.03 × 10^3	– 0.7 ± 0.01 × 10^3
ANS fluorescence spectra			
– Fluorescence intensity at 470 nm	30.6 ± 0.20	44.7 ± 0.60	33.5 ± 3.50
– Emission maximum (nm)	470 ± 0.00	489 ± 1.15	485 ± 0.58
Tryptophan fluorescence spectra			
– Fluorescence intensity at 336 nm	1,111.2 ± 1.31	655.2 ± 13.15	964.8 ± 3.50
– Emission maximum (nm)	336 ± 0.58	343 ± 1.00	338 ± 0.00

Each value is expressed as the mean ± SD of three independent experiments.
[a] Calculated by the method of Chen et al. (1972).

3.2.2.2. Near-UV CD spectra

Figure 3.24 shows the near-UV CD spectra of 5.9 M urea-denatured ovalbumin in the absence and the presence of 20% (w/v) SHSC as well as that of the native ovalbumin. The near-UV CD spectrum of the native ovalbumin was identified by the presence of five peaks at 260 nm, 268 nm, 276 nm, 282 nm and 292 nm, which was similar to that shown in an earlier report (Naeem et al., 2011). Occurrence of these peaks can be assigned to the presence of disulphide bonds and aromatic chromophores in the protein (Kelly et al., 2005). The MRE values of the three major peaks occurring at 260 nm, 268 nm and 276 nm, in different states of ovalbumin are listed in Table 3.10. Presence of 5.9 M urea affected the near-UV CD spectrum of the native ovalbumin by reducing the MRE values of all peaks, suggesting significant loss in the tertiary structure. However, presence of 20% (w/v) SHSC prevented disruption of the tertiary structure of the protein to a significant extent as revealed by the increased MRE values (Table 3.10), indicating tertiary structure stabilization by 20% (w/v) SHSC.

3.2.2.3. UV-difference spectra

The UV-difference spectra of 5.9 M urea-denatured ovalbumin in the absence and the presence of 20% (w/v) SHSC are shown in Figure 3.25. Presence of two negative peaks at 287 nm and 293 nm along with a shoulder around 281 nm defined the UV-difference spectrum of 5.9 M urea-denatured ovalbumin. Appearance of a negative peak at 287 nm and a shoulder at 281 nm in the UV-difference spectrum characterized the microenvironmental alteration around Tyr residues while a negative signal around 293 nm indicated change in the polarity around Trp residues. An earlier report has also identified similar spectral features in the UV-difference spectrum of ovalbumin under various denaturation conditions (Qasim & Salahuddin, 1978). A significant reduction (71%) in the molar difference extinction coefficient values at 287 nm and 293 nm in the

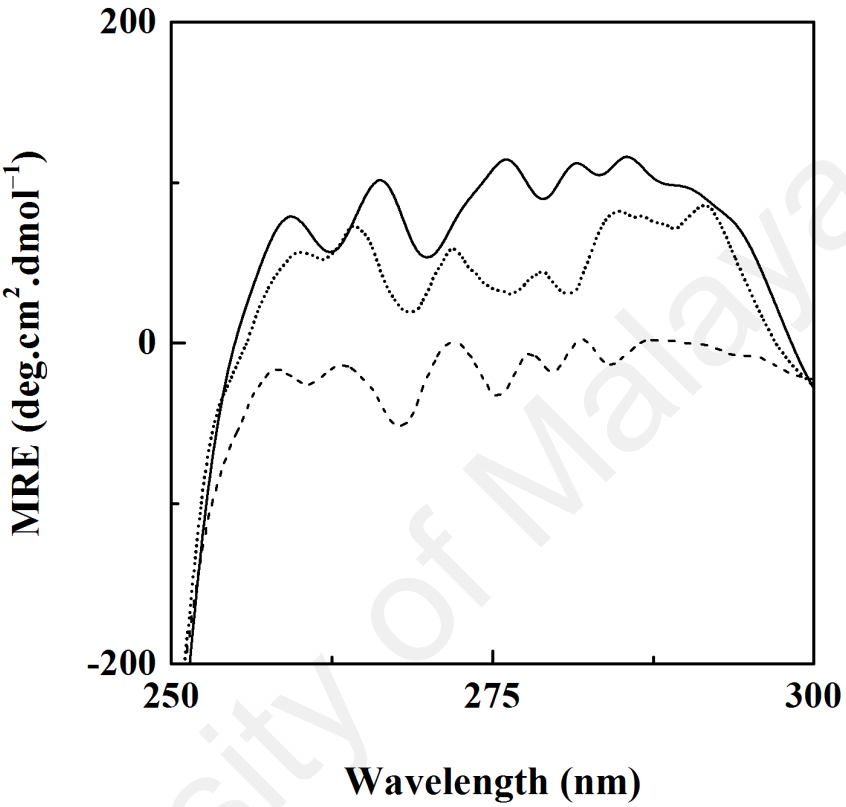

Figure 3.24. Near-UV CD spectra of ovalbumin (——) and 5.9 M urea-denatured ovalbumin in the absence (- - -) and the presence (·····) of 20% (w/v) SHSC at pH 7.4. The protein concentration was 40 μM.

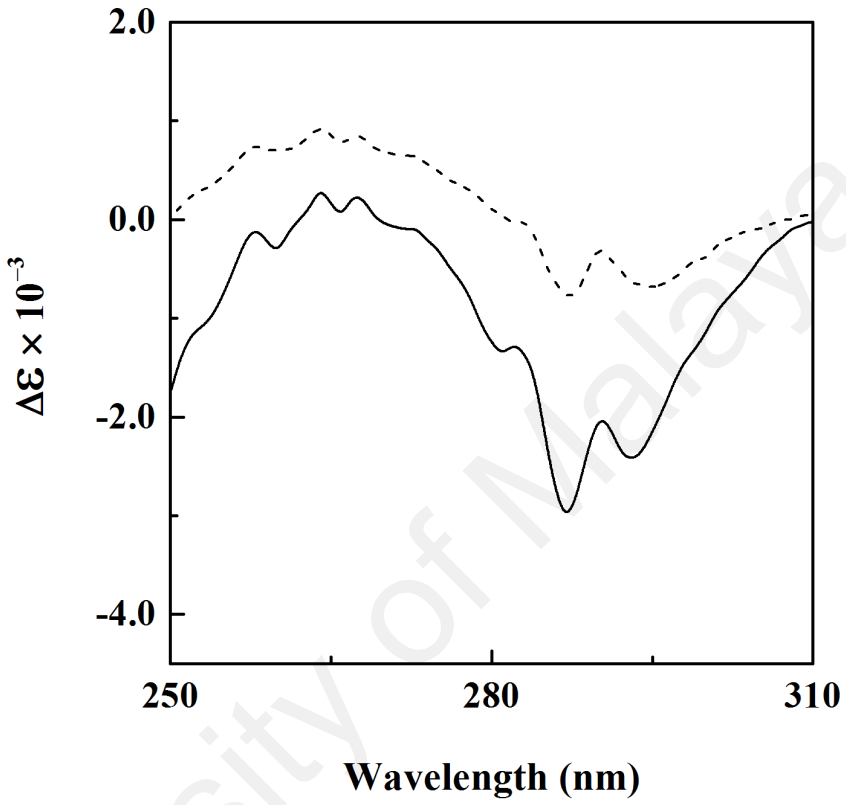

Figure 3.25. UV-difference spectra of 5.9 M urea-denatured ovalbumin in the absence (——) and the presence (- - -) of 20% (w/v) SHSC at pH 7.4. The protein concentration was 40 μM.

presence of 20% (w/v) SHSC compared to those observed in its absence (Figure 3.25; Table 3.10) clearly indicated SHSC-induced tertiary structure stabilization of 5.9 M urea-denatured ovalbumin.

3.2.2.4. ANS fluorescence spectra

ANS fluorescence spectra of the native ovalbumin as well as 5.9 M urea-denatured ovalbumin in the absence and the presence of 20% (w/v) SHSC are shown in Figure 3.26. Native ovalbumin produced significant ANS fluorescence due to surface hydrophobicity and was in agreement with a previous report (Naeem et al., 2011). ANS fluorescence intensity of 5.9 M urea-denatured ovalbumin at 470 nm showed 46% increase along with 19 nm red shift in the emission maxima (Figure 3.26; Table 3.10), which were suggestive of the exposure of buried hydrophobic regions in 5.9 M urea-denatured ovalbumin (Naeem et al., 2011). However, addition of 20% (w/v) SHSC in the incubation mixture produced significant retention in the fluorescence characteristics (Figure 3.26; Table 3.10), indicating stabilization of the folded tertiary structure in 5.9 M urea-denatured ovalbumin.

3.2.2.5. Tryptophan fluorescence spectra

Figure 3.27 shows the effect of 20% (w/v) SHSC on the Trp fluorescence characteristics of 5.9 M urea-denatured ovalbumin. The fluorescence intensity of 5.9 M urea-denatured ovalbumin at 336 nm decreased by 41% along with 7 nm red shift in the emission maxima (Figure 3.27; Table 3.10), in comparison to the fluorescence characteristics of the native ovalbumin. Such changes in the fluorescence characteristics indicated alteration in the microenvironment around Trp residues from non-polar to polar, owing to tertiary structure destabilization. A recovery in the fluorescence intensity (28%) of 5.9 M urea-denatured ovalbumin in the presence of 20% (w/v) SHSC along with normalization of the emission maxima (Figure 3.27; Table 3.10) were suggestive of lesser

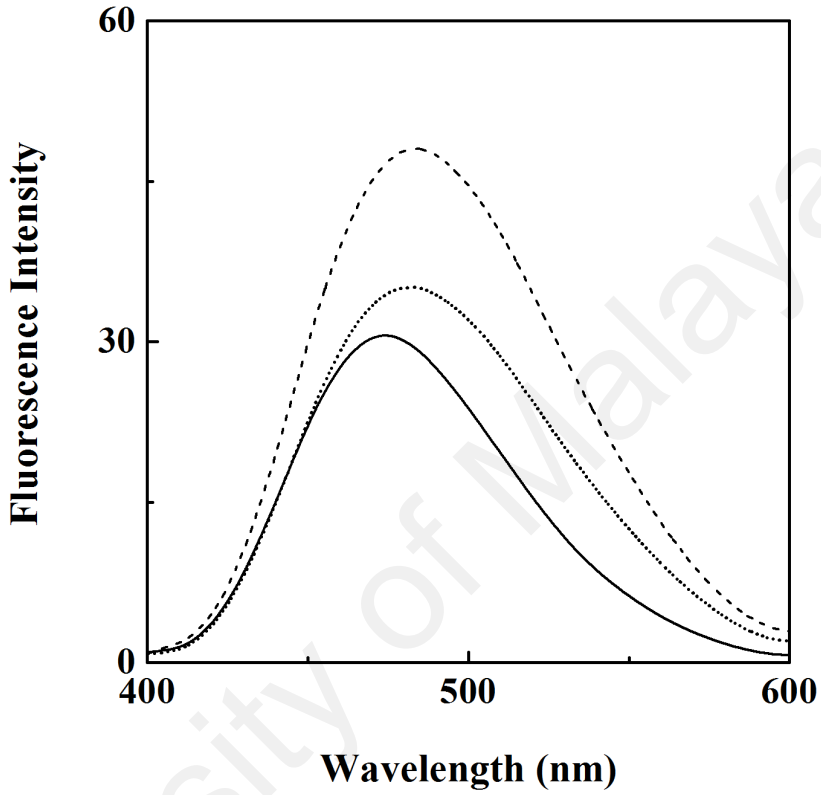

Figure 3.26. ANS fluorescence spectra of ovalbumin (——) and 5.9 M urea-denatured ovalbumin in the absence (- - -) and the presence (·····) of 20% (w/v) SHSC at pH 7.4 upon excitation at 380 nm. The protein concentration was 0.2 μM while the ANS concentration was set as 20 μM.

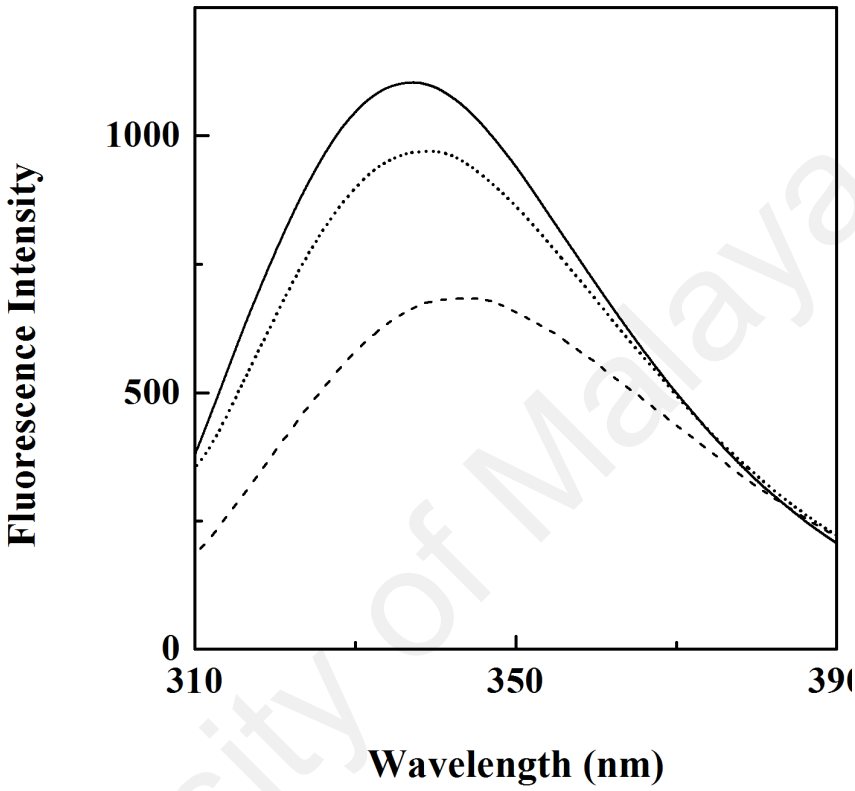

Figure 3.27. Tryptophan fluorescence spectra of ovalbumin (——) and 5.9 M urea-denatured ovalbumin in the absence (- - -) and the presence (·····) of 20% (w/v) SHSC at pH 7.4 upon excitation at 295 nm. The protein concentration was 2.5 μM. The spectrum of 5.9 M urea-denatured ovalbumin in the presence of 20% (w/v) SHSC was normalized with the help of the spectrum of native ovalbumin, obtained in the presence of 20% (w/v) SHSC.

perturbation in the microenvironment around Trp residues, implying tertiary structure stabilization by 20% (w/v) SHSC.

3.2.2.6. Three-dimensional fluorescence spectra

Three-dimensional fluorescence spectral measurements were carried out to get more insight about tertiary structural changes in ovalbumin under different experimental conditions. Figures 3.28 and 3.29 show the 3-D fluorescence spectra and corresponding contour maps of the native and 5.9 M urea-denatured ovalbumins in the absence and the presence of 20% (w/v) SHSC, respectively. Similar to those observed with BSA, the four peaks were identified in the 3-D fluorescence spectra of the native and 5.9 M urea-denatured ovalbumins under these conditions. Out of these peaks, peak 1 (λ_{ex} = 280 nm) and peak 2 (λ_{ex} = 230 nm) represented protein fluorescence peaks, which were indicative of spectral behavior of Tyr and Trp residues in the protein. The fluorescence intensity of both peaks '1' and '2' in 5.9 M urea-denatured ovalbumin was significantly decreased in a ratio of 0.80:1.00 and 0.31:1.00, respectively, compared to that obtained with the native ovalbumin (Figures 3.28; Table 3.11). A red shift of 7 nm and 4 nm in the emission maxima of peaks '1' and '2', respectively, was also noticed (Table 3.11). Both these observations were suggestive of microenvironmental changes around Tyr and Trp residues from non-polar to polar due to 5.9 M urea-induced tertiary structural disruption. However, a recovery in the fluorescence intensity along with normalization of the emission maxima of both peaks '1' and '2' were observed in the presence of 20% (w/v) SHSC (Figure 3.29; Table 3.11), which suggested tertiary structure stabilization of 5.9 M urea-denatured ovalbumin by 20% (w/v) SHSC.

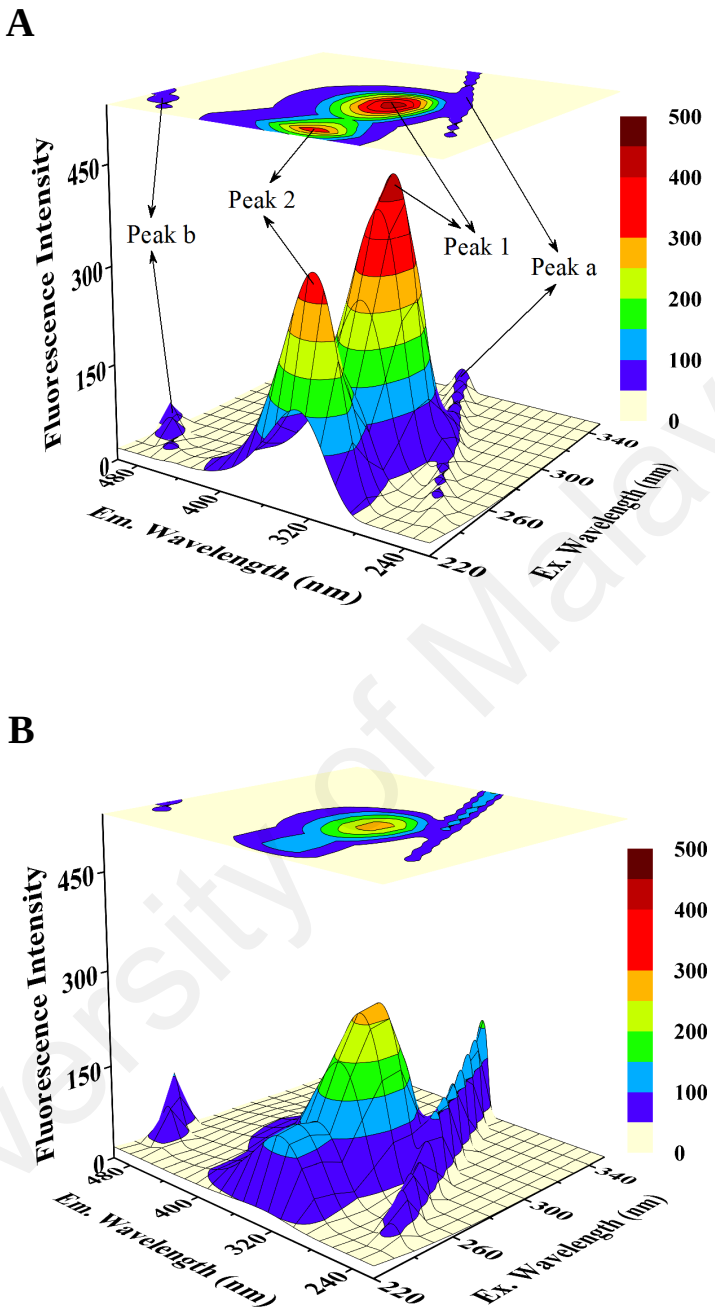

Figure 3.28. Three-dimensional fluorescence spectra and corresponding contour maps of ovalbumin (A) and 5.9 M urea-denatured ovalbumin (B). The protein concentration was 2.5 μM.

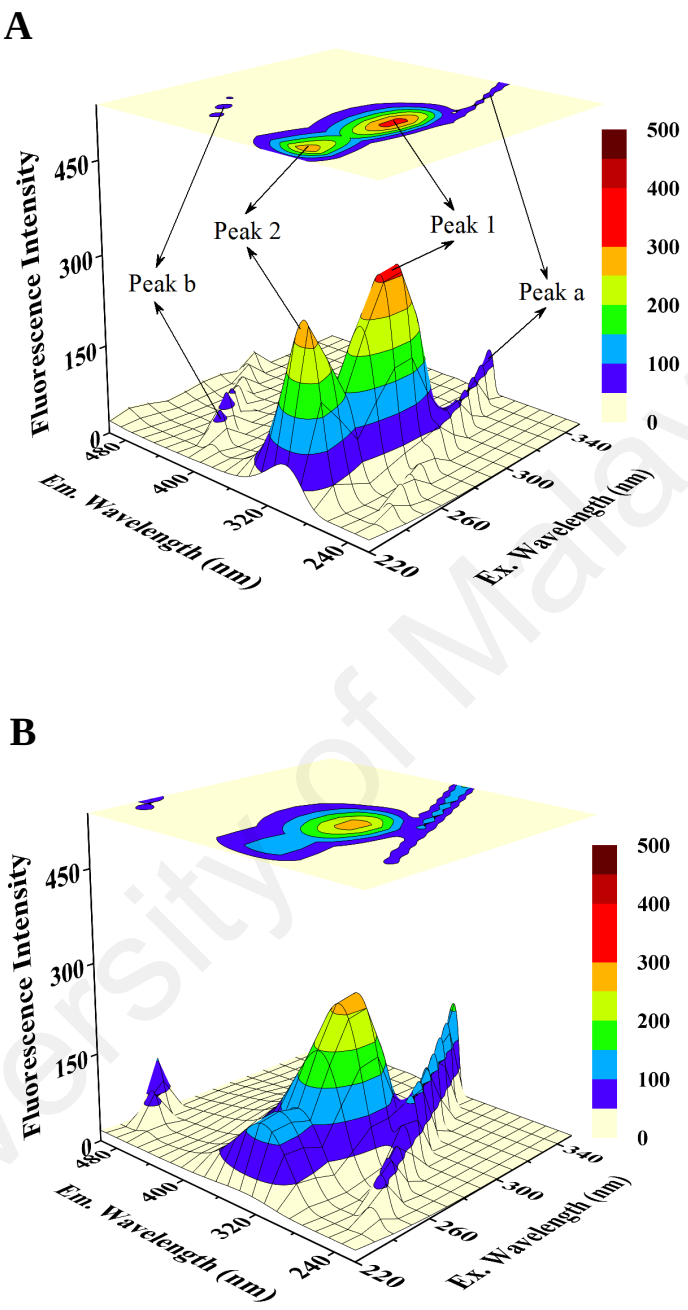

Figure 3.29. Three-dimensional fluorescence spectra and corresponding contour maps of ovalbumin (A) and 5.9 M urea-denatured ovalbumin (B) both in the presence of 20% (w/v) SHSC. The protein concentration was 2.5 μM.

Table 3.11. Three-dimensional fluorescence spectral characteristics of ovalbumin under various experimental conditions.

Protein sample	Peak	Peak position [$\lambda_{ex}/\lambda_{em}$ (nm/nm)]	Intensity
Native ovalbumin	a	230/230 → 350/350	17.5 → 37.5
	b	250/500	49.4
	1	280/334	445.0
	2	230/333	363.2
5.9 M urea-denatured ovalbumin	a	230/230 → 350/350	18.2 → 279.6
	b	250/500	168.7
	1	280/341	354.6
	2	230/337	112.5
Native ovalbumin + 20% (w/v) SHSC	a	230/230 → 350/350	17.5 → 76.9
	b	250/500	76.6
	1	280/334	314.9
	2	230/333	287.8
5.9 M urea-denatured ovalbumin + 20% (w/v) SHSC	a	230/230 → 350/350	16.1 → 161.5
	b	250/500	106.0
	1	280/334	269.5
	2	230/334	122.6

3.2.3. GdnHCl denaturation of ovalbumin in the absence and the presence of SHSC

Protein stabilizing effect of SHSC on ovalbumin against GdnHCl denaturation was studied using far-UV CD spectroscopy. The far-UV CD spectra of ovalbumin in the presence of increasing GdnHCl concentrations (Figure 3.30) were found similar to those observed in the presence of urea (Figure 3.19), showing a progressive decrease in the MRE values with increasing denaturant concentrations. The far-UV CD spectra of ovalbumin at lower (< 1.2 M) and higher (> 5.0 M) GdnHCl concentrations are omitted due to their overlapping nature. Furthermore, high signal to noise ratio in the far-UV CD spectra of ovalbumin, observed in the presence of GdnHCl, prevented the spectral recording below 210–220 nm.

Figure 3.31 shows normalized GdnHCl denaturation curves of ovalbumin, as monitored by MRE_{222nm} measurements. GdnHCl denaturation of ovalbumin exhibited a single-step transition, starting at 1.0 M GdnHCl and completed at 5.0 M GdnHCl with the occurrence of the mid-point at 2.2 M GdnHCl (Figure 3.31; Table 3.12). This result was in accordance with a previous report on GdnHCl denaturation of ovalbumin, as monitored by UV-difference absorption spectroscopy (Ahmad & Salahuddin, 1976). In the presence of 20% (w/v) SHSC, the transition curve shifted towards higher GdnHCl concentrations (Figure 3.31), showing increase in the start- and the mid-point values to 1.6 M and 2.5 M GdnHCl, respectively (Table 3.12). These results suggested SHSC-induced secondary structure stabilization of ovalbumin against GdnHCl denaturation.

Figure 3.32 shows the far-UV CD spectra of the native ovalbumin and the partially-denatured ovalbumin, obtained at the mid-point of transition (2.2 M GdnHCl-denatured ovalbumin) in the absence and the presence of 20% (w/v) SHSC. The secondary structure of 2.2 M GdnHCl-denatured ovalbumin was significantly reduced, as revealed by a large

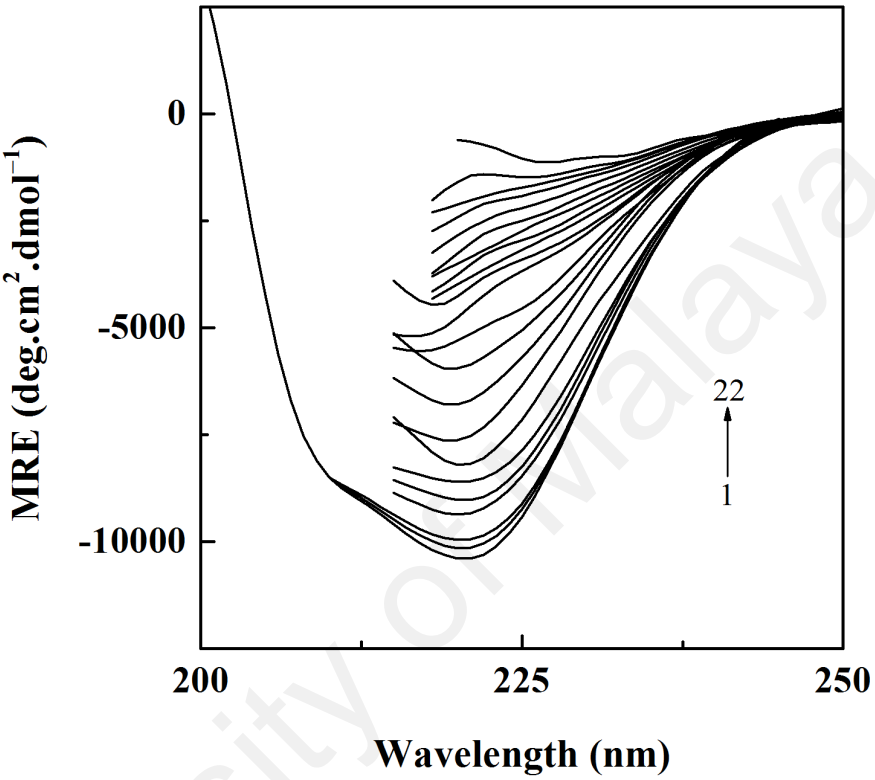

Figure 3.30. Far-UV CD spectra of ovalbumin (5 μM), obtained in 60 mM sodium phosphate buffer, pH 7.4 in the absence and the presence of increasing GdnHCl concentrations (0–5.0 M GdnHCl). The GdnHCl concentrations (from bottom to top) were: 0, 1.2, 1.3, 1.5, 1.6, 1.7, 1.8, 2.0, 2.1, 2.2, 2.4, 2.6, 2.8, 3.0, 3.2, 3.4, 3.5, 3.75, 4.0, 4.25, 4.5 and 5.0 M.

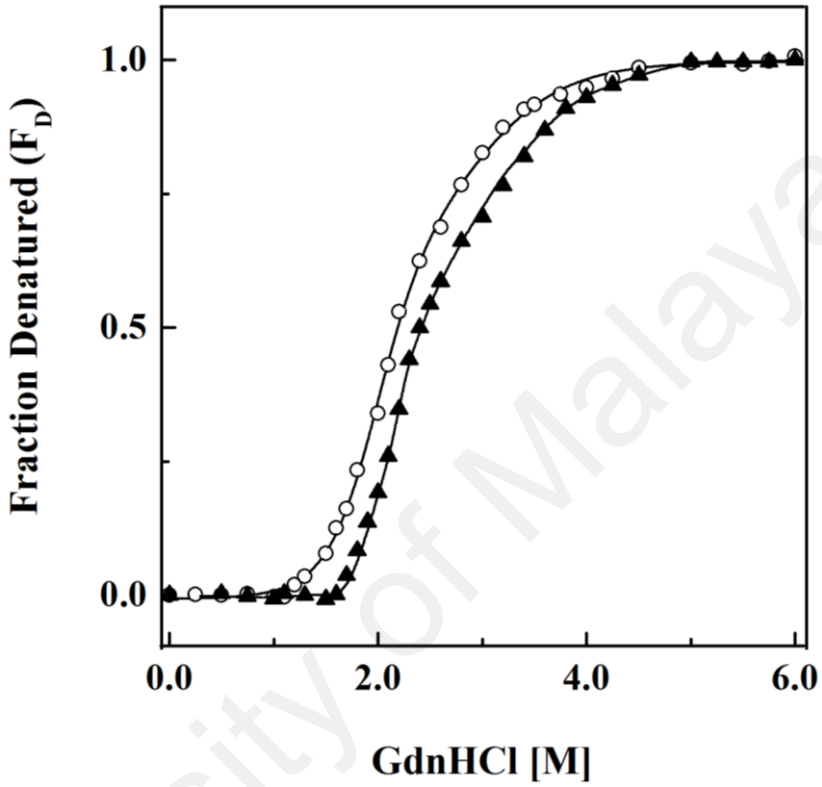

Figure 3.31. Normalized GdnHCl denaturation curves of ovalbumin (5 μM) in 60 mM sodium phosphate buffer, pH 7.4, as studied by MRE_{222nm} measurements in the absence (○) and the presence of 20% (▲) (w/v) SHSC.

Table 3.12. Characteristics of GdnHCl denaturation of ovalbumin in the absence and the presence of 20% (w/v) SHSC, as monitored by MRE_{222nm} measurements

Characteristics	Ovalbumin	Ovalbumin + 20% (w/v) SHSC
GdnHCl-induced transition		
– Start-point [M]	1.0 ± 0.06	1.6 ± 0.06
– Mid-point [M]	2.2 ± 0.06	2.5 ± 0.06
– End-point [M]	5.0 ± 0.00	5.0 ± 0.00
Far-UV CD spectra		
– MRE at 222 nm ($deg.cm^2.dmol^{-1}$) [α-Helical content[a]]		
• Native	–10,426.6 ± 208 [~27 ± 0.68%]	–10,632.0 ± 208 [~27 ± 0.68%]
• 2.2 M GdnHCl-denatured	–5,579.3 ± 88 [~11 ± 0.29%]	–7,590.5 ± 125 [~19 ± 0.42%]

Each value is expressed as the mean ± SD of three independent experiments.
[a] Calculated by the method of (Chen et al., 1972).

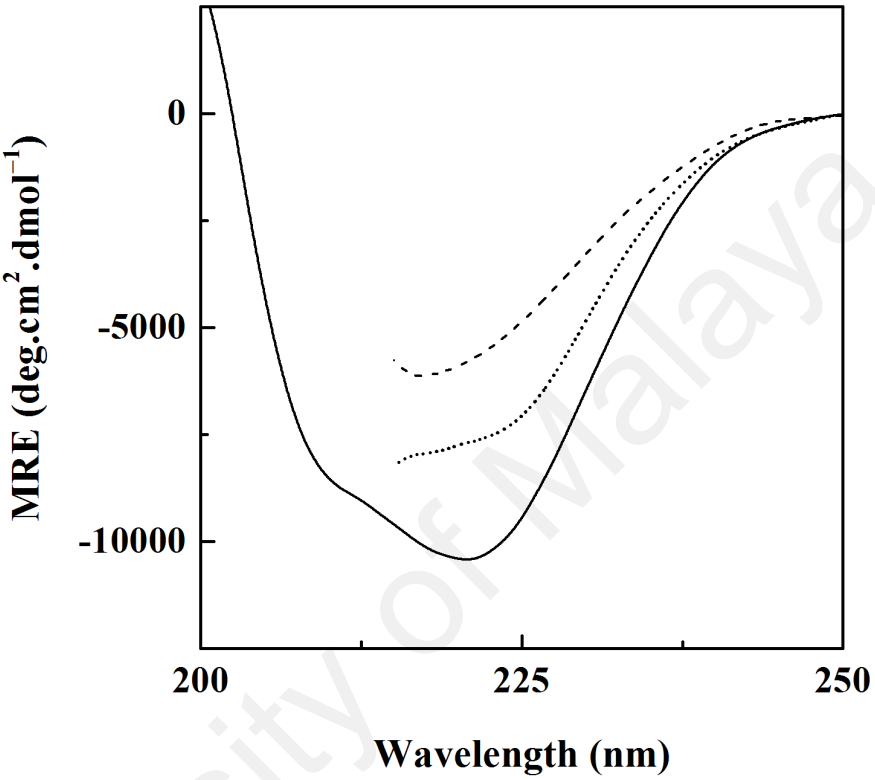

Figure 3.32. Far-UV CD spectra of ovalbumin (——) and 2.2 M GdnHCl-denatured ovalbumin in the absence (- - -) and the presence (·····) of 20% (w/v) SHSC at pH 7.4. The protein concentration was 5 μM.

decrease (46%) in the MRE_{222nm} value, compared to that of the native ovalbumin (Table 3.12). However, the MRE_{222nm} value of 2.2 M GdnHCl-denatured ovalbumin was increased by 17% in the presence of 20% (w/v) SHSC, indicating secondary structure stabilization by SHSC (Figure 3.32; Table 3.12). More evidently, the α-helical content of ovalbumin decreased from ~27% to ~11% in the presence of 2.2 M GdnHCl, but showed significant retention (~19%) in the presence of 20% (w/v) SHSC (Table 3.12). All these results were suggestive of the stabilization of ovalbumin against GdnHCl denaturation by 20% (w/v) SHSC.

3.2.4. Thermal denaturation of ovalbumin in the absence and the presence of SHSC

Thermal stabilizing potential of 20% (w/v) SHSC on ovalbumin was studied by far-UV CD spectral measurements. Figure 3.33 shows the thermal denaturation curves of ovalbumin in the temperature range, 20–95°C, obtained in the absence and the presence of 20% (w/v) SHSC. As can be seen from the figure, the thermal transition curve of ovalbumin was characterized by the occurrence of the start-, the mid- and the end-points at 60°C, 68.5°C and 80°C, respectively (Table 3.13). These results were similar to those published earlier on thermal denaturation of ovalbumin using FTIR and far-UV CD spectroscopy (Dong et al., 2000). In the presence of 20% (w/v) SHSC, the start-, the mid- and the end-points of the thermal transition curve of ovalbumin were shifted towards higher temperatures *i.e.* 62.5°C, 73.8°C and 87.5°C, respectively (Figure 3.33; Table 3.13), suggesting thermal stabilization of the ovalbumin by SHSC.

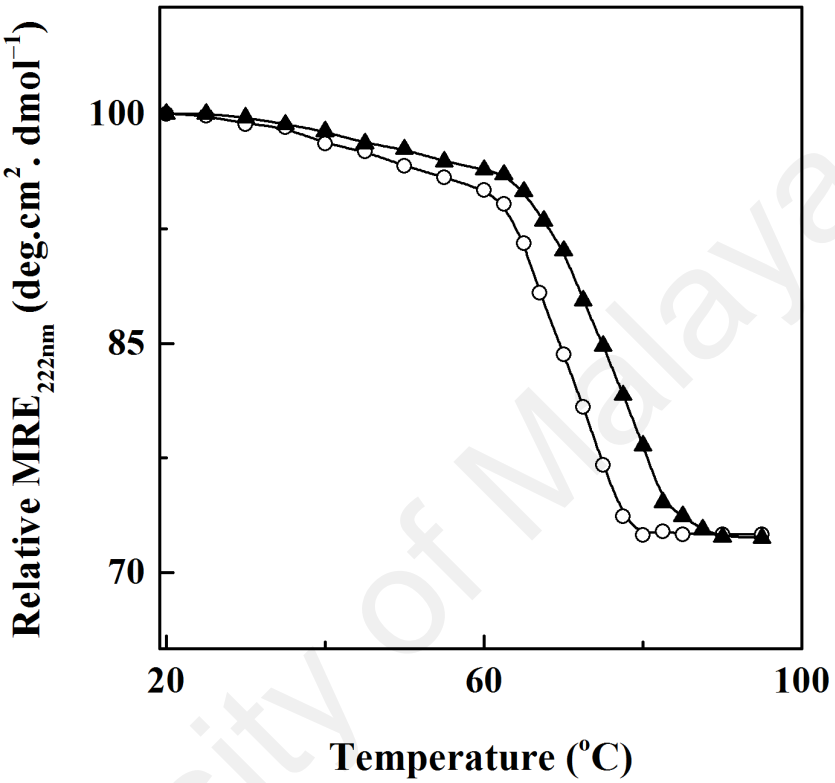

Figure 3.33. Thermal denaturation curves of ovalbumin (5 μM) in 60 mM sodium phosphate buffer, pH 7.4, as studied by MRE_{222nm} measurements in the absence (○) and the presence of 20% (▲) (w/v) SHSC.

Table 3.13. Characteristics of thermal denaturation of ovalbumin in the absence and the presence of 20% (w/v) SHSC, as monitored by MRE_{222nm} measurements

Characteristics	Ovalbumin	Ovalbumin + 20% (w/v) SHSC
Thermal-induced transition		
– Start-point (°C)	60.0 ± 0.58	62.5 ± 0.29
– Mid-point (°C)	68.5 ± 0.06	73.8 ± 0.21
– End-point (°C)	80.0 ± 1.53	87.5 ± 0.50

Each value is expressed as the mean ± SD of three independent experiments.

3.3. SHSC-induced stabilization of lysozyme

The protein stabilizing effect of SHSC against chemical and thermal denaturations of another model protein, lysozyme was investigated using CD and fluorescence spectroscopy.

3.3.1. GdnHCl denaturation of lysozyme in the absence and the presence of SHSC

GdnHCl denaturation of lysozyme was studied in the absence and the presence of increasing SHSC concentrations, using far-UV CD and Trp fluorescence measurements.

3.3.1.1. Far-UV CD spectra

Figure 3.34 shows the far-UV CD spectra of lysozyme, obtained in the absence and the presence of increasing GdnHCl (3.4–5.0 M) concentrations. Due to the coinciding nature of the far-UV CD spectra at lower (< 3.4 M) and higher (> 5.0 M) GdnHCl concentrations, these spectra are not included in the figure. Moreover, presence of GdnHCl increased the signal to noise ratio, which hampered the spectral recording below 218–220 nm. Presence of the α-helical structure in lysozyme was evident from the occurrence of two minima at 208 nm and 222 nm in the far-UV CD spectra (Figure 3.34). GdnHCl-induced denaturation of lysozyme can be clearly seen from the gradual decrease in the MRE values with increasing GdnHCl concentrations.

Figure 3.35 represents F_D curves of GdnHCl denaturation of lysozyme in the absence and the presence of SHSC, obtained after treating the denaturation data according to the procedure described in the section 2.2.6.3. Various characteristics of the transition curve of lysozyme in terms of the start-, the mid and the end-points are given in Table 3.14. As shown in the Figure 3.35, GdnHCl denaturation of lysozyme followed a single-step, two-state transition, which started at 3.3 M and ended at 5.0 M GdnHCl with the mid-point of the transition occurring at 4.0 M GdnHCl (Table 3.14). These results were

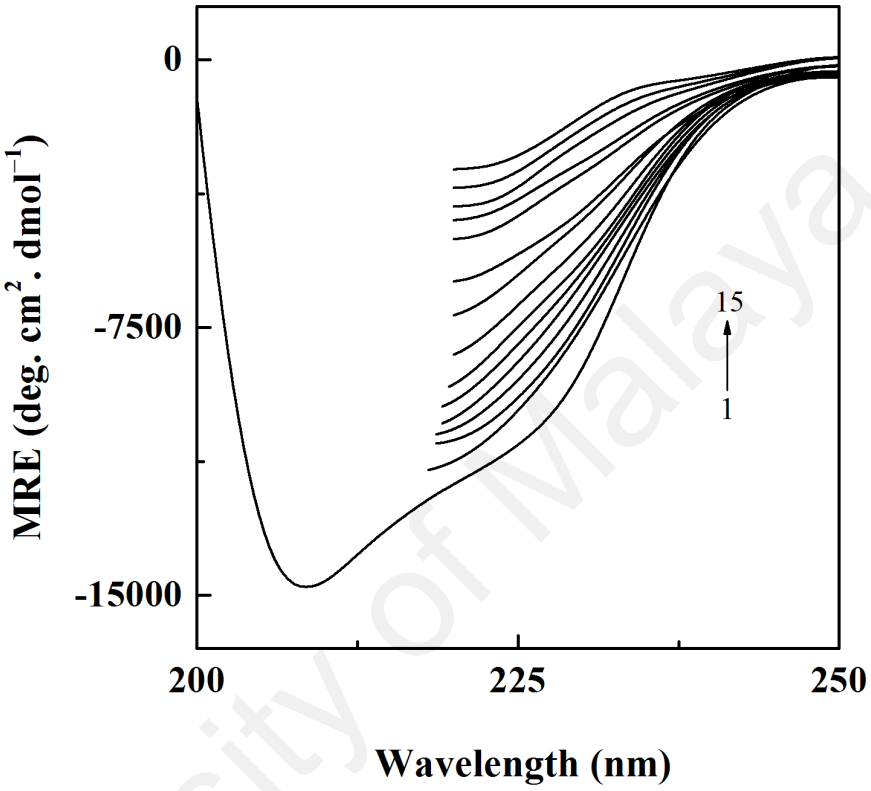

Figure 3.34. Far-UV CD spectra of lysozyme (10 μM), obtained in 60 mM sodium phosphate buffer, pH 7.0 in the absence and the presence of increasing GdnHCl concentrations (0–5.0 M GdnHCl). The GdnHCl concentrations (from bottom to top) were: 0, 3.4, 3.6, 3.7, 3.8, 3.85, 3.9, 4.0, 4.1, 4.2, 4.3, 4.4, 4.5, 4.75 and 5.0 M.

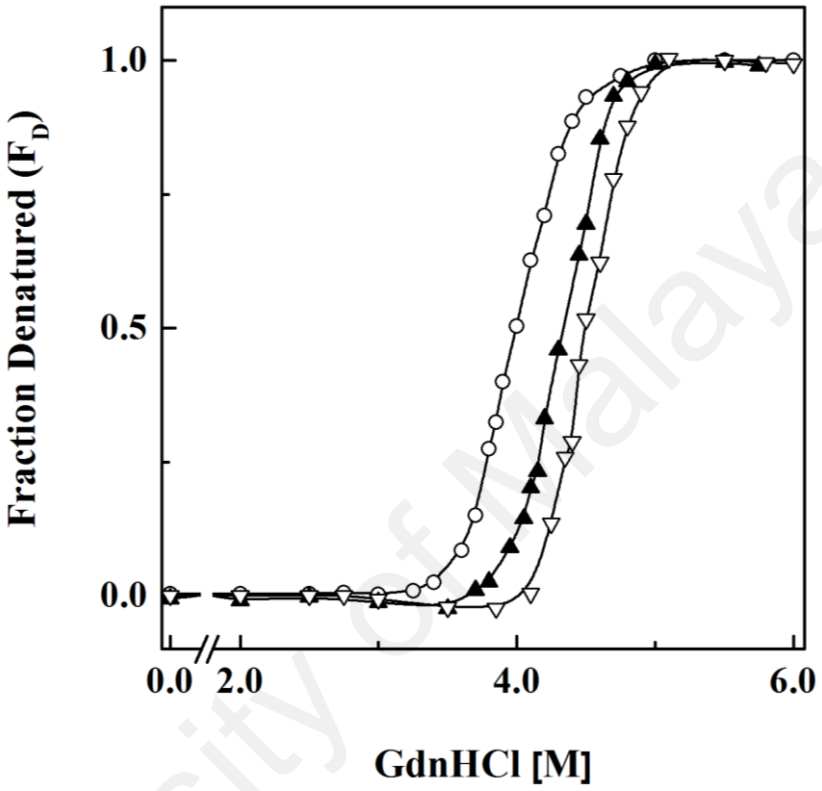

Figure 3.35. Normalized GdnHCl denaturation curves of lysozyme (10 μM) in 60 mM sodium phosphate buffer, pH 7.0, as studied by MRE_{222nm} measurements in the absence (○) and the presence of 20% (▲) or 30% (▽) (w/v) SHSC.

Table 3.14. Characteristics of GdnHCl denaturation of lysozyme in the absence and the presence of different SHSC concentrations, as monitored by MRE_{222nm} measurements.

Protein sample	GdnHCl-induced transition		
	Start-point [M]	Mid-point [M]	End-point [M]
Lysozyme	3.3 ± 0.06	4.0 ± 0.05	5.0 ± 0.10
Lysozyme + 20% (w/v) SHSC	3.5 ± 0.06	4.3 ± 0.06	5.0 ± 0.03
Lysozyme + 30% (w/v) SHSC	3.9 ± 0.10	4.5 ± 0.10	5.0 ± 0.06

Each value is expressed as the mean ± SD of three independent experiments.

similar to those reported by Wu et al. (2008). Presence of different SHSC concentrations [20% and 30% (w/v)] significantly shifted the transition curve towards higher GdnHCl concentrations, with the start- and the mid-points of the transition occurring at 3.9 M and 4.5 M GdnHCl, respectively, in the presence of 30% (w/v) SHSC (Figure 3.35; Table 3.14). Even with 20% (w/v) SHSC, shift in the start- and the mid-points of the transition was significant (Figure 3.35; Table 3.14). These results suggested SHSC-induced secondary structure stabilization of lysozyme, which was found concentration dependent, being more pronounced in the presence of 30% (w/v) SHSC.

3.3.1.2. Tryptophan fluorescence spectra

The stabilizing effect of SHSC on the tertiary structure of lysozyme against GdnHCl denaturation was studied using Trp fluorescence spectroscopy. Figure 3.36 shows the Trp fluorescence spectra of lysozyme in the absence and the presence of increasing GdnHCl (3.3–4.8 M) concentrations upon excitation at 295 nm. The fluorescence spectra obtained at both extremes of the GdnHCl concentration range (< 3.3 M and > 4.8 M GdnHCl) are excluded for clarity. The fluorescence spectrum of lysozyme showed the emission maxima at 338 nm, suggesting presence of Trp residues (Lakowicz, 1999). The fluorescence characteristics of lysozyme were significantly affected in the presence of GdnHCl, as a progressive increase in the fluorescence intensity along with red shift in the emission maxima were observed with increasing GdnHCl concentrations. Such changes in the spectral behavior of lysozyme in the presence of GdnHCl indicated tertiary structure disruption of lysozyme.

The shift in the emission maxima was used to probe tertiary structural disruption of lysozyme induced by GdnHCl. The denaturation data, obtained in the absence and the presence of different SHSC concentrations were transformed into F_D values according to the procedure described above and were plotted against GdnHCl concentration.

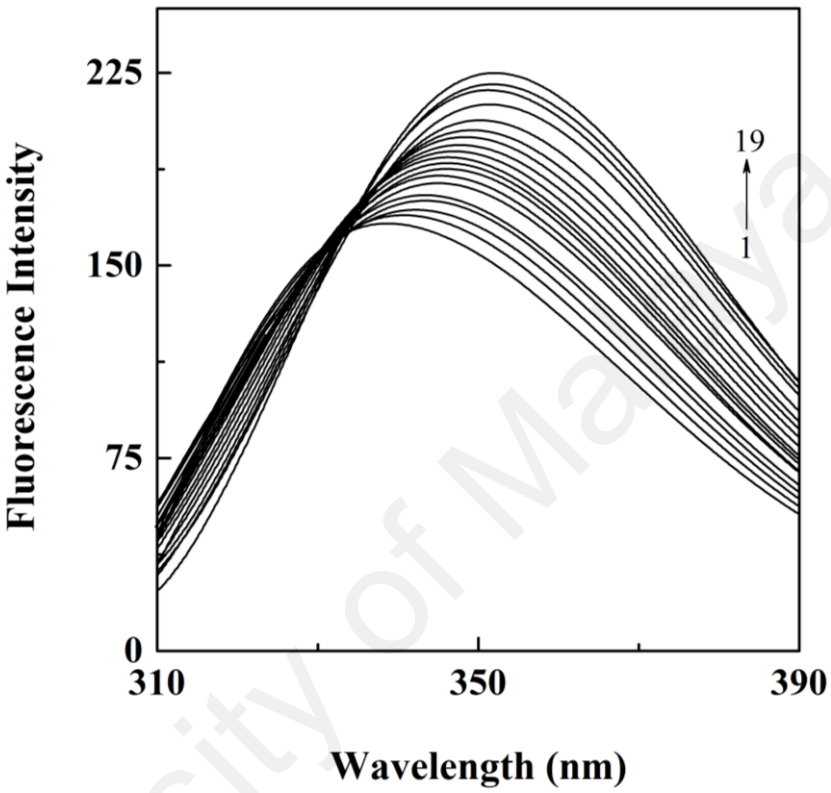

Figure 3.36. Fluorescence spectra of lysozyme (1 μM), obtained in 60 mM sodium phosphate buffer, pH 7.0 in the absence and the presence of increasing GdnHCl concentrations (0 – 4.8 M GdnHCl) upon excitation at 295 nm. The GdnHCl concentrations (from bottom to top) were: 0, 3.3, 3.45, 3.55, 3.65, 3.75, 3.85, 3.9, 3.95, 4.0, 4.05, 4.1, 4.15, 4.2, 4.25, 4.3, 4.4, 4.5 and 4.8 M.

Figure 3.37 shows normalized GdnHCl denaturation curves of lysozyme in the absence and the presence of 20% and 30% (w/v) SHSC, as studied by the shift in the emission maxima of Trp fluorescence. The denaturation curves were found similar to those obtained with MRE_{222nm} measurements, showing a single-step, two-state transition (Figure 3.35). The small variation in the values of the start-, the mid- and the end-points of the transition is commonly observed when using different probes (Hung & Chang, 2001; Santra et al., 2004; Kishore et al., 2012). The start-, the mid- and the end-points of the transition curve of lysozyme were found to be 3.1 M, 4.0 M and 4.8 M GdnHCl, respectively (Table 3.15), which were in close agreement with the results published earlier (Ong et al., 2009; Arumugam et al., 2010). These transition characteristics were changed to 3.8 M, 4.4 M and 4.8 M GdnHCl, respectively, in the presence of 30% (w/v) SHSC (Table 3.15). The shift in the transition curve towards higher GdnHCl concentration (Figure 3.37) along with an increase in the start- and the mid-point values indicated stabilization of lysozyme in the presence of SHSC.

3.3.2. Characterization of the partially-denatured lysozyme in the absence and the presence of SHSC

Far-UV CD, near-UV CD and ANS fluorescence measurements were made to study the stabilizing effect of SHSC on the conformation of 4.0 M GdnHCl-denatured lysozyme, representing the partially-denatured state at the mid-point of the transition.

3.3.2.1. Far-UV CD spectra

The far-UV CD spectra of 4.0 M GdnHCl-denatured lysozyme in the absence and the presence of 20% and 30% (w/v) SHSC could not be recorded below 220 nm due to high signal to noise ratio. The far-UV CD spectrum of 4.0 M GdnHCl-denatured lysozyme retained the minima at 222 nm but showed a significant (30%) decrease in the MRE_{222nm} value from –11034.9 $deg.cm^2.dmol^{-1}$ (for native lysozyme) to

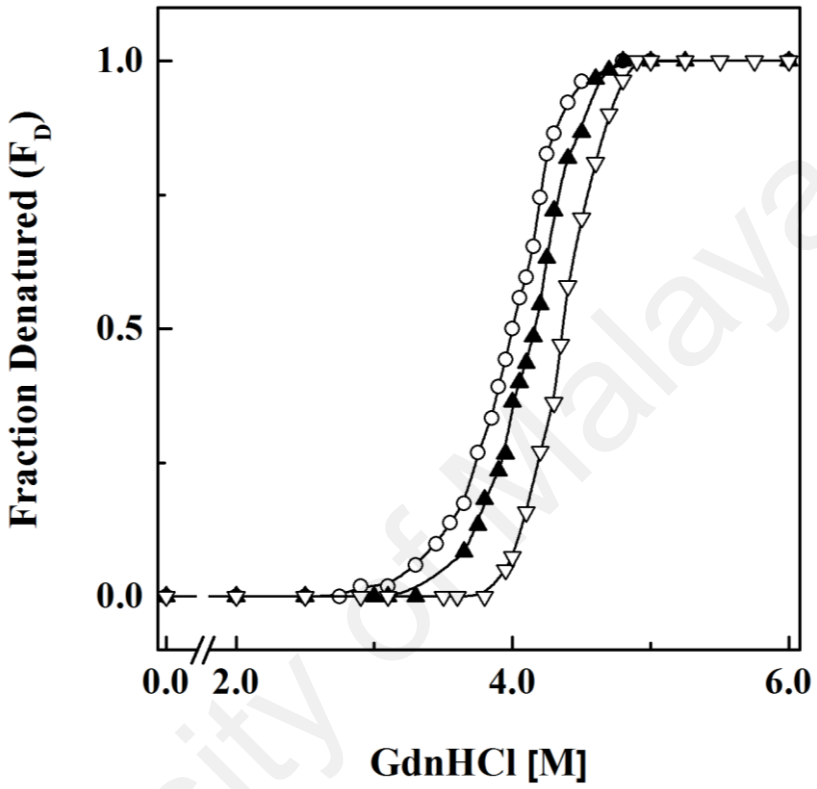

Figure 3.37. Normalized GdnHCl denaturation curves of lysozyme (1 μM) in 60 mM sodium phosphate buffer, pH 7.0, as studied by emission maxima of Trp fluorescence measurements upon excitation at 295 nm in the absence (○) and the presence of 20% (▲) or 30% (▽) (w/v) SHSC.

Table 3.15. Characteristics of GdnHCl denaturation of lysozyme in the absence and the presence of different SHSC concentrations, as monitored by tryptophan fluorescence measurements (Emission maxima) upon excitation at 295 nm.

Protein sample	GdnHCl-induced transition		
	Start-point [M]	Mid-point [M]	End-point [M]
Lysozyme	3.1 ± 0.06	4.0 ± 0.05	4.8 ± 0.05
Lysozyme + 20% (w/v) SHSC	3.3 ± 0.06	4.2 ± 0.06	4.8 ± 0.03
Lysozyme + 30% (w/v) SHSC	3.8 ± 0.06	4.4 ± 0.07	4.8 ± 0.06

Each value is expressed as the mean ± SD of three independent experiments.

–7770.7 deg.cm^2.dmol^{-1} (Figure 3.38; Table 3.16), suggesting partial denaturation of lysozyme with the loss in the α-helical structure. In contrast, significant retention in the MRE_{222nm} value of 4.0 M GdnHCl-denatured lysozyme, showing 17% and 8% decrease, was noticed in the presence of 20% and 30% (w/v) SHSC, respectively. These results indicated secondary structure stabilization of 4.0 M GdnHCl-denatured lysozyme by SHSC (Figure 3.38; Table 3.16).

The calculation of the α-helical content from the MRE_{222nm} value showed ~29% α-helical content in the native lysozyme, which was in agreement with a previous report (Chen et al., 1972). The α-helical content was decreased to ~18% in 4.0 M GdnHCl-denatured lysozyme (Table 3.16), but significant retention of the α-helical structure *i.e.* ~22% and ~26%, observed in the presence of 20% and 30% (w/v) SHSC, respectively, clearly suggested protein's secondary structure stabilization.

3.3.2.2. Near-UV CD spectra

The tertiary structure stabilization of 4.0 M GdnHCl-denatured lysozyme was evident from the near-UV CD spectral results (Figure 3.39). The near-UV CD spectrum of the native lysozyme was characterized by the presence of three major peaks around 282 nm, 288 nm and 294 nm along with a few minor peaks in the wavelength range, 255–270 nm (Figure 3.39). The spectral features of the native lysozyme were similar to those reported earlier (Barnes et al., 1972) and can be attributed to the presence of aromatic chromophores and disulphide bonds in the native protein (Kelly et al., 2005). The MRE values at the above three wavelengths were significantly reduced in 4.0 M GdnHCl-denatured lysozyme, while an increase in the MRE values was noticed in the wavelength range, 255–270 nm (Figure 3.39; Table 3.16). These results were suggestive of partial denaturation of the enzyme with loss in its tertiary structure. Surprisingly, the MRE values of all three major peaks showed significant increase,

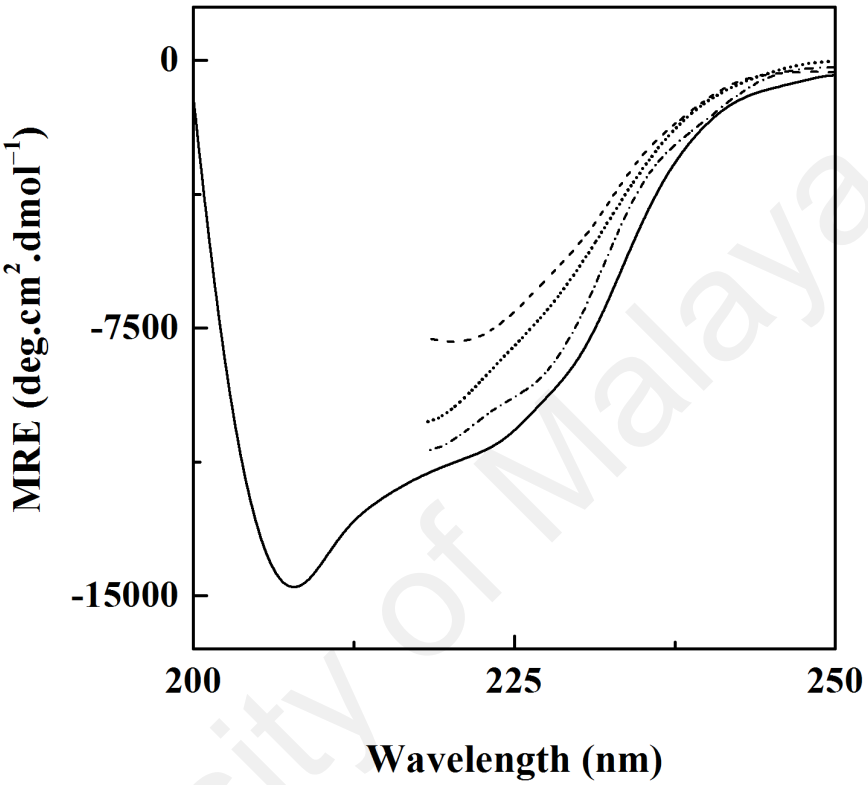

Figure 3.38. Far-UV CD spectra of lysozyme (——) and 4.0 M GdnHCl-denatured lysozyme in the absence (- - -) and the presence of 20% (·····) or 30% (-·-) (w/v) SHSC at pH 7.0. The protein concentration was 10 µM.

Table 3.16. Spectral characteristics of lysozyme under various experimental conditions, as monitored by different probes.

Spectral characteristics	Native lysozyme	4.0 M GdnHCl-denatured lysozyme	4.0 M GdnHCl-denatured lysozyme + 20% (w/v) SHSC	4.0 M GdnHCl-denatured lysozyme + 30% (w/v) SHSC
Far-UV CD spectra				
– MRE at 222 nm (deg.cm^2.dmol^{-1})	–11,034.9 ± 280	–7,770.7 ± 107	–9,125.3 ± 150	–10,156.3 ± 207
– α-Helical content[a]	~29 ± 0.6%	~18 ± 0.7%	~22 ± 0.8%	~26 ± 0.5%
Near-UV CD spectra				
– MRE at 282 nm (deg.cm^2.dmol^{-1})	2,498.8 ± 62	1,310.3 ± 20	2,459.0 ± 47	ND[b]
– MRE at 288 nm (deg.cm^2.dmol^{-1})	3,232.7 ± 80	1,699.7 ± 26	2,763.6 ± 55	ND[b]
– MRE at 294 nm (deg.cm^2.dmol^{-1})	2,192.6 ± 55	745.6 ± 11	1,280.3 ± 26	ND[b]
ANS fluorescence spectra				
– Fluorescence intensity at 524 nm	76.2 ± 4	103.2 ± 5	92.0 ± 3	86.6 ± 2

Each value is expressed as the mean ± SD of three independent experiments.

[a] Calculated by the method of Chen et al. (1972).

[b] ND = Not determined.

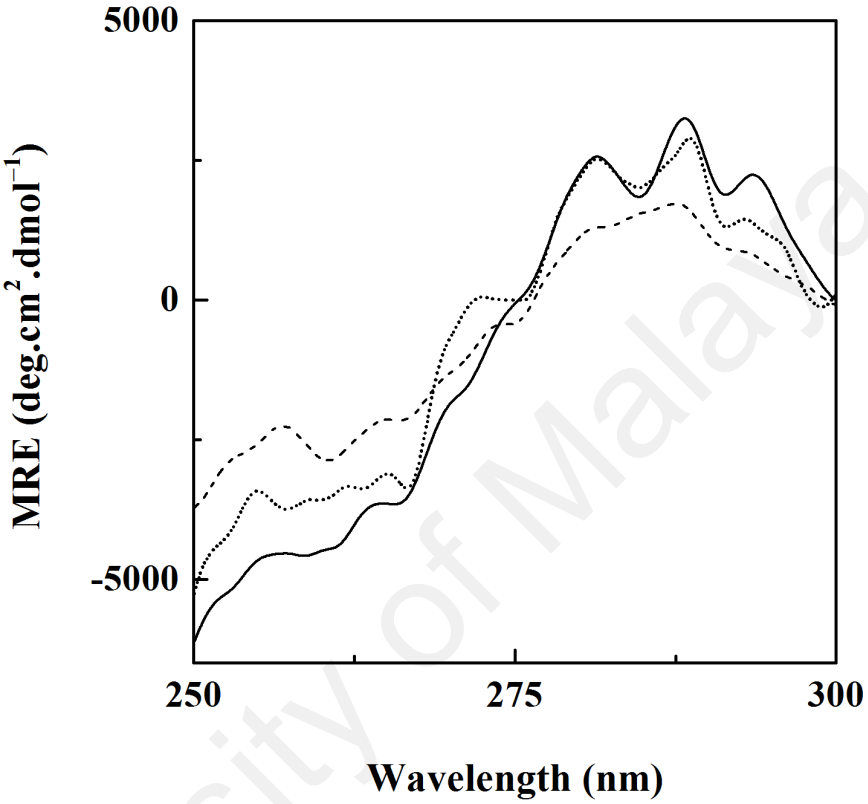

Figure 3.39. Near-UV CD spectra of lysozyme (——) and 4.0 M GdnHCl-denatured lysozyme in the absence (- - -) and the presence (·····) of 20% (w/v) SHSC at pH 7.0. The protein concentration was 25 μM.

approaching native characteristics in the presence of 20% (w/v) SHSC (Table 3.16). Similarly, improvement in the MRE values in the wavelength range, 255–270 nm was also noticed in the presence of 20% (w/v) SHSC (Figure 3.39). Both these results suggested tertiary structure stabilization of 4.0 M GdnHCl-denatured lysozyme induced by SHSC. The near-UV CD spectrum of 4.0 M GdnHCl-denatured lysozyme could not be recorded in the presence of 30% (w/v) SHSC due to high signal to noise ratio throughout the wavelength range, 250–300 nm.

3.3.2.3. ANS fluorescence spectra

Figure 3.40 shows ANS fluorescence spectra of 4.0 M GdnHCl-denatured lysozyme in the absence and the presence of 20% and 30% (w/v) SHSC. ANS fluorescence spectrum of the native lysozyme is also included for comparison. As evident from the figure, ANS fluorescence spectrum of the native lysozyme showed an emission maximum at 524 nm upon excitation at 380 nm, which was similar to the one published earlier (Samuel et al., 2000). The small value of the ANS fluorescence intensity (~76), observed with the native lysozyme indicated lesser surface hydrophobicity due to burial of hydrophobic residues in the protein interior (Samuel et al., 2000). However, significant increase (35%) in the ANS fluorescence intensity was observed in the presence of 4.0 M GdnHCl, demonstrating greater exposure of the hydrophobic regions due to tertiary structural alteration. Similar increase in the ANS fluorescence intensity has also been noticed in the urea-denatured lysozyme (Sugahara et al., 2002). Interestingly, 4.0 M GdnHCl-denatured lysozyme showed only 21% and 14% increase in the ANS fluorescence intensity in the presence of 20% and 30% (w/v) SHSC, respectively (Figure 3.40; Table 3.16). These results suggested lesser exposure of the hydrophobic regions in the protein and were consistent with the near-UV CD spectral results, showing retention of the folded structure in 4.0 M GdnHCl-denatured lysozyme in the presence of SHSC.

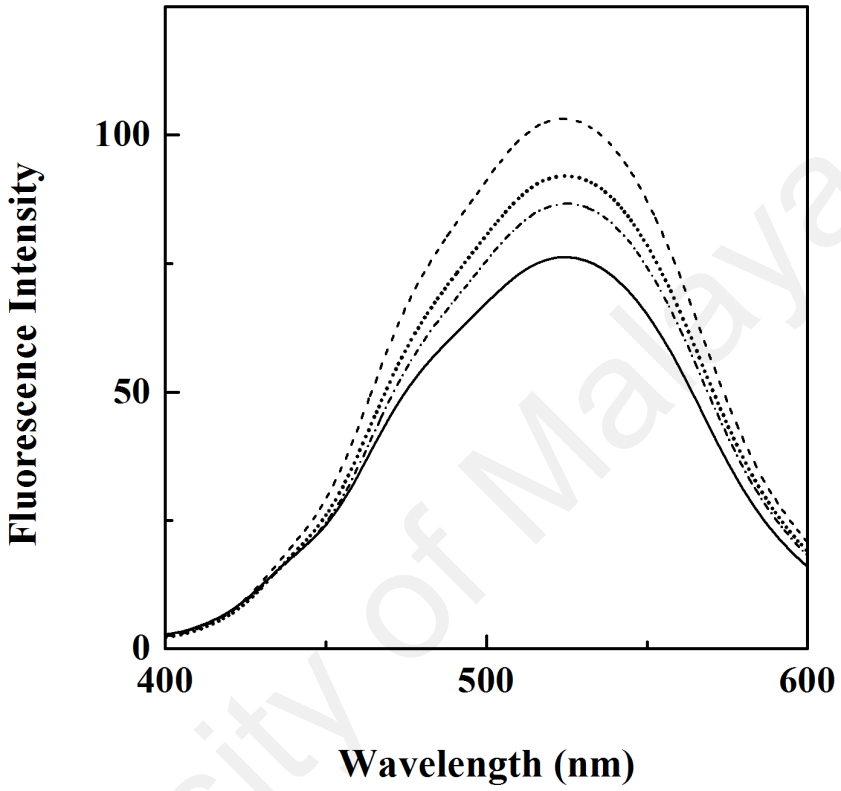

Figure 3.40. ANS fluorescence spectra of lysozyme (——) and 4.0 M GdnHCl-denatured lysozyme in the absence (- - -) and the presence of 20% (·····) or 30% (-·-) (w/v) SHSC at pH 7.0. The protein concentration was 1.0 μM while the ANS concentration was set as 100 μM.

3.3.3. Thermal denaturation of lysozyme in the absence and the presence of SHSC

Figure 3.41 shows the normalized thermal denaturation curves of lysozyme in the absence and the presence of 20% and 30% (w/v) SHSC, as monitored by MRE_{222nm} measurements. Thermal denaturation of lysozyme was also found to follow a single-step transition (Figure 3.41), which started at 60°C and completed at 90°C with the mid-point of the transition (T_m), occurring at 72°C (Table 3.17). Thermal transition curve of lysozyme shown in Figure 3.41 was in agreement with a previous report (Yamamoto et al., 2006). Interestingly, greater thermal stability of lysozyme was observed in the presence of 20% and 30% (w/v) SHSC, as the thermal denaturation curve was shifted towards higher temperature range in the presence of SHSC. For example, the start- and the mid-points of the transition curve increased from 60°C and 72°C (for lysozyme) to 66°C and 78°C, respectively, in the presence of 30% (w/v) SHSC (Table 3.17). The shift in the transition curve of lysozyme in the presence of SHSC was also found to be concentration dependent, as observed in GdnHCl denaturation experiments, suggesting thermal stabilization of lysozyme by SHSC.

Thermal stabilizing effect of SHSC on lysozyme at 72°C was also recognized from the far-UV CD spectra of the heat-denatured (72°C) lysozyme, obtained in the absence and the presence of SHSC (Figure 3.42). A comparison of the spectra, obtained at 25°C and 72°C showed significant reduction in the MRE_{222nm} value from –11034.9 (25°C) to –7684.9 $deg.cm^2.dmol^{-1}$ (72°C) (Table 3.17), indicating loss in the secondary structure of lysozyme. This was more evident from the calculation of the α-helical content, which showed 11% loss of the α-helical content at 72°C (Table 3.17). Due to high signal to noise ratio, far-UV CD spectra could not be recorded below 220 nm. Presence of 20% and 30% (w/v) SHSC in the incubation mixture prevented the loss in the secondary structure to a significant extent, as the MRE_{222nm} values of lysozyme at 72°C were found to be significantly higher than those obtained in the absence of SHSC (Table 3.17). The

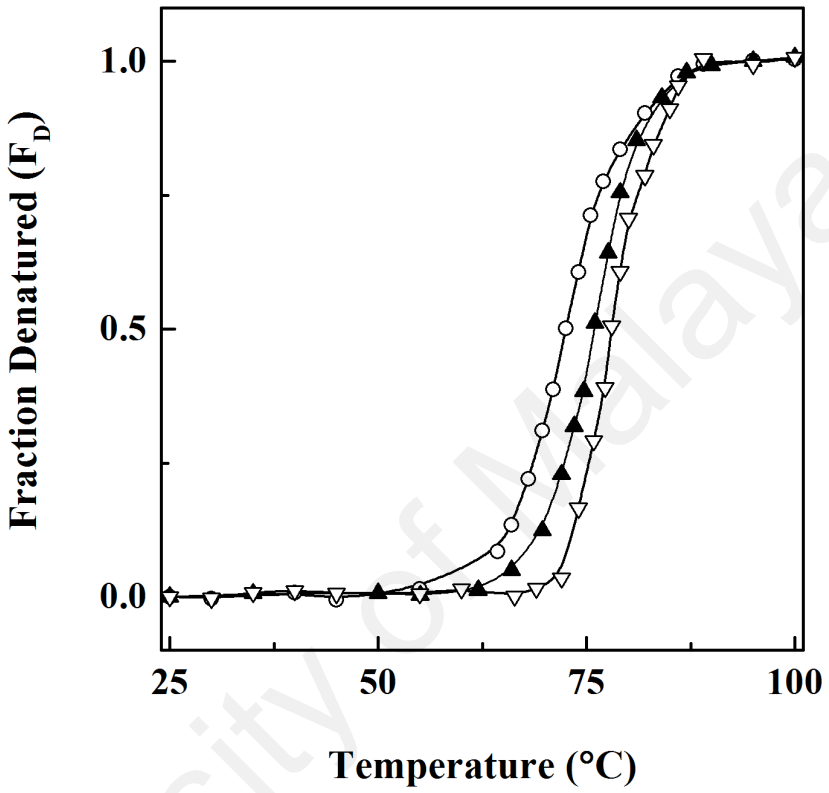

Figure 3.41. Normalized thermal denaturation curves of lysozyme (10 μM) in 60 mM sodium phosphate buffer, pH 7.0, as studied by MRE_{222nm} measurements in the absence (○) and the presence of 20% (▲) or 30% (▽) (w/v) SHSC.

Table 3.17. Characteristics of thermal denaturation of lysozyme in the absence and the presence of 20% or 30% (w/v) SHSC, as monitored by MRE_{222nm} measurements.

Characteristics	Lysozyme	Lysozyme + 20% (w/v) SHSC	Lysozyme + 30% (w/v) SHSC
Thermal-induced transition			
– Start-point (°C)	60 ± 0.6	62 ± 0.6	66 ± 1.0
– Mid-point (°C)	72 ± 0.5	76 ± 0.4	78 ± 0.2
– End-point (°C)	90 ± 0.6	90 ± 0.6	90 ± 0.3
Far-UV CD spectra			
– MRE at 222 nm ($deg.cm^2.dmol^{-1}$) [α-Helical content[a]]			
• 25°C	–11,034.9 ± 210 [~29 ± 0.6%]	–10,979.0 ± 190 [~29 ± 0.6%]	–10,972.7 ± 150 [~29 ± 0.6%]
• 72°C	–7,684.9 ± 150 [~18 ± 0.5%]	–8,598.9 ± 118 [~21 ± 0.4%]	–9,349.5 ± 225 [~23 ± 0.4%]

Each value is expressed as the mean ± SD of three independent experiments.
[a] Calculated by the method of Chen et al. (1972).

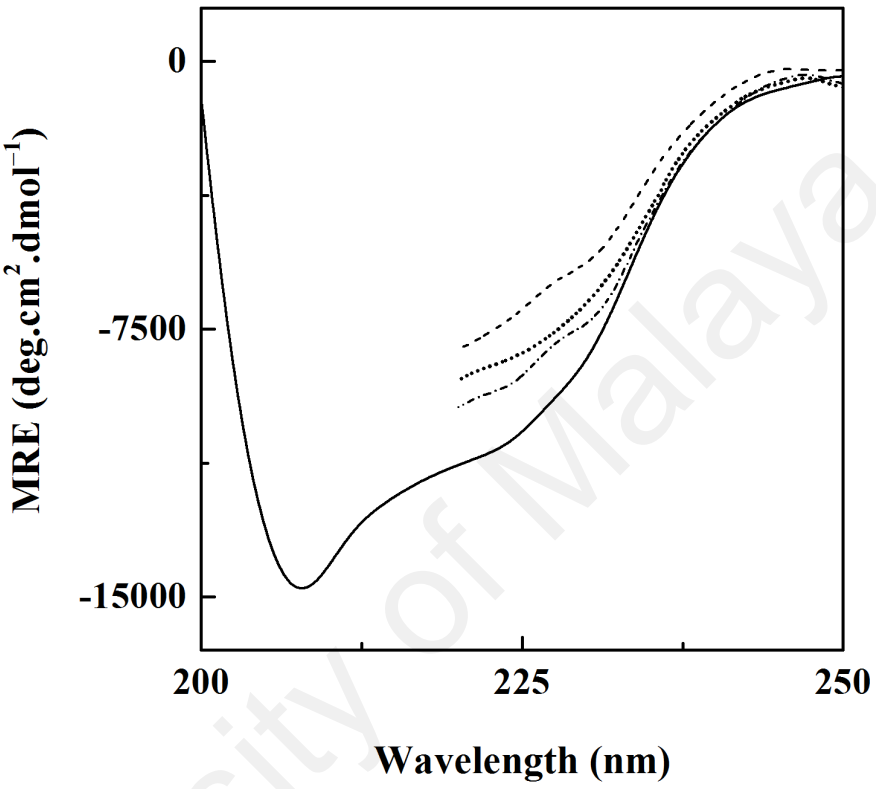

Figure 3.42. Far-UV CD spectra of lysozyme at 25°C (——) and 72°C in the absence (– – –) and the presence of 20% (·····) or 30% (– · –) (w/v) SHSC at pH 7.0. The protein concentration was 10 μM.

calculated values of the α-helical content also showed an increase from ~18% (for lysozyme at 72°C) to ~21% and ~23% in the presence of 20% and 30% (w/v) SHSC, respectively, suggesting thermal stabilization of lysozyme by SHSC (Table 3.17).

3.4. Honey-induced protein stabilization

Honey contains several other compounds such as flavonoids, polyphenols, vitamins, minerals and amino acids in addition to sugars, which may contribute towards protein stabilizing potential of honey. Hence, protein stabilization studies were also made in the presence of honey, using BSA as the model protein.

3.4.1. Honey interference with protein's intrinsic fluorescence

Figure 3.43 shows the effect of increasing honey concentrations on the intrinsic fluorescence spectrum of BSA (2 μM) upon excitation at 280 nm. The top spectrum shown in the figure represents the fluorescence spectrum of BSA in the absence of honey. The spectrum was characterized by the presence of an emission maxima at 341 nm, which was in agreement with previous reports (Khan et al., 1987; Kumaran & Ramamurthy, 2011). Addition of increasing concentrations of honey [0.15–15% (w/v)] to BSA produced a concentration dependent decrease in the fluorescence intensity (Figure 3.43). However, the emission maxima remained unaltered in the presence of honey. Absolute quenching of the protein fluorescence was observed in the presence of 5% (w/v) honey. Interestingly, the pure honey sample (without BSA) also produced the fluorescence spectra in the same wavelength range upon excitation at 280 nm (inset of Figure 3.43), which can be ascribed to the presence of proteins or aromatic amino acids in the honey sample (Bogdanov et al., 2008). Approximately 0.5% (w/v) of the total honey weight constitutes proteins and amino acids in different honey samples (Bogdanov et al., 2008). Although, the magnitude of the fluorescence intensity observed with the pure honey sample was found to be much smaller (~5%) than that of BSA, a similar decrease in the fluorescence intensity was also observed upon increasing the concentration of the honey present in the sample (inset of Figure 3.43). Since the fluorescence spectra of BSA in the presence of different honey concentrations shown in Figure 3.43 were obtained after

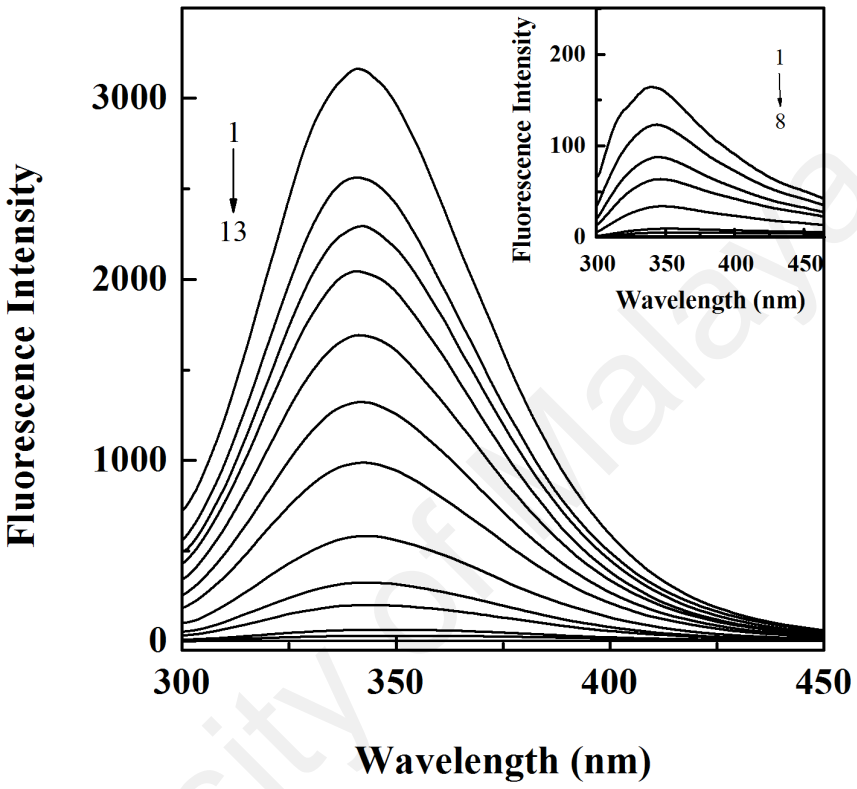

Figure 3.43. Fluorescence spectra of BSA (2 μM), obtained in 60 mM sodium phosphate buffer, pH 7.4 in the absence and the presence of increasing honey concentrations (0–15%, w/v honey) upon excitation at 280 nm. The honey concentrations (from top to bottom) were: 0, 0.15, 0.25, 0.35, 0.50, 0.75, 1.0, 1.5, 2.0, 3.0, 4.0, 5.5 and 15.0% (w/v). Inset shows fluorescence spectra of honey with increasing concentrations as 1.0, 2.0, 3.0, 4.0, 5.5, 7.5, 10 and 15% (w/v) upon excitation at 280 nm.

subtracting the fluorescence spectra produced by honey alone, the fluorescence contribution from the proteins present in the honey can be ruled out.

A quantitative evaluation of the influence of honey on the BSA fluorescence was made by transforming the fluorescence intensity values of BSA at 341 nm, obtained in various honey concentrations into relative fluorescence intensity by taking the fluorescence intensity of BSA (without honey) at 341 nm as 100. Figure 3.44 shows the variation in the relative fluorescence intensity of BSA at 341 nm with increasing honey concentrations. A drastic decrease in the fluorescence intensity was observed over the 0–1.5% (w/v) honey concentration range. An approximate 82% decrease in the relative fluorescence intensity at 341 nm was noted in the presence of 1.5% (w/v) honey. A further small decrease in the relative fluorescence intensity was observed up to 4% (w/v) honey. The complete quenching of the fluorescence intensity was achieved at 5% (w/v) honey and any further increase in the honey concentration up to 15% (w/v) did not show any recovery in the fluorescence intensity. Increasing the protein concentration to 5 μM failed to produce any significant change in the fluorescence quenching behaviour of honey as the fluorescence quenching curve superimposed the data obtained with 2 μM BSA. However, slightly weaker quenching was noted with 5 μM protein over a similar honey concentration range. Such a remarkable quenching effect of honey on BSA fluorescence can be ascribed to the presence of a vast variety of substances including polyphenolic compounds, minerals and vitamins in the honey samples (Bogdanov et al., 2008), which might have acted as protein fluorescence quenchers. This seems to be feasible because several polyphenolic compounds, flavonoids and vitamins, which are commonly found in honey, *i.e.*, caffeic acid, galangin, kaempferol, naringenin, rutin, quercetin, vitamin B_2 (riboflavin), vitamin C (ascorbic acid) and vitamin K (Andrade et al., 1997; Bogdanov et al., 2008; Kaškonienė et al., 2009) have shown a fluorescence quenching effect on serum

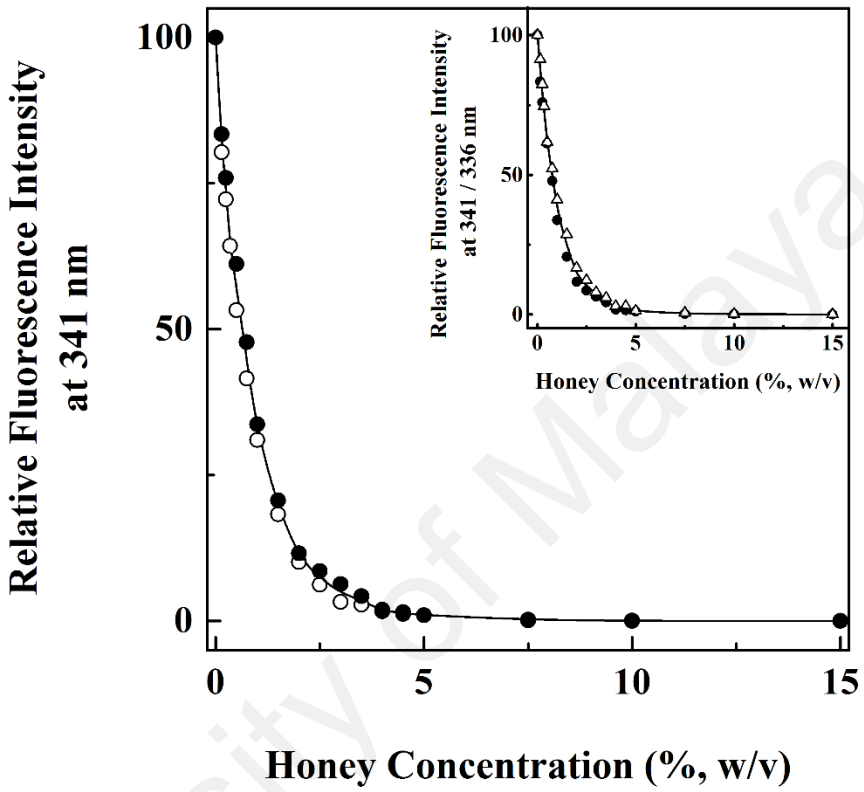

Figure 3.44. Plot showing variation in the relative fluorescence intensity at 341 nm of 2 µM (○) and 5 µM (●) BSA with increasing honey concentrations upon excitation at 280 nm. Inset shows the decrease in the relative fluorescence intensity of 5.0 µM BSA at 341 nm (●) and 5.0 µM ovalbumin at 336 nm (△) with increasing honey concentrations upon excitation at 280 nm.

albumin (Papadopoulou et al., 2005; Shaikh et al., 2007; Wang et al., 2008; Fu et al., 2012; Skrt et al., 2012; Li et al., 2014). Similar quenching effect produced by honey on the fluorescence of BSA was also observed with ovalbumin (inset of Figure 3.44). These results suggested that the quenching effect was not specific towards BSA, but was common to other proteins including ovalbumin. Presence of such quenchers in the honey was also evident from the inset of Figure 3.43, showing marked quenching effect of the honey samples at higher concentrations, producing complete quenching at 15% (w/v) honey. In view of this, the intrinsic fluorescence of a protein cannot be used as a probe to study protein denaturation / stabilization in the presence of honey.

To further validate the conclusion that intrinsic fluorescence of proteins is not a suitable probe to study protein denaturation / stabilization in the presence of honey, urea denaturation of BSA was studied both in the absence and the presence of 5% (w/v) honey, using intrinsic fluorescence signal at 341 nm. Figure 3.45 shows urea denaturation profiles of BSA, obtained by using the intrinsic fluorescence signal at 341 nm at different urea concentrations in the absence and the presence of 5% (w/v) honey. The urea denaturation profile of BSA, obtained in the absence of honey matched closely with the urea denaturation results studied earlier by different groups, showing a two-step, three-state transition with the start- and the end-points occurring at 2.0 M and 7.75 M urea, respectively, along with the accumulation of an intermediate around 4.5–5.0 M urea (Ahmad & Qasim, 1995; Tayyab et al., 2000; Tayyab et al., 2002). In contrast, urea denaturation of BSA in the presence of 5% (w/v) honey produced a small fluorescence signal (~200) compared to ~3200, obtained in the absence of honey, which remained constant throughout the urea concentration range without showing any transition. Hence, these results suggested that the intrinsic fluorescence of proteins cannot be used as a probe to study protein denaturation / stabilization in the presence of honey. Other probes such

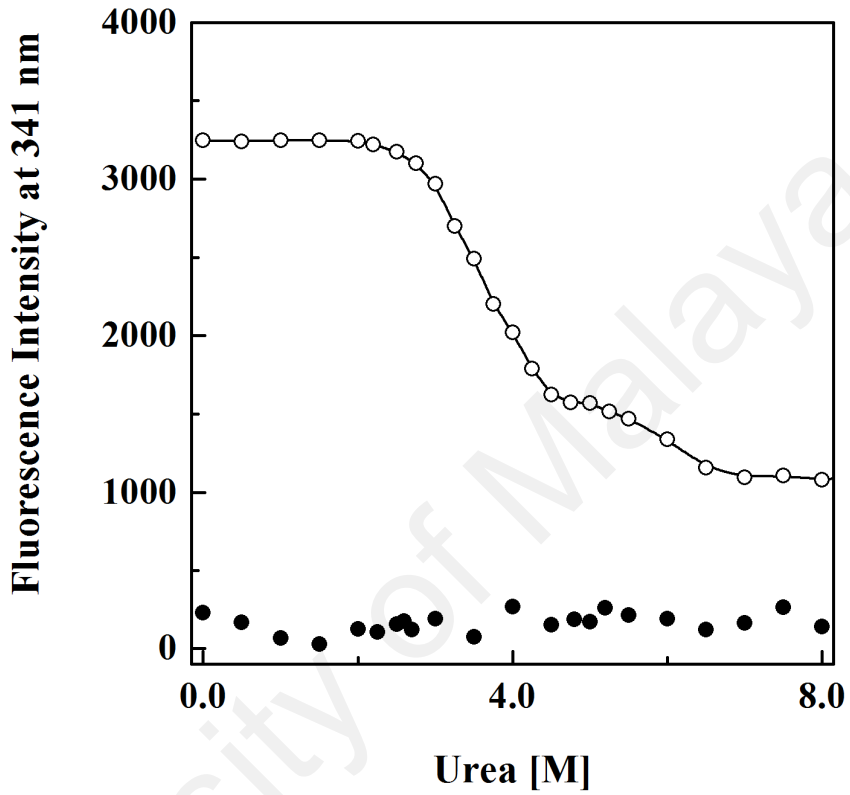

Figure 3.45. Plot showing urea denaturation curves of BSA (2 µM) in 60 mM sodium phosphate buffer, pH 7.4, as studied by intrinsic fluorescence measurements at 341 nm upon excitation at 280 nm in the absence (○) and the presence (●) of 5% (w/v) honey.

as far-UV CD spectral signal or ANS fluorescence may be more suitable to study protein denaturation / stabilization in the presence of honey.

3.4.2 Honey versus SHSC-induced protein stabilization

A comparative analysis of the protein stabilizing effect of honey *versus* SHSC was made using a model protein, BSA against chemical and thermal denaturations.

3.4.2.1. Urea denaturation of BSA in the absence and the presence of honey or SHSC

Far-UV CD and ANS fluorescence spectral measurements were employed to study urea denaturation of BSA in the absence and the presence of honey / SHSC.

i. Far-UV CD spectra: Information about honey / SHSC-induced secondary structure stabilization of BSA was obtained from the far-UV CD spectral results. Figure 3.46 shows normalized urea denaturation curves of BSA, obtained in the absence and the presence of 20% (w/v) SHSC or honey, as monitored by MRE_{222nm} measurements. As discussed earlier in the section 3.1.1.1, presence of 20% (w/v) SHSC transformed the two-step, three-state urea transition of BSA into a single-step, two-state transition along with abolishment of the intermediate state (Figure 3.46). Furthermore, the whole transition curve was shifted towards higher urea concentrations in the presence of 20% (w/v) SHSC. Both shift in the transition curve towards higher urea concentrations, as reflected from the increase in the start-point from 2.0 M (for BSA) to 3.6 M urea [in the presence of 20% (w/v) SHSC] and abolishment of the intermediate (Table 3.18; Figure 3.46) clearly demonstrated SHSC-induced protein stabilization.

As envisioned, stability of BSA against urea denaturation was greatly enhanced in the presence of 20% (w/v) honey, as the denaturation curve showed a more pronounced shift towards higher urea concentrations compared to that obtained in the presence of 20% (w/v) SHSC (Figure 3.46). Unequivocally, the start- and the mid-points of the transition

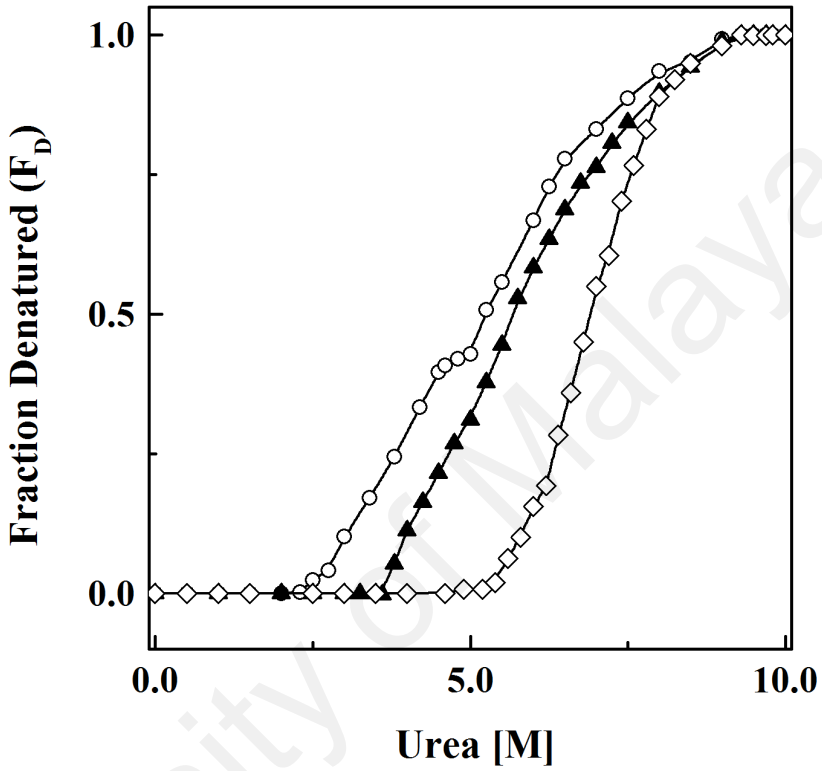

Figure 3.46. Normalized urea denaturation curves of BSA (2 μM) in 60 mM sodium phosphate buffer, pH 7.4, as studied by MRE_{222nm} measurements in the absence (○) and the presence of 20% (w/v) SHSC (▲) or honey (◇).

Table 3.18. Characteristics of urea denaturation of BSA in the absence and the presence of 20% (w/v) SHSC or honey, as monitored by MRE_{222nm} measurements.

Protein sample	Urea-induced transition		
	Start-point [M]	Mid-point [M]	End-point [M]
BSA			
– First transition	2.0 ± 0.06	3.6 ± 0.07	4.6 ± 0.06
– Second transition	5.0 ± 0.06	6.1 ± 0.08	9.3 ± 0.06
BSA + 20% (w/v) SHSC	3.6 ± 0.06	5.5 ± 0.06	9.3 ± 0.00
BSA + 20% (w/v) Honey	4.9 ± 0.06	6.9 ± 0.09	9.3 ± 0.00

Each value is expressed as the mean ± SD of three independent experiments.

curve were greatly shifted to 4.9 M and 6.9 M urea, respectively, in the presence of 20% (w/v) honey, compared to 3.6 M and 5.5 M urea, obtained with 20% (w/v) SHSC (Table 3.18). These results clearly suggested greater protein stabilizing potential of honey than SHSC.

ii. ANS fluorescence spectra: Information about protein's tertiary structure stabilization in the presence of honey / SHSC was obtained from ANS fluorescence spectral results. Figure 3.47 shows normalized urea denaturation curves of BSA, obtained in the absence and the presence of 20% (w/v) SHSC or honey, as monitored by ANS fluorescence measurements at 470 nm upon excitation at 380 nm. As can be seen from the Figure 3.47, urea denaturation of BSA showed a two-step, three-state transition, with the start- and the end-points occurring at 1.0 M and 8.0 M urea, respectively (Table 3.19), along with an intermediate centered around 4.0–4.25 M urea. Several earlier reports have shown single-step urea transition of serum albumin with ANS fluorescence (Hayakawa et al., 1992; Muzammil et al., 2000a). The possible reason for the failure in detecting the intermediate in earlier studies seems to be the selection of relatively larger urea concentration interval in denaturation experiments. The urea transition characteristics showed an early transition with ANS fluorescence measurements (Table 3.19) compared to that obtained with MRE_{222nm} measurements (Table 3.18). Such differences in the transition characteristics were not unusual and have been reported in the literature with different probes (Santra et al., 2004; Kishore et al., 2012). The transition became a single-step transition and was shifted towards higher urea concentrations in the presence of 20% (w/v) SHSC or honey, being more pronounced in the presence of 20% (w/v) honey. This was reflected from the shift in the start- and the mid-points of the transition curve to 5.0 M and 6.5 M urea, respectively, in the presence of 20% (w/v) honey compared to 2.0 M and 4.8 M urea, respectively, observed in the presence of 20% (w/v) SHSC (Table 3.19). These results further advocated greater stabilization of BSA in the presence of

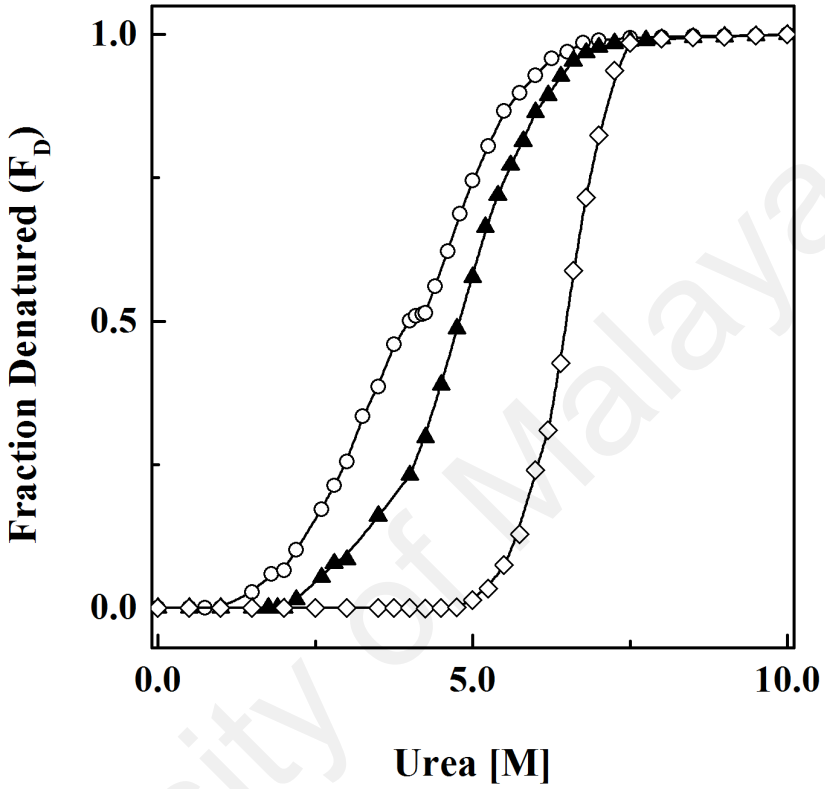

Figure 3.47. Normalized urea denaturation curves of BSA in 60 mM sodium phosphate buffer, pH 7.4, as studied by ANS fluorescence measurements at 470 nm upon excitation at 380 nm in the absence (○) and the presence of 20% (w/v) SHSC (▲) or honey (◇). The protein concentration was 1.5 μM while the ANS concentration was set as 75 μM.

Table 3.19. Characteristics of urea denaturation of BSA in the absence and the presence of 20% (w/v) SHSC or honey, as monitored by ANS fluorescence measurements at 470 nm upon excitation at 380 nm.

Protein sample	Urea-induced transition		
	Start-point [M]	Mid-point [M]	End-point [M]
BSA			
– First transition	1.0 ± 0.06	2.9 ± 0.03	4.0 ± 0.06
– Second transition	4.25 ± 0.06	5.1 ± 0.04	8.0 ± 0.14
BSA + 20% (w/v) SHSC	2.0 ± 0.06	4.8 ± 0.04	8.0 ± 0.06
BSA + 20% (w/v) Honey	5.0 ± 0.14	6.5 ± 0.02	8.0 ± 0.00

Each value is expressed as the mean ± SD of three independent experiments.

20% (w/v) honey, compared to 20% (w/v) SHSC.

3.4.2.2. Characterization of the partially-denatured BSA in the absence and the presence of SHSC or honey

A comparison of the protein stabilizing potentials of SHSC and honey was also made using the partially-denatured BSA, obtained in the presence of 4.6 M urea and studying its far-UV CD spectral characteristics in the absence and the presence of 20% (w/v) SHSC or honey. The far-UV CD spectra of the native BSA and 4.6 M urea-denatured BSA in the absence and the presence of 20% (w/v) SHSC or honey are given in Figure 3.48. The far-UV CD spectral features of the native BSA and 4.6 M urea-denatured BSA were found similar to those described above (Figure 3.7; Table 3.4). As can be seen from the Figure 3.48, the spectral signal at 208 nm of the partially-denatured BSA in the absence and the presence of SHSC or honey could not be detected due to high signal to noise ratio below 215 nm. Although addition of 20% (w/v) SHSC to 4.6 M urea-denatured BSA produced a significant increase in its MRE_{222nm} value from –11,923.1 deg.cm^2.dmol^{-1} to –15,188.4 deg.cm^2.dmol^{-1}, spectral overlap and an MRE_{222nm} value (–19,925.1 deg.cm^2.dmol^{-1}) comparable to that of the native BSA (–19,988.7 deg.cm^2.dmol^{-1}) were achieved in the presence of 20% (w/v) honey (Figure 3.48). Furthermore, both native BSA and 4.6 M urea-denatured BSA in the presence of 20% (w/v) honey were found to possess similar (~58%) α-helical content. These results proved that 20% (w/v) honey was sufficient to maintain the native protein conformation of BSA even in the presence of 4.6 M urea, which was otherwise not possible with 20% (w/v) SHSC.

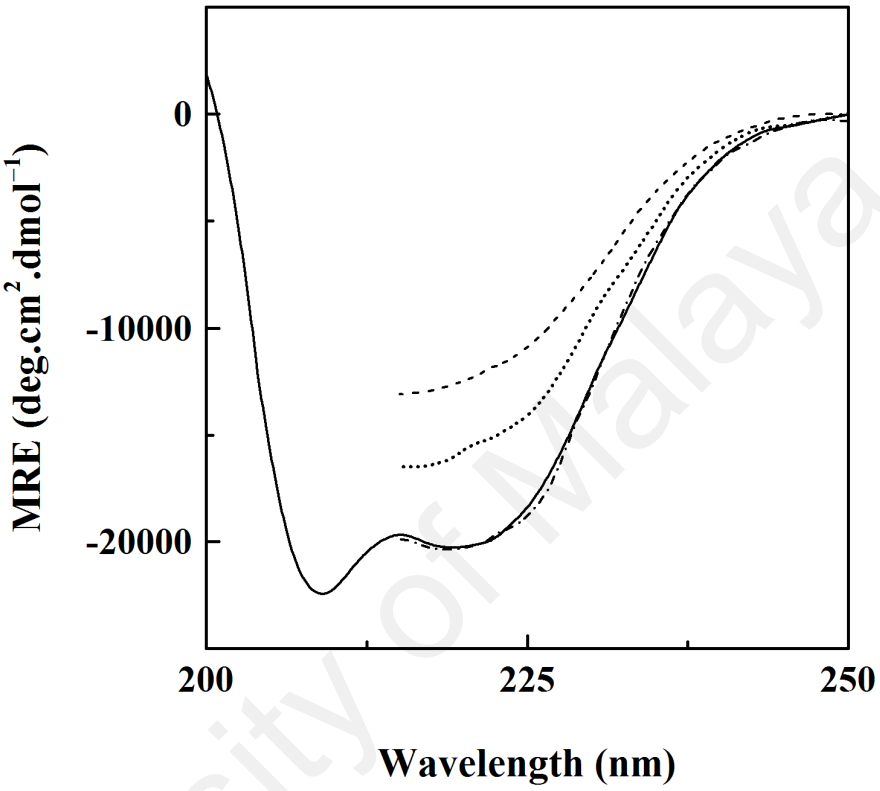

Figure 3.48. Far-UV CD spectra of BSA (——) and 4.6 M urea-denatured BSA in the absence (– – –) and the presence of 20% (w/v) SHSC (·····) or honey (– · –) at pH 7.4. The protein concentration was 2 μM.

3.4.2.3. Thermal denaturation of BSA in the absence and the presence of honey or SHSC

Thermal stabilizing potentials of SHSC and honey on BSA were compared using far-UV CD spectroscopy. Figure 3.49 shows thermal denaturation curves of BSA in the absence and the presence of 20% (w/v) SHSC or honey, as monitored by MRE_{222nm} measurements. The thermal denaturation curves of BSA in the absence and the presence of 20% (w/v) SHSC were similar to those described in the section 3.1.4 (Figure 3.17), showing a shift in the transition towards higher temperature range in the presence of SHSC. Interestingly, degree of thermal stabilization of BSA offered by 20% (w/v) honey was found greater than that observed in the presence of 20% (w/v) SHSC at all temperatures, as denaturation was further delayed, showing major structural changes beyond 70°C (Figure 3.49).

Figure 3.50 shows the far-UV CD spectra of BSA, obtained at 65°C in the absence and the presence of 20% (w/v) SHSC or honey. The far-UV CD spectrum of the native BSA at 25°C is also included in the figure for comparison. Similar to that shown in Figure 3.18, about 36% decrease in the MRE_{222nm} value (24% decrease in the α-helical content) of BSA was observed at 65°C, compared to the characteristics (MRE_{222nm}= –19,963.2 deg.cm^2.dmol^{-1}; α-helix= ~58%) of the native BSA at 25°C. In accordance with the results shown in the section 3.1.4, such loss in the secondary structure was partially reverted (representing 20% and 13% decrease in the MRE_{222nm} value and the α-helical content, respectively) in the presence of 20% (w/v) SHSC, suggesting SHSC-induced protein stabilization. On the other hand, greater protein stabilization was noticed in the presence of 20% (w/v) honey as the MRE_{222nm} value (–17,493.8 deg.cm^2.dmol^{-1}) and the α-helical content (~50%) showed only 12% and 8% decrease, respectively, from those

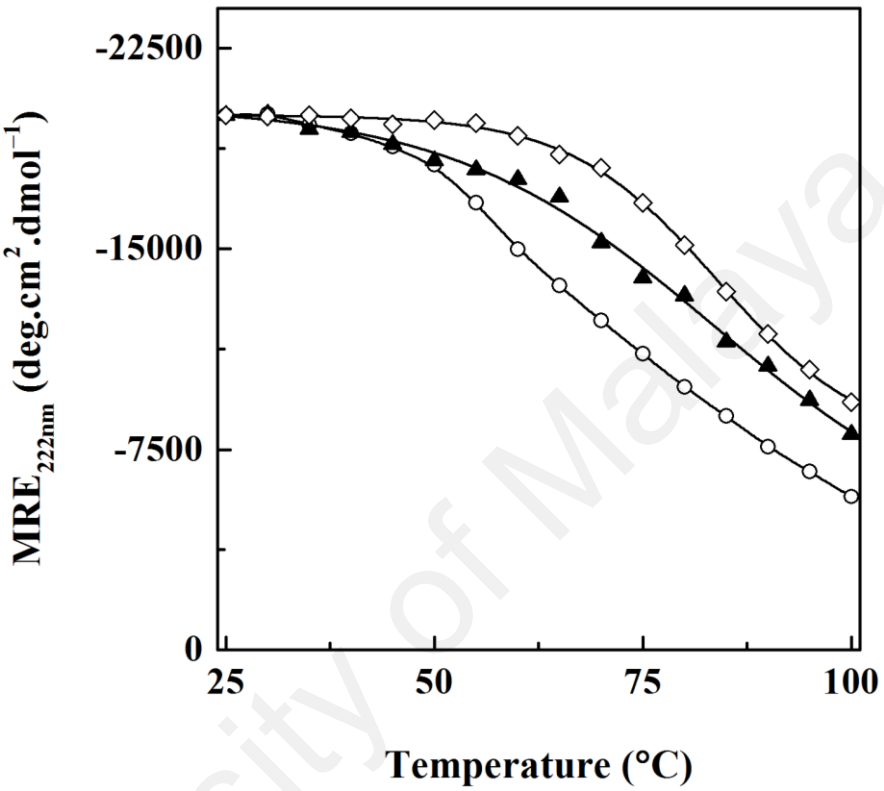

Figure 3.49. Thermal denaturation curves of BSA (2 μM) in 60 mM sodium phosphate buffer, pH 7.4, as studied by MRE_{222nm} measurements in the absence (○) and the presence of 20% (w/v) SHSC (▲) or honey (◇).

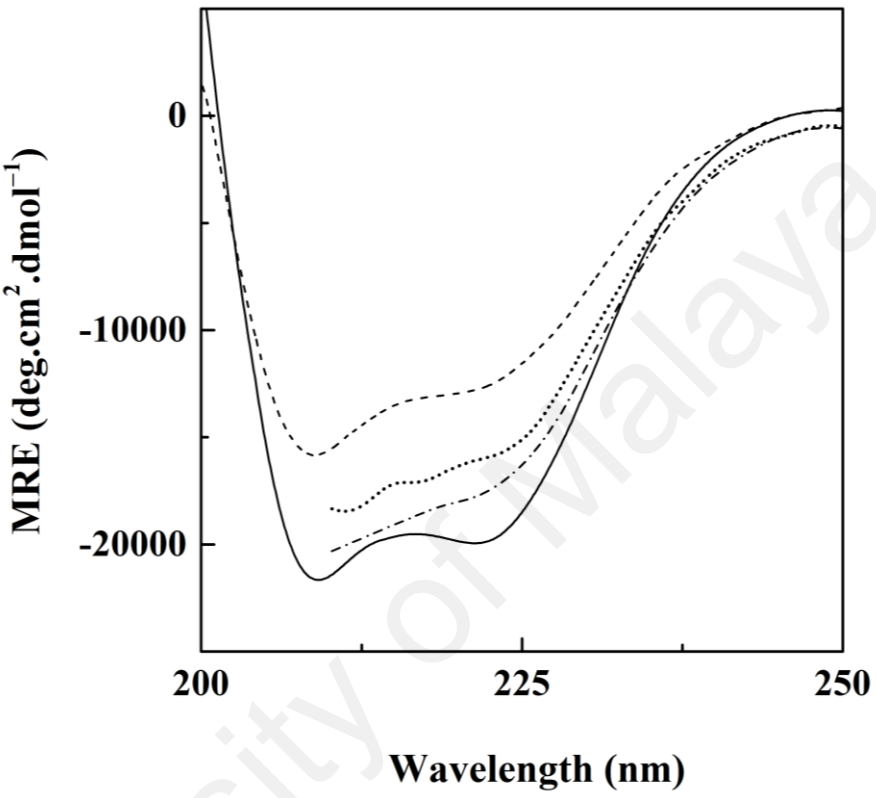

Figure 3.50. Far-UV CD spectra of BSA at 25°C (——) and 65°C in the absence (– – –) and the presence of 20% (w/v) SHSC (·····) or honey (– · –) at pH 7.4. The protein concentration was 2 μM.

obtained with the native BSA (Figure 3.50). These results also supported greater thermal stabilizing potential of honey on BSA, compared to SHSC.

Although SHSC was formulated using the same sugar composition as that found in the honey, nonetheless, presence of several additional compounds (amino acids and proteins (~500 mg%), flavonoids and polyphenolic compounds (~50 mg%), minerals (~200 mg%) and vitamins (~5 mg%) (Bogdanov *et al.*, 2008) in honey would have contributed to the greater protein stabilizing potential of honey. This is supported by various reports, suggesting protein stabilizing effects of amino acids, flavonoids and polyphenolic compounds *etc* (Taneja & Ahmad, 1994; Rawel *et al.*, 2002; Ozdal *et al.*, 2013).

3.5. Honey / SHSC-induced protein stabilization mechanism

Many studies have shown the stabilizing potential of sugars (mono-, di- and trisaccharides) on proteins against different denaturing conditions, particularly, thermal denaturation (Baier & McClements, 2001; Miroliaei & Nemat-Gorgani, 2001; Kaushik & Bhat, 2003; Gheibi et al., 2006; Miroliaei et al., 2007; Poddar et al., 2008; Bellavia et al., 2009; Naika et al., 2009; Yadav & Prakash, 2009; Singh et al., 2011). Several mechanisms have been proposed in support of sugar-induced protein stabilization (Gerlsma, 1968; 1970; Back et al., 1979; Lee & Timasheff, 1981; Arakawa & Timasheff, 1982; Bolen & Baskakov, 2001). However, no single mechanism can be generalized to explain the protein stabilization phenomenon in the presence of sugars.

According to Timasheff and his group (Lee & Timasheff, 1981; Arakawa & Timasheff, 1982; 1985; Lin & Timasheff, 1996; Timasheff, 2002), sugar-induced protein stabilization can be explained on the basis of 'preferential hydration' of protein, which is noted to be a common feature in the presence of sugars, irrespective of the kind of protein and solvent conditions (Arakawa & Timasheff, 1982). The preferential hydration of a protein implies that either the concentration of sugars in the vicinity of protein is less compared to that available in the bulk solvent or it is totally excluded (Lee & Timasheff, 1981). This can be understood from Figure 3.51, showing preferential interactions, which include preferential binding of the co-solute or its preferential exclusion (preferential hydration) from the protein surface (Timasheff, 2002). As shown in the figure, upon addition of co-solute (sugar) into the solution, the co-solute either binds to the protein surface, manifesting 'preferential binding' or excluded from the protein surface (preferential exclusion). Preferential binding of co-solute may lead to preferential exclusion of water. Similarly, preferential exclusion of co-solute may result in preferential hydration of proteins. However, the experimental results from Timasheff and his group indicated that the sugar molecules are preferentially excluded from the protein

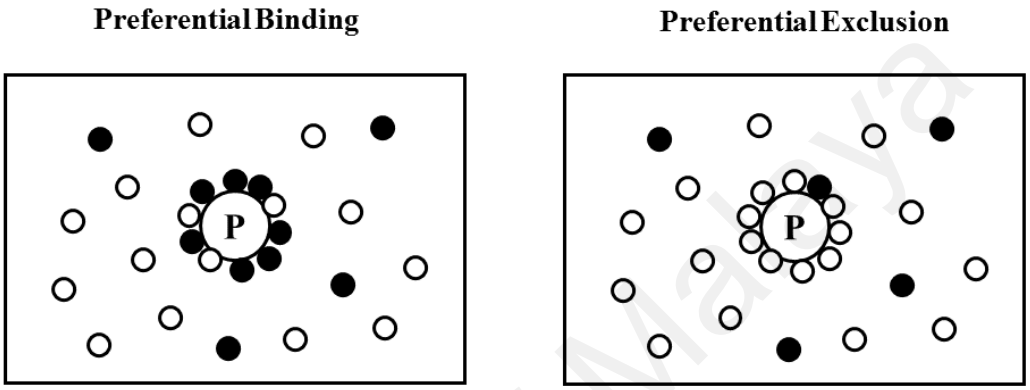

Figure 3.51. Molecular distribution of water and co-solutes in the preferential interactions. Different symbols used are water (○) and co-solute (●) molecules.

surface, thus supporting the preferential exclusion / preferential hydration phenomena (Lee & Timasheff, 1981). Addition of sugars to protein solution increases the surface tension of water and are therefore, preferentially excluded from the protein surface, thus manifesting preferential hydration of protein (Arakawa & Timasheff, 1985). Besides, steric repulsions may result in a little volume fraction occupied by sugar molecules at the protein surface and further contribute to the preferential hydration (Bhat & Timasheff, 1992; Xie & Timasheff, 1997).

The preferential hydration of proteins in the presence of sugars signifies that addition of sugars to a protein solution is an unfavourable process, characterized by a positive free energy change (Arakawa & Timasheff, 1982). This positive free energy change is assumed to be higher in the denatured state of the protein due to greater surface area, compared to its native counterpart (Timasheff et al., 1976; Arakawa & Timasheff, 1982). In other words, sugar-protein interactions are thermodynamically more unfavourable in the denatured state than the native state of the protein (Arakawa & Timasheff, 1982). Hence, the equilibrium between the native and the denatured states of a protein would have shifted towards its native state, thus favouring protein stabilization (Lee & Timasheff, 1981).

To understand the thermodynamic stabilization of a protein in the presence of sugars, thermodynamic cycle of the native and the denatured states of the protein in the absence and the presence of co-solute (sugar) is shown in Figure 3.52. The free energy changes for the transformation of the protein from its native state to the denatured state in water and the sugar solution are marked as ΔG_1 and ΔG_4, respectively, while ΔG_3 and ΔG_2 represent free energy change for the transfer reactions of the native and the denatured states of a protein from water to sugar solution, respectively. Since the conformation of the native state and the denatured state of the protein remains identical in the absence and

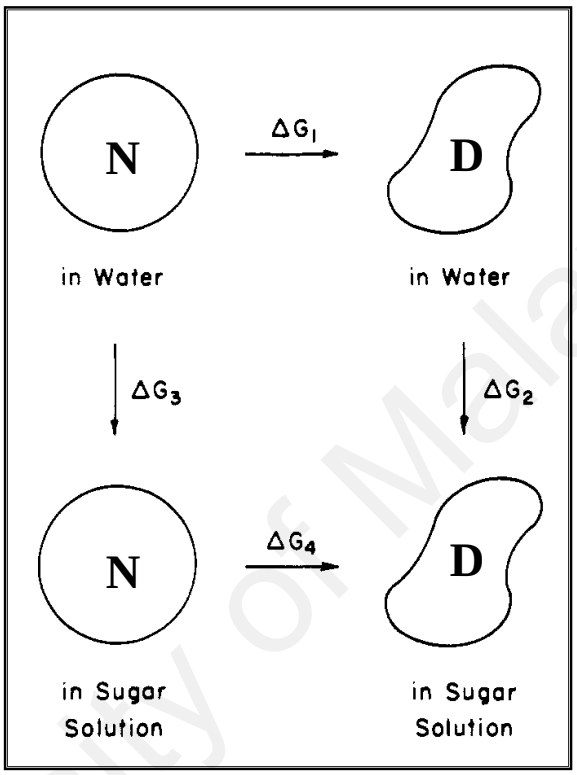

Figure 3.52. Scheme showing thermodynamic cycle of the native (N) and the denatured (D) states of a protein in the absence and the presence of sugars. (Adapted from Arakawa and Timasheff, 1982)

the presence of sugars, hence, $\Delta G_1 + \Delta G_2$ should be equal to $\Delta G_3 + \Delta G_4$. However, ΔG_2 will be higher than ΔG_3 due to greater increase in the positive chemical potential of the denatured state in the presence of sugar, thus leading to $\Delta G_1 < \Delta G_4$. This phenomenon can be better visualized from the relative free energy diagram for the transfer reactions of the native and the denatured states of a protein from water to sugar solution, as shown in Figure 3.53. Hence, the equilibrium will shift towards the native state in the presence of sugar, favouring protein stabilization.

In accordance to Timasheff's mechanism, Bolen and co-workers (Liu & Bolen, 1995; Qu et al., 1998; Bolen & Baskakov, 2001) have also suggested an increase in the Gibbs free energy of the protein molecule in the presence of osmolytes (sugars). However, according to them, the chemical origin of the increase in the Gibbs free energy in both native and denatured states of a protein in the presence of osmolytes lies in the unfavourable (solvophobic) interactions between the osmolytes and the polypeptide backbone, which is termed as 'osmophobic effect' (Liu & Bolen, 1995; Bolen & Baskakov, 2001). In view of the greatly exposed polypeptide backbone structure in the denatured state of a protein, this osmophobic effect would be more pronounced, thus increase in the Gibbs free energy of the denatured state would be far greater than its native counterpart (Qu et al., 1998; Bolen & Baskakov, 2001). Hence, addition of osmolytes would have favoured the native state of the protein due to the displacement of the equilibrium between the native and the denatured states of the protein towards the native state (Qu et al., 1998; Bolen & Baskakov, 2001).

Smith and co-workers (Back et al., 1979) have conceived the idea of protein stabilization by sugars through alteration in the water structure, which in turn determines the strength of the hydrophobic interactions. Presence of sugars in the solvent would have changed the solvent properties in the vicinity of the protein molecule, leading to stronger

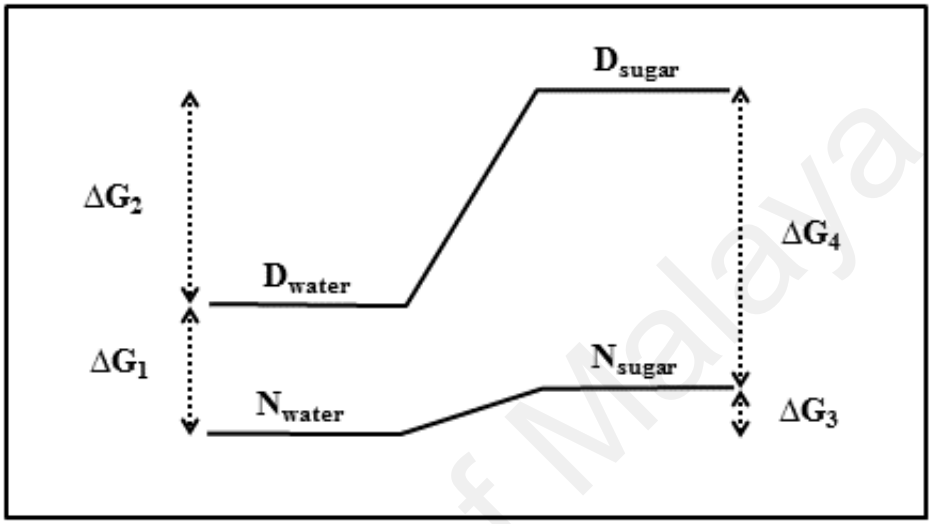

Figure 3.53. Relative free energy diagram for the transfer reactions of the native and the denatured states of a protein from water to sugar solution. N_{water} and D_{water} represent native and denatured states of a protein in water, respectively, while N_{sugar} and D_{sugar} are the native and denatured states of the protein in sugar solution, respectively. (Adapted from Qu et al., 1998)

hydrophobic interactions in the protein (Back et al., 1979). This change in the solvent properties would have also been responsible for reducing the hydrogen rupturing potency of surrounding water molecules in the vicinity of the protein, thus leading to protein stabilization (Gerlsma, 1970). This seems reasonable as water molecules connect different sugar molecules to each other as well as to the protein surface via hydrogen bonds, forming a water–mediated hydrogen bond network (Cottone et al., 2002; Cottone, 2007). This hydrogen bond network renders the interaction between the protein and the water molecules less favourable as compared to that in the absence of sugar. In view of the above, water molecules are hindered from penetrating the protein interior and breaking the internal hydrogen bonds (Schiffer et al., 1995). Besides, this network also hinders the water molecules at the protein surface from breaking the surface hydrogen bonds formed between the surface polar residues.

Since SHSC / honey represents a mixture of sugars, mainly fructose and glucose, presence of SHSC / honey would have displaced the equilibrium between the native and the denatured states of a protein towards the native state through both preferential hydration as well as osmophobic effect, as described by Timasheff (Lee & Timasheff, 1981; Arakawa & Timasheff, 1982; 1985; Lin & Timasheff, 1996; Timasheff, 2002) and Bolen (Liu & Bolen, 1995; Qu et al., 1998; Bolen & Baskakov, 2001), respectively. Furthermore, an increase in the hydrophobic interactions in the protein and reduced hydrogen bond rupturing potency of surrounding water molecules could have also played a role in maintaining native structure of the protein.

An earlier report (Poddar et al., 2008) has shown greater stabilizing effect of equimolar mixture of monosaccharide constituents of various disaccharides than that observed with the respective disaccharides. In other words, protein stabilizing potential of monosaccharide mixtures has been suggested as additive and synergistic. A molecular

simulation study has also supported synergistic protein stabilizing effect of monosaccharide mixtures. Cluster formation involving monosaccharide mixtures through short-range interactions, has been suggested an important factor for synergistic action (Poddar et al., 2010). The formed clusters would have larger molecular radius than their respective disaccharides (Poddar et al., 2010). The tendency of the cluster formation depends on the hydrogen bond forming capacity of various sugars, in which monosaccharides have higher capability as part of the hydroxyl groups is used to form chemical bond in disaccharides (Lerbret et al., 2005). Such increase in the molecular radius would have induced more hydration shells around the protein molecule, thus leading towards greater protein stabilization (Poddar et al., 2010). This can be clearly seen from the Figure 3.54, showing higher cluster formation of monosaccharide mixtures at higher sugar concentrations, which leads to greater hydration of the protein.

Since SHSC / honey is a mixture of sugars, comprised of different mono- and disaccharides, clusters could have been formed among different monosaccharide molecules, leading to an increased molecular radius, thus promoting greater hydration shell around protein molecules and greater stabilization. On this basis, SHSC / honey would have provided greater protein stabilization than equal concentrations of individual sugars and this would have significantly reduced the concentration of sugar requirement to achieve similar extent of stabilization.

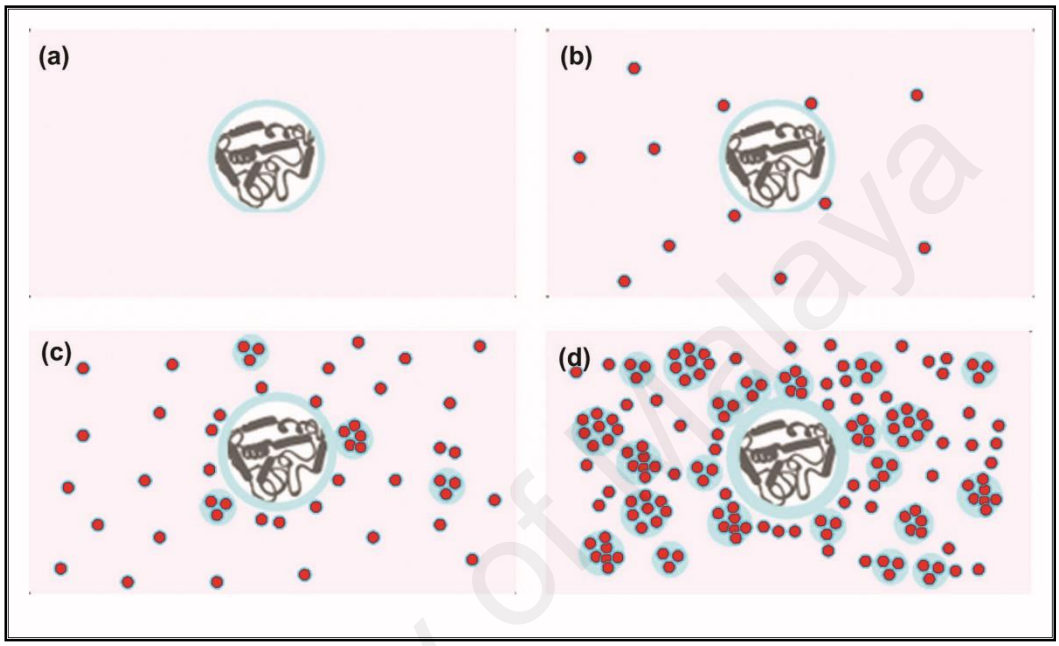

Figure 3.54. Geometrical model describing the increase in cluster formation with increasing monosaccharide mixture concentration. (A) protein molecule in solvent water; (B) small amount of sugar along with protein in water; (C) cluster formation begins at intermediate sugar concentration; (D) more cluster formation at higher sugar concentration. The blue colour shows hydration and red colour shows sugar molecules. (Adapted from Poddar et al., 2010)

CHAPTER 4

Conclusions

4. CONCLUSIONS

The chemical and thermal stability of BSA, ovalbumin and lysozyme were enhanced in the presence of SHSC as reflected by the shift of the transition curves (urea, GdnHCl and thermal) towards higher denaturant concentrations. Furthermore, SHSC-induced protein stabilization was found to be concentration dependent, being more pronounced at higher SHSC concentrations. The spectral characterization of the partially-denatured states of BSA, ovalbumin and lysozyme in the absence and the presence of SHSC also suggested significant retention of both secondary and tertiary structures of the protein in the presence of SHSC. Therefore, SHSC can be used as a solvent additive for protein stabilization.

The intrinsic fluorescence of BSA was quenched in the presence of honey in a concentration dependent manner, showing complete quenching in the presence of 5% (w/v) honey. Similar quenching effect was also observed with ovalbumin, suggesting this phenomenon as a general effect on many proteins. Due to the fluorescence quenching behavior of honey, urea denaturation studies on BSA using intrinsic fluorescence as a probe failed to produce any transition in the presence of 5% (w/v) honey. Hence, intrinsic fluorescence cannot be used as a spectral probe in protein denaturation / stabilization studies in the presence of honey.

Greater increase in the chemical and thermal stability of BSA was observed in the presence of honey compared to SHSC, as evident by the larger shift in the transition curve towards higher denaturant concentrations in the presence of honey. In other words, the protein stabilizing potential of honey was found to be greater than that observed with SHSC, which may be due to the presence of several other components such as amino acids, proteins, minerals, vitamins, polyphenolic compounds and flavonoids in honey.

CHAPTER 5

References

5. REFERENCES

Acharya, P., Rajakumara, E., Sankaranarayanan, R. and Rao, N. M. (2004). Structural basis of selection and thermostability of laboratory evolved *Bacillus subtilis* lipase. *Journal of Molecular Biology, 341*(5): 1271–1281.

Ahmad, B., Ahmed, M. Z., Haq, S. K. and Khan, R. H. (2005). Guanidine hydrochloride denaturation of human serum albumin originates by local unfolding of some stable loops in domain III. *Biochimica et Biophysica Acta, 1750*(1): 93–102.

Ahmad, F. and Salahuddin, A. (1976). Reversible unfolding of the major fraction of ovalbumin by guanidine hydrochloride. *Biochemistry, 15*(23): 5168–5175.

Ahmad, F. and Bigelow, C. C. (1982). Estimation of the free energy of stabilization of ribonuclease A, lysozyme, α-lactalbumin, and myoglobin. *Journal of Biological Chemistry, 257*(21): 12935–12938.

Ahmad, F., Contaxis, C. C. and Bigelow, C. C. (1983). Free energy changes in lysozyme denaturation. *Journal of Biological Chemistry, 258*(13): 7960–7963.

Ahmad, F., Yadav, S. and Taneja, S. (1992). Determining stability of proteins from guanidinium chloride transition curves. *Biochemical Journal, 287*: 481–485.

Ahmad, N. and Qasim, M. A. (1995). Fatty acid binding to bovine serum albumin prevents formation of intermediate during denaturation. *European Journal of Biochemistry, 227*(1-2): 563–565.

Akanuma, S., Qu, C., Yamagishi, A., Tanaka, N. and Oshima, T. (1997). Effect of polar side chains at position 172 on thermal stability of 3-isopropylmalate dehydrogenase from *Thermus thermophilus*. *FEBS Letters, 410*(2–3): 141-144.

Al-Mamary, M., Al-Meeri, A. and Al-Habori, M. (2002). Antioxidant activities and total phenolics of different types of honey. *Nutrition Research, 22*(9): 1041–1047.

Alderton, G., Ward, W. H. and Fevold, H. L. (1945). Isolation of lysozyme from egg white. *Journal of Biological Chemistry, 157*(1): 43–58.

Alleoni, A. C. C. (2006). Albumen protein and functional properties of gelation and foaming. *Scientia Agricola, 63*: 291–298.

Allison, S. D., Dong, A. and Carpenter, J. F. (1996). Counteracting effects of thiocyanate and sucrose on chymotrypsinogen secondary structure and aggregation during freezing, drying, and rehydration. *Biophysical Journal, 71*(4): 2022–2032.

Andrade, P., Ferreres, F., Gil, M. I. and Tomás-Barberán, F. A. (1997). Determination of phenolic compounds in honeys with different floral origin by capillary zone electrophoresis. *Food Chemistry, 60*(1): 79–84.

Anfinsen, C. B. (1973). Principles that govern the folding of protein chains. *Science, 181*(4096): 223–230.

Aoki, K., Sato, K., Nagaoka, S., Kamada, M. and Hiramatsu, K. (1973). Heat denaturation of bovine serum albumin in alkaline pH region. *Biochimica et Biophysica Acta, 328*(2): 323–333.

Arai, S. and Hirai, M. (1999). Reversibility and hierarchy of thermal transition of hen egg-white lysozyme studied by small-angle x-ray scattering. *Biophysical Journal, 76*(4): 2192–2197.

Arakawa, T. and Timasheff, S. N. (1982). Stabilization of protein structure by sugars. *Biochemistry, 21*(25): 6536–6544.

Arakawa, T. and Timasheff, S. N. (1985). The stabilization of proteins by osmolytes. *Biophysical Journal, 47*(3): 411–414.

Arakawa, T., Ejima, D., Tsumoto, K., Obeyama, N., Tanaka, Y., Kita, Y. and Timasheff, S. N. (2007). Suppression of protein interactions by arginine: A proposed mechanism of the arginine effects. *Biophysical Chemistry, 127*(1-2): 1–8.

Arumugam, B., Kadir, H. A. and Tayyab, S. (2010). Effect of charge neutralization at lysine residues on the free energy of stabilization of hen egg white lysozyme. *Romanian Journal of Biochemistry, 47*(2): 115–133.

Aune, K. C. and Tanford, C. (1969). Thermodynamics of the denaturation of lysozyme by guanidine hydrochloride. II. Dependence on denaturant concentration at 25°. *Biochemistry, 8*(11): 4586–4590.

Back, J. F., Oakenfull, D. and Smith, M. B. (1979). Increased thermal stability of proteins in the presence of sugars and polyols. *Biochemistry, 18*(23): 5191–5196.

Baier, S. and McClements, D. J. (2001). Impact of preferential interactions on thermal stability and gelation of bovine serum albumin in aqueous sucrose solutions. *Journal of Agricultural and Food Chemistry, 49*(5): 2600–2608.

Baptista, R. P., Cabral, J. M. and Melo, E. P. (2000). Trehalose delays the reversible but not the irreversible thermal denaturation of cutinase. *Biotechnology and Bioengineering, 70*(6): 699–703.

Barnes, K. P., Warren, J. R. and Gordon, J. A. (1972). Effect of urea on the circular dichroism of lysozyme. *Journal of Biological Chemistry, 247*(6): 1708–1712.

Batra, P., Sasa, K., Ueki, T. and Takeda, K. (1989). Circular dichroic study of conformational changes in ovalbumin. *Journal of Protein Chemistry, 8*(2): 221–229.

Batra, P. P. and Uetrecht, D. (1990). Helix stability in succinylated and acetylated ovalbumins: Effect of high ph, urea and guanidine hydrochloride. *Biochimica et Biophysica Acta, 1040*: 102–108.

Bellavia, G., Cottone, G., Giuffrida, S., Cupane, A. and Cordone, L. (2009). Thermal denaturation of myoglobin in water-disaccharide matrixes: Relation with the glass transition of the system. *Journal of Physical Chemistry B, 113*(33): 11543–11549.

Ben Mabrouk, S., Aghajari, N., Ben Ali, M., Ben Messaoud, E., Juy, M., Haser, R. and Bejar, S. (2011). Enhancement of the thermostability of the maltogenic amylase MAUS149 by Gly312Ala and Lys436Arg substitutions. *Bioresource Technology, 102*(2): 1740–1746.

Berg, J. M., Tymoczko, J. L. and Stryer, L. (2002). *Biochemistry* (5 ed.). New York: W.H. Freeman.

Beychok, S. and Warner, R. C. (1959). Denaturation and electrophoretic behavior of lysozyme. *Journal of the American Chemical Society, 81*(8): 1892–1897.

Bhat, R. and Timasheff, S. N. (1992). Steric exclusion is the principal source of the preferential hydration of proteins in the presence of polyethylene glycols. *Protein Science, 1*(9): 1133–1143.

Bieniarz, C., Cornwell, M. J. and Young, D. F. (1998). Alkaline phosphatase activatable polymeric cross-linkers and their use in the stabilization of proteins. *Bioconjugate Chemistry, 9*(3): 390–398.

Bisgaard-Frantzen, H., Svendsen, A., Norman, B., Pedersen, S., Kjaerulff, S., Outtrup, H. and Borchert, T. V. (1999). Development of industrially important α-amylases. *Journal of Applied Glycoscience, 46*(2): 199–206.

Blake, C. C., Johnson, L. N., Mair, G. A., North, A. C., Phillips, D. C. and Sarma, V. R. (1967). Crystallographic studies of the activity of hen egg-white lysozyme. *Proceedings of the Royal Society of London. Series B: Biological Sciences, 167*(1009): 378–388.

Blake, C. C. F., Koenig, D. F., Mair, G. A., North, A. C. T., Phillips, D. C. and Sarma, V. R. (1965). Structure of hen egg-white lysozyme: A three-dimensional fourier synthesis at 2 Å resolution. *Nature, 206*(4986): 757–761.

Bogdanov, S., Haldimann, M., Luginbühl, W. and Gallmann, P. (2007). Minerals in honey: Environmental, geographical and botanical aspects. *Journal of Apicultural Research, 46*(4): 269–275.

Bogdanov, S., Jurendic, T., Sieber, R. and Gallmann, P. (2008). Honey for nutrition and health: A review. *Journal of the American College of Nutrition, 27*(6): 677–689.

Bolen, D. W. and Baskakov, I. V. (2001). The osmophobic effect: Natural selection of a thermodynamic force in protein folding. *Journal of Molecular Biology, 310*(5): 955–963.

Bonincontro, A., Cinelli, S., Onori, G. and Stravato, A. (2004). Dielectric behavior of lysozyme and ferricytochrome-c in water / ethylene-glycol solutions. *Biophysical Journal, 86*(2): 1118–1123.

Botelho, M. G., Gralle, M., Oliveira, C. L., Torriani, I. and Ferreira, S. T. (2003). Folding and stability of the extracellular domain of the human amyloid precursor protein. *Journal of Biological Chemistry, 278*(36): 34259–34267.

Brandt, J. and Andersson, L.-O. (1976). Heat denaturation of human serum albumin. Migration of bound fatty acids. *International Journal of Peptide and Protein Research, 8*(1): 33–37.

Brannigan, J. A. and Wilkinson, A. J. (2002). Protein engineering 20 years on. *Nature Reviews Molecular Cell Biology, 3*(12): 964–970.

Brown, J. R. (1977). Serum albumin: Amino acid sequence. In V. M. Rosenoer, M. Oratz and M. A. Rothschild (Eds.), *Albumin: Structure, Function and Uses* (pp. 27–52). New York: Pergamon Press.

Bryan, P. N. (2000). Protein engineering of subtilisin. *Biochimica et Biophysica Acta, 1543*(2): 203–222.

Burley, R. W. and Vadehra, D. V. (1989). The albumen: Chemistry. In R. W. Burley and D. V. Vadehra (Eds.), *The Avian Egg: Chemistry and Biology* (pp. 65–128). New York: Wiley.

Bustos-Jaimes, I., Mora-Lugo, R., Calcagno, M. L. and Farres, A. (2010). Kinetic studies of Gly28:Ser mutant form of *Bacillus pumilus* lipase: Changes in k(cat) and thermal dependence. *Biochimica et Biophysica Acta, 1804*(12): 2222–2227.

Callewaert, L. and Michiels, C. W. (2010). Lysozymes in the animal kingdom. *Journal of Biosciences, 35*(1): 127–160.

Canfield, R. E. (1963a). Peptides derived from tryptic digestion of egg white lysozyme. *Journal of Biological Chemistry, 238*(8): 2691–2697.

Canfield, R. E. (1963b). The amino acid sequence of egg white lysozyme. *Journal of Biological Chemistry, 238*(8): 2698–2707.

Canfield, R. E. and Liu, A. K. (1965). The disulfide bonds of egg white lysozyme (muramidase). *Journal of Biological Chemistry*, *240*: 1997–2002.

Cann, J. R. (1949). Electrophoretic analysis of ovalbumin. *Journal of the American Chemical Society, 71*(3): 907–909.

Cardamone, M. and Puri, N. K. (1992). Spectrofluorimetric assessment of the surface hydrophobicity of proteins. *Biochemical Journal, 282*: 589–593.

Carrotta, R., Manno, M., Giordano, F. M., Longo, A., Portale, G., Martorana, V. and Biagio, P. L. (2009). Protein stability modulated by a conformational effector: Effects of trifluoroethanol on bovine serum albumin. *Physical Chemistry Chemical Physics, 11*(20): 4007–4018.

Carter, D. C. and Ho, J. X. (1994). Structure of serum albumin. *Advances in Protein Chemistry, 45*: 153–203.

Catanzano, F., Gambuti, A., Graziano, G. and Barone, G. (1997). Interaction with D-glucose and thermal denaturation of yeast hexokinase B: A DSC study. *Journal of Biochemistry, 121*(3): 568–577.

Chang, J. Y. and Li, L. (2002). The unfolding mechanism and the disulfide structures of denatured lysozyme. *FEBS Letters, 511*(1-3): 73–78.

Chebotareva, N. A., Kurganov, B. I. and Livanova, N. B. (2004). Biochemical effects of molecular crowding. *Biochemistry (Moscow), 69*(11): 1239–1251.

Chen, Y. H., Yang, J. T. and Martinez, H. M. (1972). Determination of the secondary structures of proteins by circular dichroism and optical rotatory dispersion. *Biochemistry, 11*(22): 4120–4131.

Chio, K. S. and Tappel, A. L. (1969). Inactivation of ribonuclease and other enzymes by peroxidizing lipids and by malonaldehyde. *Biochemistry, 8*(7): 2827–2832.

Clarke, J. and Fersht, A. R. (1993). Engineered disulfide bonds as probes of the folding pathway of barnase: Increasing the stability of proteins against the rate of denaturation. *Biochemistry, 32*(16): 4322–4329.

Cohn, E. J., Hughes, W. L. and Weare, J. H. (1947). Preparation and properties of serum and plasma proteins. Xiii. Crystallization of serum albumins from ethanol – water mixtures. *Journal of the American Chemical Society, 69*(7): 1753–1761.

Conchie, J. and Strachan, I. (1978). The carbohydrate units of ovalbumin: Complete structures of three glycopeptides. *Carbohydrate Research, 63*: 193–213.

Cottone, G., Ciccotti, G. and Cordone, L. (2002). Protein–trehalose–water structures in trehalose coated carboxy-myoglobin. *The Journal of Chemical Physics, 117*(21): 9862–9866.

Cottone, G. (2007). A comparative study of carboxy myoglobin in saccharide-water systems by molecular dynamics simulation. *Journal of Physical Chemistry. B, 111*(13): 3563–3569.

Covaciu, M., Olaru, F. and Petrescu, I. (2004). Ovalbumin isoforms - purification and denaturation / renaturation studies. *Analele Stiintifice Ale Universitatii Alexandru Ioan Cuza din Iasi,Sectiunea II A : Genetica si Biologie Moleculara, 5* (1), 6 pages.

Crane, E. (1983). *The Archaeology of Beekeeping*. London: Gerald Duckworth & Co.

Cunningham, L. W., Wilburn Clouse, R. and Ford, J. D. (1963). Heterogeneity of the carbohydrate moiety of crystalline ovalbumin. *Biochimica et Biophysica Acta, 78*(2): 379–381.

Davies, R. C., Neuberger, A. and Wilson, B. M. (1969). The dependence of lysozyme activity on pH and ionic strength. *Biochimica et Biophysica Acta, 178*(2): 294–305.

Dayhoff, M. O., Perlmann, G. E. and MacInnes, D. A. (1952). The partial specific volumes, in aqueous solution, of three proteins. *Journal of the American Chemical Society, 74*(10): 2515–2517.

Deng, F. Y. and Liu, Y. (2012). Study of the interaction between tosufloxacin tosylate and bovine serum albumin by multi-spectroscopic methods. *Journal of Luminescence, 132*(2): 443–448.

Dill, K. A. (1990). Dominant forces in protein folding. *Biochemistry, 29*(31): 7133–7155.

Dill, K. A. and Shortle, D. (1991). Denatured states of proteins. *Annual Review of Biochemistry, 60*(1): 795–825.

Dobson, C. M. (2003). Protein folding and misfolding. *Nature, 426*(6968): 884–890.

Dombkowski, A. A., Sultana, K. Z. and Craig, D. B. (2014). Protein disulfide engineering. *FEBS Letters, 588*(2): 206–212.

Doner, L. W. (1977). The sugars of honey–a review. *Journal of the Science of Food and Agriculture, 28*(5): 443–456.

Doner, L. W. (2003). Honey. In B. Caballero (Ed.), *Encyclopedia of Food Sciences and Nutrition (Second Edition)* (pp. 3125–3130). Oxford: Academic Press.

Dong, A. C., Meyer, J. D., Brown, J. L., Manning, M. C. and Carpenter, J. F. (2000). Comparative fourier transform infrared and circular dichroism spectroscopic analysis of α_1-proteinase inhibitor and ovalbumin in aqueous solution. *Archives of Biochemistry and Biophysics, 383*(1): 148–155.

Ellis, R. J. and Hartl, F. U. (1999). Principles of protein folding in the cellular environment. *Current Opinion in Structural Biology, 9*(1): 102–110.

Evrard, C., Fastrez, J. and Declercq, J. P. (1998). Crystal structure of the lysozyme from bacteriophage lambda and its relationship with V and C-type lysozymes. *Journal of Molecular Biology, 276*(1): 151–164.

Fágáin, C. Ó. (1995). Understanding and increasing protein stability. *Biochimica et Biophysica Acta, 1252*(1): 1–14.

Fágáin, C. Ó. (2003). Enzyme stabilization—recent experimental progress. *Enzyme and Microbial Technology, 33*(2): 137–149.

Farruggia, B., Nerli, B., Di Nuci, H., Rigatusso, R. and Pico, G. (1999). Thermal features of the bovine serum albumin unfolding by polyethylene glycols. *International Journal of Biological Macromolecules, 26*(1): 23–33.

Farruggia, B. and Pico, G. A. (1999). Thermodynamic features of the chemical and thermal denaturations of human serum albumin. *International Journal of Biological Macromolecules, 26*(5): 317–323.

Feeney, R. E., Yamasaki, B. B. and Geoghegan, K. F. (1982). Chemical modification of proteins: An overview. In R. E. Feeney and J. R. Whitaker (Eds.), *Modification of Proteins: Food, Nutritional and Pharmacological Aspects* (Vol. 198, pp. 3–55): American Chemical Society.

Fenel, F., Leisola, M., Janis, J. and Turunen, O. (2004). A de novo designed N-terminal disulphide bridge stabilizes the *Trichoderma reesei* endo-1,4-beta-xylanase II. *Journal of Biotechnology, 108*(2): 137–143.

Fenel, F., Zitting, A. J. and Kantelinen, A. (2006). Increased alkali stability in *Trichoderma reesei* endo-1, 4-beta-xylanase II by site directed mutagenesis. *Journal of Biotechnology, 121*(1): 102–107.

Foster, J. F. (1960). Plasma albumin. In F. W. Putnam (Ed.), *The Plasma Proteins* (Vol. 1, pp. 179–239). New York: Academic Press.

Foster, J. F. (1977). Some aspects of the structure and conformational properties of serum albumin. In V. M. Rosenoer, M. Oratz and M. A. Rothschild (Eds.), *Albumin: Structure, Function and Uses* (pp. 53–84). New York: Pergamon Press.

Fothergill, L. A. and Fothergill, J. E. (1968). Disulphide bonds of ovalbumins. *Biochemical Journal, 110*(3): 36P–37P.

Fothergill, L. A. and Fothergill, J. E. (1970). Structural comparison of ovalbumins from nine different species. *European Journal of Biochemistry, 17*(3): 529–532.

Fu, Z. D., Chen, X. Q. and Jiao, F. P. (2012). Study of the interaction of galangin, kaempferol and quercetin with BSA. *Latin American Applied Research, 42*: 211–216.

Gaertner, H. F. and Puigserver, A. J. (1992). Increased activity and stability of poly(ethylene glycol)-modified trypsin. *Enzyme and Microbial Technology, 14*(2): 150–155.

Gagen, W. L. and Holme, J. (1964). The denaturation and aggregation of ovalbumin by urea in neutral solutions. *The Journal of Physical Chemistry, 68*(4): 723–730.

Galantini, L., Leggio, C., Konarev, P. V. and Pavel, N. V. (2010). Human serum albumin binding ibuprofen: A 3D description of the unfolding pathway in urea. *Biophysical Chemistry, 147*(3): 111–122.

Gerlsma, S. Y. (1968). Reversible denaturation of ribonuclease in aqueous solutions as influenced by polyhydric alcohols and some other additives. *Journal of Biological Chemistry, 243*(5): 957–961.

Gerlsma, S. Y. (1970). The effects of polyhydric and monohydric alcohols on the heat induced reversible denaturation of chymotrypsinogen A. *European Journal of Biochemistry, 14*(1): 150–153.

Gheibi, N., Saboury, A. A., Haghbeen, K. and Moosavi-Movahedi, A. A. (2006). The effect of some osmolytes on the activity and stability of mushroom tyrosinase. *Journal of Biosciences, 31*(3): 355–362.

Gheldof, N. and Engeseth, N. J. (2002). Antioxidant capacity of honeys from various floral sources based on the determination of oxygen radical absorbance capacity and inhibition of *in vitro* lipoprotein oxidation in human serum samples. *Journal of Agricultural and Food Chemistry, 50*(10): 3050–3055.

Glazer, A. N., McKenzie, H. A. and Wake, R. G. (1963). The denaturation of proteins II. Ultraviolet absorption spectra of bovine serum albumin and ovalbumin in urea and in acids. *Biochimica et Biophysica Acta, 69*: 240–248.

Gómez, L., Ramírez, H. and Villalonga, R. (2000). Stabilization of invertase by modification of sugar chains with chitosan. *Biotechnology Letters, 22*(5): 347–350.

Gómez, L. and Villalonga, R. (2000). Functional stabilization of invertase by covalent modification with pectin. *Biotechnology Letters, 22*(14): 1191–1195.

Greene, R. F., Jr. and Pace, C. N. (1974). Urea and guanidine hydrochloride denaturation of ribonuclease, lysozyme, α-chymotrypsin, and β-lactoglobulin. *Journal of Biological Chemistry, 249*(17): 5388–5393.

Greenfield, N. J. and Fasman, G. D. (1969). Computed circular dichroism spectra for the evaluation of protein conformation. *Biochemistry, 8*(10): 4108–4116.

Gurung, N., Ray, S., Bose, S. and Rai, V. (2013). A broader view: Microbial enzymes and their relevance in industries, medicine, and beyond. *BioMed Research International, 2013*, 18 pages. doi:10.1155/2013/329121

Guzzi, R., Andolfi, L., Cannistraro, S., Verbeet, M. P., Canters, G. W. and Sportelli, L. (2004). Thermal stability of wild type and disulfide bridge containing mutant of poplar plastocyanin. *Biophysical Chemistry, 112*(1): 35–43.

Hamaguchi, K. and Kurono, A. (1963). Structure of muramidase (lysozyme). I. The effect of guanidine hydrochloride on muramidase. *Journal of Biochemistry, 54*: 111–122.

Haque, I., Singh, R., Moosavi-Movahedi, A. A. and Ahmad, F. (2005). Effect of polyol osmolytes on DeltaG(D), the Gibbs energy of stabilisation of proteins at different pH values. *Biophysical Chemistry, 117*(1): 1–12.

Harding, S. E. (1981). Could egg albumin be egg shaped? *International Journal of Biological Macromolecules, 3*(6): 398–399.

Hassan, N., Messina, P. V., Dodero, V. I. and Ruso, J. M. (2011). Rheological properties of ovalbumin hydrogels as affected by surfactants addition. *International Journal of Biological Macromolecules, 48*(3): 495–500.

Hayakawa, I., Kajihara, J., Morikawa, K., Oda, M. and Fujio, Y. (1992). Denaturation of bovine serum albumin (BSA) and ovalbumin by high pressure, heat and chemicals. *Journal of Food Science, 57*(2): 288–292.

Holt, J. C. and Creeth, J. M. (1972). Studies of the denaturation and partial renaturation of ovalbumin. *Biochemical Journal, 129*(3): 665–676.

Horowitz, P. M. and Butler, M. (1993). Interactive intermediates are formed during the urea unfolding of rhodanese. *Journal of Biological Chemistry, 268*(4): 2500–2504.

Huang, B. X., Kim, H. Y. and Dass, C. (2004). Probing three-dimensional structure of bovine serum albumin by chemical cross-linking and mass spectrometry. *Journal of the American Society for Mass Spectrometry, 15*(8): 1237–1247.

Hughson, F. M. and Baldwin, R. L. (1989). Use of site-directed mutagenesis to destabilize native apomyoglobin relative to folding intermediates. *Biochemistry, 28*(10): 4415–4422.

Hung, H. C. and Chang, G. G. (2001). Multiple unfolding intermediates of human placental alkaline phosphatase in equilibrium urea denaturation. *Biophysical Journal, 81*(6): 3456–3471.

Hunter, M. J. (1966). A method for the determination of protein partial specific volumes. *The Journal of Physical Chemistry, 70*(10): 3285–3292.

Hutson, S. M., Stinson-Fisher, C., Shiman, R. and Jefferson, L. S. (1987). Regulation of albumin synthesis by hormones and amino acids in primary cultures of rat hepatocytes. *American Journal of Physiology, 252*(3 Pt 1): E291–298.

Imoto, T., Johnson, L. N., North, A. C. T., Phillips, D. C. and Rupley, J. A. (1972). Vertebrate lysozymes. In D. B. Paul (Ed.), *The Enzymes* (Vol. 7, pp. 665–868). New York: Academic Press.

Imoto, T. and Yamada, H. (1989). Chemical modification. In T. E. Creighton (Ed.), *Protein Function: A Practical Approach* (pp. 247–277). Oxford: IRL Press.

Iyer, P. V. and Ananthanarayan, L. (2008). Enzyme stability and stabilization—aqueous and non-aqueous environment. *Process Biochemistry, 43*(10): 1019–1032.

Jacobson, R. H., Matsumura, M., Faber, H. R. and Matthews, B. W. (1992). Structure of a stabilizing disulfide bridge mutant that closes the active-site cleft of T4 lysozyme. *Protein Science, 1*(1): 46–57.

Janatova, J., Fuller, J. K. and Hunter, M. J. (1968). The heterogeneity of bovine albumin with respect to sulfhydryl and dimer content. *Journal of Biological Chemistry, 243*(13): 3612–3622.

Jollès, J., Jauregui-Adell, J., Bernier, I. and Jollès, P. (1963). The chemical structure of hen's egg white lysozyme: Detailed study. *Biochimica et Biophysica Acta, 78*(4): 668–689.

Jollès, P. (1960). Lysozyme. In P. D. Boyer, H. Lardy and K. Myrback (Eds.), *The Enzymes* (2 ed., Vol. 4, pp. 431–445). New York: Academic Press.

Jollès, P. (1969). Lysozymes: A chapter of molecular biology. *Angewandte Chemie International Edition in English, 8*(4): 227–239.

Jollès, P. and Jollès, J. (1984). What's new in lysozyme research? *Molecular and Cellular Biochemistry, 63*(2): 165–189.

Kanaya, S., Katsuda, C., Kimura, S., Nakai, T., Kitakuni, E., Nakamura, H., Katayanagi, K., Morikawa, K. and Ikehara, M. (1991). Stabilization of *Escherichia coli* ribonuclease H by introduction of an artificial disulfide bond. *Journal of Biological Chemistry, 266*(10): 6038–6044.

Kaškonienė, V., Maruška, A. and Kornyšova, O. (2009). Quantitative and qualitative determination of phenolic compounds in honey. *Chemical Technology, 52*(3): 74–80.

Kato, A. and Takagi, T. (1988). Formation of intermolecular β-sheet structure during heat denaturation of ovalbumin. *Journal of Agricultural and Food Chemistry, 36*(6): 1156–1159.

Kaushik, J. K. and Bhat, R. (2003). Why is trehalose an exceptional protein stabilizer? An analysis of the thermal stability of proteins in the presence of the compatible osmolyte trehalose. *Journal of Biological Chemistry, 278*(29): 26458–26465.

Kaysen, G. A., Jones, H., Martin, V. and Hutchison, F. N. (1989). A low-protein diet restricts albumin synthesis in nephrotic rats. *Journal of Clinical Investigation, 83*(5): 1623–1629.

Kelly, S. M., Jess, T. J. and Price, N. C. (2005). How to study proteins by circular dichroism. *Biochimica et Biophysica Acta, 1751*(2): 119–139.

Khajeh, K., Naderi-Manesh, H., Ranjbar, B., Moosavi-Movahedi, A. A. and Nemat-Gorgani, M. (2001). Chemical modification of lysine residues in Bacillus α-amylases: Effect on activity and stability. *Enzyme and Microbial Technology, 28*(6): 543–549.

Khan, M. Y., Agarwal, S. K. and Hangloo, S. (1987). Urea-induced structural transformations in bovine serum albumin. *Journal of Biochemistry, 102*(2): 313–317.

Kidwai, S. A., Ansari, A. A. and Salahuddin, A. (1976). Effect of succinylation (3-carboxypropionylation) on the conformation and immunological activity of ovalbumin. *Biochemical Journal, 155*(1): 171–180.

Kim, Y.-S., Jones, L. S., Dong, A., Kendrick, B. S., Chang, B. S., Manning, M. C., Randolph, T. W. and Carpenter, J. F. (2003). Effects of sucrose on conformational equilibria and fluctuations within the native-state ensemble of proteins. *Protein Science, 12*(6): 1252–1261.

Kishore, D., Kundu, S. and Kayastha, A. M. (2012). Thermal, chemical and pH induced denaturation of a multimeric β-galactosidase reveals multiple unfolding pathways. *PloS One, 7*(11), 9 pages. doi:10.1371/journal.pone.0050380

Knapp, S., Ladenstein, R. and Galinski, E. A. (1999). Extrinsic protein stabilization by the naturally occurring osmolytes β-hydroxyectoine and betaine. *Extremophiles, 3*(3): 191–198.

Koseki, T., Kitabatake, N. and Doi, E. (1989). Irreversible thermal denaturation and formation of linear aggregates of ovalbumin. *Food Hydrocolloids, 3*(2): 123–134.

Kragh-Hansen, U., Saito, S., Nishi, K., Anraku, M. and Otagiri, M. (2005). Effect of genetic variation on the thermal stability of human serum albumin. *Biochimica et Biophysica Acta, 1747*(1): 81–88.

Kumar, A., Attri, P. and Venkatesu, P. (2010). Trehalose protects urea-induced unfolding of α-chymotrypsin. *International Journal of Biological Macromolecules, 47*(4): 540–545.

Kumar, A., Dutt, S., Bagler, G., Ahuja, P. S. and Kumar, S. (2012). Engineering a thermo-stable superoxide dismutase functional at sub-zero to >50°C, which also tolerates autoclaving. *Scientific Reports, 2*, 8 pages. doi:10.1038/srep00387

Kumaran, R. and Ramamurthy, P. (2011). Denaturation mechanism of BSA by urea derivatives: Evidence for hydrogen-bonding mode from fluorescence tools. *Journal of Fluorescence, 21*(4): 1499–1508.

Lakowicz, J. R. (1999). *Principles of Fluorescence Spectroscopy* (2 ed.). Plenum: Kluwer Academic.

Laurents, D. V. and Baldwin, R. L. (1997). Characterization of the unfolding pathway of hen egg white lysozyme. *Biochemistry, 36*(6): 1496–1504.

Le, Q. A., Joo, J. C., Yoo, Y. J. and Kim, Y. H. (2012). Development of thermostable *Candida antarctica* lipase B through novel in silico design of disulfide bridge. *Biotechnology and Bioengineering, 109*(4): 867–876.

Leader, B., Baca, Q. J. and Golan, D. E. (2008). Protein therapeutics: A summary and pharmacological classification. *Nature Reviews: Drug Discovery, 7*(1): 21–39.

Lee, H.-L., Chang, C.-K., Jeng, W.-Y., Wang, A. H.-J. and Liang, P.-H. (2012). Mutations in the substrate entrance region of β-glucosidase from *Trichoderma reesei* improve enzyme activity and thermostability. *Protein Engineering Design and Selection, 25*(11): 733–740.

Lee, J. C. and Timasheff, S. N. (1981). The stabilization of proteins by sucrose. *Journal of Biological Chemistry, 256*(14): 7193–7201.

Lee, J. Y. and Hirose, M. (1992). Partially folded state of the disulfide-reduced form of human serum albumin as an intermediate for reversible denaturation. *Journal of Biological Chemistry, 267*(21): 14753–14758.

Lee, S., Lee, D. G., Jang, M. K., Jeon, M. J., Jang, H. J. and Lee, S. H. (2011). Improvement in the catalytic activity of beta-agarase AgaA from *Zobellia galactanivorans* by site-directed mutagenesis. *Journal of Microbiology and Biotechnology, 21*(11): 1116–1122.

Lee, Y. C. and Montgomery, R. (1962). Glycopeptides from ovalbumin: The structure of the peptide chains. *Archives of Biochemistry and Biophysics, 97*(1): 9–17.

Lee, Y. C., Wu, Y.-C. and Montgomery, R. (1964). Modification of emulsin action on asparaginyl-carbohydrate from ovalbumin by dinitrophenylation. *Biochemical Journal, 91*(2): 9C–19C.

Leggio, C., Galantini, L., Konarev, P. V. and Pavel, N. V. (2009). Urea-induced denaturation process on defatted human serum albumin and in the presence of palmitic acid. *Journal of Physical Chemistry B, 113*(37): 12590–12602.

Leisola, M. and Turunen, O. (2007). Protein engineering: opportunities and challenges. *Applied Microbiology and Biotechnology, 75*(6): 1225–1232.

Léonis, J. (1956). Preliminary investigation of the behavior of lysozyme in urea solutions. *Archives of Biochemistry and Biophysics, 65*(1): 182–193.

Lerbret, A., Bordat, P., Affouard, F., Descamps, M. and Migliardo, F. (2005). How homogeneous are the trehalose, maltose, and sucrose water solutions? An insight from molecular dynamics simulations. *Journal of Physical Chemistry. B, 109*(21): 11046–11057.

Lesnierowski, G. and Kijowski, J. (2007). Lysozyme. In R. Huopalahti, R. López-Fandiño, M. Anton and R. Schade (Eds.), *Bioactive Egg Compounds* (pp. 33–42). New York: Springer Berlin Heidelberg.

Li, D. J., Zhu, M., Xu, C. and Ji, B. M. (2011). Characterization of the baicalein-bovine serum albumin complex without or with Cu^{2+} or Fe^{3+} by spectroscopic approaches. *European Journal of Medicinal Chemistry, 46*(2): 588–599.

Li, X., Wang, G., Chen, D. and Lu, Y. (2014). Binding of ascorbic acid and α–tocopherol to bovine serum albumin: A comparative study. *Molecular BioSystems, 10*(2): 326–337.

Lin, T. Y. and Timasheff, S. N. (1996). On the role of surface tension in the stabilization of globular proteins. *Protein Science, 5*(2): 372–381.

Liu, Y. and Bolen, D. W. (1995). The peptide backbone plays a dominant role in protein stabilization by naturally occurring osmolytes. *Biochemistry, 34*(39): 12884–12891.

Longsworth, L. G., Cannan, R. K. and MacInnes, D. A. (1940). An electrophoretic study of the proteins of egg white. *Journal of the American Chemical Society, 62*(10): 2580–2590.

Longsworth, L. G. and Jacobsen, C. F. (1949). An electrophoretic study of the binding of salt ions by β-lactoglobulin and bovine serum albumin. *Journal of Physical and Colloid Chemistry, 53*(1): 126–135.

Lundblad, R. L. and Noyes, C. M. (1984). *Chemical Reagents for Protein Modification,* (Vol. 1 and 2). Boca Raton, Florida: CRC Press.

Makhatadze, G. I., Kim, K. S., Woodward, C. and Privalov, P. L. (1993). Thermodynamics of BPTI folding. *Protein Science, 2*(12): 2028–2036.

Marshall, S. A., Lazar, G. A., Chirino, A. J. and Desjarlais, J. R. (2003). Rational design and engineering of therapeutic proteins. *Drug Discovery Today, 8*(5): 212–221.

Matsumura, M., Becktel, W. J., Levitt, M. and Matthews, B. W. (1989). Stabilization of phage T4 lysozyme by engineered disulfide bonds. *Proceedings of the National Academy of Sciences, USA, 86*(17): 6562–6566.

Matthews, B., Nicholson, H. and Becktel, W. (1987). Enhanced protein thermostability from site-directed mutations that decrease the entropy of unfolding. *Proceedings of the National Academy of Sciences, USA, 84*(19): 6663–6667.

McKenzie, H. A., Smith, M. B. and Wake, R. G. (1963). The denaturation of proteins. I. Sedimentation, diffusion, optical rotation, viscosity and gelation in urea solutions of ovalbumin and bovine serum albumin. *Biochimica et Biophysica Acta, 69*: 222–239.

McKenzie, H. A. and Frier, R. D. (2003). The behavior of R-ovalbumin and its individual components A1, A2, and A3 in urea solution: kinetics and equilibria. *Journal of Protein Chemistry, 22*(3): 207–214.

McMillan, D. E. (1974). A comparison of five methods for obtaining the intrinsic viscosity of bovine serum albumin. *Biopolymers, 13*(7): 1367–1376.

Means, G. E. and Feeney, R. E. (1990). Chemical modifications of proteins: History and applications. *Bioconjugate Chemistry, 1*(1): 2–12.

Meiering, E. M., Serrano, L. and Fersht, A. R. (1992). Effect of active site residues in barnase on activity and stability. *Journal of Molecular Biology, 225*(3): 585–589.

Meng, F.-G., Hong, Y.-K., He, H.-W., Lyubarev, A. E., Kurganov, B. I., Yan, Y.-B. and Zhou, H.-M. (2004). Osmophobic effect of glycerol on irreversible thermal denaturation of rabbit creatine kinase. *Biophysical Journal, 87*(4): 2247–2254.

Miroliaei, M. and Nemat-Gorgani, M. (2001). Sugars protect native and apo yeast alcohol dehydrogenase against irreversible thermoinactivation. *Enzyme and Microbial Technology, 29*(8): 554–559.

Miroliaei, M., Ranjbar, B., Naderi-Manesh, H. and Nemat-Gorgani, M. (2007). Thermal denaturation of yeast alcohol dehydrogenase and protection of secondary and tertiary structural changes by sugars: CD and fluorescence studies. *Enzyme and Microbial Technology, 40*(4): 896–901.

Mitchinson, C. and Wells, J. A. (1989). Protein engineering of disulfide bonds in subtilisin BPN'. *Biochemistry, 28*(11): 4807–4815.

Monkos, K. (1997). Concentration and temperature dependence of viscosity in lysozyme aqueous solutions. *Biochimica et Biophysica Acta (BBA) - Protein Structure and Molecular Enzymology, 1339*(2): 304–310.

Montgomery, R., Wu, Y.-C. and Lee, Y. C. (1965). Periodate oxidation of glycopeptides from ovalbumin. *Biochemistry, 4*(3): 578–587.

Moosavi-Movahedi, A., Bordbar, A., Taleshi, A., Naderimanesh, H. and Ghadam, P. (1996). Mechanism of denaturation of bovine serum albumin by dodecyl trimethylammonium bromide. *International Journal of Biochemistry and Cell Biology, 28*(9): 991–998.

Moriyama, Y., Kawasaka, Y. and Takeda, K. (2003). Protective effect of small amounts of sodium dodecyl sulfate on the helical structure of bovine serum albumin in thermal denaturation. *Journal of Colloid and Interface Science, 257*(1): 41–46.

Moriyama, Y., Watanabe, E., Kobayashi, K., Harano, H., Inui, E. and Takeda, K. (2008). Secondary structural change of bovine serum albumin in thermal denaturation up to 130 degrees C and protective effect of sodium dodecyl sulfate on the change. *Journal of Physical Chemistry B, 112*(51): 16585–16589.

Mouton, A. and Jolles, J. (1969). On the identity of human lysozymes isolated from normal and abnormal tissues or secretions. *FEBS Letters, 4*(4): 337–340.

Mozhaev, V. V., Šikšnis, V. A., Melik-Nubarov, N. S., Galkantaite, N. Z., Denis, G. J., Butkus, E. P., Zaslavsky, B. Y., Mestechkina, N. M. and Martinek, K. (1988). Protein stabilization via hydrophilization. *European Journal of Biochemistry, 173*(1): 147–154.

Mulqueen, P. M. and Kronman, M. J. (1982). Binding of naphthalene dyes to the N and A conformers of bovine α–lactalbumin. *Archives of Biochemistry and Biophysics, 215*(1): 28–39.

Murphy, K. P. (1995). Noncovalent forces important to the conformational stability of protein structures. In B. A. Shirley (Ed.), *Protein Stabiliy and Folding: Theory and Practice* (Vol. 40, pp. 1–34). New York: Humana Press.

Mustafa, M., Dar, T. and Ali, S. (2011). Polyols stabilize the denatured states of multidomain protein ovomucoid. *International Journal of Biological Chemistry, 5*: 327–341.

Muzammil, S., Kumar, Y. and Tayyab, S. (2000a). Anion-induced stabilization of human serum albumin prevents the formation of intermediate during urea denaturation. *Proteins: Structure, Function, and Genetics, 40*(1): 29–38.

Muzammil, S., Kumar, Y. and Tayyab, S. (2000b). Anion-induced refolding of human serum albumin under low pH conditions. *Biochimica et Biophysica Acta, 1476*(1): 139–148.

Naeem, A., Khan, T. A., Muzaffar, M., Ahmad, S. and Saleemuddin, M. (2011). A partially folded state of ovalbumin at low pH tends to aggregate. *Cell Biochemistry and Biophysics, 59*(1): 29–38.

Naika, G. S., Prakash, V. and Tiku, P. K. (2009). Effect of cosolvents on the structural stability of endoglucanase from *Aspergillus aculeatus*. *Journal of Agricultural and Food Chemistry, 57*(21): 10450–10456.

Narita, K. (1961). N-terminal group of ovalbumin. *Biochemical and Biophysical Research Communications, 5*(2): 160–164.

Nicholson, H., Becktel, W. J. and Matthews, B. W. (1988). Enhanced protein thermostability from designed mutations that interact with α-helix dipoles. *Nature, 336*(6200): 651–656.

Nielsen, J. E. and Borchert, T. V. (2000). Protein engineering of bacterial α-amylases. *Biochimica et Biophysica Acta, 1543*(2): 253–274.

Nisbet, A. D., Saundry, R. H., Moir, A. J. G., Fothergill, L. A. and Fothergill, J. E. (1981). The complete amino-acid sequence of hen ovalbumin. *European Journal of Biochemistry, 115*(2): 335–345.

Okajima, T., Kawata, Y. and Hamaguchi, K. (1990). Chemical modification of tryptophan residues and stability changes in proteins. *Biochemistry, 29*(39): 9168–9175.

Ong, H. N., Arumugam, B. and Tayyab, S. (2009). Succinylation-induced conformational destabilization of lysozyme as studied by guanidine hydrochloride denaturation. *Journal of Biochemistry, 146*(6): 895–904.

Pace, C. N. (1975). The stability of globular proteins. *CRC Critical Reviews in Biochemistry, 3*(1): 1–43.

Pace, C. N. (1986). Determination and analysis of urea and guanidine hydrochloride denaturation curves. *Methods in Enzymology, 131*: 266–280.

Pace, C. N., Shirley, B. A., McNutt, M. and Gajiwala, K. (1996). Forces contributing to the conformational stability of proteins. *FASEB Journal, 10*(1): 75–83.

Pace, C. N. and Scholtz, J. M. (1997). Measuring the conformational stability of a protein. In T. E. Creighton (Ed.), *Protein Structure: A Practical Approach* (pp. 299-321). Oxford: Oxford University Press.

Pantoliano, M. W., Whitlow, M., Wood, J. F., Rollence, M. L., Finzel, B. C., Gilliland, G. L., Poulos, T. L. and Bryan, P. N. (1988). The engineering of binding affinity at metal ion binding sites for the stabilization of proteins: Subtilisin as a test case. *Biochemistry, 27*(22): 8311–8317.

Papadopoulou, A., Green, R. J. and Frazier, R. A. (2005). Interaction of flavonoids with bovine serum albumin: a fluorescence quenching study. *Journal of Agricultural and Food Chemistry, 53*(1): 158–163.

Park, S. K., Bae, D. H. and Rhee, K. C. (2000). Soy protein biopolymers cross-linked with glutaraldehyde. *Journal of the American Oil Chemists' Society, 77*(8): 879–884.

Pearce, F. G., Mackintosh, S. H. and Gerrard, J. A. (2007). Formation of amyloid-like fibrils by ovalbumin and related proteins under conditions relevant to food processing. *Journal of Agricultural and Food Chemistry, 55*(2): 318–322.

Pelton, J. T. and McLean, L. R. (2000). Spectroscopic methods for analysis of protein secondary structure. *Analytical Biochemistry, 277*(2): 167–176.

Perlmann, G. E. (1952). Enzymatic dephosphorylation of ovalbumin and plakalbumin. *Journal of General Physiology, 35*(5): 711–726.

Peters, T., Jr. and Anfinsen, C. B. (1950). Net production of serum albumin by liver slices. *Journal of Biological Chemistry, 186*(2): 805–813.

Peters, T., Jr. (1985). Serum albumin. *Advances in Protein Chemistry, 37*: 161–245.

Peters, T., Jr. (1996). *All about Albumin: Biochemistry, Genetics and Medical Applications*. New York: Academic Press.

Phillips, D. C. (1967). The hen egg-white lysozyme molecule. *Proceedings of the National Academy of Sciences, USA, 57*(3): 483–495.

Pico, G. A. (1997). Thermodynamic features of the thermal unfolding of human serum albumin. *International Journal of Biological Macromolecules, 20*(1): 63–73.

Poddar, N. K., Ansari, Z. A., Singh, R. K. B., Moosavi-Movahedi, A. A. and Ahmad, F. (2008). Effect of monomeric and oligomeric sugar osmolytes on Delta G_D, the Gibbs energy of stabilization of the protein at different pH values: Is the sum effect of monosaccharide individually additive in a mixture? *Biophysical Chemistry, 138*(3): 120–129.

Poddar, N. K., Ansari, Z. A., Singh, R. K., Moosavi Movahedi, A. A. and Ahmad, F. (2010). Effect of oligosaccharides and their monosaccharide mixtures on the stability of proteins: A scaled particle study. *Journal of Biomolecular Structure and Dynamics, 28*(3): 331–341.

Qasim, M. A. and Salahuddin, A. (1978). Changes in conformation and immunological activity of ovalbumin during its modification with different acid anhydrides. *Biochimica et Biophysica Acta, 536*(1): 50–63.

Qasim, M. A. and Salahuddin, A. (1979). The conformational consequences of maleylation of amino groups in ovalbumin. *Journal of Biochemistry, 85*(4): 1029–1035.

Qu, Y., Bolen, C. L. and Bolen, D. W. (1998). Osmolyte-driven contraction of a random coil protein. *Proceedings of the National Academy of Sciences, USA, 95*(16): 9268–9273.

Raftery, M. A. and Dahlquist, F. W. (1969). The chemistry of lysozyme. *Progress in the Chemistry of Organic Natural Products, 27*: 340–381.

Ramos, A., Raven, N., Sharp, R. J., Bartolucci, S., Rossi, M., Cannio, R., Lebbink, J., Van Der Oost, J., De Vos, W. M. and Santos, H. (1997). Stabilization of enzymes against thermal stress and freeze-drying by mannosylglycerate. *Applied and Environmental Microbiology, 63*(10): 4020–4025.

Ratnaparkhi, M. P., Chaudhari, S. P. and Pandya, V. A. (2011). Peptides and proteins in pharmaceuticals. *International Journal of Current Pharmaceutical Research, 3*(2): 1–9.

Reed, R. G., Feldhoff, R. C., Clute, O. L. and Peters, T. (1975). Fragments of bovine serum albumin produced by limited proteolysis. Conformation and ligand binding. *Biochemistry, 14*(21): 4578–4583.

Robinson, A., Meredith, C. and Austen, B. M. (1986). Isolation and properties of the signal region from ovalbumin. *FEBS Letters, 203*(2): 243–246.

Royer, C. A. (2006). Probing protein folding and conformational transitions with fluorescence. *Chemical Review, 106*(5): 1769–1784.

Ryan, O., Smyth, M. R. and Fágáin, C. Ó. (1994). Thermostabilized chemical derivatives of horseradish peroxidase. *Enzyme and Microbial Technology, 16*(6): 501–505.

Rybak-Chmielewska, H. and Szczęsna, T. (1995). Composition and properties of Polish buckwheat honey. In T. Matano and A. Vjihara (Eds.), *Current Advances in Buckwheat Research* (pp. 793–799). Shinshu: Shinshu University Press.

Saadati, Z. and Bordbar, A. K. (2008). Stability of β-lactoglobulin A in the presence of sugar osmolytes estimated from their guanidinium chloride-induced transition curves. *Protein Journal, 27*(7-8): 455–460.

Saber, M. A., Stockbauer, P., Moravek, L. and Meloun, B. (1977). Disulphide bonds in human serum albumin. *Collection of Czechoslovak Chemical Communications, 42*: 564–579.

Samuel, D., Kumar, T. K., Ganesh, G., Jayaraman, G., Yang, P. W., Chang, M. M., Trivedi, V. D., Wang, S. L., Hwang, K. C., Chang, D. K. and Yu, C. (2000). Proline inhibits aggregation during protein refolding. *Protein Science, 9*(2): 344–352.

Santra, M. K., Banerjee, A., Krishnakumar, S. S., Rahaman, O. and Panda, D. (2004). Multiple-probe analysis of folding and unfolding pathways of human serum albumin. Evidence for a framework mechanism of folding. *European Journal of Biochemistry, 271*(9): 1789–1797.

Sasvari, Z. and Asboth, B. (1999). Crosslinking of glucoamylases via carbohydrates hardly affects catalysis but impairs stability. *Biotechnology and Bioengineering, 63*(4): 459–463.

Sathish, H. A., Kumar, P. R. and Prakash, V. (2007). Mechanism of solvent induced thermal stabilization of papain. *International Journal of Biological Macromolecules, 41*(4): 383–390.

Schein, C. H. (1990). Solubility as a function of protein structure and solvent components. *Nature Biotechnology, 8*(4): 308–317.

Schiffer, C. A., Doetsch, V., Wuethrich, K. and van Gunsteren, W. F. (1995). Exploring the role of the solvent in the denaturation of a protein: A molecular dynamics study of the DNA binding domain of the 434 repressor. *Biochemistry, 34*(46): 15057–15067.

Shahani, M., Mahgvan, P. V., Tadayon, R., Rostami, A., Ramandi, M. and Mohammadian, T. (2014). Drug comparion and characterizing regarded with human serum albumin from years 2006 to 2012. *Journal of Paramedical Sciences, 5*(1): 81–91.

Shaikh, S. M. T., Seetharamappa, J., Kandagal, P. B. and Manjunatha, D. H. (2007). In vitro study on the binding of anti-coagulant vitamin to bovine serum albumin and the influence of toxic ions and common ions on binding. *International Journal of Biological Macromolecules, 41*(1): 81–86.

Sheehan, H., O'Kennedy, R. and Kilty, C. (1990). Investigation of the properties of bovine heart creatine kinase cross-linked with dimethyl suberimidate. *Biochimica et Biophysica Acta, 1041*(2): 141–145.

Shoichet, B. K., Baase, W. A., Kuroki, R. and Matthews, B. W. (1995). A relationship between protein stability and protein function. *Proceedings of the National Academy of Sciences, USA, 92*(2): 452–456.

Siadat, O., Lougarre, A., Lamouroux, L., Ladurantie, C. and Fournier, D. (2006). The effect of engineered disulfide bonds on the stability of *Drosophila melanogaster* acetylcholinesterase. *BMC Biochemistry, 7*(12), 7 pages. doi:10.1186/1471-2091-7-12

Simko, J. P. and Kauzmann, W. (1962). The kinetics of the urea denaturation of hemoglobin. I. Beef oxyhemoglobin*. *Biochemistry, 1*(6): 1005–1017.

Simpson, R. B. and Kauzmann, W. (1953). The kinetics of protein denaturation. I. The behavior of the optical rotation of ovalbumin in urea solutions. *Journal of the American Chemical Society, 75*(21): 5139–5152.

Singh, L., Poddar, N., Dar, T., Rahman, S., Kumar, R. and Ahmad, F. (2011). Forty years of research on osmolyte-induced protein folding and stability. *Journal of the Iranian Chemical Society, 8*(1): 1–23.

Singh, R. K., Tiwari, M. K., Singh, R. and Lee, J.-K. (2013). From protein engineering to immobilization: Promising strategies for the upgrade of industrial enzymes. *International Journal of Molecular Sciences, 14*(1): 1232–1277.

Skrt, M., Benedik, E., Podlipnik, Č. and Ulrih, N. P. (2012). Interactions of different polyphenols with bovine serum albumin using fluorescence quenching and molecular docking. *Food Chemistry, 135*(4): 2418–2424.

Slusarczyk, H., Felber, S., Kula, M.-R. and Pohl, M. (2000). Stabilization of NAD-dependent formate dehydrogenase from *Candida boidinii* by site-directed mutagenesis of cysteine residues. *European Journal of Biochemistry, 267*(5): 1280–1289.

Sogami, M. and Ogura, S. (1973). Structural transitions of bovine plasma albumin. Location of tyrosyl and tryptophyl residues by solvent perturbation difference spectra. *Journal of Biochemistry, 73*(2): 323–334.

Sophianopoulos, A. J., Rhodes, C. K., Holcomb, D. N. and Van Holde, K. E. (1962). Physical studies of lysozyme: I. Characterization. *Journal of Biological Chemistry, 237*(4): 1107–1112.

Sørensen, S. P. L., Linderstrøm-Lang, K. and Lund, E. (1927). The influence of salts upon the ionisation of egg albumin. *The Journal of General Physiology, 8*(6): 543–599.

Squire, P. G., Moser, P. and O'Konski, C. T. (1968). The hydrodynamic properties of bovine serum albumin monomer and dimer. *Biochemistry, 7*(12): 4261–4272.

Srikrishnan, S., Randall, A., Baldi, P. and Da Silva, N. A. (2012). Rationally selected single-site mutants of the *Thermoascus aurantiacus* endoglucanase increase hydrolytic activity on cellulosic substrates. *Biotechnology and Bioengineering, 109*(6): 1595–1599.

Sriprang, R., Asano, K., Gobsuk, J., Tanapongpipat, S., Champreda, V. and Eurwilaichitr, L. (2006). Improvement of thermostability of fungal xylanase by using site-directed mutagenesis. *Journal of Biotechnology, 126*(4): 454–462.

Sriprapundh, D., Vieille, C. and Zeikus, J. G. (2000). Molecular determinants of xylose isomerase thermal stability and activity: Analysis of thermozymes by site-directed mutagenesis. *Protein Engineering, 13*(4): 259–265.

Stein, P. E., Leslie, A. G. W., Finch, J. T., Turnell, W. G., McLaughlin, P. J. and Carrell, R. W. (1990). Crystal structure of ovalbumin as a model for the reactive centre of serpins. *Nature, 347*(6288): 99–102.

Stein, P. E., Leslie, A. G., Finch, J. T. and Carrell, R. W. (1991). Crystal structure of uncleaved ovalbumin at 1.95 A resolution. *Journal of Molecular Biology, 221*(3): 941–959.

Steiner, R. F. (1964). Structural transitions of lysozyme. *Biochimica et Biophysica Acta, 79*(1): 51–63.

Steven, F. S. and Tristram, G. R. (1959). The denaturation of ovalbumin. Changes in optical rotation, extinction and viscosity during serial denaturation in solutions of urea. *Biochemical Journal, 73*(1): 86–90.

Stryer, L. (1965). The interaction of a naphthalene dye with apomyoglobin and apohemoglobin. A fluorescent probe of non-polar binding sites. *Journal of Molecular Biology, 13*(2): 482–495.

Sugahara, T., Yamada, Y., Yano, S. and Sasaki, T. (2002). Heat denaturation enhanced immunoglobulin production stimulating activity of lysozyme from hen egg white. *Biochimica et Biophysica Acta, 1572*(1): 19–24.

Sun, D. P., Sauer, U., Nicholson, H. and Matthews, B. W. (1991). Contributions of engineered surface salt bridges to the stability of T4 lysozyme determined by directed mutagenesis. *Biochemistry, 30*(29): 7142–7153.

Sun, Y., Yang, H. and Wang, W. (2011). Improvement of the thermostability and enzymatic activity of cholesterol oxidase by site-directed mutagenesis. *Biotechnology Letters, 33*(10): 2049–2055.

Tai, T., Yamashita, K., Ogata-Arakawa, M., Koide, N., Muramatsu, T., Iwashita, S., Inoue, Y. and Kobata, A. (1975). Structural studies of two ovalbumin glycopeptides in relation to the endo-beta-N-acetylglucosaminidase specificity. *Journal of Biological Chemistry, 250*(21): 8569–8575.

Tai, T., Yamashita, K., Ito, S. and Kobata, A. (1977). Structures of the carbohydrate moiety of ovalbumin glycopeptide III and the difference in specificity of endo-beta-N-acetylglucosaminidases CII and H. *Journal of Biological Chemistry, 252*(19): 6687–6694.

Takahashi, K., Lou, X.-F., Ishii, Y. and Hattori, M. (2000). Lysozyme-glucose stearic acid monoester conjugate formed through the maillard reaction as an antibacterial emulsifier. *Journal of Agricultural and Food Chemistry, 48*(6): 2044–2049.

Taneja, S. and Ahmad, F. (1994). Increased thermal stability of proteins in the presence of amino acids. *Biochemical Journal, 303*: 147–153.

Tanford, C. (1961). *Physical Chemistry of Macromolecules* New York: Wiley.

Tanford, C. (1968). Protein denaturation. In C. B. Anfinsen, M. L. Anson, J. T. Edsall and F. M. Richards (Eds.), *Advances in Protein Chemistry* (Vol. 23, pp. 121–282). New York: Academic Press.

Tani, F., Shirai, N., Venelle, F., Yasumoto, K. and Onishi, T. (1997). Temperature control for kinetic refolding of heat-denatured ovalbumin. *Protein Science, 6*(7): 1491–1502.

Tani, F., Shirai, N., Nakanishi, Y., Yasumoto, K. and Kitabatake, N. (2004). Role of the carbohydrate chain and two phosphate moieties in the heat-induced aggregation of hen ovalbumin. *Bioscience, Biotechnology, and Biochemistry, 68*(12): 2466–2476.

Taravati, A., Shokrzadeh, M., Ebadi, A., Valipour, P., Hassan, A. T. M. and Farrokhi, F. (2007). Various effects of sugar and polyols on the protein structure and function: Role as osmolyte on protein stability. *World Applied Sciences Journal, 2*: 353–362.

Taverna, D. M. and Goldstein, R. A. (2002). Why are proteins marginally stable? *Proteins: Structure, Function, and Genetics, 46*(1): 105–109.

Tayyab, S., Sharma, N. and Khan, M. M. (2000). Use of domain specific ligands to study urea-induced unfolding of bovine serum albumin. *Biochemical and Biophysical Research Communications, 277*(1): 83–88.

Tayyab, S., Ahmad, B., Kumar, Y. and Khan, M. M. (2002). Salt-induced refolding in different domains of partially folded bovine serum albumin. *International Journal of Biological Macromolecules, 30*(1): 17–22.

Thompson, A. R. (1955). Amino acid sequence in lysozyme. 1. Displacement chromatography of peptides from a partial hydrolysate on ion-exchange resins. *Biochemical Journal, 60*(3): 507–515.

Timasheff, S. N. and Gorbunoff, M. J. (1967). Conformation of proteins. *Annual Review of Biochemistry, 36*: 13–54.

Timasheff, S. N., Lee, J. C., Pittz, E. P. and Tweedy, N. (1976). The interaction of tubulin and other proteins with structure-stabilizing solvents. *Journal of Colloid and Interface Science, 55*(3): 658–663.

Timasheff, S. N. (1993). The control of protein stability and association by weak interactions with water: how do solvents affect these processes? *Annual Review of Biophysics and Biomolecular Structure, 22*(1): 67–97.

Timasheff, S. N. (2002). Protein hydration, thermodynamic binding, and preferential hydration. *Biochemistry, 41*(46): 13473–13482.

Tiwari, A. and Bhat, R. (2006). Stabilization of yeast hexokinase A by polyol osmolytes: Correlation with the physicochemical properties of aqueous solutions. *Biophysical Chemistry, 124*(2): 90–99.

Tomás-Barberán, F. A., Martos, I., Ferreres, F., Radovic, B. S. and Anklam, E. (2001). HPLC flavonoid profiles as markers for the botanical origin of European unifloral honeys. *Journal of the Science of Food and Agriculture, 81*(5): 485–496.

Treetharnmathurot, B., Ovartlarnporn, C., Wungsintaweekul, J., Duncan, R. and Wiwattanapatapee, R. (2008). Effect of PEG molecular weight and linking chemistry on the biological activity and thermal stability of PEGylated trypsin. *International Journal of Pharmaceutics, 357*(1): 252–259.

Ueda, T., Masumoto, K., Ishibashi, R., So, T. and Imoto, T. (2000). Remarkable thermal stability of doubly intramolecularly cross-linked hen lysozyme. *Protein Engineering, 13*(3): 193–196.

Uversky, V. N. (1993). Use of fast protein size-exclusion liquid chromatography to study the unfolding of proteins which denature through the molten globule. *Biochemistry, 32*(48): 13288–13298.

Vadehra, D. V., Nath, K. R. and Forsythe, R. (1973). Eggs as a source of protein. *C R C Critical Reviews in Food Technology, 4*(2): 193–309.

van den Berg, B., Chung, E. W., Robinson, C. V., Mateo, P. L. and Dobson, C. M. (1999a). The oxidative refolding of hen lysozyme and its catalysis by protein disulfide isomerase. *EMBO Journal, 18*(17): 4794–4803.

van den Berg, B., Chung, E. W., Robinson, C. V. and Dobson, C. M. (1999b). Characterisation of the dominant oxidative folding intermediate of hen lysozyme. *Journal of Molecular Biology, 290*(3): 781–796.

van der Veen, M., Norde, W. and Stuart, M. C. (2004). Electrostatic interactions in protein adsorption probed by comparing lysozyme and succinylated lysozyme. *Colloids and Surfaces B: Biointerfaces, 35*(1): 33–40.

van der Veen, M., Norde, W. and Stuart, M. C. (2005). Effects of succinylation on the structure and thermostability of lysozyme. *Journal of Agricultural and Food Chemistry, 53*(14): 5702–5707.

Venkataramani, S., Truntzer, J. and Coleman, D. R. (2013). Thermal stability of high concentration lysozyme across varying pH: A Fourier transform infrared study. *Journal of Pharmacy and Bioallied Sciences, 5*(2): 148–153.

Wagner, M. L. and Scheraga, H. (1956). Gouy diffusion studies of bovine serum albumin. *The Journal of Physical Chemistry, 60*(8): 1066–1076.

Waldmann, T. A. (1977). Albumin catabolism. In V. M. Rosenoer, M. Oratz and M. A. Rothschild (Eds.), *Albumin: Structure, Function and Uses* (pp. 255–273). New York: Pergamon Press.

Wang, F., Huang, W. and Dai, Z. (2008). Spectroscopic investigation of the interaction between riboflavin and bovine serum albumin. *Journal of Molecular Structure, 875*(1–3): 509-514.

Warner, R. C. (1954). Egg proteins. In H. Neurath and K. Bailey (Eds.), *The Proteins* (Vol. 2, pp. 435–485). New York: Academic Press.

Wetter, L. R. and Deutsch, H. F. (1951). Immunological studies on egg white proteins: IV. Immunochemical and physical studies of lysozyme. *Journal of Biological Chemistry, 192*(1): 237–242.

Wetzel, R., Perry, L. J., Baase, W. A. and Becktel, W. J. (1988). Disulfide bonds and thermal stability in T4 lysozyme. *Proceedings of the National Academy of Sciences, USA, 85*(2): 401–405.

White, J. W. and Kushnir, I. (1967). Composition of honey. VII. Proteins. *Journal of Apicultural Research, 6*(3): 163–178.

White, J. W. (1975). Composition of honey. In E. Crane (Ed.), *Honey. A Comprehensive Survey* (pp. 157–206). London: Heinemann.

White, J. W. (1978). Honey. In C. O. Chichester (Ed.), *Advances in Food Research* (Vol. 24, pp. 287–374). San Diego: Academic Press.

Wong, S. S. and Wong, L.-J. C. (1992). Chemical crosslinking and the stabilization of proteins and enzymes. *Enzyme and Microbial Technology, 14*(11): 866–874.

Wright, A. K. and Thompson, M. R. (1975). Hydrodynamic structure of bovine serum albumin determined by transient electric birefringence. *Biophysical Journal, 15*(2): 137–141.

Wright, H. T., Qian, H. X. and Huber, R. (1990). Crystal structure of plakalbumin, a proteolytically nicked form of ovalbumin: Its relationship to the structure of cleaved α-1-proteinase inhibitor. *Journal of Molecular Biology, 213*(3): 513–528.

Wu, L. Z., Ma, B. L., Sheng, Y. B. and Wang, W. (2008). Equilibrium and kinetic analysis on the folding of hen egg lysozyme in the aqueous-glycerol solution. *Journal of Molecular Structure, 891*(1-3): 167–172.

Xie, G. and Timasheff, S. N. (1997). The thermodynamic mechanism of protein stabilization by trehalose. *Biophysical Chemistry, 64*(1–3): 25–43.

Yadav, J. K. and Prakash, V. (2009). Thermal stability of α–amylase in aqueous cosolvent systems. *Journal of Biosciences, 34*(3): 377–387.

Yamamoto, T., Fukui, N., Hori, A. and Matsui, Y. (2006). Circular dichroism and fluorescence spectroscopy studies of the effect of cyclodextrins on the thermal stability of chicken egg white lysozyme in aqueous solution. *Journal of Molecular Structure, 782*(1): 60–66.

Yancey, P. H., Clark, M. E., Hand, S. C., Bowlus, R. D. and Somero, G. N. (1982). Living with water stress: evolution of osmolyte systems. *Science, 217*(4566): 1214–1222.

Yancey, P. H. (2003). Proteins and counteracting osmolytes. *Biologist, 50*: 126–131.

Yancey, P. H. (2004). Compatible and counteracting solutes: Protecting cells from the Dead Sea to the deep sea. *Science Progress, 87*(1): 1–24.

Yancey, P. H. (2005). Organic osmolytes as compatible, metabolic and counteracting cytoprotectants in high osmolarity and other stresses. *Journal of Experimental Biology, 208*(Pt 15): 2819–2830.

Zaroog, M. S. and Tayyab, S. (2012). Formation of molten globule-like state during acid denaturation of *Aspergillus niger* glucoamylase. *Process Biochemistry, 47*(5): 775–784.

Zemser, M., Friedman, M., Katzhendler, J., Greene, L., Minsky, A. and Gorinstein, S. (1994). Relationship between functional properties and structure of ovalbumin. *Journal of Protein Chemistry, 13*(2): 261–274.

Zhang, N., Liu, F.-F., Dong, X.-Y. and Sun, Y. (2013). Counteraction of trehalose on urea-induced protein unfolding: Thermodynamic and kinetic studies. *Biochemical Engineering Journal, 79*(0): 120–128.

LIST OF PUBLICATIONS / PRESENTATIONS

Publications

1. **Wong Yin How** and Saad Tayyab (2012). Protein stabilizing potential of simulated honey sugar cocktail under various denaturation conditions. ***Process Biochemistry*** **47**: 1933–1943.

2. **Wong Yin How**, Habsah Abdul Kadir and Saad Tayyab (2013). Honey-induced protein stabilization as studied by fluorescein isothiocyanate fluorescence. ***Scientific World Journal*** Article ID 981902, 8 pages.

3. **Wong Yin How**, Lim Chze Huey, Habsah Abdul Kadir and Saad Tayyab (2014). Towards increasing chemical and thermal stability of lysozyme with a simulated honey sugar cocktail. ***RSC Advances*** **4**: 53891–53898.

4. **Wong Yin How**, Habsah Abdul Kadir and Saad Tayyab (2015). Targeting chemical and thermal stability of ovalbumin by simulated honey sugar cocktail. ***International Journal of Biological Macromolecules*** **73**: 207–214.

5. Pralad Manoharan, **Wong Yin How** and Saad Tayyab (2015). Stabilization of human serum albumin against urea denaturation by diazepam and ketoprofen. ***Protein & Peptide Letters*** **22**: 611–617.

6. **Wong Yin How**, Habsah Abdul Kadir and Saad Tayyab (2015). Intrinsic fluorescence as a spectral probe for protein denaturation studies in the presence of honey. ***Journal of Applied Spectroscopy*** **82**: 788–791.

7. Nurul Iman Ahmed Kameel, **Wong Yin How**, Adawiyah Suriza Shuib and Saad Tayyab (2016). Conformational analysis of champedak galactose-binding lectin under different urea concentrations. ***Plant Physiology and Biochemistry*** **98**: 57–63.

8. **Wong Yin How**, Habsah Abdul Kadir and Saad Tayyab (2016). A comparative analysis of protein stabilizing potential of honey and simulated honey sugar cocktail. – Communicated.

Presentations

1. **Wong Yin How** and Saad Tayyab (2012). Simulated honey sugar cocktail as a protein stabilizer. Proceedings of the 9th International Conference on Protein Stability, held at Lisbon, Portugal on May 2 – 4, 2012. Abstract No. P35, pp. 35.

2. **Wong Yin How** and Saad Tayyab (2012). Structural stabilization of ovalbumin by simulated honey sugar cocktail against urea denaturation. Proceedings of the 37th Annual Conference of the Malaysian Society for Biochemistry & Molecular Biology, held at Kuala Lumpur, Malaysia on July 18 – 19, 2012. Abstract No. O8, pp. 39.

3. **Wong Yin How**, Habsah Abdul Kadir and Saad Tayyab (2012). Fluorescein isothiocyanate as a probe to study protein denaturation in the presence of honey. Proceedings of the 17th Biological Sciences Graduate Congress, held at Bangkok, Thailand on December 8 – 10, 2012. Abstract No. BC–OR 16, pp. 82.

4. **Wong Yin How** and Saad Tayyab (2014). Interference of honey with protein's intrinsic fluorescence and honey-induced protein stabilization. Proceedings of the 2014 International Conference on Biological and Chemical Sciences (ICBCS 2014), held at Shanghai, China on March 29 – 30, 2014. Abstract No. CB051, pp. 6 – 7.

5. **Wong Yin How** and Saad Tayyab (2014). Improved chemical and thermal stability of proteins in the presence of simulated honey sugar cocktail. Proceedings of the 10th International Conference on Protein Stability, held at Stresa, Italy on May 7 – 9, 2014. Abstract No. C11, pp. 74.

6. Salanee Kandandapani, **Wong Yin How**, Adawiyah Suriza Shuib and Saad Tayyab (2015). Guanidine hydrochloride-denatured states of *Bacillus licheniformis* α-amylase under different buffer conditions. Proceedings of the 40th Annual Conference of the Malaysian Society for Biochemistry & Molecular Biology, held at Sepang, Malaysia on June 10 – 11, 2015. Abstract No. P16, pp. 56.

7. Nurul Iman Ahamed Kameel, **Wong Yin How**, Adawiyah Suriza Shuib and Saad Tayyab (2015). Urea-induced structural transitions in Champedak galactosidase-binding lectin. Proceedings of the 40th Annual Conference of the Malaysian Society for Biochemistry & Molecular Biology, held at Sepang, Malaysia on June 10 – 11, 2015. Abstract No. P24, pp. 64.

BIOGRAPHY

Wong Yin How was born in Kuala Lumpur, Malaysia on October 30, 1988. He received his pre-university education from SMK Seri Garing, Selangor in 2006–2007. He then enrolled in the programme of Bachelor of Science in Biochemistry at the University of Malaya in the year 2008. He obtained his B.Sc. degree in Biochemistry and has been awarded the Best Student of Biochemistry Award in the year 2011. He then joined University of Malaya for his Master of Science degree in Biochemistry in the year 2012. During 2012–2013, he also served the Institute of Biological Sciences, Faculty Science, University of Malaya as a Tutor of Biochemistry. In 2013, he converted his candidature from M. Sc. to Ph.D. degree. He has been awarded the University Malaya Fellowship Scheme for the period, 2012–2015. He has also been the recipient of University of Malaya Postgraduate Research Grant from 2013–2015.

Process Biochemistry 47 (2012) 1933–1943

Contents lists available at SciVerse ScienceDirect

Process Biochemistry

journal homepage: www.elsevier.com/locate/procbio

Protein stabilizing potential of simulated honey sugar cocktail under various denaturation conditions

Yin-How Wong, Saad Tayyab*

Biomolecular Research Group, Biochemistry Programme, Institute of Biological Sciences, Faculty of Science, University of Malaya, 50603 Kuala Lumpur, Malaysia

ARTICLE INFO

Article history:
Received 7 March 2012
Received in revised form 26 June 2012
Accepted 26 June 2012
Available online 4 July 2012

Keywords:
Simulated honey sugar cocktail
Protein stabilization
Urea denaturation
Bovine serum albumin

ABSTRACT

Protein stabilizing potential of simulated honey sugar cocktail (SHSC) against chemical and thermal denaturations was studied using bovine serum albumin (BSA) as the model protein. The two-step, three-state transition of urea denaturation of BSA became a single-step, two-state transition along with the shift in the whole transition curve towards higher urea concentrations in the presence of increasing SHSC concentrations [8–20% (w/v)] as revealed by far-UV CD, fluorescence and UV difference spectroscopic results. Far-UV and near-UV CD spectra, UV difference spectra, ANS fluorescence and three-dimensional fluorescence results suggested significant retention of native-like conformation in 4.6 M urea-denatured BSA in the presence of 20% (w/v) SHSC. A significant shift was also noticed in thermal and GdnHCl denaturation curves of BSA in the presence of 20% (w/v) SHSC. Taken together, all these results suggested significant stabilization of BSA against urea, GdnHCl and thermal denaturations by SHSC.

1. Introduction

Over the past 40 years, protein stability remains a critical issue in the field of biotechnology due to increasing applications and escalating demands of proteins in various industries as biocatalysts, analytical tools, therapeutic agents, clinical diagnostic materials, etc. [1–3]. Proteins are relatively unstable and progressively loose their functionality and native conformation under in vitro conditions such as extreme temperature, pH, pressure as well as in presence of various chemicals and solvents. Such environmental conditions are frequently met in the biotechnology industry and call for further research in order to achieve greater storage and operational stability of proteins including increased shelf life and functionality under these conditions [1].

Although a number of strategies have been demonstrated for increasing protein stability, none of them is proved successful as a general approach for commercialization. These strategies include protein engineering, chemical modification and site-directed mutagenesis [1,4]. Naturally occurring small organic molecules present in the organisms, have shown greater potential to provide significant stabilization to proteins. These small organic molecules such as sugars, polyols, salts, amino acids and their derivatives are collectively termed as osmolytes. Most of the osmolytes have been found compatible with most of the macromolecules in biological systems, hence do not affect the protein functionality or biological activity [2,5,6]. Recently, osmolytes have also been recognized as chemical chaperones due to their protein structure stabilizing ability as well as restoring the folding of the misfolded proteins in biological systems [2]. Exploitation of the above characteristics of osmolytes in stabilizing proteins' structures has given the birth of another phenomenon, known as solvent engineering [7]. Such a strategy has been found promising over to other strategies, particularly in its use for therapeutic agents in treatment of protein misfolding diseases and biocatalysts in the food industry [1,2].

Honey has been used in traditional medicine and as a food supplement since ancient civilization due to its high medicinal and nutritional values. Recent researches have concluded antimicrobial, antibacterial and wound healing properties of honey, which have allowed the use of honey in the treatment of some gastrointestinal, respiratory and ophthalmic disorders and as a topical agent in wound healing treatment [8]. Honey is a mixture of compounds with high-carbohydrate content and rich diversity of minor constituents such as minerals, amino acids, proteins and vitamins. Major component of the honey is sugar, constituting more than 95% of honey dry weight [8]. Various studies have shown that sugars can act as effective osmolytes in increasing protein stability especially, thermal-stability [3,9–17]. Sugars have been shown to provide stabilization to proteins under various stresses such as dehydration, variable pH, freezing, high salinity and in presence of chemical denaturants [1,3,18]. The stabilization mechanism of sugars

Abbreviations: ANS, 1-anilinonaphthalene-8-sulfonate; BSA, bovine serum albumin; CD, circular dichroism; GdnHCl, guanidine hydrochloride; MRE, mean residue ellipticity; SHSC, simulated honey sugar cocktail; Trp, tryptophan; Tyr, tyrosine.

* Corresponding author. Tel.: +60 3 7967 7118; fax: +60 3 7967 4178.
E-mail address: saadtayyab2004@yahoo.com (S. Tayyab).

1359-5113/$ – see front matter © 2012 Elsevier Ltd. All rights reserved.
http://dx.doi.org/10.1016/j.procbio.2012.06.028

Hindawi Publishing Corporation
The Scientific World Journal
Volume 2013, Article ID 981902, 8 pages
http://dx.doi.org/10.1155/2013/981902

Research Article

Honey-Induced Protein Stabilization as Studied by Fluorescein Isothiocyanate Fluorescence

Yin How Wong, Habsah Abdul Kadir, and Saad Tayyab

Biomolecular Research Group, Biochemistry Programme, Institute of Biological Sciences, Faculty of Science, University of Malaya, 50603 Kuala Lumpur, Malaysia

Correspondence should be addressed to Saad Tayyab; saadtayyab2004@yahoo.com

Received 11 July 2013; Accepted 22 August 2013

Academic Editors: H. Mobasheri and P. Pohl

Protein stabilizing potential of honey was studied on a model protein, bovine serum albumin (BSA), using extrinsic fluorescence of fluorescein isothiocyanate (FITC) as the probe. BSA was labelled with FITC using chemical coupling, and urea and thermal denaturation studies were performed on FITC-labelled BSA (FITC-BSA) both in the absence and presence of 10% and 20% (w/v) honey using FITC fluorescence at 522 nm upon excitation at 495 nm. There was an increase in the FITC fluorescence intensity upon increasing urea concentration or temperature, suggesting protein denaturation. The results from urea and thermal denaturation studies showed increased stability of protein in the presence of honey as reflected from the shift in the transition curve along with the start point and the midpoint of the transition towards higher urea concentration/temperature. Furthermore, the increase in $\Delta G_D^{H_2O}$ and $\Delta G_D^{25^\circ C}$ in presence of honey also suggested protein stabilization.

1. Introduction

Protein stability has been regarded as a critical issue in biotechnology due to increasing demands of proteins in various applications, such as industrial enzymes, analytical tools, therapeutics agents, clinical diagnostic materials, and so forth [1–3]. However, many proteins suffer from the drawback of poor storage and operational stability and lose their functionality and native conformation over a period of time [1]. On the other hand, various industrial processes require operational conditions such as extreme temperature, pH, pressure, and the presence of various chemicals and solvents, which may lead to protein destabilization and denaturation. Hence, there is a need to increase the stability of proteins used in industrial processes.

Several attempts have been made to increase protein stability using chemical modification, site-directed mutagenesis, introduction of disulphide bonds, and anion binding sites as well as solvent engineering [4–7]. However, only a few modified enzymes have displayed commercial viability [8, 9]. Solvent engineering has shown an edge over other methods of protein stabilization as osmolytes are known to be functionally and biologically compatible with most of the proteins [2, 10, 11]. Sugars and amino acids are well-known naturally occurring osmolytes, showing great protein stabilizing potential against different denaturing conditions including chemical (urea and guanidine hydrochloride) and thermal denaturations [1, 12–14]. With a few exceptions [12, 15, 16], most of the osmolyte-induced protein stabilization studies have been focused on using a single osmolyte [3, 13, 14].

Honey is a natural mixture of compounds with high-sugar content (~38% fructose, ~32% glucose, ~1.7% maltose, ~1.4% sucrose, ~1% turanose, ~0.8% isomaltose, ~0.4% erlose, etc.) and minor constituents such as amino acids, proteins, vitamins, minerals, and polyphenols [17, 18]. Due to the presence of these compounds, honey has been regarded as the traditional medicine and food supplement since prehistorical time. Modern science has also recognized the antibacterial, antioxidant, anti-inflammatory, and wound healing properties of honey [18]. Due to the presence of a number of osmolytes, honey can be used as a potential protein stabilizer. Recently, an attempt has been made to study

RSC Advances

PAPER

View Article Online
View Journal | View Issue

Cite this: *RSC Adv.*, 2014, **4**, 53891

Towards increasing chemical and thermal stability of lysozyme with a simulated honey sugar cocktail

Yin How Wong, Chze Huey Lim, Habsah Abdul Kadir and Saad Tayyab*

Received 2nd September 2014
Accepted 10th October 2014

DOI: 10.1039/c4ra09606a

www.rsc.org/advances

Guanidine hydrochloride (GdnHCl) and thermal denaturation studies on lysozyme were made in the absence and the presence of a simulated honey sugar cocktail (SHSC). GdnHCl denaturation curve was shifted towards higher denaturant concentration along with an increase in $\Delta G_D^{H_2O}$ value in the presence of SHSC, when studied by $MRE_{222\ nm}$ and tryptophan fluorescence measurements. Far- and near-UV CD as well as ANS fluorescence spectra of the partially-denatured lysozyme indicated greater retention of the folded structure in the presence of SHSC. The thermal transition curve showed a shift towards the higher temperature range along with an increase in the melting temperature in the presence of SHSC, when studied by $MRE_{222\ nm}$ and DSC measurements. Taken together, all these results suggested SHSC-induced chemical and thermal stabilization of lysozyme.

1. Introduction

Many new applications of proteins such as analytical tools, therapeutic agents, clinical diagnostic materials and industrial enzymes have evolved due to recent progress in biotechnology.[1–3] However, the intrinsic properties of the protein, in being stable under *in vitro* conditions have remained a major issue in these applications as the isolated protein fails to maintain its function and activity over a longer period.[3] Over the past decade, lots of efforts have been directed towards protein folding/unfolding studies with the aim to acquire some insights on protein stabilization.[1–3] Although several approaches such as protein engineering, chemical modification and solvent engineering have been adapted to improve protein stability,[1] none of them has shown promising results.[4] Solvent engineering seems to be a better choice for increasing protein stability, as osmolytes have been shown compatible with most proteins.[3] Various reports have demonstrated protein stabilizing effect of osmolytes against different denaturing conditions.[5–8] Potential of honey as a protein stabilizer can be attributed to its high sugar content (natural osmolytes). However, presence of other minor constituents in the honey has restricted its use in protein stabilization studies involving various spectroscopic probes. Hence, simulated honey sugar cocktail (SHSC), containing same sugar composition as that found in the honey can be used to study its effect on chemical and thermal stability of proteins.

Lysozyme (EC 3.2.1.17), also known as β-1,4-*N*-acetylmuramidase catalyzes hydrolysis of β-1,4-glycosidic bond between *N*-acetylmuramic acid and *N*-acetyl-D-glucosamine residues in peptidoglycan cell wall of Gram positive bacteria. Due to this biological activity, lysozyme is widely used in food preservation, pharmaceutical, medicinal and veterinary industries.[9–15] The anti-bacterial property of lysozyme has made its impact in cheese, wine and brewing industries to maintain quality of the products.[13,14] The enzyme has also got its application as an antibiotic in poultry industry in being used in chicken feed to promote healthy growth of chicks.[15] In this manuscript, an attempt was made to study the effect of SHSC on lysozyme against chemical (guanidine hydrochloride) and heat denaturations using far-UV and near-UV circular dichroism (CD), tryptophan (Trp) fluorescence as well as differential scanning calorimetry (DSC).

Biomolecular Research Group, Biochemistry Programme, Institute of Biological Sciences, Faculty of Science, University of Malaya, 50603 Kuala Lumpur, Malaysia. E-mail: saadtayyab2004@yahoo.com; Fax: +60 3 79674178; Tel: +60 3 7967 7118

2. Experimental

2.1. Materials

Lysozyme from chicken egg white (type L-6876), guanidine hydrochloride (GdnHCl) (type G-4505), 8-anilino-1-naphthalenesulfonic acid (ANS) (type A-3125), D-(−)-fructose (type F-0127), D-(+)-glucose (type G-8270) and D-(+)-trehalose dihydrate (type T-9449) were supplied by Sigma-Aldrich Co., USA. Maltose (type 3538-00) and sucrose (type SU250-00) were purchased from R&M Chemicals, USA and SYSTERM®, Malaysia, respectively. All other reagents used were of analytical grade purity.

2.2. Analytical procedures

The stock solutions of lysozyme (200 μM) and GdnHCl (8.0 M) were prepared in 60 mM sodium phosphate buffer, pH 7.0. The corrected pH of the stock GdnHCl solution was found to be 6.81 ± 0.02, following the procedure described by Garcia-Mira & Sanchez-Ruiz.[16] This solution was used without any further pH adjustment. The protein concentration was determined

International Journal of Biological Macromolecules 73 (2015) 207–214

Contents lists available at ScienceDirect

International Journal of Biological Macromolecules

journal homepage: www.elsevier.com/locate/ijbiomac

Targeting chemical and thermal stability of ovalbumin by simulated honey sugar cocktail

Yin How Wong, Habsah A. Kadir, Saad Tayyab*

Biomolecular Research Group, Biochemistry Programme, Institute of Biological Sciences, Faculty of Science, University of Malaya, 50603 Kuala Lumpur, Malaysia

ARTICLE INFO

Article history:
Received 28 October 2014
Received in revised form
21 November 2014
Accepted 21 November 2014
Available online 28 November 2014

Keywords:
Chemical denaturation
Thermal denaturation
Protein stabilization
Ovalbumin
Simulated honey sugar cocktail

ABSTRACT

Effect of simulated honey sugar cocktail (SHSC) on chemical and thermal stability of ovalbumin (OVA) was investigated using multiple-spectroscopic techniques. Urea-induced denaturation of OVA produced a transition, characterized by the start-, the mid- and the end-points at 3.2 M, 5.9/5.6 M and 8.5/8.0 M urea, respectively, when studied by MRE_{222nm} and tryptophan fluorescence measurements. Presence of 10% or 20% (w/v) SHSC in the incubation mixture shifted the transition curve towards higher urea concentration in a concentration dependent manner. A comparison of far- and near-UV CD, UV-difference, ANS fluorescence and 3-D fluorescence spectral results of native OVA and 5.9 M urea-denatured OVA (U-OVA), obtained in the absence and the presence of 20% (w/v) SHSC suggested SHSC-induced stabilization of U-OVA. Furthermore, a significant shift towards higher denaturant concentration was also noticed in the GdnHCl and thermal transition curves of OVA in the presence of 20% (w/v) SHSC. Taken together, all these results suggested stabilization of OVA against chemical and thermal denaturations by SHSC.

1. Introduction

Chicken egg white proteins (EWP) have been regarded as one of the most extensively used ingredients in food processing and manufacturing industries due to their gelling, foaming and emulsifying properties [1]. The foams produced maintain the texture and structure of the food products such as cakes, crackers, ice creams and breads during or after food processing [2]. The gelling ability of EWP has also made its impact in meat and noodle manufacture industries to improve their texture and food sensory [1].

Efficacy of EWP to serve as a foaming or gelling agent depends on the stability of the foam or the gel produced. The foam's stability in turn depends on the configuration and stability of the proteins involved. However, the proteins' stability is sensitive towards external factors such as pH, ionic strength, heating, presence of salts and composition of the medium [2]. These external factors might be responsible for protein denaturation and aggregation, thereby reducing the foam's stability. Similarly, hardness of the gel formed is also affected by the pH and the ionic strength of the gelling medium [1].

Recently, food technologists have recognized the nutritional benefits of honey and have incorporated it in various types of food products *e.g.* baked products, confectionary, breakfast cereals, beverages, milk products and many preserved food ingredients [3]. Since honey contains high sugar content, it seems to stabilize the native protein conformation [4–7]. Presence of honey in some food products could have stabilized EWP against various external factors involved in the industrial processing and it is meaningful to examine protein stabilizing effect of honey. However, presence of other components such as flavonoids and polyphenolic compounds in honey has interfered in protein stabilization studies using spectroscopic probes (unpublished data). Hence, simulated honey sugar cocktail (SHSC) was formulated using the same sugar composition as that found in honey, in order to elucidate its stabilizing effect on EWP. Since ovalbumin (OVA) is the major component of EWP, contributing ~54% to its total protein content, stability of EWP should mainly be reflected by OVA stability against various external factors [8]. Therefore, in this manuscript we report our results on SHSC-induced stabilization of OVA against chemical and thermal denaturations, as studied by various spectroscopic techniques.

2. Materials and methods

2.1. Materials

Ovalbumin, urea ultrapure, guanidine hydrochloride (GdnHCl), 1-anilinonaphthalene-8-sulfonate (ANS), D (−) fructose, D (+) trehalose dihydrate and D (+) glucose were obtained from

* Corresponding author. Tel.: +60 379677118; fax: +60 379674178.
E-mail address: saadtayyab2004@yahoo.com (S. Tayyab).

http://dx.doi.org/10.1016/j.ijbiomac.2014.11.015
0141-8130/

Send Orders for Reprints to reprints@benthamscience.ae

Protein & Peptide Letters, 2015, *22*, 611-617

Stabilization of Human Serum Albumin against Urea Denaturation by Diazepam and Ketoprofen

Pralad Manoharan, Yin H. Wong and Saad Tayyab*

Biomolecular Research Group, Biochemistry Programme, Institute of Biological Sciences, Faculty of Science, University of Malaya, 50603 Kuala Lumpur, Malaysia

Saad Tayyab

Abstract: Stabilizing effect of diazepam and ketoprofen, Sudlow's site II markers on human serum albumin (HSA) against urea denaturation was studied using fluorescence spectroscopy. The two-step, three-state urea transition of HSA was transformed into a single-step, two-state transition with the abolishment of the intermediate state along with a shift of the transition curve towards higher urea concentrations in the presence of diazepam or ketoprofen. Interestingly, a greater shift in the transition curve of HSA was observed in the presence of ketoprofen compared to diazepam. A comparison of the intrinsic fluorescence and three-dimensional fluorescence spectra of HSA and partially-denatured HSAs, obtained in the absence and the presence of diazepam or ketoprofen suggested significant retention of native-like conformation in the partially-denatured states of HSA in the presence of Sudlow's site II markers. Taken together, all these results suggested stabilization of HSA in the presence of diazepam or ketoprofen, being greater in the presence of ketoprofen.

Keywords: Diazepam, Fluorescence spectroscopy, Human serum albumin, Ketoprofen, Protein stabilization, Urea denaturation.

INTRODUCTION

Proteins fold into their native three-dimensional conformations from the linear polypeptide chains driven by non-covalent forces such as hydrogen bonding, *van der Waals*, electrostatic and hydrophobic interactions along with disulphide linkages, if present [1]. However, many globular proteins are only marginally stable over their denatured counterparts as the free energy of unfolding of most proteins has been reported to be around – 10 kcal/mol [2-5]. Since proteins have many applications in pharmaceutical and industrial sectors, their stability has become a major issue in these applications [6]. In order to increase the stability of proteins under *in vitro* conditions, various approaches such as protein engineering, chemical modification, solvent engineering and use of protein-specific ligands have been employed [6,7].

Human serum albumin (HSA) is a non-glycosylated protein with 585 amino acid residues, arranged into three homologous domains *i.e.* I, II and III, with their subsequent division into subdomains A and B [8]. Being the major transport protein in blood circulation, HSA is known to bind a number of endogenous and exogenous compounds in the circulation, which include fatty acids, heme, steroids, amino acids and various drugs [9,10]. Binding of these compounds to HSA mainly occurs in two regions, characterized as Sudlow's site I and II, which are located in subdomains IIA and IIIA, respectively [10,11]. Diazepam (a psychoactive drug) and ketoprofen (a non-steroidal anti-inflammatory drug), whose chemical structures are shown in Fig. **1**, have been frequently used as the Sudlow's site II-specific markers in various ligand-protein interaction studies since binding of these drugs to Sudlows's Site II is well established [11-13].

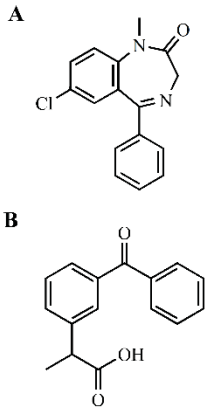

Figure 1. Chemical structures of diazepam (**A**) and ketoprofen (**B**).

Protein denaturation studies are usually made to determine the stability of a protein [14,15]. The denaturation behavior of HSA in the presence of chaotropic agent, urea is characterized by the unfolding of domain III, followed by unfolding of domains I and II [16,17]. Since subdomain IIIA

*Address correspondence to this author at the Biomolecular Research Group, Biochemistry Programme, Institute of Biological Sciences, Faculty of Science, University of Malaya, 50603 Kuala Lumpur, Malaysia; Tel/Fax: +603 7967 7118, +603 7967 4178; E-mail: saadtayyab2004@yahoo.com

1875-5305/15 $58.00+.00

INTRINSIC FLUORESCENCE AS A SPECTRAL PROBE FOR PROTEIN DENATURATION STUDIES IN THE PRESENCE OF HONEY

Y. H. Wong, H. A. Kadir, S. Tayyab*

Institute of Biological Sciences, University of Malaya,
50603, Kuala Lumpur, Malaysia; e-mail: saadtayyab2004@yahoo.com

Honey was found to quench the intrinsic fluorescence of bovine serum albumin (BSA) in a concentration dependent manner, showing complete quenching in the presence of 5% (w/v) honey. Increasing the protein concentration up to 5.0 μM did not lead to the recovery of the protein fluorescence. Urea denaturation of BSA, which otherwise shows a two-step, three-state transition, using intrinsic fluorescence of the protein as the probe failed to produce any result in the presence of 5% (w/v) honey. Thus, intrinsic fluorescence cannot be used as a spectral probe for protein denaturation studies in the presence of honey.

Keywords: *bovine serum albumin, fluorescence spectroscopy, fluorimetric interference, honey, protein denaturation.*

МЕТОД СОБСТВЕННОЙ ФЛУОРЕСЦЕНЦИИ ДЛЯ ИССЛЕДОВАНИЯ ДЕНАТУРАЦИИ БЕЛКА В ПРИСУТСТВИИ МЕДА

Y. H. Wong, H. A. Kadir, S. Tayyab*

УДК 535.372:547.96

Институт биологии Университета Малайзии,
50603, Куала-Лумпур, Малайзия; e-mail: saadtayyab2004@yahoo.com

(Поступила 16 октября 2014)

Обнаружено, что мед подавляет собственную флуоресценцию бычьего сывороточного альбумина (BSA) с эффективностью, зависящей от концентрации. Полное тушение флуоресценции белка наступает при 5% содержании меда. Повышение концентрации белка до 5.0 мкМ не приводит к восстановлению флуоресценции белка. Денатурация BSA мочевиной, которая в других случаях проявляется как двухшаговый переход через три состояния, не обнаруживается методом собственной флуоресценции белка, если в пробе присутствует 5% меда. Показано, что в присутствии меда метод собственной флуоресценции не может быть использован для исследований денатурации белка.

Ключевые слова: *бычий сывороточный альбумин, флуоресцентная спектроскопия, интерференция, мед, денатурация белка.*

Introduction. Proteins have many important applications such as industrial enzymes, analytical tools, therapeutics agents, and clinical diagnostic materials [1–3]. However, many proteins suffer from the drawback of poor storage and operational stability, thus losing their functionality and native conformation over a period of time. Poor protein stability is of significant concern in various industrial processes, which require extreme operational conditions such as extreme temperature, pH, pressure, and the presence of various chemicals and solvents. Hence, protein stabilization has been regarded as a critical issue in biotechnology.

Honey is a natural mixture of compounds with a high sugar content and minor constituents including amino acids, proteins, vitamins, minerals, and polyphenols [4]. Because of the presence of these compounds, honey has been regarded as a traditional medicine and food supplement since prehistoric times. Modern science has also recognized the antibacterial, antioxidant, anti-inflammatory, and wound healing properties of honey [4–6]. Honey can be used as a protein stabilizer because of its high sugar content. Recently, the protein stabilizing potential of honey using a simulated honey sugar cocktail (SHSC) was examined [7]. However, the presence of other osmolytes in honey, such as amino acids, would have further added to the stabilizing potential of SHSC. Thus, the protein stabilizing potential of honey can only be accurately examined using honey rather than an alternative cocktail.

Protein stabilization studies mainly involve denaturation studies, which can be carried out by a variety of spectroscopic techniques, i.e., circular dichroism (CD), fluorescence, and UV-difference absorption. Since fluo-

Plant Physiology and Biochemistry 98 (2016) 57–63

Contents lists available at ScienceDirect

Plant Physiology and Biochemistry

journal homepage: www.elsevier.com/locate/plaphy

Research article

Conformational analysis of champedak galactose-binding lectin under different urea concentrations

Nurul Iman Ahamed Kameel, Yin How Wong, Adawiyah Suriza Shuib, Saad Tayyab*

Biomolecular Research Group, Biochemistry Programme, Institute of Biological Sciences, Faculty of Science, University of Malaya, 50603, Kuala Lumpur, Malaysia

ARTICLE INFO

Article history:
Received 2 September 2015
Received in revised form
2 November 2015
Accepted 16 November 2015
Available online xxx

Keywords:
Champedak galactose-binding lectin
Conformational analysis
Far-UV CD
Hemagglutination
Tryptophan fluorescence
Urea denaturation

ABSTRACT

Conformational analysis of champedak galactose-binding (CGB) lectin under different urea concentrations was studied in phosphate-buffered saline (pH 7.2) using far-ultraviolet circular dichroism (far-UV CD), tryptophan (Trp) fluorescence and ANS fluorescence. In all cases, CGB lectin displayed a two-step, three-state transition. The first transition (from the native state to the intermediate state) started at ~2.0 M urea and ended at ~4.5 M urea, while the second transition (from the intermediate state to the completely denatured state) was characterized by the start- and end-points at ~5.75 M and ~7.5 M urea, respectively, when analyzed by the emission maximum of Trp fluorescence. A marked increase in the Trp fluorescence, ANS fluorescence and −CD values at 218 nm ($-CD_{218\ nm}$) represented the first transition, whereas a decrease in these parameters defined the second transition. On the other hand, emission maximum of the Trp fluorescence showed a continuous increase throughout the urea concentration range. Transformation of tetramer into monomer represented the first transition, whereas the second transition reflected the unfolding of monomer. Far-UV CD, Trp fluorescence and ANS fluorescence spectra were used to characterize the native, the intermediate and the completely denatured states of CGB lectin, obtained at 0.0 M, 5.0 M and 9.0 M urea, respectively. The intermediate state was characterized by the presence of higher secondary structures, increased ANS binding as well as increased Trp fluorescence intensity. A gradual decrease in the hemagglutination activity of CGB lectin was observed with increasing urea concentrations, showing complete loss at 4.0 M urea.

1. Introduction

Protein denaturation studies have gained much interest in the pursuit of understanding the conformational stability and the structure–function relationship of proteins (Privalov, 2012; Wong et al., 2014). Out of various denaturants, chemical denaturants such as urea and guanidine hydrochloride have been found popular in protein denaturation studies in being effective to disrupt all noncovalent interactions (O'Brien et al., 2007), which are known to stabilize the native protein conformation. The denaturation of multimeric proteins is more complex than the monomeric proteins due to the presence of intersubunit interactions in addition to the intrasubunit interactions within the protein (Biswas and Kayastha, 2004; Sinha et al., 2005; Dev et al., 2006).

Lectins are ubiquitous carbohydrate-binding proteins, possessing at least one specific sugar-binding site (Goldstein, 1980; Peumans and Van Damme, 1995). In plant seeds, they constitute up to 5% of the total protein content (Van Damme, 2008). The physiological importance of lectins in plants has been accredited due to their role in plant defense against pathogens, plant development and symbiotic plant–microbe interactions (Brill et al., 2001; De Hoff et al., 2009; Yamaji et al., 2012). Due to their sugar-binding properties, plant lectins have also been harnessed as tools in the characterization of glycoconjugates, carriers in drug delivery systems and for their potential anti-tumor applications (Gabor et al., 2002; Wu et al., 2009; Fu et al., 2011).

Champedak (*Artocarpus integer*) is a fruit tree species of the same genus as of the jackfruit and is local to Southeast Asia. Champedak seeds are the source for champedak galactose-binding (CGB) lectin, which has been well characterized for its molecular properties, including hemagglutinating activity (Hashim et al.,

Abbreviations: ANS, 1-anilinonaphthalene-8-sulfonate; CGB, champedak galactose-binding; CD, circular dichroism; Trp, tryptophan.

* Corresponding author.
E-mail addresses: imankameel@gmail.com (N.I.A. Kameel), zack_wong123@yahoo.com (Y.H. Wong), adawiyah@um.edu.my (A.S. Shuib), saadtayyab2004@yahoo.com (S. Tayyab).

http://dx.doi.org/10.1016/j.plaphy.2015.11.007
0981-9428/